Biocatalytic Conversion of Cellulose towards Itaconic Acid

Von der Fakultät für Maschinenwesen
der Rheinisch-Westfälischen Technischen Hochschule Aachen
zur Erlangung des akademischen Grades
eines Doktors der Naturwissenschaften
genehmigte Dissertation

vorgelegt von

Gernot Jäger

Berichter: Universitätsprofessor Dr.-Ing. Jochen Büchs
               Universitätsprofessor Dr. rer. nat. Ulrich Schwaneberg

Tag der mündlichen Prüfung: 08. August 2012

Biocatalytic Conversion of Cellulose towards Itaconic Acid

Gernot Jäger

Vorwort

Die vorliegende Dissertation entstand während meiner Tätigkeit als wissenschaftlicher Mitarbeiter am Lehrstuhl für Bioverfahrenstechnik (Aachener Verfahrenstechnik) der RWTH Aachen. Diese Arbeit war eingegliedert in das Exzellenzcluster 236 „Maßgeschneiderte Kraftstoffe aus Biomasse".

Mein besonderer Dank gilt Professor Jochen Büchs für die Betreuung dieser Arbeit und für die Möglichkeit am Lehrstuhl für Bioverfahrenstechnik zu promovieren. Seine Unterstützung, seine Anregungen und seine Offenheit gegenüber neuen Ideen waren Voraussetzung für das Gelingen dieser Arbeit. Für die Förderung meiner wissenschaftlichen Laufbahn möchte ich mich ausdrücklich bei ihm bedanken. Mein Dank gilt auch Professor Ulrich Schwaneberg für die Übernahme des Koreferates und für die Zusammenarbeit im Rahmen des Exzellenzclusters. Professor Stefan Pischinger danke ich für die Übernahme des Prüfungsvorsitzes und für die Leitung und Organisation des Exzellenzclusters.

Die Grundlage für die Bearbeitung dieser interdisziplinären Arbeit war die sehr gute Zusammenarbeit innerhalb des Exzellenzclusters. Besonders möchte ich mich bei den folgenden Kooperationspartnern für die konstruktiven Diskussionen und die gewinnbringende Zusammenarbeit bedanken: Tobias Klement, Marco Scheidle und Michael Zavrel (AVT – Lehrstuhl für Bioverfahrenstechnik); Philip Engel, Helene Wulfhorst und Professor Antje Spiess (AVT – Lehrstuhl für Enzymprozesstechnik); Roberto Rinaldi und Hans Bongard (Max-Planck-Institut für Kohlenforschung); Michele Girfoglio, Michael Küpper, Ulrich Commandeur und Professor Rainer Fischer (Lehrstuhl für molekulare Biotechnologie); Stefano Di Fiore (Fraunhofer-Institut für Molekularbiologie und angewandte Ökologie); Professor Christos Georgakis (Department of Chemical & Biological Engineering, Tufts University).

Besonderer Dank gebührt meinen Studenten und wissenschaftlichen Hilfskräften (HiWi), die mich durch ihre Arbeiten wesentlich unterstützt haben. Ich danke Florian Dollo (Abschlussarbeit + HiWi), Efthimia Ellinidou (Abschlussarbeit), Kerstin Garschhammer (Abschlussarbeit + HiWi), Martin Pöhnlein (Abschlussarbeit), Christin Schlegel (Abschlussarbeit), Zhuojun Wu (HiWi) und Erik Zeithammel (Abschlussarbeit).

Nicht zu vergessen sind meine Kollegen innerhalb der Aachener Verfahrenstechnik. Ihnen danke ich für die überaus angenehme Arbeitsatmosphäre und die freundschaftliche Verbundenheit.

Zu guter Letzt danke ich ganz herzlich meiner Familie für all ihre Unterstützung während der Anfertigung dieser Arbeit. Ohne sie wäre eine erfolgreiche, persönliche Entwicklung sowohl vor als auch während dieser Arbeit nicht möglich gewesen.

Erkelenz, Dezember 2011   Gernot Jäger

Chi poco pensa molto erra.

(Wer wenig denkt, der irrt viel.)

Leonardo da Vinci (1452 - 1519)

A) Aspects of this thesis have been published previously:

Main author:

1) Jäger G, Wu Z, Garschhammer K, Engel P, Klement T, Rinaldi R, Spiess AC, Büchs J. 2010. Practical screening of purified cellobiohydrolases and endoglucanases with alpha-cellulose and specification of hydrodynamics. Biotechnol Biofuels 3:18[#].

2) Jäger G, Wulfhorst H, Zeithammel EU, Ellinidou E, Spiess AC, Büchs J. 2011. Screening of cellulases for biofuel production: Online monitoring of the enzymatic hydrolysis of insoluble cellulose using high-throughput scattered light detection. Biotechnol J 6:74-85.

3) Jäger G, Girfolgio M, Dollo F, Rinaldi R, Bongard H, Commandeur U, Fischer R, Spiess AC, Büchs J. 2011. How recombinant swollenin from *Kluyveromyces lactis* affects cellulosic substrates and accelerates their hydrolysis. Biotechnol Biofuels 4:33[#].

4) Wulfhorst* H, Jäger* G, Ellinidou E, Büchs J, Spiess AC. 2010. Charakterisierung von Cellulasepräparationen mittels Streulicht. Chem Ing Tech 82(1-2):117-120.

B) Contributions to associated publications during this thesis:

Main author:

5) Eberhard* W, Jäger* G, Pinto J, Spiess AC, Büchs J. 2012. Determining complete suspension of immobilized enzymes by analysis of digital camera images. Chem Eng Commun 199:720-736.

Co-author:

6) Engel P, Mladenov R, Wulfhorst H, Jäger G, Spiess AC. 2010. Point by point analysis: how ionic liquid affects the enzymatic hydrolysis of native and modified cellulose. Green Chem 12(11):1959-1966.

7) Huber R, Wulfhorst H, Maksym L, Stehr R, Pöhnlein M, Jäger G, Spiess AC, Büchs J. 2011. Screening for enzyme activity in turbid suspensions with scattered light. Biotechnol Progr 27:555-561.

8) Klement T, Milker S, Jäger G, Grande PM, Domínguez de María P, Büchs J. 2012. Biomass pretreatment affects *Ustilago maydis* in producing itaconic acid. Microb Cell Fact 11:43[#].

[#] Last numbers indicate article numbers and no page numbers.

* Authors contributed equally to the respective publication.

Abstract

Naturally occurring cellulose can be used as a renewable resource for the sustainable production of platform chemicals such as itaconic acid. The biocatalytic conversion of cellulose is a very promising approach due to its high selectivity, mild conditions, and low exergy loss. However, such biocatalytic processes are still seldom applied at the industrial scale since the single conversion steps (pretreatment, hydrolysis, and fermentation) exhibit low efficiencies or high costs. To allow a knowledge-based optimization, each step was analyzed in detail within this thesis. Thereby, new (integrated) approaches and screening technologies were also established.

To pretreat cellulose in an environmentally friendly manner, the non-hydrolyzing protein swollenin was applied. A new and efficient method to produce recombinant swollenin was established by using the robust yeast *Kluyveromyces lactis*. During the pretreatment of different cellulosic substrates, swollenin induced deagglomeration and decrystallization of cellulose. As a result, swollenin caused a significant decrease in particle size as well as in crystallinity of the cellulosic substrates, thereby substantially increasing their accessibility. Moreover, pretreatment with swollenin – even in non-saturating concentrations – significantly accelerated the subsequent cellulose hydrolysis. A correlation for hydrolysis rates based on particle size and crystallinity illustrated the hydrolysis-accelerating effect of swollenin. For the first time, it was quantified and elucidated in detail how swollenin affects relevant physical properties of cellulosic substrates and how it improves their subsequent hydrolysis.

The efficiency of cellulose hydrolysis also depends on selecting optimal cellulases and hydrolysis conditions. To screen for these optimal parameters, practical cellulosic substrates and sophisticated cellulase assays are essential. Within this thesis, insoluble α-cellulose was found to be an excellent practical substrate to screen and characterize cellulase adsorption and activity. At first, a reproducible purification method was established to prepare the major cellulases from *Trichoderma reesei* with high purity. The adsorption isotherms and kinetics of these cellulases were modeled and analyzed in detail by using α-cellulose. The activities of all purified cellulases were determined, and a semi-mechanistic model was developed to precisely predict the kinetics of cellulose hydrolysis. Moreover, optimal hydrolysis conditions (pH, temperature, and hydrodynamics) were identified. Here, it was shown for the first time how different hydrodynamic conditions affect cellulase adsorption as well as the correlation

between the adsorption and the activity of cellulases. In particular, the complete suspension of cellulose particles was ensured in order to optimize cellulase adsorption and activity.

Up to now, most cellulase assays are slow, tedious, or based on artificial soluble substrates that do not reflect real insoluble cellulose. Here, the first sophisticated cellulase assay was developed which simultaneously combines high-throughput, online analysis, and insoluble cellulose in one simple system. This assay is based on the BioLector, which monitors the scattered light intensities of cellulose suspensions in a continuously shaken microtiter plate. By using the BioLector, cellulase activities towards different insoluble cellulosic substrates were quantified. At low cellulase/cellulose ratios, the determined Michaelis-Menten parameters were mainly affected by cellulose crystallinity; at high ratios, the cellulose particle size was the key determining factor. Moreover, cellulase adsorption and the non-hydrolytic deagglomeration of cellulose were studied using the BioLector. In conclusion, the developed assay will considerably simplify and accelerate fundamental research on cellulase screening.

As yet, itaconic acid has solely been produced by separate fermentations necessitating directly fermentable carbon sources such as glucose. Here, the first integrated process was presented to directly convert cellulose to itaconic acid via simultaneous saccharification and fermentation (SSF). In just one SSF step, α-cellulose was hydrolyzed by cellulases, and the released glucose was simultaneously converted to itaconic acid by the fungus *Ustilago maydis*. It was shown that the enzymatic cellulose hydrolysis can be performed under SSF conditions. Moreover, an inhibitory effect of itaconic acid on the cellulases could be disproved. The SSF was comprehensively analyzed and compared with an ordinary batch fermentation using glucose as sole carbon source. During SSF, the cellulose was almost completely hydrolyzed, and the itaconic acid yield was comparable to that of the batch fermentation.

Within this thesis, a detailed understanding of the biocatalytic conversion of cellulose to itaconic acid was generated. Not only all essential conversion steps were investigated in detail, but also novel (integrated) approaches as well as technologies were developed. In the future, the conversion steps need to be further harmonized, and (*in-situ*) product recovery should be implemented, as well as the recycling of water, cellulases, microorganisms, and unconverted cellulose. Moreover, cellulases and microorganisms need to be improved and adapted to integrated process configuration such as SSF. In conclusion, the results presented within this thesis are the fundamental basis for a further knowledge-based improvement and pave the way for an economically feasible production process converting cellulose to itaconic acid.

Kurzfassung

Biokatalytische Umwandlung von Cellulose zu Itaconsäure

Cellulose ist ein natürlicher, nachwachsender Rohstoff, der für die nachhaltige Produktion von Plattformchemikalien (z.B. Itaconsäure) verwendet werden kann. Die biokatalytische Umwandlung von Cellulose stellt dabei eine äußerst vielversprechende Prozessvariante dar, die sowohl hohe Selektivität, niedrige Exergieverluste als auch milde Reaktionsbedingungen vereinigt. Solche biokatalytischen Prozesse werden allerdings selten industriell umgesetzt, da die einzelnen Umwandlungschritte (Vorbehandlung, Hydrolyse, Fermentation) eine geringe Effizienz oder hohe Kosten aufweisen. Um diese Umwandlungschritte gezielt optimieren zu können, wurde im Rahmen der vorliegenden Arbeit jeder dieser drei Schritte ausführlich untersucht. Des Weiteren wurden dabei neue (integrierte) Verfahren und Screeningtechnologien entwickelt.

Um die Cellulose vorzubehandeln, wurde das nicht-hydrolytische Protein Swollenin eingesetzt. Das dafür benötigte Swollenin konnte mit Hilfe der Hefe *Kluyveromyces lactis* in einem neuen und effizienten Expressionsverfahren rekombinant hergestellt werden. Während der Vorbehandlung von verschiedenen cellulosehaltigen Substraten induzierte Swollenin eine Deagglomeration und Dekristallisation der Cellulose. Hierbei konnte sowohl eine signifikante Reduktion der Partikelgröße und der Kristallinität als auch eine deutliche Steigerung der Cellulosezugänglichkeit nachgewiesen werden. Außerdem führte die Vorbehandlung mit Swollenin zu einer signifikanten Beschleunigung der anschließenden enzymatischen Cellulosehydrolyse. Die gesteigerten Hydrolyseraten konnten eindeutig auf die von Swollenin induzierten Effekte zurückgeführt werden, indem die Hydrolyseraten mit der Partikelgröße und der Kristallinität von Cellulose korreliert wurden. Folglich wurde somit zum ersten Mal quantitativ nachgewiesen, wie Swollenin die physikalischen Eigenschaften von Cellulose beeinflusst und deren nachfolgende Hydrolyse steigert.

Die Effizienz der enzymatischen Cellulosehydrolyse hängt des Weiteren maßgeblich von der Wahl geeigneter Cellulasen und geeigneter Hydrolysebedingungen ab. Um diese zu ermitteln, müssen sowohl praxisnahe cellulosehaltige Substrate als auch fortschrittliche Analyseverfahren eingesetzt werden. Innerhalb dieser Arbeit konnte α-Cellulose als hervorragendes praxisnahes Substrat identifiziert werden, um die Adsorption und die Aktivität von gereinigten Cellulasen zu untersuchen. Um zunächst gereinigte Cellulasen zu

erhalten, wurde eine neue und reproduzierbare Reinigungsmethode entwickelt. Mit Hilfe dieser Methode konnten verschiedene Cellulasen (Cellobiohydrolasen und Endoglucanasen) von *Trichoderma reesei* isoliert werden. Anschließend wurden die Adsorptionsisothermen und Adsorptionskinetiken dieser Cellulasen modelliert und ausführlich analysiert. Die Aktivitäten der Cellulasen wurden ebenfalls bestimmt. Basierend auf diesen Versuchen konnte ein semi-mechanistisches Modell entwickelt werden, um die Kinetik der Cellulosehydrolyse präzise vorauszusagen. Des Weiteren wurden die optimalen Bedingungen (pH-Wert, Temperatur, Hydrodynamik) für die Hydrolyse von α-Cellulose ermittelt. Dabei konnte zum ersten Mal gezeigt werden, wie verschiedene hydrodynamische Zustände sowohl die Cellulaseadsorption als auch die Korrelation von Adsorption und Aktivität beeinflussen. Die vollständige Suspension der Cellulosepartikel musste insbesondere gewährleistet werden, um eine optimale Cellulaseadsorption und -aktivität zu erzielen.

Die meisten derzeit angewandten Analyseverfahren für Cellulasen sind langwierig, arbeitsaufwendig oder basieren auf artifiziellen wasserlöslichen Substraten, die die reale unlösliche Cellulose nicht korrekt abbilden können. Im Rahmen dieser Arbeit wurde jedoch das erste Analyseverfahren für Cellulasen entwickelt, welches Hochdurchsatzscreening, Online-Analytik und den Einsatz unlöslicher Cellulose in einem einfach zu bedienenden System vereinigt. Dieses Verfahren basiert auf dem BioLector, mit dem die Streulichtintensität von Cellulosesuspensionen in einer kontinuierlich geschüttelten Mikrotiterplatte gemessen werden kann. Mit Hilfe des BioLectors konnten Cellulaseaktivitäten gegenüber verschiedenen unlöslichen Cellulosevarianten quantifiziert werden. Entsprechend des verwendeten Cellulase/Cellulose-Verhältnisses, waren die Cellulaseaktivitäten und abgeleiteten Michaelis-Menten-Parameter entweder durch die Kristallinität oder die Partikelgröße der Cellulose limitiert. Des Weiteren konnten die Cellulaseadsorption und die nicht-hydrolytische Deagglomeration von Cellulose im BioLector untersucht werden. Schließlich weist das entwickelte Analyseverfahren das Potential auf, um die Charakterisierung und das Screening von Cellulasen deutlich zu vereinfachen und zu beschleunigen.

Itaconsäure wurde bisher lediglich mit konventionellen Fermentationen hergestellt, die auf direkt fermentierbaren Kohlenstoffquellen wie Glucose basieren. Im Rahmen dieser Arbeit wurde jedoch der erste integrierte Prozess entwickelt (SSF, „simultaneous saccharification and fermentation"), mit dem Cellulose direkt zu Itaconsäure umgewandelt werden kann. Während dieses SSF-Prozesses wurde die Cellulose durch Cellulasen hydrolysiert und die

resultierende Glucose simultan von dem Pilz *Ustilago maydis* zu Itaconsäure umgewandelt. Hierbei wurde nachgewiesen, dass die enzymatische Cellulosehydrolyse auch unter den Bedingungen eines SSF durchgeführt werden kann und die Cellulasen durch das Produkt Itaconsäure nicht inhibiert werden. Der SSF-Versuch wurde umfassend analysiert und mit einer konventionellen Batch-Fermentation auf Basis von Glucose verglichen. Während des SSF wurde die Cellulose fast vollständig hydrolysiert und eine mit der konventionellen Fermentation vergleichbare Itaconsäureausbeute erreicht.

Im Rahmen dieser Dissertation wurde ein grundlegendes Verständnis für die biokatalytische Umwandlung von Cellulose zu Itaconsäure generiert. Dabei wurden nicht nur alle essentiellen Umwandlungsschritte detailliert untersucht, sondern auch innovative (integrierte) Verfahren und Technologien entwickelt. In zukünftigen Arbeiten müssen die Umwandlungsschritte weiter aufeinander abgestimmt und die (*in-situ*) Reinigung der Itaconsäure als finaler Prozessschritt implementiert werden. Das Recycling von Wasser, Cellulasen, Mikroorganismen und restlicher Cellulose sollte ebenfalls ein Schwerpunkt zukünftiger Forschung sein. Um die Ausbeute und Produktivität des gesamten Prozesses zu erhöhen, müssen die Biokatalysatoren optimiert und an die Bedingungen von integrierten Prozessschritten (z.B. SSF) angepasst werden. Das im Rahmen dieser Arbeit generierte Verständnis bildet schließlich die Grundlage, um weitere Verbesserung zu erzielen und einen ökonomischen Prozess zur Umwandlung von Cellulose zu Plattformchemikalien zu etablieren.

Contents

Nomenclature

Abbreviations

a.u.	arbitrary units
AGU	anhydroglucose units
BCA	bicinchoninic acid
BSA	bovine serum albumin
CBH	cellobiohydrolase
CBP	consolidated bioprocessing
CMC	carboxymethyl cellulose
DNS	dinitrosalicylic acid
DoE	U.S. Department of Energy
DSMZ	German collection of microorganisms and cell cultures
EC	enzyme commission number
EG	endoglucanase
FITC	fluorescein isothiocyanate
FPU	filter paper units
HMF	5-hydroxymethylfurfural
HPLC	high-performance liquid chromatography
IA	itaconic acid
mAU	milli-absorbance units
MBP	maltose-binding protein
MTHF	methyltetrahydrofuran
NBT/BCIP	nitro blue tetrazolium / 5-bromo-4-chloro-3-indolyl phosphate
PAHBAH	*p*-hydroxybenzoic acid hydrazide

PBST   phosphate buffered saline containing Tween-20

rpm   rounds per minute

RAMOS   respiration activity monitoring system

SDS   sodium dodecyl sulfate

SHF   separate hydrolysis and fermentation

SHCF   separate hydrolysis and co-fermentation

SSF   simultaneous saccharification and fermentation

SSCF   simultaneous saccharification and co-fermentation

TMFB   tailor-made fuels from biomass

XRD   X-ray diffraction

YPGal   medium containing yeast extract, peptone and galactose

Roman Symbols

a   non-linear Gaussian cumulative function parameter   [-]

A   adsorbed protein $[\mu mol_{protein}/g_{cellulose}]$*

A_{EQ} adsorbed protein at equilibrium $[\mu mol_{protein}/g_{cellulose}]$*

A_{max} maximum protein adsorption $[\mu mol_{protein}/g_{cellulose}]$*

A_{pre} pre-exponential factor   [1/s]

b   non-linear Gaussian cumulative function parameter   [-]

c   non-linear Gaussian cumulative function parameter   [-]

C   cellulose concentration   [g/L]

C_0 initial cellulose concentration   [g/L]

CrI   crystallinity index   [%]

d   non-linear Gaussian cumulative function parameter   [-]

d_0 shaking diameter   [mm]

d_P	geometric mean particle size	[µm]
DP	degree of polymerization	[AGU]
DP_w	weight-average apparent degree of polymerization	[AGU]
D_t	inner tube diameter	[mm]
e	non-linear Gaussian cumulative function parameter	[-]
E	free protein concentration	[µmol$_{protein}$/L]*
E_0	initial protein concentration	[µmol$_{protein}$/L]*
E_{ad}	adsorbed protein concentration	[µmol$_{protein}$/L]*
$E_{ad,EQ}$	adsorbed protein concentration at equilibrium	[µmol$_{protein}$/L]*
E_A	activation energy	[kJ/mol]
f	non-linear Gaussian cumulative function parameter	[-]
g	non-linear Gaussian cumulative function parameter	[-]
I_{002}	maximum intensity of crystalline plane reflection	[1/s]
I_{AM}	XRD scattering at 18° (amorphous) in cellulose-I	[1/s]
k_{ad}	pseudo-first-order adsorption rate constant	[1/s]
$k_{cat,app}$	apparent turnover number	[1/s]
K_a	acid dissociation constant	[mol/L]
K_A	association constant	[L/µmol$_{protein}$]*
K_D	dissociation constant	[µmol$_{protein}$/L]*
K_i	inhibition constant	[g/L]
$K_{M,app}$	apparent Michaelis constant	[g/L]
n	shaking frequency	[rpm]
n_{crit}	critical shaking frequency for liquid mixing	[rpm]
OTR	oxygen transfer rate	[mmol/(L·h)]
p	probability for significant scores (protein matching)	[-]

pK_a	negative logarithm of acid dissociation constant	[-]
P	reducing sugar concentration	[g/L]
$P_{glucose}$	glucose concentration	[g/L]
R	ideal gas constant	[J/(mol·K)]
R^2	coefficient of determination	[-]
T	temperature	[°C] or [K]
t	time	[s]
V	cellulase activity	[g/(L·h)]
V_L	total filling volume	[mL]
$V_{max,app}$	apparent maximum cellulase activity	[g/(L·h)]
$V_{pH,optimal}$	cellulase activity at optimal pH value	[g/(L·h)]
$Y_{P/S}$	product yield of itaconic acid	[$g_{IA}/g_{glucose}$] or [$g_{IA}/g_{cellulose}$]

* Instead of molar amounts, mass units can be applied. The correlation is based on the molecular masses of the respective proteins.

Greek Symbols

θ	diffraction angle	[°]
λ	wavelength	[Å] or [nm]
ρ_L	liquid density	[kg/L]
σ	surface tension	[N/m]

List of Figures

List of Tables

1   Introduction

1.1   Lignocellulose: Production Rates and Structure

Plants use solar energy to convert carbon dioxide and water into carbohydrate building blocks $(CH_2O)_n$ and oxygen (Huber et al., 2006; Kaltschmitt et al., 2009). This process – known as photosynthesis – allows the (photo-)autotrophic growth of plants. The production rates of dry plant biomass are about 150 billion tons/year (Eisenbeiß and Wagner, 2006; Graziani and Fornasiero, 2006; Zhang et al., 2006), and the world's plant biomass is about 2000 billion tons (Graziani and Fornasiero, 2006). Since lignocellulose is the main component of dry plant biomass, it is the most abundant and renewable organic resource on earth (Bhat and Bhat, 1997; Zhang and Lynd, 2004). Lignocellulose can be found within plant cell walls and generally consists of cellulose, hemicellulose, and lignin (Lynd et al., 2002). Although the composition of lignocellulose strongly depends on the type and origin of the particular plant biomass, the average proportions are as follows (Jorgensen et al., 2007; Kumar et al., 2009; Lynd et al., 2002): 35-50% (w/w) cellulose, 20-35% (w/w) hemicellulose, and 5-30% (w/w) lignin.

Cellulose – the main component of lignocellulose – is a linear polymer or chain of D-anhydroglucose molecules linked together by β-1,4-glycosidic bonds (Figure 1-1A). The D-anhydroglucose $(C_6H_{10}O_5)$ molecules result from condensation reactions of D-glucose $(C_6H_{12}O_6)$. Each cellulose chain has a reducing end and a non-reducing end (Figure 1-1A) (Klemm et al., 2005). At the reducing end, the terminal hemiacetal is in equilibrium with the open-ring form, thereby revealing the reducing aldehyde group (Klemm et al., 2005). At the non-reducing end, the ring opening is prevented, since the C1-OH group in the hemiacetal is involved in the β-1,4-glycosidic bond (Mosier et al., 1999). Since adjacent D-anhydroglucose molecules are rotated by 180° to their neighbors (Zhang and Lynd, 2004), anhydrocellobiose is the structural repeating unit of cellulose (Figure 1-1A). As a consequence of this rotation, each side of the cellulose chain has the same number of hydroxyl groups, thereby leading to a symmetrical and linear structure (Zhang and Lynd, 2004). Based on this structure, hydrogen bonds and van der Waal's forces can be formed between individual cellulose chains (Zhang and Lynd, 2004). Around 30 parallel cellulose chains are assembled into larger units called

elementary fibrils or protofibrils (Figure 1-1B) (Lynd et al., 2002). These elementary fibrils are further arranged into microfibrils (Figure 1-1C) (Lynd et al., 2002; Somerville et al., 2004). Here, the parallel alignment and the extensive number of intra- and intermolecular hydrogen bonds lead to a highly organized and crystalline structure (Mansfield et al., 1999; Zhang and Lynd, 2004). Within this structure, the cellulose is tightly packed, and the penetration of enzymes or even smaller molecules (such as water) is prevented (Lynd et al., 2002). In most cases, however, cellulose does not occur in a completely crystalline form. Thus, microfibrils consist of crystalline and amorphous regions (Figure 1-1C) (Lynd et al., 2002; Mansfield et al., 1999). Moreover, cellulose microfibrils are further arranged into macrofibrils (fibers) (Figure 1-1D) (Lynd et al., 2002). To stabilize this final supramolecular structure, the smaller microfibrils are embedded in a matrix of hemicellulose and lignin (Bidlack et al., 1992; Ganan et al., 2008; Lynd et al., 2002; Mansfield et al., 1999; Somerville et al., 2004).
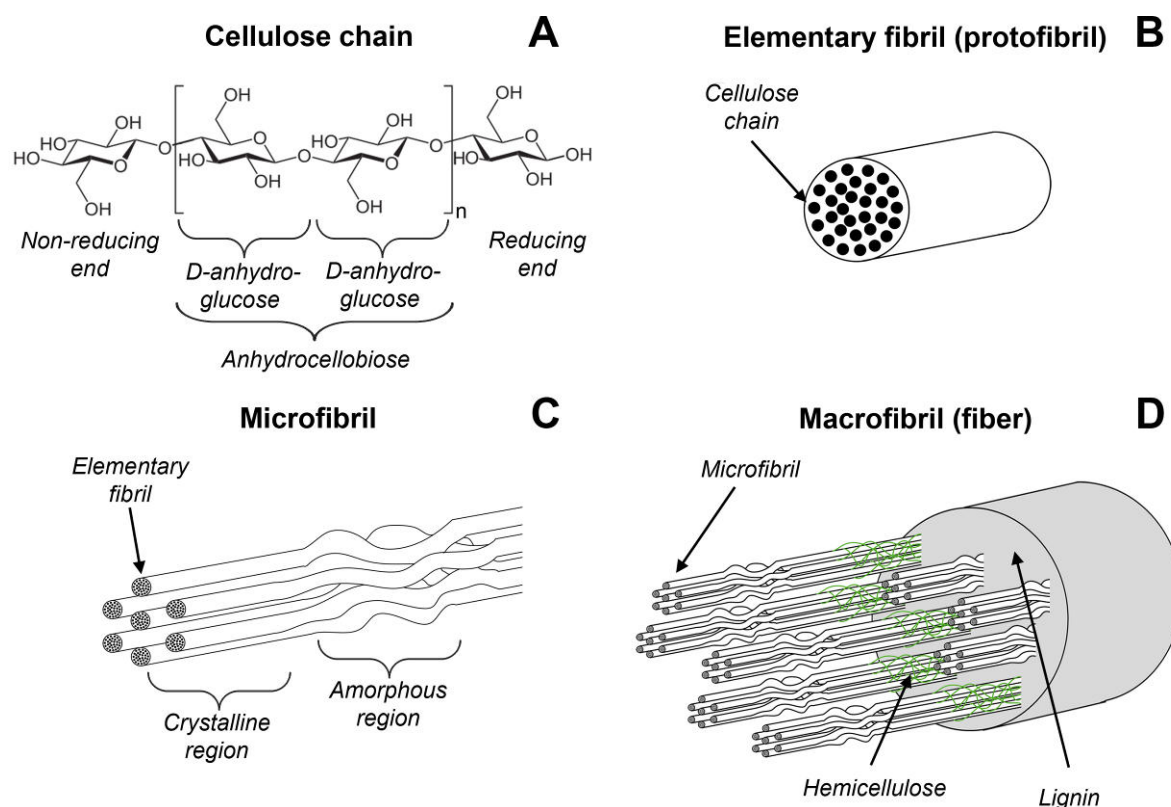
Figure 1-1:   Structure of cellulose and its association with hemicellulose and lignin (lignocellulose). Structural classifications (**A**, **B**, **C**, **D**) are described in Chapter 1.1.

Hemicellulose is an amorphous polysaccharide consisting of pentoses (usually xylose and arabinose) and hexoses (usually galactose, glucose, and mannose) (Hamelinck et al., 2005; Huber et al., 2006; Mosier et al., 2005; Shallom and Shoham, 2003; van Zyl et al., 2007). It

forms hydrogen bonds with cellulose and surrounds the individual microfibrils (Figure 1-1D) (Bidlack et al., 1992; Mosier et al., 2005; Shallom and Shoham, 2003; Somerville et al., 2004). By contrast, lignin is a highly branched polyaromatic compound consisting mainly of paracoumaryl, coniferyl, and sinapyl alcohols (Huber et al., 2006). It covalently bonds to hemicellulose and, thereby, connects the individual complexes, made of microfibrils and hemicellulose, with each other (Figure 1-1D) (Bidlack et al., 1992; Lynd et al., 2002; Shallom and Shoham, 2003; Zhang and Lynd, 2004). Finally, the tight packing of cellulose and its association with hemicellulose and lignin lead to the mechanical stability of lignocellulose (and plant cells) and hinder its degradation via chemicals, enzymes, or plant pathogens (Bidlack et al., 1992; Bresinsky et al., 2008; Weiler and Nover, 2008).

To describe the structure of (ligno-)cellulose, several physical properties have been defined. Aside from the amount of hemicellulose and lignin, these properties, in particular, are (Lynd et al., 2002; Zhang and Lynd, 2004; Zhang et al., 2006): degree of polymerization (*DP*), accessibility, and crystallinity. The degree of polymerization describes the average length of the cellulose chains and is given by the number of repeating D-anhydroglucose units (AGU) (Zhang and Lynd, 2004). Accessibility reflects the total surface area available for direct physical contact between cellulose and other substances. It is generally determined by cellulose particle size (external surface area) and the porosity of cellulose (internal surface area) (Chandra et al., 2007; Chandra et al., 2008). Furthermore, crystallinity is a relevant physical property describing the percentage of crystalline regions. Here, it should be noted that crystallinity may also affect cellulose accessibility (Arantes and Saddler, 2011; Chandra et al., 2007; Park et al., 2010). Up to now, however, their relationship has not been clearly elucidated (Chandra et al., 2007; Ramos et al., 1993).

1.2 Platform Chemicals from Lignocellulose

Because of its high availability and sustainability (Chapter 1.1), lignocellulose is a promising resource for the sustainable production of platform chemicals (Himmel et al., 1999; Himmel et al., 2007; Himmel and Bayer, 2009; Huber et al., 2006; Kaltschmitt et al., 2009; Lynd et al., 1999; Marquardt et al., 2010; Peralta-Yahya and Keasling, 2010). These platform chemicals can be converted to valuable products such as fine chemicals, polymers, or fuels (Werpy and Petersen, 2004). In 2004, the U.S. Department of Energy (DoE) published a study about the

top value-added platform chemicals from starch, cellulose, and hemicellulose – lignin was not initially included (Werpy and Petersen, 2004). Starting from a list of more than 300 platform chemicals, the DoE screened for those candidates meeting the following criteria: (1) economical production from starch, cellulose, or hemicellulose via biological or chemical reaction steps, and (2) large potential for further conversion to valuable products. By using an iterative review process based on raw material costs, processing costs, complexity of processing pathways, selling prices, market potentials, chemical functionalities, and potential uses, the top twelve value-added platform chemicals were finally chosen (Table 1-1). Moreover, it should be noted that the DoE published an additional study about the potential chemicals from lignin (Bozell et al., 2007). However, these chemicals are not addressed within this section, since there is no consensus regarding the use of lignin at industrial scale (burning or conversion) (Bozell et al., 2007).

Table 1-1:   Top twelve value-added platform chemicals from starch, cellulose, and hemicellulose.

Number of carbon atoms [-]	Platform chemicals[a]
3	glycerol, 3-hydroxy propionic acid
4	aspartic acid, 1,4-dicarboxylic acids[b,c], 3-hydroxybutyrolactone
5	glutamic acid, itaconic acid, levulinic acid, xylitol/arabinitol[c]
6	glucaric acid, sorbitol, 2,5-furan dicarboxylic acid

[a] According to Werpy and Petersen (2004).

[b] This term includes succinic acid, malic acid, and fumaric acid.

[c] These molecules have been grouped because of the potential synergy related to their structures.

As shown in Table 1-1, platform chemicals with three to six carbon atoms were selected. This can be explained by the sugar focus of the DoE study, thereby limiting the opportunities for value-added chemicals with more than six carbon atoms (Werpy and Petersen, 2004). Moreover, platform chemicals with multiple functional groups were chosen, since these substances have a much larger potential for further conversion into useful derivatives than substances with one functional group (Werpy and Petersen, 2004). Consequently, compounds with two carbon atoms, such as acetic acid or ethanol, were not considered because of their low chemical functionality. According to Table 1-1, some platform chemicals have been grouped together because of the potential synergy related to their structures. These candidate groups are xylitol/arbinitol and the 1,4-dicarboxylic acids (succinic acid, malic acid, and

fumaric acid). For each of the twelve platform chemicals, different pathways for further conversion and a number of potential derivates can be found in the DoE study (Werpy and Petersen, 2004).

In particular, a promising platform chemical is itaconic acid (methylene butanedioic acid) – a white crystalline unsaturated dicarboxylic acid (Figure 1-2) (Willke and Vorlop, 2001). Because of its high number of functional groups (methylene, carboxyl, and hydroxyl groups), a significant market opportunity for the production of established or novel products from itaconic acid exists (Werpy and Petersen, 2004). For example, itaconic acid can be applied as an additional monomer in styrene-butadiene heteropolymers (synthetic rubber) which are used in detergents and emulsion paints as well as in the fiber, pharmaceutical, and herbicide industries (Bressler and Braun, 2000; Werpy and Petersen, 2004). Furthermore, itaconic acid can be transformed to the potential biofuel 3-methyltetrahydrofuran (3-MTHF) (Geilen et al., 2010; Marquardt et al., 2010).
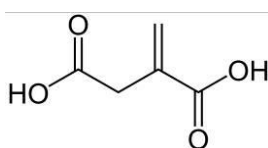
Figure 1-2:   Structural formula of itaconic acid ($C_5H_6O_4$).

Although the DoE included starch as a possible resource for the production of platform chemicals (Werpy and Petersen, 2004), it should be noted that the use of starch (as well as sucrose) comprises serious disadvantages (Palatinus et al., 2007; Pfennig, 2007; Somerville et al., 2010): (1) depletion of edible resources (competition with the food chain), and (2) conversion of only a small fraction of the plant material (in particular for wheat or corn). In the future, lignocellulose should be used as an alternative resource for the production of platform chemicals. Thereby, no interference with the food chain occurs, and the entire plant can be used (Palatinus et al., 2007; Pfennig, 2007; Somerville et al., 2010).

1.3   Non-selective / Selective Conversion of Lignocellulose

In order to convert lignocellulose to platform chemicals, two different approaches can be performed (Huber et al., 2006; Marquardt et al., 2010): (1) non-selective conversion or (2) selective conversion (Figure 1-3).

In the case of the non-selective conversion, the highly functionalized lignocellulose is completely degraded by gasification into C1 building blocks such as CO and CH_4 (Figure 1-3) (Huber et al., 2006; Huber and Dumesic, 2006; Marquardt et al., 2010). Afterwards, these building blocks are reassembled into the desired platform chemicals by, for example, Fischer-Tropsch synthesis. This non-selective approach can process different kinds of biomass simultaneously (such as lignocellulose, oil, and starch) (Marquardt et al., 2010). However, it requires capital-intensive large-scale plants and high-temperature treatments (greater than 500 °C). Moreover, it annihilates nature's synthesis power and, therefore, leads to high losses of exergy which has been initially stored within the biomass (Marquardt et al., 2010).
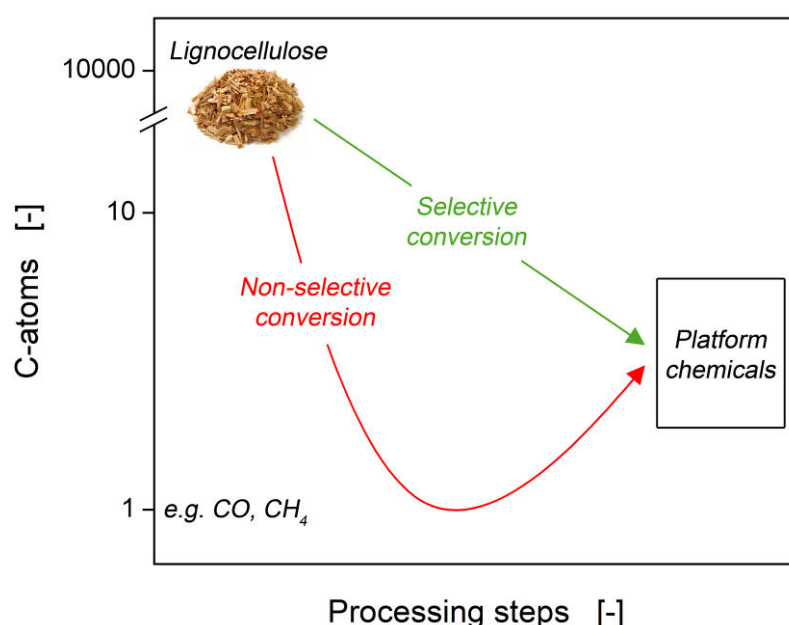
Figure 1-3:   Approaches for the non-selective and selective conversion of lignocellulose to platform chemicals.

For the selective approach, lignocellulose is selectively depolymerized to its monomers without significant degradation (Figure 1-3). Afterwards, the resulting monomers are refunctionalized into the desired platform chemicals. In contrast to the conventional non-selective approach, conversion reactions are performed under mild conditions, and nature's synthesis power is preserved to a maximum extent (Huber et al., 2006; Marquardt et al., 2010). Therefore, the selective approach offers the chance to establish processes with higher carbon efficiency and lower exergy loss. Since highly selective catalysts need to be applied during such processes, only one type of biomass can be converted at one time (Huber et al., 2006). Up to now, different types of catalysts have been applied for the selective conversion

(depolymerization and refunctionalization) of lignocellulose: chemocatalysts (Michels and Wagemann, 2010; Rinaldi et al., 2008; vom Stein et al., 2010; vom Stein et al., 2011), enzymes (Himmel et al., 2007; Zhang and Lynd, 2004), microorganisms (Stephanopoulos, 2007), or combinations of these (Rinaldi et al., 2010; Yanase et al., 2010). However, this work focuses on the selective and biocatalytic conversion of lignocellulose by using enzymes and microorganisms.

1.4 Biocatalytic Conversion of Lignocellulose

In general, the biocatalytic conversion of lignocellulose to valuable products, such as platform chemicals, consists of four major processing steps (Huber et al., 2006; Mosier et al., 2005; Wyman, 2004): pretreatment, hydrolysis, fermentation, and product recovery (Figure 1-4).
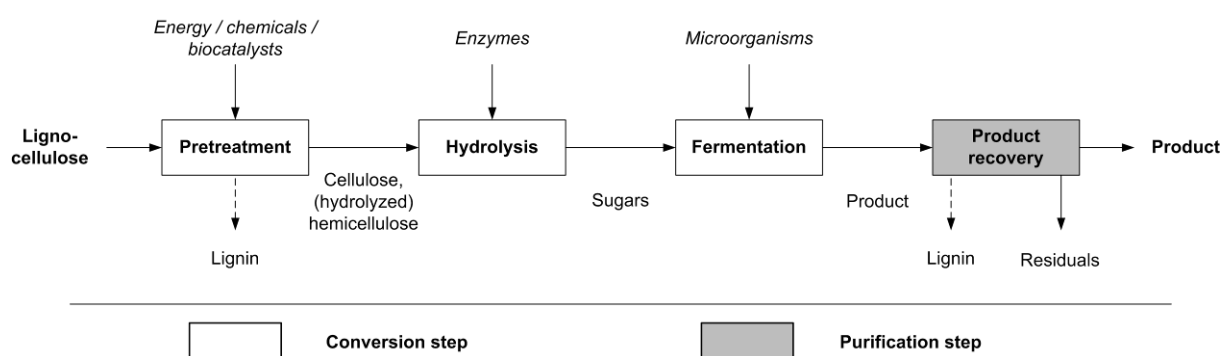
Figure 1-4:   Scheme of the selective and biocatalytic conversion of lignocellulose.

Pretreatment is required to open up the recalcitrant structure of lignocellulose (Chapter 1.1). Hence, the carbohydrate fractions (cellulose and hemicellulose) are more accessible, and their subsequent hydrolysis to monomeric sugars can be achieved more rapidly and with greater yields (Hamelinck et al., 2005; Mosier et al., 2005). Depending on the applied pretreatment technique and its driving force/catalyst (energy, chemicals, or biocatalysts), hemicellulose is already hydrolyzed, and lignin can be removed (Figure 1-4) (Hamelinck et al., 2005; Mosier et al., 2005; Olofsson et al., 2008).

After pretreatment, hydrolysis is the processing step that converts the carbohydrate fractions (cellulose and non-hydrolyzed hemicellulose) into their monomeric sugars (Figure 1-4). According to the composition of cellulose and hemicellulose (Chapter 1.1), hexoses (such as

glucose, galactose, and mannose) and pentoses (such as xylose and arabinose) result from hydrolysis. In general, the hydrolysis reaction can be catalyzed by enzymes or acids such as sulfuric acid (Huber et al., 2006). In the case of enzymatic hydrolysis, cellulose and hemicellulose are hydrolyzed by cellulases and hemicellulases, respectively (Lynd et al., 2002; Mosier et al., 2005; Zhang and Lynd, 2004). When performing the chemical hydrolysis of cellulose, undesired by-products including 5-hydroxymethylfurfural (HMF) and levulinic acid result from acid-catalyzed sugar degradation, which in turn can lead to glucose yields less than 70% (Huber et al., 2006). By contrast, the enzymatic hydrolysis can produce glucose yields above 95% and is, thus, often superior to the sole chemical hydrolysis (Huber et al., 2006).

After hydrolysis, the resulting sugars are fermented to the desired product (Figure 1-4). Because the cost-effectiveness of a lignocellulose-based process depends critically on the yield of sugar conversion to the final product (Stephanopoulos, 2007), all sugars (both hexoses and pentoses) need to be converted (Lynd et al., 2002; Mosier et al., 2005). For example, *Aspergillus terreus* or *Ustilago maydis* utilize both hexoses and pentoses (Kautola et al., 1985; Kurz and Ericson, 1962; Matsushima and Klug, 1958), and they are able to produce itaconic acid (Guevarra and Tabuchi, 1990; Kautola et al., 1985; Kobayashi, 1978; Willke and Vorlop, 2001). In addition, the applied microorganism must tolerate potentially inhibitory compounds generated during pretreatment (Lynd et al., 2002). Such compounds arise from the release of additional substances present in plant biomass (e.g. organic acids and extractives), degradation of carbohydrates to undesired by-products (e.g. furfurals), or corrosion leading to the release of inorganic ions (Lynd et al., 2002). Here, the actual amount of generated inhibitors depends greatly on the type of plant biomass and the pretreatment conditions.

Whereas molecular structures were changed during pretreatment, hydrolysis, and fermentation (conversion steps), the last processing step aims to recover the final product from the fermentation broth (Figure 1-4). Depending on the product and the impurities of the fermentation broth, one of the following unit operations can be generally applied (Chmiel et al., 2011): adsorption, chromatography, distillation, extraction, membrane separation, precipitation/crystallization, or combinations of these. For example, itaconic acid can be purified via extraction, crystallization, or membrane separation (electrodialysis) (Wasewar et al., 2011; Willke and Vorlop, 2001). Residuals – such as enzymes, microorganisms, non-

hydrolyzed cellulose, and non-hydrolyzed hemicellulose – end up during product recovery (Figure 1-4) (Mosier et al., 2005). Moreover, lignin is an additional residual accumulating during product recovery or pretreatment (Huber et al., 2006). If the energy demand for drying these residuals is relatively low, they can be burned to power the process (Mosier et al., 2005). Alternatively, some of these residuals can be converted to valuable co-products (Bozell et al., 2007; Mosier et al., 2005). In the case of lignin, no efficient biocatalytic conversion has been developed so far (Marquardt et al., 2010). However, several researches have screened and characterized first enzymes capable of depolymerizing lignin (Arora et al., 2002; Dashtban et al., 2010; Ruiz-Duenas and Martinez, 2009). Although product recovery is an essential part for the biocatalytic conversion of lignocellulose, this work focuses on pretreatment, hydrolysis, and fermentation. In the following chapters, these conversion steps will be further discussed.

1.4.1   Pretreatment

As described in Chapter 1.4, the general task of pretreatment is to open up the recalcitrant structure of lignocellulose (Chapter 1.1) and to make cellulose as well as hemicellulose more accessible. Thus, enzymes can effectively penetrate into the carbohydrate network, and both carbohydrates are hydrolyzed more rapidly and with greater yields (Hamelinck et al., 2005; Mosier et al., 2005). In general, the optimal pretreatment technique should have the following effects (Alvira et al., 2010; Chandra et al., 2007; Chandra et al., 2008; Hamelinck et al., 2005; Kumar et al., 2009; Mosier et al., 2005): (1) disaggregation of cellulose, hemicellulose, and lignin, (2) prehydrolysis of hemicellulose, (3) removal of lignin, (4) increase in cellulose accessibility (total surface area) by decreasing cellulose particle size and increasing the porosity of cellulose, (5) reduction in cellulose crystallinity, and (6) reduction in the degree of polymerization. Moreover, pretreatment should meet the following requirements (Chandra et al., 2007; Kumar et al., 2009): (1) no degradation or loss of carbohydrates, (2) no formation of by-products that inhibit subsequent hydrolysis or fermentation, (3) low capital and operating costs, and (4) applicability on a wide range of lignocellulosic materials. Up to now, no pretreatment technique can provide all of the desired effects and meet all the aforementioned requirements. Nevertheless, all developed pretreatment techniques disaggregate lignocellulose and increase cellulose accessibility (Mosier et al., 2005). Moreover, most pretreatment techniques already hydrolyze hemicellulose (Hamelinck et al., 2005; Mosier et al., 2005; Olofsson et al., 2008).

Over time, different pretreatment techniques have been developed which can be classified as follows (Galbe and Zacchi, 2007; Kumar et al., 2009): physical (e.g. milling, grinding), physicochemical (e.g. steam explosion, ammonia fiber explosion), chemical (e.g. acid or alkaline hydrolysis, organic solvents, ionic liquids), biological, electrical methods, or combinations of these methods. Unfortunately, some of these techniques require expensive equipment, harsh conditions, and high energy input (Kumar et al., 2009). By contrast, in the recent years, non-hydrolyzing proteins have been investigated that pretreat cellulosic substrates under mild conditions (Arantes and Saddler, 2010; Hall et al., 2011). After the regular pretreatment of lignocellulose, these non-hydrolyzing proteins can be added during hydrolysis (Baker et al., 2000), or they can be utilized in a second pretreatment step in which cellulose is the substrate (Hall et al., 2011). Although, these non-hydrolyzing proteins offer a promising pretreatment due to the mild conditions and low energy input, there is no systematic and quantitative analysis of the effects of non-hydrolyzing proteins on cellulosic substrates and their subsequent hydrolysis.

1.4.2   Enzymatic Hydrolysis of Cellulose

As shown in Figure 1-4, the pretreatment of lignocellulose is generally followed by the hydrolysis of the pretreated carbohydrate fractions. Since most pretreatment techniques already hydrolyze hemicellulose (Hamelinck et al., 2005; Mosier et al., 2005; Olofsson et al., 2008), this section focuses on the enzymatic hydrolysis of cellulose – the main component of lignocellulose (Chapter 1.1).

1.4.2.1   Cellulases: Activities and Structure

The hydrolysis of cellulose to glucose necessitates three different types of enzymes known as cellulases (Himmel et al., 1999; Himmel et al., 2007; Lynd et al., 2002; Mielenz, 2001; Zhang and Lynd, 2004): endoglucanase (EG, EC 3.2.1.4), cellobiohydrolase (CBH, EC 3.2.1.91), and β-glucosidase (EC 3.2.1.21). As shown in Figure 1-5, endoglucanases hydrolyze cellulose chains at internal amorphous sites, generating oligo- or polysaccharides of various lengths and, therefore, new chain ends (Lynd et al., 2002). Cellobiohydrolases, also called exoglucanases, attack the ends of cellulose chains and act in a processive manner, thereby releasing cellobiose (Lynd et al., 2002). Here, CBH I and CBH II hydrolyze from the reducing and non-reducing ends, respectively. In contrast to EGs, CBHs can hydrolyze

amorphous as well as crystalline cellulose, presumably peeling cellulose chains from the crystalline structure (Himmel et al., 2007; Rouvinen et al., 1990; Teeri, 1997). Finally, β-glucosidases convert cellobiose to glucose (Lynd et al., 2002). This hydrolytic activity is especially important, since CBHs and EGs are severely inhibited by cellobiose (Du et al., 2010; Gruno et al., 2004; Holtzapple et al., 1990). Nevertheless, glucose is also a weak inhibitor for all cellulases and reduces the final yield of cellulose hydrolysis (Holtzapple et al., 1990; Olofsson et al., 2008; Wyman, 1994). In general, cellulase systems consisting of all three cellulase types show a higher collective activity than the sum of the individual activities (Henrissat et al., 1985; Nidetzky et al., 1994a). This synergism can be explained as follows (Gruno et al., 2004; Henrissat et al., 1985; Lynd et al., 2002; Teeri, 1997; Woodward, 1991): (1) endo-exo synergy, since EGs produce new cellulose chain ends for CBHs; (2) exo-exo synergy between CBH I and CBH II, since one chain can be attacked simultaneously from the reducing and non-reducing end; and (3) synergy between β-glucosidase and the other cellulases, since β-glucosidase removes the strong inhibitor cellobiose.
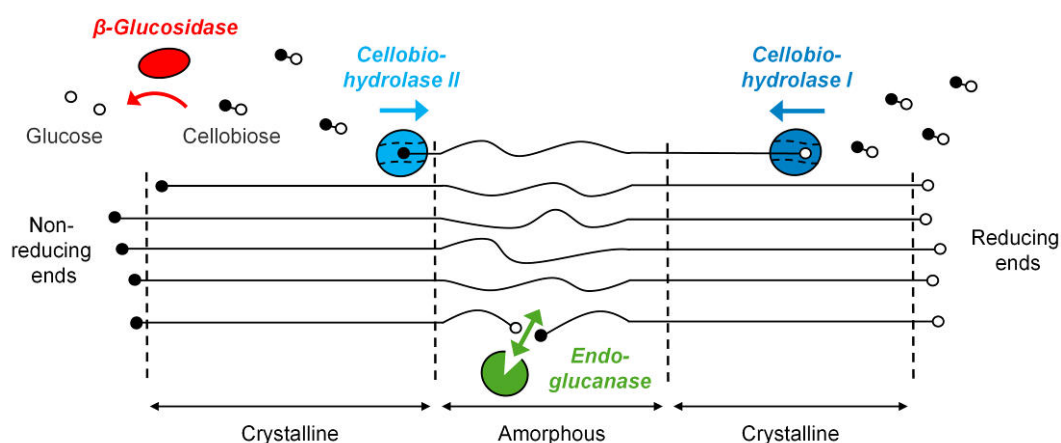
Figure 1-5:   Scheme of the enzymatic hydrolysis of cellulose.

Since CBHs and EGs hydrolyze insoluble cellulose, the adsorption of these cellulases onto cellulose is a prerequisite for hydrolysis (Lynd et al., 2002). Consequently, most CBHs and EGs have a common structure and consist of a cellulose-binding domain connected by a linker region to a catalytic domain (Himmel et al., 2007; Kubicek, 1992; Rouvinen et al., 1990). Whereas the cellulose-binding domain facilitates the efficient adsorption onto insoluble cellulose, the catalytic domain performs the hydrolysis of glycosidic bonds.

1.4.2.2   Limiting Factors for Cellulose Hydrolysis

In general, the hydrolysis of insoluble cellulose performed by CBHs and EGs is the rate-limiting step for the whole hydrolysis (Zhang et al., 2006). This enzymatic step is primarily hindered by the recalcitrant structure of cellulose and its physical properties (Chapter 1.1) (Desai and Converse, 1997; Kumar and Wyman, 2009c; Wang et al., 2006; Zhang et al., 1999). Thereby, the degree of polymerization, accessibility, and crystallinity – defined in Chapter 1.1 – are the main limiting factors (Alvira et al., 2010; Chandra et al., 2007; Hall et al., 2011; Mansfield et al., 1999). Among these, cellulose accessibility is the most important factor for hydrolysis (Arantes and Saddler, 2010; Arantes and Saddler, 2011; Chandra et al., 2007; Dasari and Berson, 2007; Mansfield et al., 1999; Yeh et al., 2010). It reflects the total surface area available for direct physical contact between cellulase and cellulose and, therefore, determines cellulase adsorption as well as the rates and yields of cellulose hydrolysis (Arantes and Saddler, 2011; Kim et al., 1988). Furthermore, crystallinity is a relevant parameter affecting the reactivity of adsorbed cellulases (Hall et al., 2010). According to various authors (Hall et al., 2010; Ooshima et al., 1983), crystallinity may also influence cellulase adsorption and, thus, cellulose accessibility (Chapter 1.1) (Arantes and Saddler, 2011; Chandra et al., 2007; Park et al., 2010). To finally achieve high cellulose hydrolysis rates and yields, the prior pretreatment (Chapters 1.4 and 1.4.1) needs to increase accessibility and to reduce crystallinity (Alvira et al., 2010; Jeoh et al., 2007; Kumar and Wyman, 2009c; Quiroz-Castaneda et al., 2011b; Rollin et al., 2011; Wyman, 2007).

1.4.2.3   Expression of Cellulases by *Trichoderma reesei*

The filamentous fungus *Trichoderma reesei* (synonym: *Hypocrea jecorina*) is an efficient cellulase producer achieving very high expression levels (> 40 g/L) and yields (0.25 g cellulase per g carbon source) of secreted cellulases (Esterbauer et al., 1991; Herpoel-Gimbert et al., 2008; Lynd et al., 2002; Tolan and Foody, 1999). Although other eukaryotes and bacteria express cellulases, *T. reesei* has been the focus of cellulase research for over 60 years (Lynd et al., 2002). *T. reesei* expresses two CBHs (CBH I and CBH II), at least five EGs (EG I, EG II, EG III, EG IV, and EG V), and two β-glucosidases (β-glucosidase I and β-glucosidase II) (Goedegebuur et al., 2002; Herpoel-Gimbert et al., 2008; Karlsson et al., 2001; Karlsson et al., 2002; Martinez et al., 2008; Nagendran et al., 2009; Ouyang et al., 2006; Rosgaard et al., 2007; Tolan and Foody, 1999). The relative amounts of the individual cellulases (g cellulase per g total cellulase) are as follows (Rosgaard et al., 2007):

CBH I (40-60%), CBH II (12-20%), EG I (5-10%), EG II (1-10%), EG III (< 1-5%), EG IV (< 1%), EG V (< 5%), β-glucosidase I (1-2%), and β-glucosidase II (< 1%). Similar values of relative cellulase levels have also been reported by Goedegebuur et al. (2002). Table 1-2 finally summarizes the molecular masses and isoelectric points of cellulases from *T. reesei*.

Table 1-2: Molecular masses and isoelectric points of cellulases from *Trichoderma reesei*.

Cellulase	Molecular mass [kDa]	Isoelectric point [-]	Reference
Cellobiohydrolase I	61-63[a]	-	(Jeoh et al., 2008)
	63	4.2	(Gama et al., 1998)
	65	3.8-4.0[a]	(Schülein, 1988)
	65	3.9	(Tomme et al., 1988)
	66	4.2	(Shoemaker et al., 1983)
	68	-	(Henrissat et al., 1985)
	47-63[a]	4.4-4.7[a]	(Herpoel-Gimbert et al., 2008)
Cellobiohydrolase II	55	-	(Henrissat et al., 1985)
	58	5.9	(Gama et al., 1998)
	58	5.9	(Tomme et al., 1988)
	30-59[a]	4.7-6.0[a]	(Herpoel-Gimbert et al., 2008)
Endoglucanase I	46	5.0	(Gama et al., 1998)
	50	-	(Henrissat et al., 1985)
	54	4.7	(Shoemaker et al., 1983)
	55	4.6	(Herpoel-Gimbert et al., 2008)
	60	4.0-5.0[a]	(Schülein, 1988)
Endoglucanase II	48	6.1	(Gama et al., 1998)
	48	7.0	(Schülein, 1988)
	48	-	(Henrissat et al., 1985)
	43-50[a]	4.5-4.8[a]	(Herpoel-Gimbert et al., 2008)
Endoglucanase III	25	-	(Karlsson et al., 2002)
	25	7.5	(Ülker and Sprey, 1990)
	25-26[a]	5.7	(Herpoel-Gimbert et al., 2008)
Endoglucanase IV	47	5.2	(Herpoel-Gimbert et al., 2008)
	55	-	(Karlsson et al., 2001)
	56	-	(Saloheimo et al., 1997)
Endoglucanase V	23	-	(Karlsson et al., 2002)
β-glucosidase I	71	8.7	(Chen et al., 1992)
	81	6.7	(Herpoel-Gimbert et al., 2008)
β-glucosidase II	114	4.8	(Chen et al., 1992)
	115	6.0	(Shoemaker et al., 1983)

[a] Different isoforms of the respective cellulase were detected.

1.4.2.4 Screening of Cellulase Activities

During the last years, cellulases have been engineered through directed evolution and rational design approaches leading to a multitude of novel or improved cellulases (Fukumura et al., 1997; Kruus et al., 1995a; Liang et al., 2010; Liang et al., 2011; Morozova et al., 2010; Zhang et al., 2006). In order to screen and characterize these variants, cellulase assays are essential (Decker et al., 2009; Zhang et al., 2006). Figure 1-6 gives an overview about cellulase assays which have been established so far. These cellulase assays can be categorized into three general approaches (Figure 1-6): (1) detection of substrate, (2) detection of product, and (3) detection of the physical properties of the substrate.

During hydrolysis, the decrease in cellulose concentration can be detected by weighing or chemical methods (Figure 1-6). When using small amounts of cellulose (e.g. 1 mg), weighing is not suitable, since the low accuracy of a balance (e.g. 0.1 mg) can lead to high coefficients of variation (e.g. 10%) (Zhang et al., 2006). In the case of chemical methods, cellulose can be directly quantified by the $K_2Cr_2O_7$-H_2SO_4 assay (Wood and Bhat, 1988) or, after liquefaction, by total sugar assays such as the phenol-H_2SO_4 (Zhang and Lynd, 2005) and the anthrone-H_2SO_4 assay (Zhang et al., 2006).

The majority of cellulase assays are based on the detection of hydrolysis products (Figure 1-6). The reducing sugar assays, in particular the dinitrosalicylic acid assay, are the most common cellulase assays (Zhang et al., 2006). Derivatized glycosides are also often applied when determining initial cellulase activities or inhibition constants (Tuohy et al., 2002; Zhang et al., 2010). After the hydrolysis of these water-soluble derivatized glycosides (such as *p*-nitrophenyl glycosides or methylumbelliferyl glycosides), the released chromophores or fluorophores can be easily detected (Zhang et al., 2006). However, such hydrolysis data based on soluble substrates are not pertinent to the realistic hydrolysis of insoluble substrates (Zhang et al., 2006), because the enzymatic hydrolysis involves, aside from the catalytic domain, also the cellulose-binding domain of cellulases (Chapter 1.4.2.1) (Lynd et al., 2002; Pristavka et al., 2000; Rabinovich et al., 1982; Yuldashev et al., 1993).

Alternatively, cellulase activities can also be determined by measuring changes in the physical properties of the cellulose. These properties, in particular, are: swollen factor, fiber strength, structure collapse, viscosity, absorbance, or scattered light. For example,

viscosimetric measurements have been frequently used to determine the initial hydrolysis rate of EGs while using soluble carboxymethyl cellulose (CMC) (Karlsson et al., 2001; Lee and Kim, 1999; Miller et al., 1960).

A detailed description of all aforementioned cellulase assays and their associated substrates (Figure 1-6) is given in the review of Zhang et al. (2006). Despite the high number of substrates, cellulases are often screened with impractical model substrates that do not reflect the real cellulosic biomass in industrial processes. In particular, the application of soluble substrates should be avoided during screening experiments, because the adsorption of cellulases onto the cellulose is ignored (Zhang et al., 2006). Moreover, there is no sophisticated cellulase assay simultaneously combining high-throughput, online analysis, and insoluble cellulosic substrates.
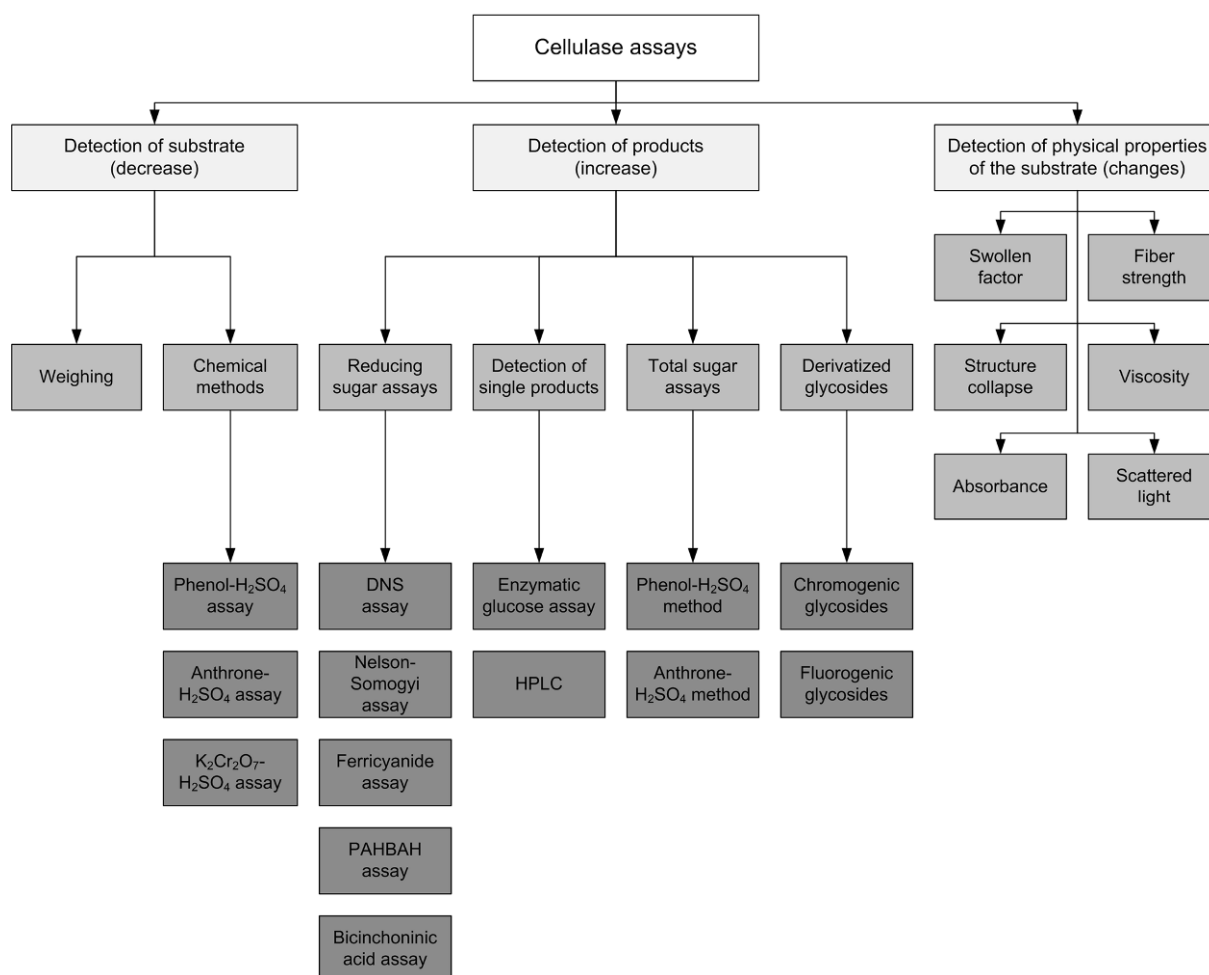
Figure 1-6:   Overview and classification of established cellulase assays. A detailed description of the assays can be found in the study of Zhang et al. (2006). Abbreviations: dinitrosalicylic acid (DNS), high-performance liquid chromatography (HPLC), *p*-hydroxybenzoic acid hydrazide (PAHBAH).

1.4.3   Fermentation

As described in Chapter 1.4, hexoses and pentoses result from the hydrolysis of cellulose and hemicellulose. During fermentation, these sugars are finally converted to the desired product (Figure 1-4). Thereby, the production of cell mass or by-products should be minimized in order to achieve high product yields (Hamelinck et al., 2005). Whereas hexoses such as glucose, galactose, and mannose are fermented by many industrially applied microorganisms, the pentoses xylose and arabinose are fermented by only a few native strains, and usually at relatively low yields (Mosier et al., 2005). However, genetic modifications of *Escherichia coli* (Ingram et al., 1998; Ingram et al., 1999), *Saccharomyces cerevisiae* (Bengtsson et al., 2009; Garcia-Sanchez et al., 2010; Runquist et al., 2011), and *Zymomonas mobilis* (Zhang et al., 1995) resulted in strains capable of co-fermenting both hexoses and pentoses to ethanol or other chemicals (Mosier et al., 2005). In addition, *Aspergillus terreus* or *Ustilago maydis* utilize both hexoses and pentoses (Kautola et al., 1985; Kurz and Ericson, 1962; Matsushima and Klug, 1958), and they are well-known producers of itaconic acid (Guevarra and Tabuchi, 1990; Kautola et al., 1985; Kobayashi, 1978; Willke and Vorlop, 2001).

In most of the former lignocellulose-based processes, the simultaneous use of all sugars by one microorganism (or a mixed-culture) was not performed (Stephanopoulos, 2007). Instead, hexoses and pentoses were sequentially converted by different microorganisms incubated in separate fermentation steps (Stephanopoulos, 2007). During the last few years, however, industrial *S. cerevisiae* strains were developed, which co-ferment both hexoses and pentoses (Garcia-Sanchez et al., 2010; Matsushika et al., 2009a). In comparison to laboratory strains, these industrial strains show higher productivities and adequate inhibitor tolerance (Matsushika et al., 2009b). Consequently, the industry focuses on applying these strains for lignocellulose-based processes.

1.4.4   Process Integration

When performing the biocatalytic conversion of lignocellulose (Chapter 1.4) by using enzymatic hydrolysis and fermentation, four biologically mediated processing steps typically occur (Lynd et al., 1999; Lynd et al., 2002): enzyme production, hydrolysis, hexose fermentation, and pentose fermentation. Process configurations of these steps can be categorized based on their level of process integration (Geddes et al., 2011; Hamelinck et al.,

2005; Lynd et al., 1999; Lynd et al., 2002; Olofsson et al., 2008; Wyman, 1994). As presented in Figure 1-7, separate hydrolysis and fermentation (SHF) involves four independent processing steps and at least four different biocatalysts. If hexoses and pentoses are co-fermented (Tian et al., 2010), the process configuration is referred to as separate hydrolysis and co-fermentation (SHCF). Simultaneous saccharification and fermentation (SSF) combine hydrolysis and hexose fermentation, with enzyme production and fermentation of pentoses occurring in separate processing steps. Simultaneous saccharification and co-fermentation (SSCF) involves just two steps: enzyme production and a second step in which hydrolysis and co-fermentation of both hexoses and pentoses are performed. Ultimately, consolidated bioprocessing (CBP) accomplishes enzyme production, hydrolysis, and co-fermentation in a single unit.
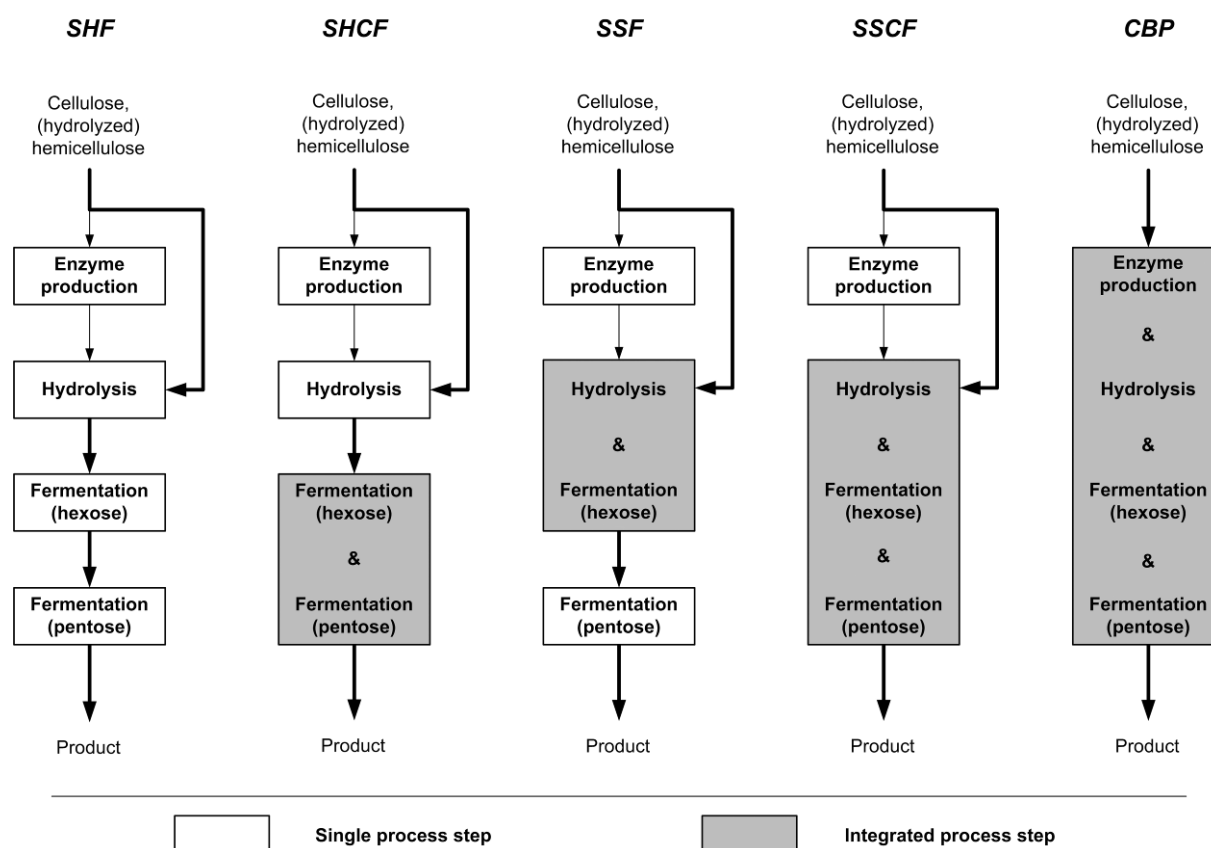
Figure 1-7:   Various (integrated) configurations of biologically mediated processing steps during the biocatalytic conversion of lignocellulose. Abbreviations according to the literature (Geddes et al., 2011; Lynd et al., 1999; Wyman, 1994): separate hydrolysis and fermentation (SHF), separate hydrolysis and co-fermentation (SHCF), simultaneous saccharification and fermentation (SSF), simultaneous saccharification and co-fermentation (SSCF), consolidated bioprocessing (CBP). The thickness of the arrows indicates the relative amounts of cellulose and (hydrolyzed) hemicellulose used for enzyme production and hydrolysis.

Lignocellulose processing technologies show a trend towards integrated process configurations (Lynd et al., 2002). Three decades ago, SHF was the preferred process configuration. Since the studies of Wright et al. (1988), SSF has been widely thought to be advantageous over SHF. Main reasons are as follows (Wyman, 1994): (1) SSF remarkably reduces the investment costs; and (2) product inhibition of the cellulases (Chapter 1.4.2.1) is prevented, since the released glucose is directly consumed by the microorganism. Currently, SSCF and CBP are considered as an economically attractive near-term goal for process development (Stephanopoulos, 2007; Xu et al., 2009). Despite the advantages of integrated process configurations, it should be noted that there is always a compromise needed to find favorable conditions for all integrated processing steps (Hamelinck et al., 2005; Olofsson et al., 2008). Consequently, some researchers suggest that cost reductions should result from optimizing the separate processing steps (Hamelinck et al., 2005).

The aforementioned trend towards integrated process configurations is most evident in the case of bioethanol production, but this trend is likely to be applicable to other chemicals as well (Lynd et al., 2002). For example, SSF processes have been applied to produce ethanol (Olofsson et al., 2008), lactic acid (Abe and Takagi, 1991; Romani et al., 2008; Wee et al., 2006; Yáñez et al., 2003), acetic acid (Borden et al., 2000), citric acid (Asenjo and Jew, 1983), and succinic acid (Chen et al., 2011). Up to now, however, no SSF process has been developed for the production of the platform chemical itaconic acid.

1.5 Interdisciplinary Collaboration (Cluster of Excellence)

In 2007, the cluster of excellence "tailor-made fuels from biomass" (TMFB) was started at the RWTH Aachen University. This fundamental research project comprises the selective conversion of lignocellulose to platform chemicals (Chapter 1.3), the catalytic transformation of platform chemicals into new synthetic fuels (fuel synthesis), and the development of novel low-temperature combustion technologies (Figure 1-8). In contrast to conventional diesel fuels, the new fuel candidates should be tailored to the requirements of the novel combustion engines with low soot and NO_x emissions (Janssen et al., 2010). Within this broad research project, scientists from different disciplines (biology, chemistry, chemical engineering, combustion engineering, mathematics, and physics) develop a CO_2-neutral process chain, ranging from lignocellulose down to the final combustion (Figure 1-8) (Janssen et al., 2010).

Among several research activities, the TMFB project also addresses the biocatalytic conversion of lignocellulose to the platform chemical itaconic acid. Here, the long-term goal is the complete conversion of cellulose as well as hemicellulose. Lignin should be burned to power the process or converted to valuable co-products (Bozell et al., 2007; Mosier et al., 2005). In order to allow a fast and detailed analysis of the essential conversion steps (pretreatment, hydrolysis, and fermentation), cellulose has been used as a model feedstock during the initial phase of the TMFB project. Moreover, cellulose is the main component of lignocellulose (Chapter 1.1) and, therefore, the efficient conversion of cellulose is especially important. Consequently, this thesis focuses on the biocatalytic conversion of cellulose to itaconic acid. However, recent studies from the TMFB project have shown that pentoses resulting from hemicellulose hydrolysis can be efficiently fermented to itaconic acid (Klement et al., 2011). Finally, itaconic acid should be further converted to 3-MTHF (Geilen et al., 2010; Marquardt et al., 2010). This potential fuel is proposed to allow a soot-free and NO_x-free combustion similar to 2-MTHF whose superior burning properties have already been validated (Janssen et al., 2010).
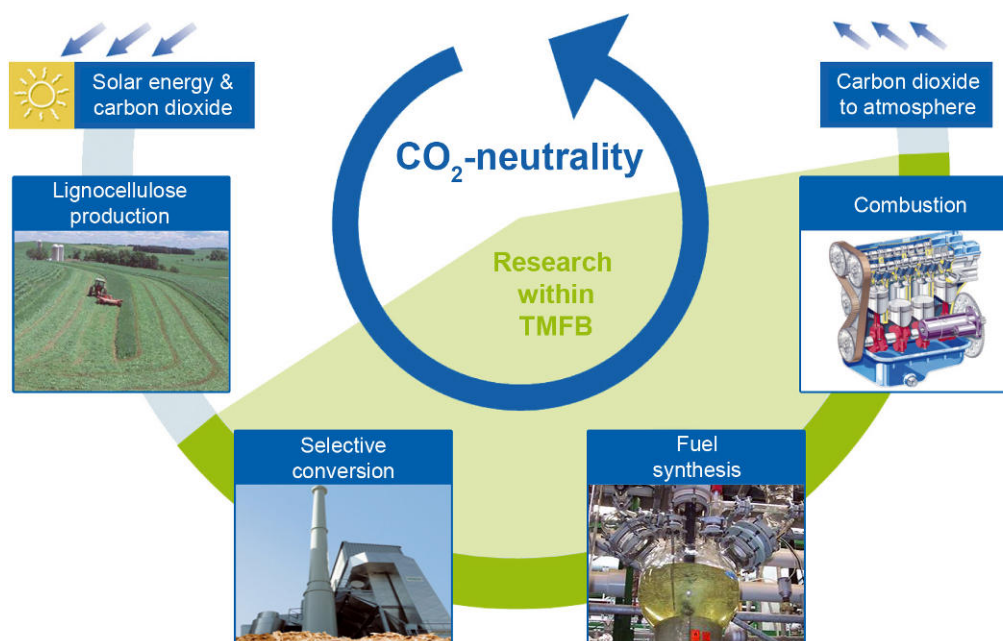
Figure 1-8: CO_2-cycle and research areas of the cluster of excellence "tailor-made fuels from biomass" (TMFB). Abbreviated from Pischinger (2009).

1.6 Objectives and Overview

This thesis investigates the aforementioned biocatalytic conversion of cellulose to itaconic acid (Chapter 1.5). According to Chapter 1.4, this process comprises three major conversion steps: pretreatment, hydrolysis, and fermentation. Within this thesis, each of the conversion steps is investigated in detail (Figure 1-9), and new approaches and technologies are developed. Rather than establishing the complete process, an in-depth understanding of the single conversion steps should be generated, and the possibility of integrated process configurations should be validated.
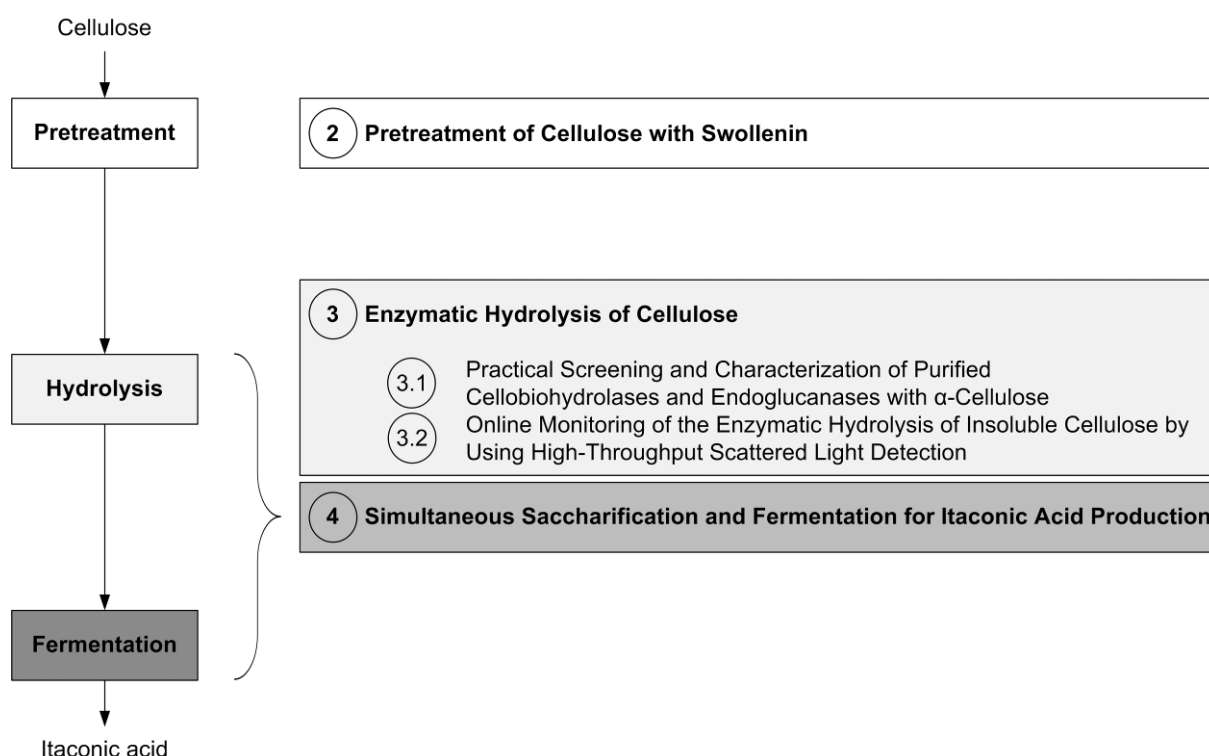
Figure 1-9:   Objectives and overview of this work: "Biocatalytic Conversion of Cellulose towards Itaconic Acid" via pretreatment, hydrolysis, and fermentation. Each number indicates one of the following chapters.

Although non-hydrolyzing proteins offer a safe and environmentally friendly pretreatment technique, there is no quantitative analysis of the effects of non-hydrolyzing proteins on cellulosic substrates (Chapter 1.4.1). Therefore, Chapter 2 addresses the pretreatment of cellulose by using the non-hydrolyzing protein swollenin. To yield sufficient swollenin for industrial applications, Chapter 2 presents a new way of producing recombinant swollenin. Furthermore, it is shown for the first time how swollenin quantitatively affects relevant

physical properties of cellulosic substrates and how it affects their subsequent enzymatic hydrolysis.

Besides the application of pretreatment techniques, the enzymatic cellulose hydrolysis can also be optimized by adjusting hydrolysis conditions. For this purpose, cellulases have to be characterized, and a better understanding of the hydrolysis mechanism needs to be established. However, CBHs and EGs are often characterized with soluble impractical model substrates that do not reflect the real cellulosic biomass in industrial processes (Chapter 1.4.2.4). In Chapter 3.1, insoluble α-cellulose is proposed as a practical substrate to characterize CBHs and EGs. In this context, a novel purification method is presented to prepare the major CBHs and EGs from *T. reesei*. Moreover, the adsorption and activity of these cellulases is modeled and analyzed. Here, a semi-mechanistic model is developed to predict the kinetics of α-cellulose hydrolysis. In addition, the influence of various hydrolysis conditions (such as pH, temperature, and hydrodynamics) is elucidated. Here, Chapter 3.1 investigates and correlates in detail the adsorption and the activity of cellulases at different hydrodynamic conditions.

Despite the high number of cellulase assays, most cellulase assays are slow, tedious, or based on soluble cellulosic substrates (Chapter 1.4.2.4). However, Chapter 3.2 presents the first sophisticated cellulase assay that simultaneously combines high-throughput, online analysis, and insoluble cellulosic substrates. It is based on the BioLector technique, which monitors the scattered light intensities of cellulose suspensions in a continuously shaken microtiter plate. By monitoring the enzymatic hydrolysis of different insoluble cellulosic substrates in the BioLector, cellulase activities are quantitatively determined. Moreover, scattered light measurements are applied to analyze cellulase adsorption as well as the non-hydrolytic effect of cellulases or swollenin on insoluble cellulose.

Up to now, itaconic acid has solely been manufactured via separate fermentations necessitating a previous step (such as cellulose hydrolysis) to produce directly fermentable carbon sources (such as glucose). However, the integration of cellulose hydrolysis and fermentation into one processing step offers several advantages (Chapter 1.4.4). Consequently, Chapter 4 deals with a new integrated SSF process to directly convert cellulose to itaconic acid. In just one step, α-cellulose should be hydrolyzed by cellulases, and the resulting glucose should be simultaneously converted to itaconic acid by *U. maydis*. In this

context, the separate enzymatic hydrolysis of cellulose is investigated under SSF conditions and compared with conventional hydrolysis conditions. Moreover, a SSF process is analyzed in detail and compared with a batch cultivation using glucose as sole carbon source.

2   Pretreatment of Cellulose with Swollenin

2.1 Introduction

As shown in Chapter 1, naturally occurring lignocellulose is a promising starting material for the sustainable production of platform chemicals and fuels (Fukuda et al., 2009; Huber et al., 2006; Klosowski et al., 2010; Okano et al., 2010; Pristavka et al., 2000; Quiroz-Castaneda et al., 2011b). For the selective and biocatalytic conversion of lignocellulose, three conversion steps are necessary (Figures 1-4 and 1-9): (1) pretreatment, (2) hydrolysis, and (3) fermentation. The general aim of pretreatment is to alter or remove structural and compositional barriers of lignocellulose so that the hydrolysis of the carbohydrate fraction (cellulose and hemicellulose) to fermentable sugars can be achieved more rapidly and with greater yields (Chapter 1.4.1) (Chandra et al., 2007; Kumar et al., 2009; Mosier et al., 2005). Since cellulose is the main fraction of lignocellulose (Chapter 1.1), the hydrolysis of cellulose is most important.

As shown in Chapter 1.4.2, the hydrolysis of cellulose to glucose necessitates a cellulase system consisting of cellobiohydrolase (CBH, E.C. 3.2.1.91), endoglucanase (EG, E.C. 3.2.1.4), and β-glucosidase (E.C. 3.2.1.21) (Himmel et al., 2007; Quiroz-Castaneda et al., 2009; Schröter et al., 2001). Besides enzyme-related factors (e.g. enzyme inactivation and product inhibition) (Zhang and Lynd, 2004), the enzymatic hydrolysis of cellulose is limited by its physical properties (Desai and Converse, 1997; Kumar and Wyman, 2009c; Wang et al., 2006; Zhang et al., 1999). As described in Chapter 1.4.2.2, these properties, in particular, are: degree of polymerization, accessibility, and crystallinity (Alvira et al., 2010; Chandra et al., 2007; Hall et al., 2011; Mansfield et al., 1999). Cellulose accessibility, which is determined by cellulose particle size (external surface area) and porosity (internal surface area), is the most important factor for hydrolysis (Arantes and Saddler, 2010; Arantes and Saddler, 2011; Chandra et al., 2007; Chandra et al., 2008; Dasari and Berson, 2007; Mansfield et al., 1999; Yeh et al., 2010). Cellulose accessibility reflects the total surface area available for direct physical contact between cellulase and cellulose and, therefore, influences cellulase adsorption as well as the rate and extent of cellulose hydrolysis (Arantes and Saddler, 2011; Kim et al., 1988). Furthermore, crystallinity is a relevant factor for cellulose hydrolysis, since

it influences the reactivity of adsorbed cellulases (Hall et al., 2010). Here, it should be noted that crystallinity may also affect cellulase adsorption (Hall et al., 2010; Ooshima et al., 1983) and, therefore, cellulose accessibility (Arantes and Saddler, 2011; Chandra et al., 2007; Park et al., 2010). Up to now, however, the relationship between crystallinity and accessibility has not been clearly understood (Chandra et al., 2007; Ramos et al., 1993). For high cellulose hydrolysis rates and yields, cellulose accessibility needs to be increased and, conversely, its crystallinity reduced (Jeoh et al., 2007; Rollin et al., 2011). To achieve this and accordingly improve subsequent hydrolysis, pretreatment techniques are essential (Alvira et al., 2010; Kumar and Wyman, 2009c; Quiroz-Castaneda et al., 2011b; Wyman, 2007).

Since pretreatment can be expensive, there is a prime motivation to screen and improve it (Decker et al., 2009; Galbe and Zacchi, 2007; Kumar et al., 2009; Mosier et al., 2005; Selig et al., 2010). Over time, many pretreatment technologies have been developed: physical, physicochemical, chemical, biological, electrical methods or combinations of these methods (Galbe and Zacchi, 2007; Kumar et al., 2009). A more detailed description of pretreatment techniques is given in Chapter 1.4.1. Some of these techniques entail expensive equipment, harsh conditions, and high energy input (Kumar et al., 2009). By contrast, non-hydrolyzing proteins have been found to pretreat cellulose under mild conditions (Arantes and Saddler, 2010; Hall et al., 2011). After the regular pretreatment of lignocellulose, these non-hydrolyzing proteins can be added during cellulose hydrolysis (Baker et al., 2000), or they can be applied in a second pretreatment step in which cellulose is the substrate (Hall et al., 2011).

During this second pretreatment step, cellulose is incubated under mild conditions with non-hydrolyzing proteins that bind to the cellulose. As a result, cellulose microfibrils (Figure 1-1; diameter: ca. 10 nm; Paiva et al., 2007; Somerville et al., 2004; Zhao et al., 2007) are dispersed, and the thicker cellulose macrofibrils or fibers (Figure 1-1; diameter: ca. 0.5-10 μm, consisting of microfibrils; Lynd et al., 2002; Paiva et al., 2007; Zhao et al., 2007) swell, thereby decreasing crystallinity and increasing accessibility (Arantes and Saddler, 2010; Coughlan, 1985; Klyosov, 1990; Rabinovich et al., 1982). This phenomenon was named amorphogenesis (Arantes and Saddler, 2010; Coughlan, 1985). Furthermore, cellulose-binding proteins can lead to deagglomeration of cellulose agglomerates (diameter: > 0.1 mm, consisting of cellulose fibers) (Chen et al., 2010; Din et al., 1991), thereby separating cellulose fibers from each other and additionally increasing cellulose accessibility. Ultimately,

amorphogenesis as well as deagglomeration promote cellulose hydrolysis (Arantes and Saddler, 2010).

Various authors have described hydrolysis-promoting effects when pretreating cellulose with single cellulose-binding domains (Hall et al., 2011), expansins from plants (Baker et al., 2000; Cosgrove, 2000; Han and Chen, 2007; Wei et al., 2010), or expansin-related proteins from *Trichoderma reesei* (Saloheimo et al., 2002), *Bacillus subtilis* (Kim et al., 2009), *Bjerkandera adusta* (Quiroz-Castaneda et al., 2011a), or *Aspergillus fumigatus* (Chen et al., 2010). A prominent expansin-related protein is swollenin from the fungus *T. reesei*. In contrast to cellulases, the expression levels of swollenin in *T. reesei* are relatively low (1 mg/L) (Saloheimo et al., 2002). Thus, swollenin from *T. reesei* has been heterologously expressed in *Saccharomyces cerevisiae* (Saloheimo et al., 2002), *Aspergillus niger* (Saloheimo et al., 2002), and *Aspergillus oryzae* (Wang et al., 2010). The expression levels in *S. cerevisiae*, however, are also low (25 µg/L) (Saloheimo et al., 2002), and only *A. oryzae* produces swollenin in higher concentrations (50 mg/L) (Wang et al., 2010). According to Saloheimo et al. (2002), swollenin can disrupt the structure of cotton fiber or the cell wall of the algae *Valonia macrophysa*. Since swollenin shows a high sequence similarity to plant expansins (Saloheimo et al., 2002), it may have a similar function and lead to the disruption of cellulosic networks within plant cell walls (Arantes and Saddler, 2010). Thus, swollenin may have an important role in the enzymatic degradation of lignocellulose by *T. reesei* (Banerjee et al., 2010). Up to now, however, there is no systematic and quantitative analysis of the effects of swollenin on cellulosic substrates and their hydrolysis.

First, Chapter 2 presents an alternative way of producing recombinant swollenin in order to generate sufficient swollenin for industrial applications. Second, the main objective is to show how recombinant swollenin quantitatively affects relevant physical properties of different cellulosic substrates and how it affects their subsequent hydrolysis.

2.2 Materials and Methods

2.2.1   Cellulosic Substrates

The cellulosic substrates Whatman filter paper No.1, α-cellulose, Avicel PH101, and Sigmacell 101 were purchased from Sigma-Aldrich (St. Louis, USA). The physical properties of filter paper were summarized by Zhang and Lynd (2004). Physical properties (solubility; purity; crystallinity index, CrI; weight-average degree of polymerization, DP_w; geometric mean particle size, d_P) and product information of the other applied cellulosic substrates are given in Chapter 3.1.2.1. Agglomerates of Whatman filter paper No.1 were prepared by using a hole-punch and quartering the resulting filter paper discs. The final filter paper agglomerates had an average diameter of approximately 3 mm.

2.2.2   Cellulase Preparation

The commercial cellulase preparation Celluclast[®] 1.5L (Novozymes, Bagsværd, DK) – a filtrated culture supernatant of *Trichoderma reesei* (Henrissat et al., 1985) – was used for the hydrolysis of the pretreated cellulosic substrates. Celluclast[®] consists of cellulases, xylanases, and a small amount of other proteins (Gama et al., 1998; Henrissat et al., 1985; Herpoel-Gimbert et al., 2008). With respect to cellulases (Chapter 1.4.2.3), *T. reesei* expresses at least two cellobiohydrolases (CBH I and CBH II), five endoglucanases (EG I, EG II, EG III, EG IV, and EG V), and two β-glucosidases (β-glucosidase I and β-glucosidase II) (Goedegebuur et al., 2002; Herpoel-Gimbert et al., 2008; Karlsson et al., 2001; Karlsson et al., 2002; Martinez et al., 2008; Nagendran et al., 2009; Ouyang et al., 2006; Rosgaard et al., 2007; Tolan and Foody, 1999). Molecular masses and isoelectric points of the cellulases from *Trichoderma reesei* are summarized in Table 1-2. According to their relative protein amount (Chapter 1.4.2.3), the main cellulases are CBH I, CBH II, EG I, and EG II (Goedegebuur et al., 2002; Nagendran et al., 2009; Rosgaard et al., 2007; Tolan and Foody, 1999).

To remove salts, sugars, and other interfering components, Celluclast[®] was previously rebuffered using column chromatography, with an Äkta FPLC (GE Healthcare, Little Chalfont, UK). For rebuffering, Celluclast[®] was loaded on Sephadex G-25 Fine (2.6 cm × 10 cm, GE Healthcare, Little Chalfont, UK), and 0.05 M sodium acetate (pH 4.8) was used as

a running buffer at 110 cm/h. Sephadex G-25 Fine exhibits an exclusion limit of 1-5 kDa which is comparable to the molecular mass cut-off of dialysis membranes for protein desalting. Since cellulases have a molecular mass of ≥ 23 kDa (Table 1-2), the mixture of cellulases was not changed during rebuffering. Chromatography was conducted at room temperature, and the automatically collected fractions were directly cooled at 4°C. To determine specific filter paper activities, different dilutions of Celluclast® and the rebuffered Celluclast® – applied for all hydrolysis experiments – were tested according to Ghose (1987). Here, the following specific filter paper activities (per g protein) were measured: 201 U/g (Celluclast®) and 279 U/g (rebuffered Celluclast®).

2.2.3   Genetic Engineering for Recombinant Swollenin

The below-mentioned cloning procedure was designed for secreted protein expression according to the *K. lactis* Protein Expression Kit (New England Biolabs, Ipswich, USA). The cDNA of the swollenin-coding region was synthesized by reverse-transcription PCR using mRNA isolated from *T. reesei* QM9414 (NCBI no. [swo1 gene]: AJ245918, NCBI no. [protein sequence]: CAB92328) and reverse transcriptase (from moloney murine leukemia virus; Promega, Fitchburg, USA) according to the manufacturer's protocol. Specific primers were applied to synthesize a cDNA starting from the 19th codon of the swollenin-coding region and, therefore, missing the secretion signal sequence of *T. reesei* (Saloheimo et al., 2002). By using these primers, SalI and SpeI restriction sites were added upstream and downstream of the swollenin-coding region, respectively. The amplified cDNA was cloned into the pCR2.1-TOPO vector (Invitrogen, Carlsbad, USA) according to the manufacturer's protocol. After DNA sequencing and isolation of a correct clone, the DNA was excised from pCR2.1-TOPO and cloned into the pKLAC1-H vector using XhoI and SpeI restriction enzymes (New England Biolabs, Ipswich, USA) according to the manufacturer's protocol. The pKLAC1-H is a modified version of the integrative pKLAC1 vector (New England Biolabs, Ipswich, USA; NCBI no. AY968582). The pKLAC1 – developed by Colussi and Taron (2005) – exhibits the α-mating factor signal sequence and can be used for the expression and secretion of recombinant proteins in *K. lactis* (Colussi and Taron, 2005). The pKLAC1-H was constructed by including an additional SpeI restriction site directly followed by a His-tag coding sequence (6 x His) between the XhoI and AvrII restriction sites of pKLAC1. The final amino acid sequence of recombinant swollenin (without the α-mating factor signal sequence) is given in Figure 2-2C. The DNA sequence and samples of the final

pKLAC1-H construct (containing the DNA coding for recombinant swollenin) were stored at the Institute of Molecular Biotechnology (RWTH Aachen University, Aachen, DE). The cloning procedure was performed in cooperation with Michele Girfoglio from the aforementioned institute.

2.2.4   Expression and Purification of Swollenin

All below-mentioned transformation, selection, and precultivation procedures – developed by Colussi and Taron (2005) – were performed according to the manufacturer's protocol (*K. lactis* Protein Expression Kit, New England Biolabs, Ipswich, USA). After cloning, *K. lactis* GG799 cells were transformed with pKLAC1-H (containing the DNA coding for recombinant swollenin), and transformed clones were selected (acetamide selection). Figure 2-1 shows a light microscopic picture of transformed *K. lactis* GG799 cells in YPGal (yeast extract, peptone, and galactose) medium.
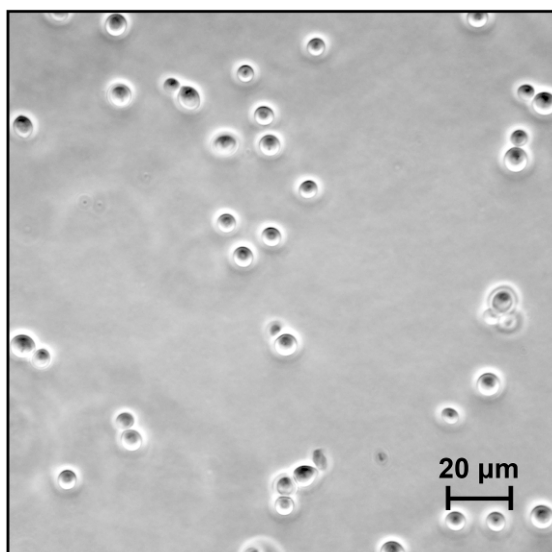
Figure 2-1:   Light microscopic picture of *Kluyveromyces lactis* GG799 in YPGal medium during the stationary growth phase; microscope: Eclipse E600 (Nikon, Tokyo, JP).

One transformed clone was precultivated in YPGal medium, consisting of 20 g/L galactose, 20 g/L peptone, and 10 g/L yeast extract – all media components were purchased from Carl Roth (Karlsruhe, DE). After inoculation with 2.5 mL of the preculture, the main culture was cultivated in triplicates in 2 L Erlenmeyer flasks with YPGal medium under the following constant conditions: temperature $T = 30°C$, total filling volume $V_L = 250$ mL, shaking diameter $d_0 = 50$ mm, shaking frequency $n = 200$ rpm. Additionally, a non-transformed

K. lactis wild type was cultivated as a reference. After incubation for 72 h, the main cultures were centrifuged (6000 g, 20 min, 4°C), and the pooled supernatants of the triplicates were treated with endoglycosidase H_f by using 20 U per µg protein for 12 h (Saloheimo et al., 2002) according to the manufacturer's protocol without denaturation (New England Biolabs, Ipswich, USA). Afterwards, the protein solution was concentrated 100-fold at 4°C using a Vivacell 100 ultrafiltration system with a molecular mass cut-off of 10 kDa (Sartorius Stedim Biotech, Göttingen, DE). For affinity chromatography, the recombinant swollenin was previously rebuffered using Sephadex G-25 Fine (2.6 cm × 10 cm, GE Healthcare, Little Chalfont, UK) at 110 cm/h with a running buffer (pH 7.4) consisting of 0.05 M sodium dihydrogen phosphate, 0.3 M sodium chloride, and 0.01 M imidazole. The rebuffered sample was loaded on Ni Sepharose 6 Fast Flow (1.6 cm × 10 cm, GE Healthcare, Little Chalfont, UK) at 120 cm/h. The bound swollenin was eluted with the aforementioned running buffer, containing 0.25 M imidazole.

2.2.5   SDS-Polyacrylamide Gel Electrophoresis of Swollenin

SDS-polyacrylamide gel electrophoresis (SDS, sodium dodecyl sulfate) was applied to analyze the molecular mass and purity of the recombinant swollenin. Novex® 12% polyacrylamide Tris-Glycine gels (Invitrogen, Carlsbad, USA) and samples were prepared according to the manufacturer's protocol. The Plus Prestained Protein Ladder (Fermentas, Burlington, CA) was used as a molecular mass marker (Appendix B). Electrophoresis was performed according to the manufacturer's protocol (Invitrogen, Carlsbad, USA). Finally, the proteins were stained with Coomassie Brilliant Blue (Wilson, 1983) by using SimplyBlue SafeStain (Invitrogen, Carlsbad, USA) and analyzed densitometrically (Tan et al., 2007) by using the scanner Perfection V700 (Epson, Suwa, JP). The molecular mass and purity of swollenin was determined using the software TotalLab TL100 (Nonlinear Dynamics, Newcastle, UK).

2.2.6   Western Blot Analysis of Swollenin

Western blot analysis was performed to identify the recombinant swollenin. Therefore, SDS-polyacrylamide gels were blotted onto a nitrocellulose membrane (Whatman, Springfield Mill, UK) according to the manufacturer's protocol (Invitrogen, Carlsbad, USA). The membranes were blocked at room temperature with 50 g/L skim milk dissolved in

phosphate buffered saline containing 0.5 g/L Tween-20 (PBST) for 30 min. To detect the recombinant swollenin, the membranes were incubated at room temperature for 1.5 h with a rabbit polyclonal antibody against His-tag (Dianova, Hamburg, DE) diluted 1:10,000 in PBST. After the membrane was washed thrice with PBST, it was incubated with alkaline phosphatase conjugated goat anti-rabbit IgG (Dianova, Hamburg, DE) diluted 1:5,000 in PBST at room temperature for 1 h. Finally, bound antibodies were visualized by incubating the membrane for 5 min with NBT/BCIP (nitro blue tetrazolium / 5-bromo-4-chloro-3-indolyl phosphate) diluted 1:100 in phosphatase buffer (100 mM Tris-HCl, 100 mM NaCl, 5 mM MgCl$_2$, pH 9.6).

2.2.7   Measurement of Protein Concentration

Protein concentrations were analyzed with the bicinchoninic acid (BCA) assay (Smith et al., 1985) using the BCA Protein Assay Kit (Thermo Fisher Scientific, Waltham, USA) and bovine serum albumin (BSA) as a standard. Depending on the protein concentration of the samples, the standard procedure (working range: 0.02-2 g/L) or the enhanced procedure (working range: 0.005-0.25 g/L) was performed according to the manufacturer's protocol. The absorbance at 562 nm was measured with a Synergy 4 microtiter plate reader (BioTek Instruments, Winooski, USA).

To quantify swollenin in the culture supernatant of *K. lactis*, the bicinchoninic acid assay was combined with the aforementioned SDS-polyacrylamide gel electrophoresis (including densitometric analysis). Here, total protein concentrations were determined and multiplied with the ratio of swollenin to total protein (purity).

2.2.8   Mass Spectrometry and Glycosylation Analysis of Swollenin

Mass spectrometry was applied to identify the expressed and purified recombinant swollenin. The protein band (~80 kDa) was excised from the SDS-polyacrylamide gel, washed in water, incubated with dithiothreitol, alkylated with iodoacetamide, and digested with trypsin (Winters and Day, 2003). Peptide analysis was carried out using a nanoHPLC (Dionex, Sunnyvale, USA) coupled to an ESI-QUAD-TOF-2 mass spectrometer (Waters Micromass, Eschborn, DE) as described by Tur et al. (2009). The mass spectrometer was used in cooperation with Michael Küpper from the Institute of Molecular Biotechnology (RWTH

Aachen University, Aachen, DE). The Mascot algorithm (Matrix Science, London, UK) was applied to correlate the mass spectrometry data with amino acid sequences in the Swissprot database. Thereby, the sequences of the analyzed peptides could be identified, and, ultimately, protein matches could be determined. The Mascot score is derived from the ions scores of the detected peptides matching the peptides in the database and reflects a non-probabilistic basis for ranking protein hits (Ramos-Fernandez et al., 2008). By using this database, the peptide mass tolerance was set at $\pm$ 0.3 Da. Additionally, the following modifications to the amino acids in brackets were allowed: carbamidomethyl (cysteine), carboxymethyl (cysteine), oxidation (methionine), and propionamide (cysteine). Moreover, potential areas for N-glycosylation and O-glycosylation were identified by using the NetNGlyc 1.0 and NetOGlyc 3.1 servers (www.cbs.dtu.dk/services/) (Julenius et al., 2005).

2.2.9 Qualitative Adsorption Study of Swollenin via Confocal Laser Scanning Microscopy

Confocal laser scanning microscopy was applied to qualitatively verify the adsorption of swollenin onto filter paper. Therefore, purified swollenin was labeled with fluorescein isothiocyanate (FITC) by using the FITC Labeling Kit (Merck, Darmstadt, DE), and FITC-labeled swollenin was subsequently dialyzed to remove excessive FITC. Two different blanks were labeled and dialyzed similarly: (1) without swollenin (= buffer) or (2) with BSA instead of swollenin. The labeling and dialysis procedure was performed according to the manufacturer's protocol. Afterwards, adsorption experiments were performed in 0.05 M sodium acetate buffer (pH 4.8) using 20 g/L untreated filter paper and 2 g/L labeled swollenin. Solutions with filter paper and solutions with labeled swollenin were preincubated separately at 45°C for 10 min, and experiments were started by mixing both solutions. The final mixtures were incubated in 2 mL Eppendorf tubes on a thermomixer MHR23 (simultaneous shaking and temperature control; HLC Biotech, Bovenden, DE) under the following constant conditions for 2 h: temperature $T = 45$°C, total filling volume $V_L = 1$ mL, shaking diameter $d_0 = 3$ mm, shaking frequency $n = 1000$ rpm. The shaking frequency was chosen to ensure the complete suspension of cellulose particles (Kato et al., 2001). To verify a specific adsorption of labeled swollenin, blanks without swollenin (= buffer) or with labeled BSA instead of labeled swollenin were incubated similarly. After incubation, the samples were put on ice and immediately analyzed.

Confocal laser scanning microscopy was carried out by using the Opera system (PerkinElmer, Waltham, USA) – a fully automated confocal laser scanning microscope with a $10 \times$ air, a $20 \times$ water, and a $40 \times$ air objective. The Opera system was used in cooperation with Stefano Di Fiore from the Fraunhofer Institute for Molecular Biology and Applied Ecology (Aachen, DE). After the aforementioned labeling, dialysis, and incubation procedures, the samples were transferred in a black 96-well microtiter plate with transparent bottom (µClear, Greiner Bio-One, Frickenhausen, DE). Afterwards, images were taken at a focal height of $\pm$ 3 mm with respect to the automatically selected focal plane above the bottom of each well. To obtain fluorescence microscopic pictures at 521 nm, exposure times of 250-2000 ms were chosen. Pseudo-coloring of the resulting grey-scale pictures was carried out by using Adobe Photoshop (Adobe Systems, San Jose, USA). To obtain light microscopic pictures, the laser was switched off, and a light-emitting diode was placed above the microtiter plate.

2.2.10 Quantitative Adsorption Experiments

Quantitative adsorption experiments were performed in 0.05 M sodium acetate buffer (pH 4.8) using 20 g/L untreated filter paper and various concentrations (0.05-1.25 g/L) of purified swollenin. Solutions with filter paper and solutions with swollenin were preincubated separately at 45°C for 10 min, and experiments were started by mixing both solutions. The final mixtures were incubated in 2 mL Eppendorf tubes on a thermomixer MHR23 (HLC Biotech, Bovenden, DE) under the following constant conditions for 2 h: temperature $T = 45$°C, total filling volume $V_L = 1$ mL, shaking diameter $d_0 = 3$ mm, shaking frequency $n = 1000$ rpm. The shaking frequency was chosen to ensure the complete suspension of cellulose particles (Kato et al., 2001). Three different blanks were incubated similarly: (1) without swollenin, (2) without filter paper, or (3) without filter paper and without swollenin. The incubation was stopped by centrifugation (8000 g, 1 min), and the supernatants were immediately analyzed for unbound swollenin by using the bicinchoninic acid assay. The adsorbed swollenin concentration was calculated as the difference between initial (blanks) and unbound swollenin concentration. Adsorption isotherm parameters were determined using the Langmuir isotherm (Bansal et al., 2009):

$$A_{EQ} = \frac{A_{max} \cdot E}{K_D + E} \tag{2-1}$$

where A_{EQ} denotes the amount of adsorbed protein at equilibrium [$\mu mol_{protein}/g_{cellulose}$], A_{max}, the maximum protein adsorption [$\mu mol_{protein}/g_{cellulose}$], E, the free protein concentration [$\mu mol_{protein}/L$], and K_D, the dissociation constant [$\mu mol_{protein}/L$]. In the literature (Nidetzky et al., 1994b), the association constant K_A [L/μmol] is sometimes used instead of the dissociation constant K_D.

To analyze the effect of swollenin pretreatment (see below) on subsequent cellulase adsorption (Rabinovich et al., 1982; Yuldashev et al., 1993), the maximum cellulase adsorption was determined by incubating various concentrations (0.7-2.5 g/L) of rebuffered Celluclast® with 10 g/L pretreated cellulosic substrates. Here, all incubations were conducted under the aforementioned conditions for 1 h, 1.5 h, and 2 h.

2.2.11 Pretreatment with Swollenin

Pretreatment experiments were performed with 20 g/L cellulosic substrates and various concentrations of swollenin in 0.05 M sodium acetate buffer (pH 4.8). The mixtures were incubated as triplicates in 2 mL Eppendorf tubes on a thermomixer MHR23 (HLC Biotech, Bovenden, DE) under the following constant conditions: temperature T = 45 °C, total filling volume V_L = 1 mL, shaking diameter d_0 = 3 mm, shaking frequency n = 1000 rpm. To exclude a sole mechanical effect on cellulosic substrates due to shaking and to verify a specific effect of swollenin, blanks without swollenin (= buffer) or with 0.4 g/L BSA instead of swollenin were incubated similarly. To detect a possible hydrolytic activity of recombinant swollenin, the sensitive p-hydroxybenzoic acid hydrazide assay (Lever, 1972) was applied by using glucose as a standard. After incubation for 48 h, the supernatants of the pretreatment solutions were analyzed, and the absorbancies were measured at 410 nm in a Synergy 4 microtiter plate reader. Subsequently, all cellulosic samples were washed to remove adsorbed proteins. Therefore, the mixtures were centrifuged (14000 × g, 10 min, 4°C), and the cellulosic pellets were washed four times with 800 μL 0.05 M citrate buffer (pH 10) and once with 800 μL distilled water (Zhu et al., 2009). Finally, the triplicates were pooled. According to Zhu et al. (2009), citrate buffer (pH 10) is an appropriate washing solution, and a single washing step with 0.05 M citrate buffer (pH 10) leads to a desorption efficiency of 61% in case of fungal

cellulases and Avicel. Since no acids or bases are formed during the washing procedure, the weak buffer capacity of citrate buffer at pH 10 can be neglected. In this study, the washing procedure was conducted four times to ensure a high desorption of swollenin. The measurements of protein concentration in the washing supernatants – by applying the aforementioned bicinchoninic acid assay (Chapter 2.2.7, working range starting from 0.005 g/L) – showed that swollenin desorbed almost completely. Already after three washing steps, a total swollenin desorption efficiency of > 90% was achieved.

2.2.12 Photography and Microscopy

Photography and microscopy were applied to visualize the effect of swollenin pretreatment on filter paper. After pretreatment with buffer, BSA, or swollenin, the different filter paper solutions were transferred into petri dishes, the particles were evenly distributed, and images were taken with an Exilim EX-FH100 camera (Casio, Tokyo, JP). Afterwards, the number of filter paper agglomerates (> 0.5 mm) was determined by image analysis using the software ImageTool 3.0 (UTHSCSA, San Antonio, USA) and a ruler as a reference. Light microscopic pictures were taken with an Eclipse E600 (Nikon, Tokyo, JP). Additionally, scanning electron microscopy was performed using a Hitachi S-5500 (Hitachi, Tokyo, JP) and a field emission of 5 kV. All washed filter paper samples were covered with a layer of carbon (3 nm) and, subsequently, with a layer of PtPd (3 nm, 80%-20%). The images were taken by using secondary electrons. Scanning electron microscopy was performed in cooperation with Roberto Rinaldi from the "Max-Planck-Institut für Kohlenforschung" (Mülheim an der Ruhr, DE).

2.2.13 Laser Diffraction

The particle-size distributions of all pretreated cellulosic substrates were measured by laser diffraction (Bowen, 2002) using a LS13320 (Beckman Coulter, Brea, USA). The geometric mean particle size d_P was calculated using the software LS version 5.01 (Beckman Coulter, Brea, USA). In the case of filter paper, particles with an average diameter of > 0.75 mm were manually removed before laser diffraction to exclude a disturbance of measurement signals.

2.2.14 X-ray Diffraction

The crystallinity index *CrI* of all pretreated cellulosic substrates was determined by powder X-ray diffraction (XRD) – in cooperation with Roberto Rinaldi from the "Max-Planck-Institut für Kohlenforschung" (Mülheim an der Ruhr, DE). XRD patterns were obtained using a STOE STADI P transmission diffractometer (STOE & Cie GmbH, Darmstadt, DE) in Debye-Scherrer geometry (Cu*Kα* radiation, λ = 1.54060 Å) with a primary monochromator and a position-sensitive detector. Thereby, XRD patterns were collected with a diffraction angle 2θ from 10° to 30° (increments of 0.01°) and a counting time of 6 s per increment. The sample was adhered to a polyester foil (biaxially-oriented polyethylene terephthalate) by using a diluted solution of adhesive. After drying the sample in open-air, the sample was covered with a second polyester foil. This set was then fixed in a sample holder. To improve statistics and level out sample orientation effects, the sample was rotated at ca. 2 Hz during XRD measurement. The *CrI* [%] was calculated using the peak height method (Cao and Tan, 2005; Park et al., 2010) and the corresponding equation:

$$CrI = \frac{I_{002} - I_{AM}}{I_{002}} \tag{2-2}$$

where I_{002} is the maximum intensity of the crystalline plane (002) reflection ($2\theta = 22.5^{\circ}$) [1/s] and I_{AM} is the intensity of the scattering for the amorphous component at about 18° in cellulose-I [1/s] (Cao and Tan, 2005). Here, it should be noted that there are several methods for calculating *CrI* from XRD data, and these methods can provide significantly different results (Park et al., 2010; Sathitsuksanoh et al., 2011). Although the applied peak height method produces *CrI* values that are higher than those of other methods, it is still the most commonly used method and ranks *CrI* values in the same order as the other methods (Park et al., 2010).

2.2.15 Hydrolysis of Swollenin-Pretreated Cellulose

Hydrolysis experiments with 10 g/L pretreated cellulosic substrate and 1 g/L rebuffered Celluclast® were conducted in 0.05 M sodium acetate buffer (pH 4.8). The mixtures were incubated as triplicates in 2 mL Eppendorf tubes on a thermomixer MHR23 (HLC Biotech, Bovenden, DE) under the following constant conditions: temperature T = 45 °C, total filling

volume $V_L = 1$ mL, shaking diameter $d_0 = 3$ mm, shaking frequency $n = 1000$ rpm. In general, attention has to be paid to cellulase inactivation which would reduce the final yield of cellulose hydrolysis (Reese, 1980). In this current study, however, a shaken system with relatively low shear forces was applied. According to Engel et al. (2010), rebuffered Celluclast® is stable under the applied incubation conditions so that cellulase inactivation could be neglected. The shaking frequency was chosen to ensure the complete suspension of cellulose particles (Kato et al., 2001) and to exclude mass transfer limitations. Three different blanks were incubated similarly: (1) without cellulase, (2) without substrate, or (3) without substrate and without cellulase. After defined time intervals, samples were taken, and the hydrolysis was stopped by boiling (10 min, 100°C). Finally, the amount of reducing sugars was analyzed by applying the dinitrosalicylic acid assay as described in Chapter 2.2.16.

Initial hydrolysis rates [g/(L·h)] were calculated by applying a linear fit to the reducing sugar concentration data from 0-6 h. Moreover, the degree of saccharification was calculated using the following equation:

$$saccharification = \frac{P \cdot \frac{162}{180}}{C_0} \tag{2-3}$$

with P denoting the detected reducing sugar concentration [g/L], C_0 denoting the initial cellulose concentration [g/L], and 162/180 denoting the correction coefficient between molecular weights of glucan monomers and glucose.

2.2.16 Dinitrosalicylic Acid Assay

The dinitrosalicylic acid assay (Miller, 1959) was applied to quantify the reducing sugars released during cellulose hydrolysis. Thereby, reducing sugar concentrations were determined by using glucose as a standard. Since the dinitrosalicylic acid assay is not sensitive at low reducing sugar concentrations (Wood and Bhat, 1988; Zhang et al., 2006), low concentrations were accurately quantified by adding 1.25 g/L glucose to the samples according to Wood and Bhat (1988). The absorbance was measured at 540 nm in a Synergy 4 microtiter plate reader (BioTek Instruments, Winooski, USA).

Since the dinitrosalicylic acid assay exhibits a lower sensitivity towards cellobiose than glucose, reducing sugar concentrations may be underestimated when glucose is used as a standard and β-glucosidase is not in excess (Zhang et al., 2006). However, under the applied hydrolysis conditions (Chapter 2.2.15), cellobiose did not accumulate (highest cellobiose to glucose ratio was measured in the case of Sigmacell after 10 h: 0.12). Therefore, this underestimation was minimal, and the addition of β-glucosidase was not needed.

2.2.17 Computational Methods

Parameters (including standard deviations) of the adsorption model were calculated by nonlinear, least squares regression analysis using MATLAB R2010 (The MathWorks, Natick, USA). TableCurve 3D 4.0 (Systat Software, Chicago, USA) was used to empirically correlate crystallinity and mean particle size with initial hydrolysis rates via the non-linear Gaussian cumulative function:

$$z = GCUMX(a, b, c) + GCUMY(d, e, f) + GCUMX(g, b, c) \cdot GCUMY(1, e, f) \qquad (2\text{-}4)$$

where a, b, c, d, e, f, and g denote the various fitting parameters of the non-linear Gaussian cumulative function [-].

2.3 Results and Discussion

2.3.1 Production and Analysis of Recombinant Swollenin

Swollenin is a cellulase-related protein and consists of an N-terminal cellulose-binding domain connected by a linker region to an expansin-homologous domain (Saloheimo et al., 2002). The cDNA of the swollenin-coding region from *T. reesei* was used as a template to clone a recombinant His-tagged swollenin (data not shown). After cloning, the recombinant swollenin was heterologously expressed by using the yeast *K. lactis* as expression host (Colussi and Taron, 2005). In addition, a non-transformed *K. lactis* wild type was cultivated as a reference. As shown by SDS-polyacrylamide gel electrophoresis (Figure 2-2A), the supernatants of the wild type (lane 1) and the transformed clone (lane 2) showed only a few

differences in protein secretion pattern. These differences could be explained by the influence of heterologous protein expression on the native secretome of *K. lactis* (Lodi et al., 2005). However, an intense protein band at ~80 kDa could be observed in the supernatant of the transformed clone which corresponds to the size of native swollenin from *T. reesei* (~75 kDa, 49 kDa based on the primary sequence) (Saloheimo et al., 2002). Furthermore, this protein band was detected as a His-tagged protein by Western blot analysis (Figure 2-2B). In order to quantify the putative swollenin in the supernatant of *K. lactis*, the total protein concentration was determined and a densitometric analysis of the SDS-polyacrylamide gel (Figure 2-2A, lane 2) was conducted. The expression level of swollenin was approximately 20-30 mg/L, which is comparable with the results for other recombinant proteins expressed in *K. lactis* (Colussi and Taron, 2005; Lodi et al., 2005). With respect to recombinant swollenin, lower or comparable expression levels were achieved by using *S. cerevisiae* (25 μg/L) (Saloheimo et al., 2002) or *A. oryzae* (50 mg/L) (Wang et al., 2010) as expression hosts. Finally, this protein was purified by immobilized metal ion affinity chromatography. According to Figure 2-2A-B, the final fraction (lane 3) showed a protein band with high purity (~75%).

To clearly identify the protein band at ~80 kDa (Figure 2-2A-B), its amino acid sequence was determined by using mass spectrometry (Schuchardt and Sickmann, 2007) and the Mascot search engine (Grosse-Coosmann et al., 2005). Figure 2-2C shows the results of mass spectrometry and the expected amino acid sequence of the recombinant swollenin. As shown by a high Mascot score of 502, the protein at ~80 kDa was clearly identified to be a variant of swollenin from *T. reesei*. Regarding the native swollenin sequence, a protein score of > 57 (homology threshold) indicates identity or extensive homology ($p < 0.05$). In addition, potential N- and O-glycosylation sites were detected by using the NetNGlyc 1.0 and NetOGlyc 3.1 servers (Julenius et al., 2005) (Figure 2-2C). Here, it should be noted that the native swollenin contains almost no N-glycosylation (Saloheimo et al., 2002). Therefore, the difference between the calculated molecular mass of 49 kDa, based on the primary sequence of swollenin, and the observed molecular mass of 80 kDa (Figure 2-2A-B) may be explained by O-glycosylation and other post-translational modifications. Proofs are given as follows: (1) the linker region of cellulases or cellulase-related proteins is highly O-glycosylated (Stals et al., 2004); (2) swollenin contains potential O-glycosylation sites within the linker region (linker: [40-232]; Figure 2-2C); (3) no peptides of the linker region were identified by mass spectrometry, since glycosylation alters the mass/charge ratio of the peptides (Figure 2-2C).
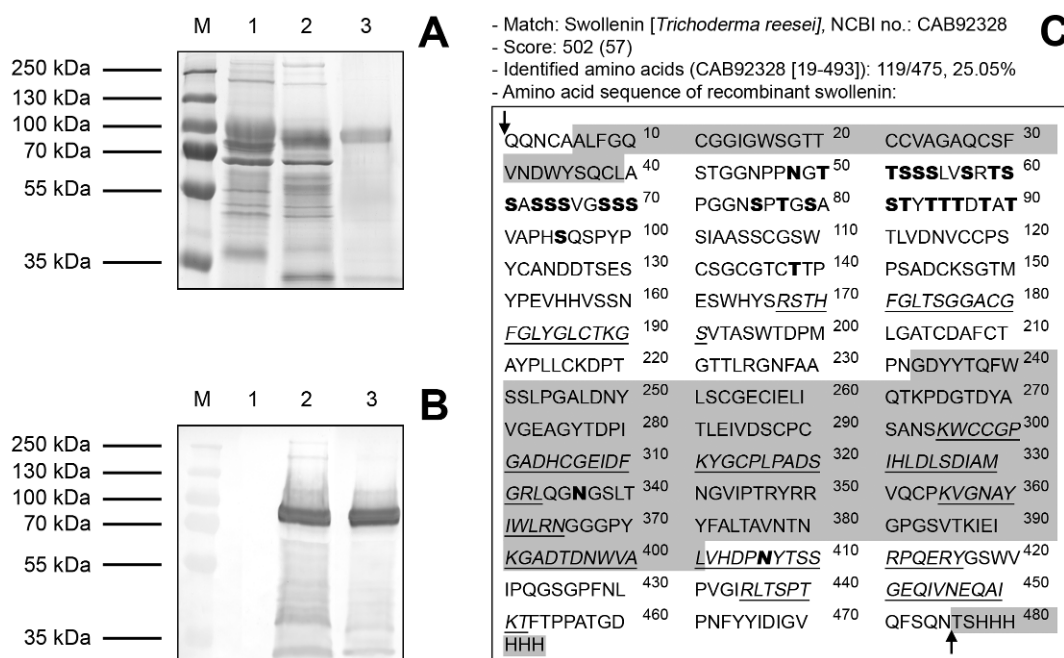
Figure 2-2: SDS-polyacrylamide gel electrophoresis, Western blot, and mass spectrometry of swollenin produced by *Kluyveromyces lactis*. (**A**) SDS-polyacrylamide gel electrophoresis and (**B**) Western blot: (M) molecular mass marker, (1) filtrated culture supernatant of *K. lactis* wild type, (2) filtrated culture supernatant of *K. lactis* expressing recombinant swollenin, (3) recombinant swollenin purified by immobilized metal affinity chromatography. 12% polyacrylamide gel, the same volume of the samples (15 μL) was loaded onto the particular slots; (**C**) mass spectrometric results and primary sequence of recombinant swollenin. The protein band (~80 kDa) was analyzed using a mass spectrometer and the Mascot database. The detected peptides are underlined and written in italic letters. The cellulose-binding domain [6-39], expansinA domain [233-401], and His-tag [476-483] are marked in grey. Potential areas for N-glycosylation and O-glycosylation are written in bold letters. The black arrows enclose the primary sequence of the native swollenin (CAB92328) without leader peptide.

2.3.2 Adsorption of Swollenin

As the adsorption of proteins is a prerequisite for amorphogenesis (Arantes and Saddler, 2010), the adsorption of purified swollenin onto filter paper was qualitatively and quantitatively analyzed.

For qualitative analysis, swollenin was labeled with the fluorophore FITC and subsequently dialyzed to remove excessive FITC. Afterwards, the labeled swollenin was incubated with filter paper for 2 h. Finally, the filter paper particles were analyzed by confocal laser scanning microscopy. As shown by Figure 2-3A, filter paper particles were fluorescent after an incubation with FITC-labeled swollenin. By contrast, filter paper incubated with FITC-

labeled BSA or buffer (negative controls) showed no fluorescent particles (data not shown). Consequently, the fluorescence was not caused by unspecific protein adsorption or direct labeling of filter paper by remaining FITC. Furthermore, the reaction of FITC with amine and sulfhydryl groups of swollenin did not inhibit its adsorption onto cellulose. As shown by Figure 2-3A, the fluorescence was not homogeneous which may be explained by different and partially inaccessible cellulose-binding sites (Carrard and Linder, 1999; Linder and Teeri, 1997). These different types of cellulose-binding sites are caused by: (1) the inhomogeneous structure of filter paper (Figure 2-3B), (2) amorphous and crystalline regions of filter paper (Zhang and Lynd, 2004), and (3) the generally porous structure of cellulose particles (Grethlein, 1985; Zhang and Lynd, 2004).
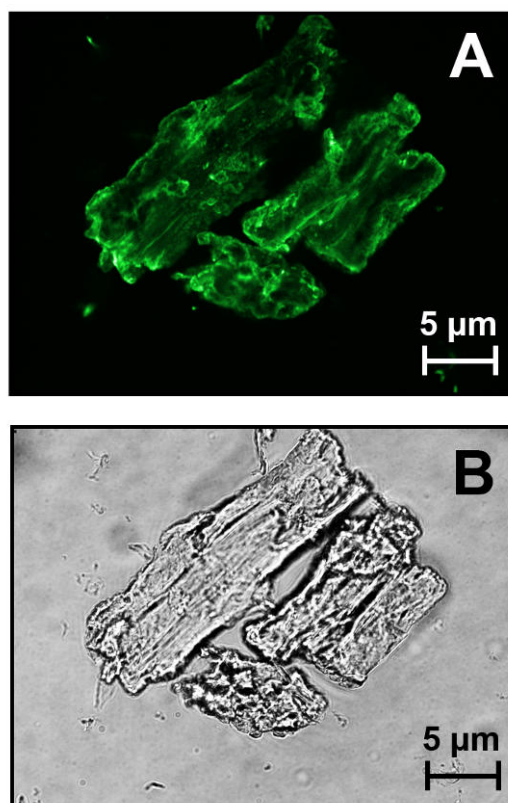
Figure 2-3:   Confocal laser scanning microscopy of filter paper after incubation with fluorescein isothiocyanate (FITC)-labeled swollenin. (**A**) Fluorescence microscopy at 521 nm; (**B**) light microscopy; labeling: FITC Labeling Kit (Merck, Darmstadt, DE) according to the manufacturer's protocol; incubation: 20 g/L Whatman filter paper No.1 in 0.05 M sodium acetate buffer (pH 4.8), 2 g/L FITC-labeled swollenin, $T = 45°C$, $V_L = 1$ mL, $n = 1000$ rpm, $d_0 = 3$ mm, incubation time 2 h; microscope: Opera system (PerkinElmer, Waltham, USA).

For quantitative analysis, the adsorption isotherm of purified, non-labeled swollenin onto filter paper was determined. Preliminary adsorption kinetics showed that an incubation time of $\leq$ 2 h was needed to reach equilibrium. Figure 2-4 illustrates that the adsorption of swollenin was a characteristic function of free swollenin concentration. After a sharp increase in adsorbed swollenin at low concentrations, a plateau was reached at higher concentrations ($>$ 5 µmol/L). As denatured swollenin, boiled for 20 min, showed no adsorption, the adsorption was specific and required a functional protein structure. The Langmuir isotherm – Eq. 2-1 – provided a good fit (Figure 2-4, R^2 = 0.91). Corresponding parameters – A_{max}(swollenin), the maximum swollenin adsorption, and K_D(swollenin), the dissociation constant of swollenin – are listed in the legend of Figure 2-4. Similar values of A_{max} and K_D were found when analyzing the adsorption of purified cellulases onto filter paper (Nidetzky et al. (1994b), CBH I: 0.17 µmol/g, 0.71 µmol/L; EG I: 0.17 µmol/g, 1.79 µmol/L). This may be attributed to the fact that swollenin exhibits a cellulose-binding domain with high homology to those of cellulases (Ouyang et al., 2006). However, A_{max} was lower for swollenin than for purified cellulases. According to Linder et al. (1995), single amino acid substitutions of cellulose-binding domains can lead to adsorption differences. Furthermore, catalytic domains of cellulases specifically adsorb onto cellulose independently of cellulose-binding domains (Lynd et al., 2002). In addition, the difference in A_{max} may be explained by the lower molecular mass of CBHs and EGs (Table 1-2) and, therefore, a better access to internal binding sites as described for other proteins and materials (Hunter and Carta, 2002; Oberholzer and Lenhoff, 1999).
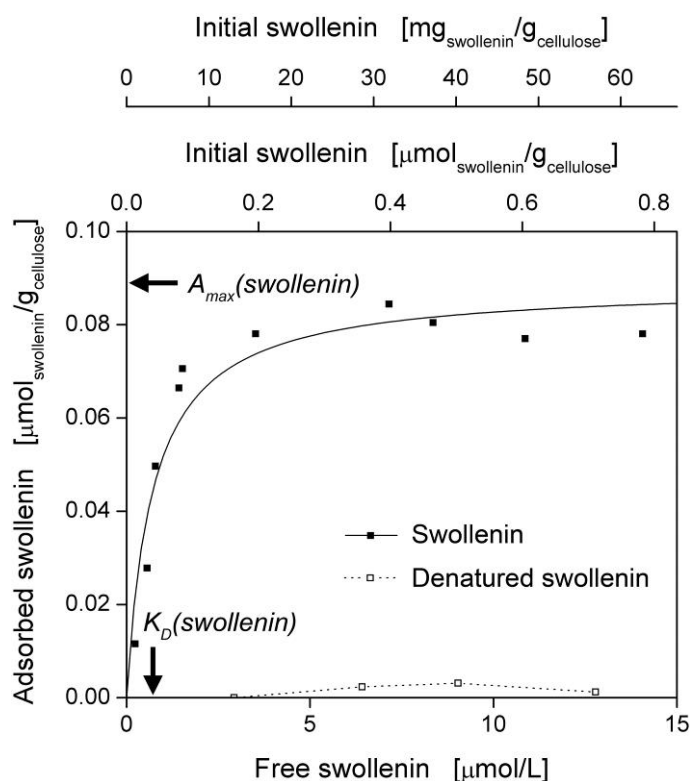
Figure 2-4:   Adsorption isotherm of purified swollenin onto filter paper. The predicted Langmuir isotherm, according to Eq. 2-1, is shown as a solid line (R^2 = 0.91), and corresponding parameters (± standard deviations) are: $A_{max}(swollenin)$ = 0.089 ± 0.006 µmol/g, $K_D(swollenin)$ = 0.707 ± 0.196 µmol/L. The initial swollenin concentration, added at the start of the incubation, is also shown for a better understanding of Figure 2-10; incubation: 20 g/L Whatman filter paper No.1 in 0.05 M sodium acetate buffer (pH 4.8), T = 45°C, V_L = 1 mL, n = 1000 rpm, d_0 = 3 mm, incubation time 2 h.

2.3.3   Pretreatment of Filter Paper with Swollenin

To verify a potential effect of recombinant swollenin on cellulose, filter paper was pretreated with buffer, bovine serum albumin (BSA), or recombinant swollenin. Here, swollenin in an initial concentration of 20 mg per g cellulose was applied (> 80% saturation, Figure 2-4). It should be noted that all pretreatments were initiated with the same initial number (= 80) of filter paper agglomerates (initial diameter: ~3 mm). As shown in Figure 2-5A, swollenin caused a deagglomeration of filter paper agglomerates (consisting of cellulose fibers, Figure 1-1). Since the cellulose fibers of a single agglomerate were separated by pretreatment with swollenin (Figure 2-5B), the number of bigger agglomerates obviously decreased (Figure 2-5A). This decrease in the number of bigger agglomerates (> 0.5 mm) was also quantified using image analysis. During pretreatment, a shaken system with relatively low shear forces was applied. However, to exclude a sole mechanical effect on cellulose agglomerates due to

shaking and to verify a specific effect of swollenin, filter paper was accordingly pretreated with buffer or the protein BSA (references). By contrast, the pretreatments with buffer or BSA showed much less deagglomeration (Figure 2-5). Consequently, the deagglomeration was specifically caused by swollenin. As no reducing sugars were detected by using the sensitive *p*-hydroxybenzoic acid hydrazide assay after an incubation with swollenin for 48 h, the reduction in the number of large agglomerates is attributed to the aforementioned adsorption of swollenin onto filter paper (Chapter 2.3.2) and the so-called non-hydrolytic deagglomeration (Arantes and Saddler, 2010).

Buffer   **BSA**   **Swollenin**

Number of agglomerates
(diameter > 0.5 mm): 80

Number of agglomerates
(diameter > 0.5 mm): 74

Number of agglomerates
(diameter > 0.5 mm): 26
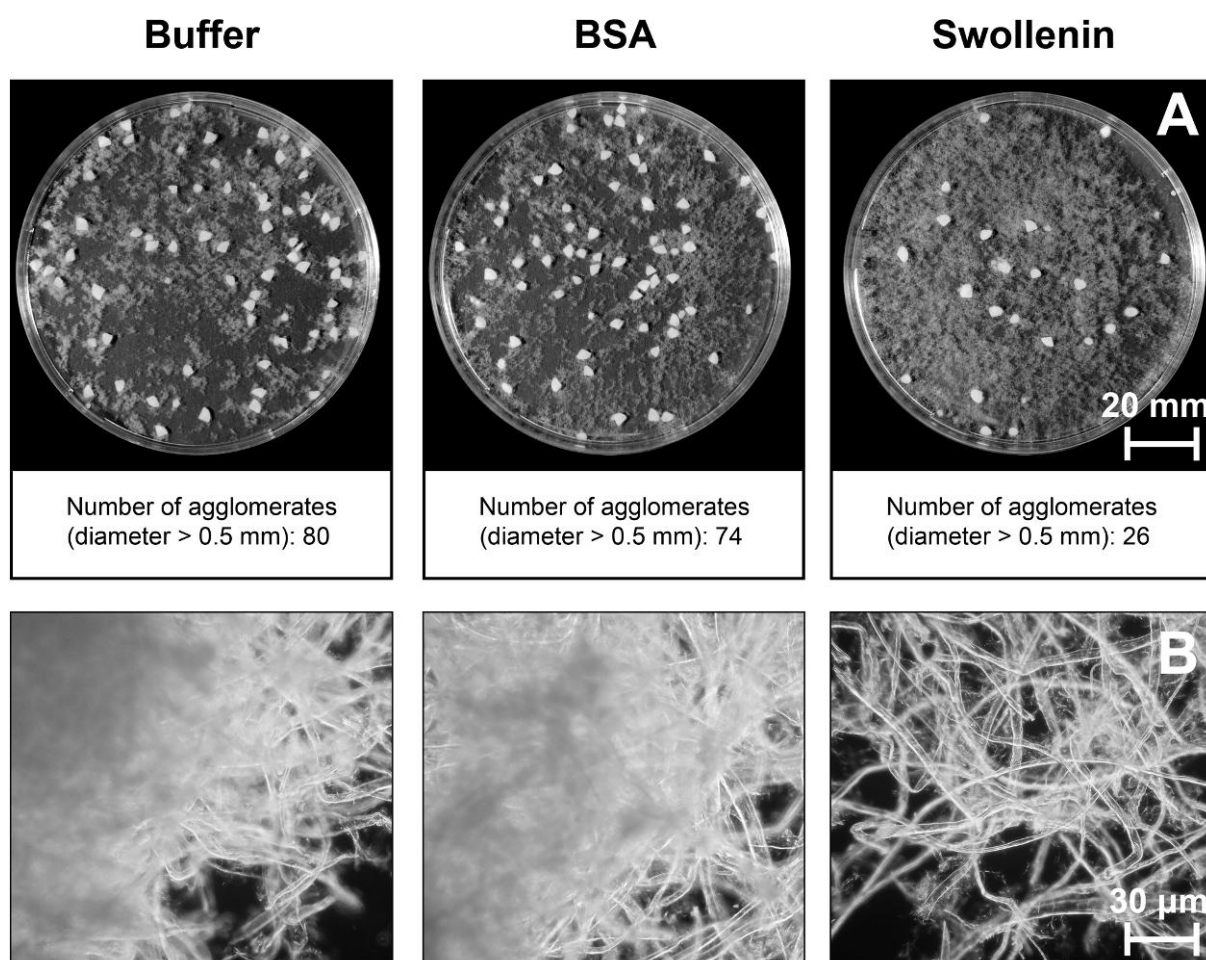
Figure 2-5:   Photography and light microscopy of filter paper after pretreatment with swollenin. (**A**) Macroscopic pictures of pretreated filter paper in petri dishes and number of agglomerates. All pretreatments were initiated with the same initial number (= 80) of filter paper agglomerates (initial diameter: ~3 mm). The number of agglomerates (> 0.5 mm) was measured by image analysis; (**B**) light microscopy of pretreated filter paper; pretreatment: 20 g/L cellulose in 0.05 M sodium acetate buffer (pH 4.8), 0.4 g/L BSA (~6 μmol/L) or swollenin (~5 μmol/L), $T = 45°C$, $V_L = 1$ mL, $n = 1000$ rpm, $d_0 = 3$ mm, incubation time 48 h; microscope: Eclipse E600 (Nikon, Tokyo, JP).

As described by Saloheimo et al. (2002), swollenin is also able to disrupt and swell cotton fibers. This phenomenon results from the dispersion of cellulose microfibrils (Figure 1-1) and is called amorphogenesis (Arantes and Saddler, 2010; Coughlan, 1985). In this current study, however, the swelling of cellulose fibers was not detected when Whatman filter paper No.1 – a different substrate – was used (Figure 2-5B). Reasons for this may be the different structure of filter paper than that of cotton used by Saloheimo et al. (2002) or the low resolution of light microscopy. Therefore, scanning electron microscopy was applied to visualize the effect of swollenin on cellulose microfibrils (Figure 2-6). After pretreatments with buffer or BSA, the microfibrils were not dispersed, thereby resulting in a smooth and uniform surface of the whole fiber. By contrast, swollenin caused the microfibrils to disperse, thereby creating a rough and amorphic surface on the cellulose fibers. Other authors found similar results via scanning electron microscopy after treating cellulose with cellulose-binding domains of cellulases (Din et al., 1991; Gao et al., 2001; Hall et al., 2011). However, the results of this study indicate that recombinant swollenin from *K. lactis* may induce amorphogenesis of cellulosic substrates.
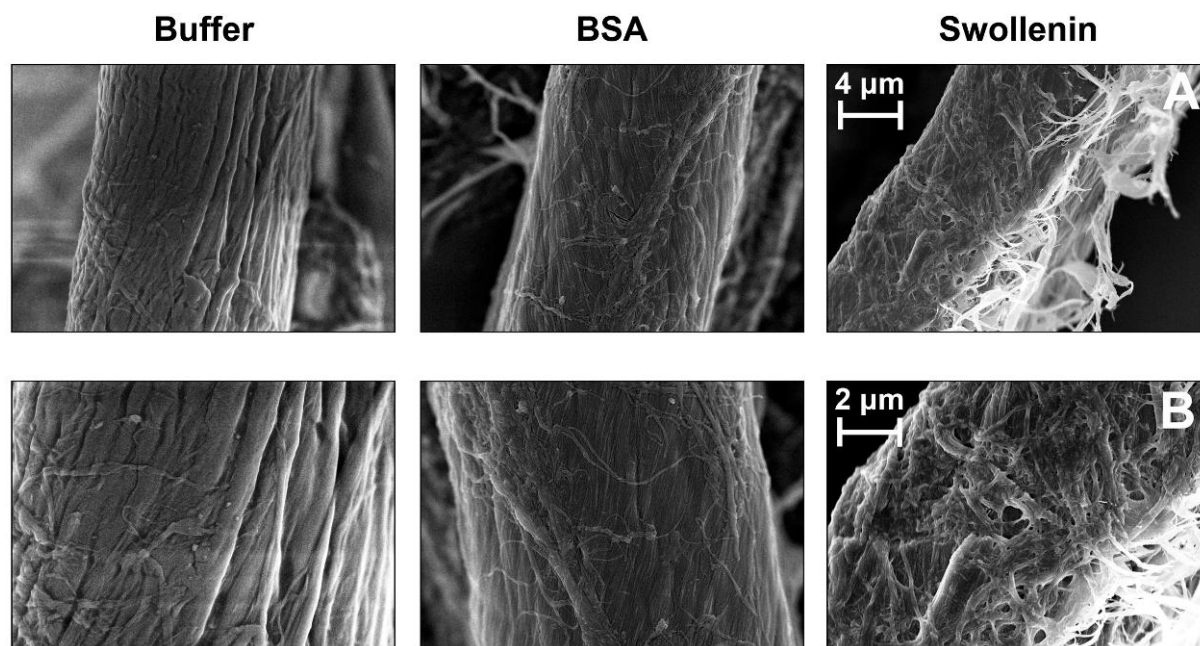
Figure 2-6:   Scanning electron microscopy of filter paper after pretreatment with swollenin. Pictures were taken at two different magnifications (**A, B**): see scale markers; pretreatment: 20 g/L cellulose in 0.05 M sodium acetate buffer (pH 4.8), 0.4 g/L BSA (~6 µmol/L) or swollenin (~5 µmol/L), $T = 45°C$, $V_L = 1$ mL, $n = 1000$ rpm, $d_0 = 3$ mm, incubation time 48 h; microscope: Hitachi S-5500 (Hitachi, Tokyo, JP).

The non-hydrolytic deagglomeration (Figure 2-5) or amorphogenesis (Figure 2-6) of cellulose was also described for single cellulose-binding domains of cellulases (Din et al., 1991; Gao et al., 2001; Hall et al., 2011) and for other expansin-related proteins from *Bacillus subtilis* (Kim et al., 2009), *Aspergillus fumigatus* (Chen et al., 2010), or *Bjerkandera adusta* (Quiroz-Castaneda et al., 2011a). However, there is no detailed and quantitative analysis of different cellulosic substrates after pretreatment with non-hydrolyzing proteins, especially with regard to swollenin.

2.3.4   Effect of Swollenin on the Physical Properties of Cellulose

To analyze in detail the effect of recombinant swollenin on cellulose, different cellulosic substrates were pretreated with buffer, BSA, or recombinant swollenin. After pretreatment and removal of bound proteins, the physical properties of the pretreated cellulosic substrates were analyzed by laser diffraction, cellulase adsorption studies, and crystallinity measurements.

2.3.4.1   Effect of Swollenin on the Particle Size of Cellulose

As seen in Figure 2-7A-D, the cellulosic substrates showed broad and inhomogeneous particle-size distributions. Upon considering the same cellulosic substrate, the pretreatments with buffer or BSA led to no differences in particle-size distributions and in the resulting geometric mean particle sizes (Figure 2-7E-H). After swollenin pretreatment, however, the particle-size distributions shifted to lower values, and large cellulose agglomerates were predominantly deagglomerated to smaller particles. The bigger the initial particle size of the corresponding cellulosic substrate was, the greater the total reduction in mean particle size by swollenin pretreatment was (filter paper > α-cellulose > Avicel). In the case of Sigmacell, all particle-size distributions were identical (Figure 2-7D), and the mean particle sizes did not change significantly by pretreatment with swollenin (Figure 2-7H). This may be explained by the small initial particle size of Sigmacell and the absence of cellulose agglomerates.
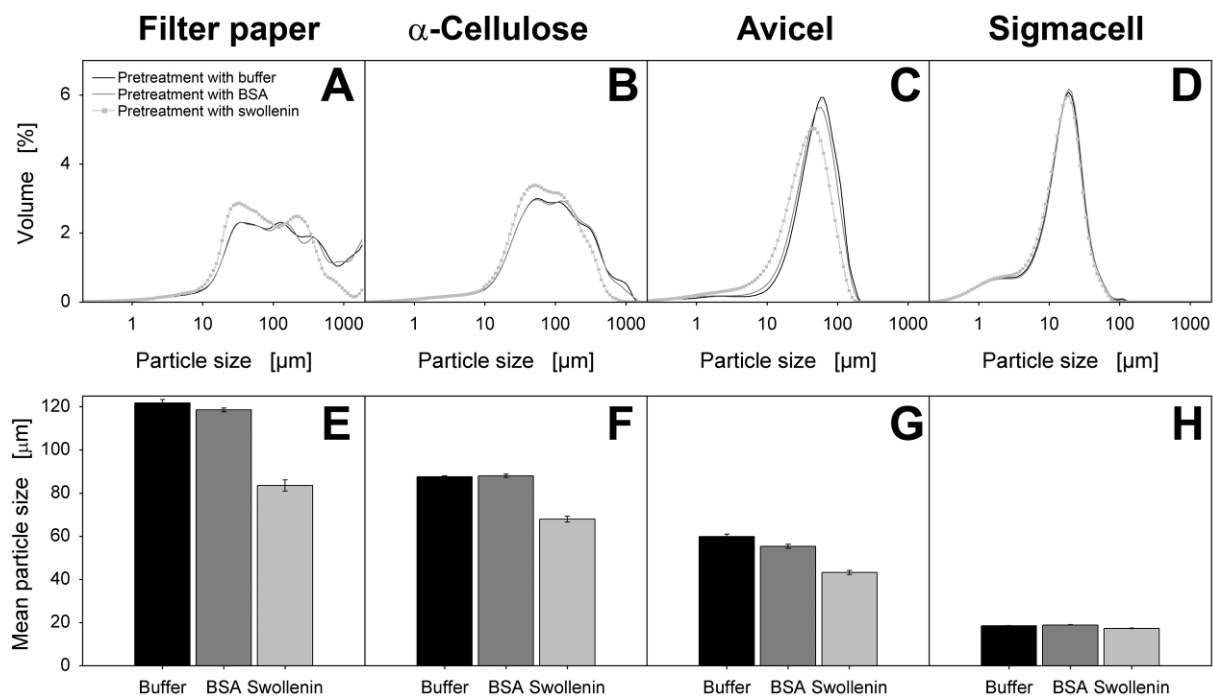
Figure 2-7: Particle size of cellulosic substrates after pretreatment with swollenin. (**A, B, C, D**) Volumetric particle-size distribution of pretreated cellulosic substrates: (**A**) Whatman filter paper No.1, (**B**) α-cellulose, (**C**) Avicel PH101, (**D**) Sigmacell 101; (**E, F, G, H**) geometric mean particle size of pretreated cellulosic substrates: (**E**) Whatman filter paper No.1, (**F**) α-cellulose, (**G**) Avicel PH101, (**H**) Sigmacell 101. Errors are given as standard deviations; pretreatment: 20 g/L cellulose in 0.05 M sodium acetate buffer (pH 4.8), 0.4 g/L BSA (~6 μmol/L) or 0.4 g/L swollenin (~5 μmol/L), $T = 45°C$, $V_L = 1$ mL, $n = 1000$ rpm, $d_0 = 3$ mm, incubation time 48 h; particles (< 2 mm) were analyzed using the particle size analyzer LS13320 (Beckman Coulter, Brea, USA).

2.3.4.2 Effect of Swollenin on the Accessibility of Cellulose

Since cellulosic particle sizes (external surface areas) influence cellulose accessibility (Chandra et al., 2007; Chandra et al., 2008), they also affect the adsorption of cellulases (Kim et al., 1988) and are an indication for the maximum cellulase adsorption (Arantes and Saddler, 2011). To investigate if swollenin pretreatment could actually affect cellulose accessibility, cellulase adsorption was analyzed after pretreatment with buffer or swollenin. According to various authors, the adsorption of total cellulase mixtures is not interpretable by simple Langmuir isotherms due to multicomponent cellulase adsorption (Beldman et al., 1987; Zhang and Lynd, 2004). Consequently, only the maximum cellulase adsorption $A_{max}(cellulase)$ was determined by applying different incubation times and a total cellulase mixture at high concentrations. Since no further increase in cellulase adsorption was detected after 1.5 h (data not shown), adsorption equilibrium was verified. According to the literature,

cellulase adsorption is rapid, and adsorption equilibrium is usually reached within 0.5-1.5 h (Lynd et al., 2002). Saturation of all applied cellulosic substrates was reached when using the following cellulase/cellulose ratios: $\geq$ 100 mg/g (in the case of filter paper or α-cellulose), $\geq$ 150 mg/g (Avicel), $\geq$ 200 mg/g (Sigmacell).

Table 2-1 finally summarizes the maximum cellulase adsorption (= adsorption capacity) onto all applied cellulosic substrates after pretreatment with buffer or swollenin. In general, the determined $A_{max}(cellulase)$ values are consistent with the adsorption data reported in the literature (Hong et al., 2007; Lynd et al., 2002; Zhang and Lynd, 2004). However, the pretreatment with swollenin caused a significant increase in maximum cellulase adsorption except for Sigmacell. The relative increase in cellulase adsorption between the pretreatment with swollenin and the pretreatment with buffer (filter paper > α-cellulose > Avicel > Sigmacell) showed a similar series as the relative reduction in mean particle size (filter paper > Avicel > α-cellulose > Sigmacell, Figure 2-7). Consequently, the increase in adsorption capacities of the swollenin-pretreated samples resulted primarily from the reduction in particle size and the corresponding increase in cellulose accessibility. However, in the case of α-cellulose, the increase in maximum cellulase adsorption was disproportionately higher. This can be explained by the effect of swollenin on other physical properties of cellulose, such as crystallinity, which may influence cellulase adsorption according to various authors (Hall et al., 2010; Ooshima et al., 1983). Moreover, since all applied cellulosic substrates do not contain lignin, its influence on cellulose accessibility (Rollin et al., 2011; Sathitsuksanoh et al., 2011; Selig et al., 2007; Selig et al., 2009) could be neglected.

Table 2-1:   Maximum cellulase adsorption onto cellulosic substrates after pretreatment with swollenin.

Substrate	Pretreatment with buffer $A_{max}(cellulase)$ [$mg_{cellulase}/g_{cellulose}$]	Pretreatment with swollenin $A_{max}(cellulase)$ [$mg_{cellulase}/g_{cellulose}$]
Whatman filter paper No. 1	16	31
α-Cellulose	21	35
Avicel PH101	52	73
Sigmacell 101	119	122

The coefficients of variation were below 7.5% for each value.

$A_{max}(cellulase)$ denotes the maximum cellulase adsorption.

2.3.4.3   Effect of Swollenin on the Crystallinity of Cellulose

To additionally determine the influence of swollenin on the crystallinity of cellulose, the *CrI* of all pretreated cellulosic substrates was analyzed by X-ray diffraction (XRD) measurements (Figure 2-8). A recrystallization of cellulose by incubation with aqueous solutions (Ouajai and Shanks, 2006; Wormald et al., 1996) was not observed, because the initial *CrI* of untreated substrates was higher than that of cellulosic substrates treated with buffer (data not shown). As illustrated by Figure 2-8, the pretreatment with buffer or BSA caused no differences in *CrI*; the *CrI* values were identical upon considering the same cellulosic substrate. By contrast, swollenin pretreatment specifically reduced the *CrI* as follows: filter paper (-10%), α-cellulose (-22%), and Avicel (-13%). However, in the case of Sigmacell, no effect of swollenin pretreatment on *CrI* was detected (Figure 2-8D) which can be explained by the low initial *CrI* and the amorphous structure of Sigmacell (Dourado et al., 1999). In the case of α-cellulose (Figure 2-8B), the strongest reduction in *CrI* was measured. Since α-cellulose is fibrous and can consist of up to 22% xylan (Gupta and Lee, 2009), it may be more sensitive to non-hydrolytic decrystallization (Whitney et al., 2000). Moreover, the strong reduction in the *CrI* of α-cellulose explains the disproportionate increase in maximum cellulase adsorption onto α-cellulose (Table 2-1), since cellulase adsorption can increase with decreasing *CrI* (Hall et al., 2010). As reported in the literature, similar reductions in crystallinity were found by using other non-hydrolyzing proteins: (1) *CrI* of Avicel decreased by 9-12% after pretreatment with single cellulose-binding domains (Hall et al., 2011); (2) *CrI* of filter paper decreased by 11.8% after pretreatment with Zea h, a protein from postharvest corn stover (Han and Chen, 2007). Up to now, however, the influence of swollenin on the *CrI* of different cellulosic substrates has not been quantified. Therefore, Chapter 2.3.4 and its subchapters provide the first proof that swollenin does induce deagglomeration of cellulose agglomerates as well as amorphogenesis (decrystallization) (Arantes and Saddler, 2010; Coughlan, 1985).
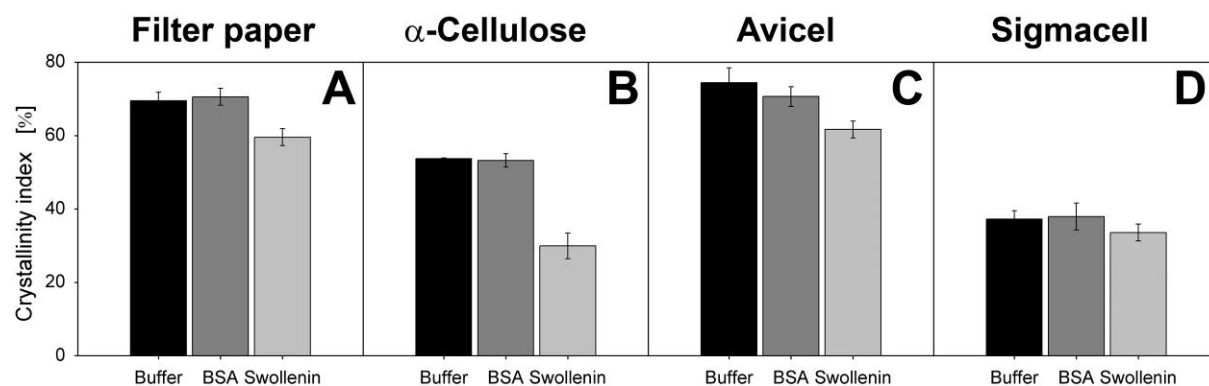
Figure 2-8:   Crystallinity index of cellulosic substrates after pretreatment with swollenin. **(A)** Whatman filter paper No.1; **(B)** α-cellulose; **(C)** Avicel PH101; **(D)** Sigmacell 101. Errors are given as standard deviations; pretreatment: 20 g/L cellulose in 0.05 M sodium acetate buffer (pH 4.8), 0.4 g/L BSA (~6 μmol/L) or 0.4 g/L swollenin (~5 μmol/L), T = 45°C, V_L = 1 mL, n = 1000 rpm, d_0 = 3 mm, incubation time 48 h; X-ray diffractometer: STADI P transmission diffractometer (STOE & Cie GmbH, Darmstadt, DE).

2.3.5   Hydrolysis of Swollenin-Pretreated Cellulose

Upon using the same cellulase mixture, enzymatic hydrolysis rates are especially affected by the physical properties of the applied cellulose (Kumar and Wyman, 2009c; Zhang and Lynd, 2004). Since swollenin pretreatment affected cellulose particle size, maximum cellulase adsorption as well as crystallinity, the resulting effects on subsequent hydrolysis of all pretreated cellulosic substrates were analyzed by using rebuffered Celluclast®. As shown in Figure 2-9A-C, swollenin pretreatment significantly accelerated cellulose hydrolysis, and the saccharification after 72 h was increased. In contrast, the corresponding hydrolysis curves for buffer and BSA were almost the same by comparing the same cellulosic substrate. This is attributed to the fact that pretreatment with buffer and BSA had no significant effect on particle size (Figure 2-7), maximum cellulase adsorption (Table 2-1) as well as on *CrI* (Figure 2-8). In the case of filter paper (Figure 2-9A), the hydrolysis-accelerating effect of swollenin pretreatment was stronger than that for α-cellulose (Figure 2-9B) and Avicel (Figure 2-9C). This may be explained by the substantial decrease in mean particle size (Figure 2-7) and the strong increase in maximum cellulase adsorption (Table 2-1) for filter paper by swollenin pretreatment. Figure 2-9D shows that the hydrolysis curves of Sigmacell were almost the same, since swollenin pretreatment did not change the physical properties of Sigmacell.
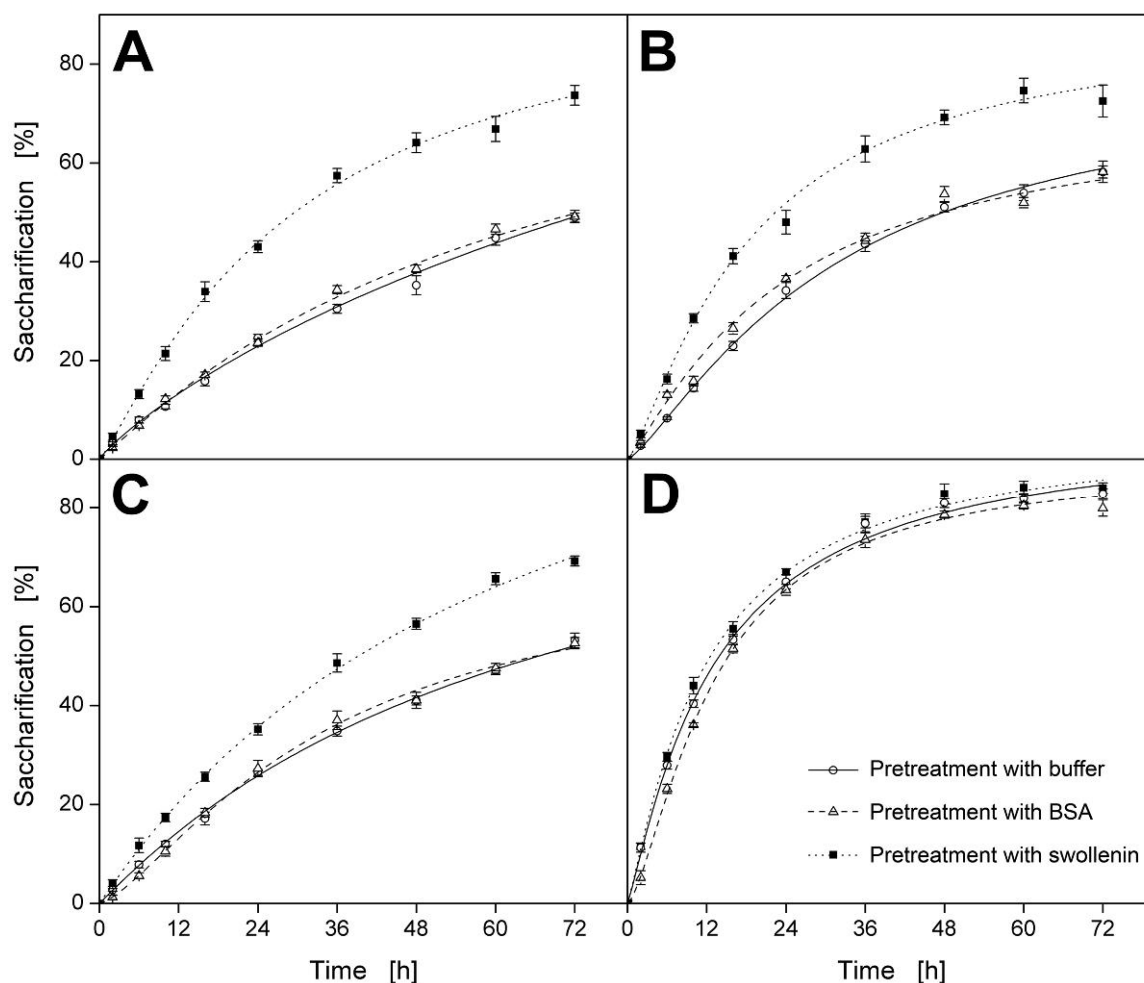
Figure 2-9:   Hydrolysis of cellulosic substrates after pretreatment with swollenin. (**A**) Whatman filter paper No.1; (**B**) α-cellulose; (**C**) Avicel PH101; (**D**) Sigmacell 101. Errors are given as standard deviations; pretreatment: 20 g/L cellulose in 0.05 M sodium acetate buffer (pH 4.8), 0.4 g/L BSA (~6 μmol/L) or 0.4 g/L swollenin (~5 μmol/L), $T = 45°C$, $V_L = 1$ mL, $n = 1000$ rpm, $d_0 = 3$ mm, incubation time 48 h; hydrolysis: 10 g/L pretreated cellulose in 0.05 M sodium acetate buffer (pH 4.8), 1 g/L rebuffered Celluclast®, $T = 45°C$, $V_L = 1$ mL, $n = 1000$ rpm, $d_0 = 3$ mm.

Furthermore, the relationship between the hydrolysis-accelerating effect and the amount of swollenin applied during pretreatment was investigated (Figure 2-10). Compared to the aforementioned experiments (Figures 2-9 and 2-10; 20 mg swollenin per g cellulose), less swollenin (5 mg per g cellulose) caused a less accelerated hydrolysis, and the final concentration of reducing sugars was 0.85-fold smaller (Figure 2-10). However, when the amount of swollenin was decreased merely from 20 mg/g to 15 mg/g, the same reducing sugar concentration was detected after 72 h. Since maximum swollenin adsorption was reached at higher initial swollenin concentrations (> 60 mg/g for 95% saturation, Figure 2-4), these results show that even non-saturating swollenin concentrations of 15-20 mg/g are sufficient

for a maximum hydrolysis-accelerating effect. This may be explained as follows: (1) not all accessible cellulose-binding sites must be occupied for a maximum hydrolysis-accelerating effect; (2) swollenin reversibly binds to cellulose, thereby performing further deagglomeration and amorphogenesis at multiple cellulose-binding sites. The reversible adsorption onto cellulose-binding sites was already reported for cellulases containing cellulose-binding domains (Linder and Teeri, 1996).
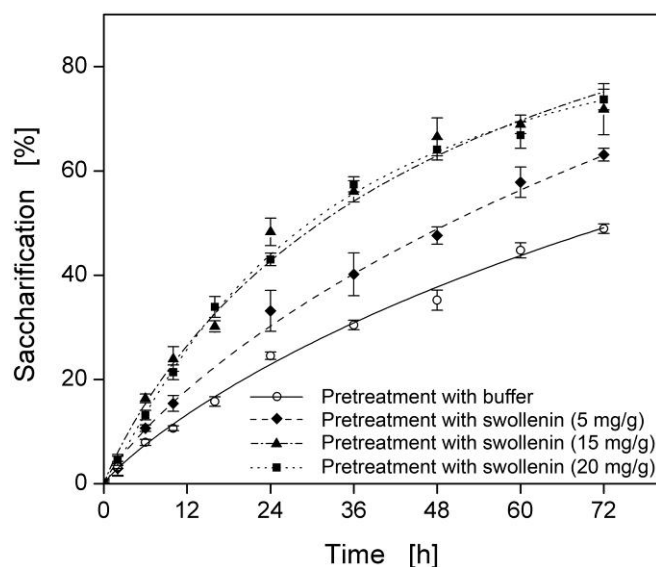
Figure 2-10:   Hydrolysis of filter paper after pretreatment with different swollenin concentrations. Errors are given as standard deviations; pretreatment: 20 g/L Whatman filter paper No.1 in 0.05 M sodium acetate buffer (pH 4.8), different concentrations of swollenin, $T = 45°C$, $V_L = 1$ mL, $n = 1000$ rpm, $d_0 = 3$ mm, incubation time 48 h; hydrolysis: 10 g/L pretreated cellulose in 0.05 M sodium acetate buffer (pH 4.8), 1 g/L rebuffered Celluclast®, $T = 45°C$, $V_L = 1$ mL, $n = 1000$ rpm, $d_0 = 3$ mm.

2.3.6   Correlating Hydrolysis Rates with the Physical Properties of Cellulose

Finally, an empirical correlation for initial hydrolysis rates based on *CrI* and mean particle size was determined for the pretreated cellulosic substrates (Figure 2-11). In this investigation, the correlation showed that the swollenin-induced reduction in *CrI* and particle size resulted in high cellulose hydrolysis rates. Furthermore, Figure 2-11 illustrates the aforementioned differences in cellulose hydrolysis rates (Figure 2-9) for various substrates and pretreatments. In addition, it confirms the following findings of other authors: (1) since smaller cellulose particle sizes lead to increased cellulase adsorption (Kim et al., 1988)

(Chapter 2.3.4.2), hydrolysis rates increase with decreasing cellulose particle size (Dasari and Berson, 2007; Yeh et al., 2010); (2) since a reduction in *CrI* leads to increased cellulase adsorption and higher reactivity of adsorbed cellulases, hydrolysis rates correlate inversely with the *CrI* of the applied cellulose (Hall et al., 2010). However, it should be noted that Figure 2-11 shows an empirical correlation for the conducted hydrolysis experiments. By applying other concentrations or types of cellulases and cellulosic substrates, different physical properties of the substrate (e.g. porosity, Huang et al., 2010) might predominate.
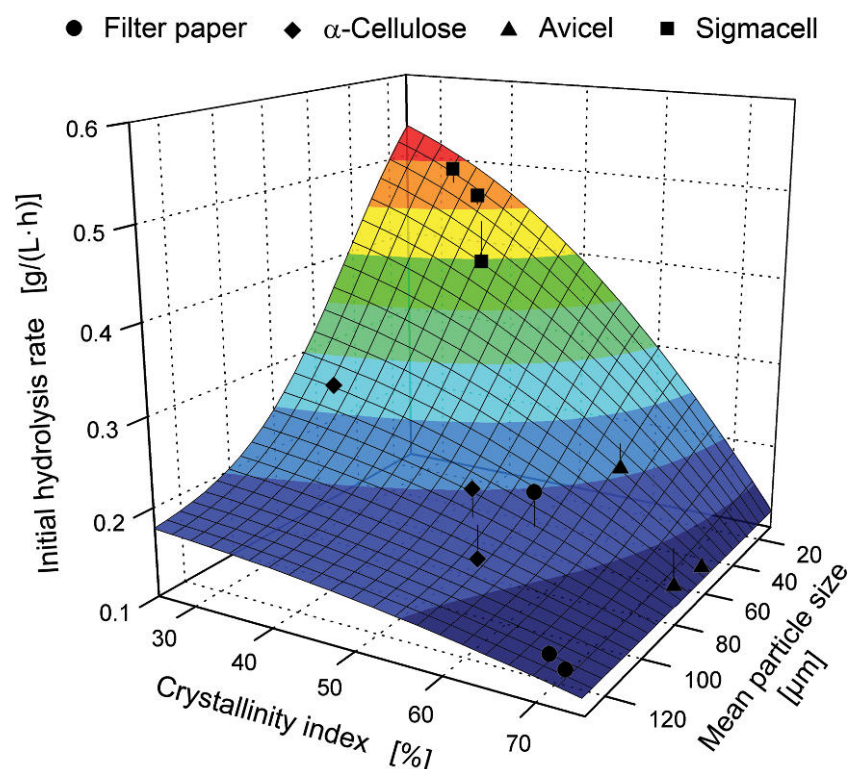
Figure 2-11:   Influence of crystallinity and mean particle size on the hydrolysis of cellulosic substrates. Data points were obtained from Figure 2-7 (mean particle size), Figure 2-8 (crystallinity index), and Figure 2-9 (initial hydrolysis rate from 0-6 h). TableCurve 3D was used to determine an empirical surface fit ($R^2 = 0.93$) based on a non-linear Gaussian cumulative function (Eq. 2-4).

2.4   Conclusions

Recombinant swollenin was easily produced with the yeast *K. lactis* and purified by affinity chromatography. Additionally, the adsorption of swollenin onto cellulose was quantified for the first time, and its adsorption parameters (A_{max}, K_D) were comparable to those of individual cellulases. The pretreatment with swollenin caused a significant decrease in particle size as

well as in crystallinity of the cellulosic substrates, thereby substantially increasing maximum cellulase adsorption. Moreover, pretreatment of the cellulosic substrates with swollenin – even in non-saturating concentrations – significantly accelerated the hydrolysis. By correlating particle size and crystallinity with initial hydrolysis rates, it could be shown that high initial hydrolysis rates resulted from the swollenin-induced reduction in particle size and crystallinity. Consequently, Chapter 2 shows an efficient means to produce recombinant swollenin with the robust yeast *K. lactis*. Moreover, it is shown that swollenin induces deagglomeration of cellulose agglomerates as well as amorphogenesis (decrystallization). For the first time, Chapter 2 quantifies and elucidates in detail how swollenin affects cellulosic substrates and their subsequent hydrolysis. Since standard assays are missing for deagglomeration, amorphogenesis, and the comparison of different non-hydrolyzing proteins, Chapter 2 may serve as an initial means to establish such assays.

A pretreatment of cellulosic substrates has been presented which is simply based on the incubation of recombinant swollenin under mild conditions. Since the enzymatic hydrolysis of cellulose is a rate-limiting processing step in biorefineries (Lynd et al., 2002), this pretreatment could significantly improve hydrolysis rates. To finally understand the action of swollenin on the cellulose surface, additional experiments need to be performed by using the single domains of swollenin (cellulose-binding domain and expansin-homologous domain). Thereby, it may be elucidated to what extend the single domains contribute to the swollenin-induced deagglomeration and amorphogenesis of cellulosic substrates. With respect to the action of swollenin, Saloheimo et al. (2002) already hypothesized that the expansin-homologous domain is able to stretch along the cellulose fiber. This ability may be important for the action of swollenin and primarily lead to its effects on cellulosic substrates.

To exclude possible side-effects between swollenin and cellulase, swollenin pretreatment was performed as a separate step within this study. After pretreatment, all cellulosic substrates were washed to remove adsorbed swollenin. From an industrial point of view, this additional desorption procedure may be too expensive. In future studies, swollenin should be directly added during cellulose hydrolysis. Here, possible side-effects between swollenin and cellulase, such as cooperative or competitive adsorption (Jeoh et al., 2002), need to be investigated.

3   Enzymatic Hydrolysis of Cellulose

As shown by the Figures 1-4 and 1-9, the pretreatment of (ligno-)cellulose is generally followed by the hydrolysis of cellulose. In Chapter 2, it was quantitatively shown how swollenin pretreatment affects relevant physical properties of cellulosic substrates and how it improves their subsequent hydrolysis. Besides the application of pretreatment techniques, the enzymatic hydrolysis of cellulose can also be improved by adjusting hydrolysis conditions or applying novel cellulases. To allow a knowledge-based improvement, the enzymatic cellulose hydrolysis needs to be characterized and a better understanding of its mechanism needs to be established (Lynd et al., 2002; Zhang and Lynd, 2004).

When characterizing the enzymatic hydrolysis of cellulose, practical insoluble cellulosic substrates and sophisticated cellulase assays are essential (Chapter 1.4.2.4). Therefore, within Chapter 3.1, insoluble α-cellulose is proposed as a practical cellulosic substrate to characterize cellulase adsorption and activity. Here, the influence of various hydrolysis conditions (such as hydrodynamics) is elucidated in detail. In Chapter 3.2, a new sophisticated cellulase assay is presented which combines high-throughput, online analysis, and insoluble cellulosic substrates.

3.1   Practical Screening and Characterization of Purified Cellobiohydrolases and Endoglucanases with α-Cellulose

3.1.1   Introduction

For the industrial use of lignocellulose, the hydrolysis of its main component cellulose to glucose is essential. As shown in Chapter 1.4.2.1, at least three different types of cellulases are involved during the enzymatic hydrolysis of cellulose (Himmel et al., 1999; Himmel et al., 2007; Lynd et al., 2002; Mielenz, 2001): cellobiohydrolase (CBH, EC 3.2.1.91), endoglucanase (EG, EC 3.2.1.4), and β-glucosidase (EC 3.2.1.21). As the cellulose depolymerization performed by CBHs and EGs is the rate-limiting step for the whole hydrolysis (Zhang et al., 2006), screening for CBHs and EGs is important. However, CBHs

and EGs are often characterized with different impractical model substrates that do not mimic the real biomass in biorefineries (Chapter 1.4.2.4) (Zhang et al., 2006). Thus, screening experiments need to be conducted with a more practical substrate such as α-cellulose so that proper cellulases are selected which best hydrolyze the biomass actually used in biorefineries.

α-Cellulose is a solid residue of lignocellulose after extraction with strong alkali (Adams and Bishop, 1953; Green, 1963; Sjöström and Alén, 1999) and mainly consists of cellulose and a small amount of hemicellulose (up to 22% (w/w) xylan; Gupta and Lee, 2009). α-Cellulose exhibits similar crystallinity and porosity to wood biomass (Zhang and Lynd, 2004) and shows the natural structure of cellulose fibers (Figure 3-1). Up to now, it has just been used for assaying total cellulase activity (Zhang et al., 2006). In contrast, conventional model substrates, further processed from α-cellulose, are more artificial (Sjöström and Alén, 1999), because they are dyed, derivatized, or water-soluble and show unnatural physical properties (such as accessibility, crystallinity, degree of polymerization) (Zhang et al., 2006). In particular, hydrolysis data based on water-soluble substrates are not pertinent to the realistic hydrolysis of insoluble substrates (Zhang et al., 2006), because the adsorption of cellulases onto the cellulosic substrate is ignored (Lynd et al., 2002; Pristavka et al., 2000; Rabinovich et al., 1982; Yuldashev et al., 1993). Consequently, insoluble α-cellulose is more natural and most similar to alkaline-pretreated cellulosic biomass used in biorefineries (Zhang et al., 2006).

Since α-cellulose is insoluble, the adsorption of cellulases onto α-cellulose is a prerequisite for hydrolysis (Lynd et al., 2002; Tanaka et al., 1986; Zhang and Lynd, 2004). Cellulase adsorption is usually analyzed using the Langmuir isotherm (Bansal et al., 2009). It assumes a single, reversible adsorption step to uniform cellulose-binding sites without interactions among cellulases. However, according to various authors, the cellulase adsorption onto the respective cellulose was found to be irreversible (Kyriacou et al., 1989; Ma et al., 2008; Palonen et al., 1999). In addition, cellulase interactions, cellulose heterogeneity, and porosity were also cited (Beldman et al., 1987; Carrard and Linder, 1999; Grethlein, 1985; Jeoh et al., 2002; Linder and Teeri, 1997). Consequently, several alternative adsorption models were developed (Linder and Teeri, 1996; Medve et al., 1997; Stahlberg et al., 1991; Woodward et al., 1988). Nevertheless, the Langmuir isotherm is the most common model for cellulase adsorption and is easily interpretable (Hoshino et al., 1992; Kumar and Wyman, 2009b; Lynd et al., 2002; Zhang and Lynd, 2004). Besides the applied cellulases and substrates,

temperature is especially important as it affects cellulase adsorption. Here, the amount of adsorbed cellulase is decreased with increasing temperature (Kim et al., 1992; Kyriacou et al., 1989; Medve et al., 1994; Ooshima et al., 1983).
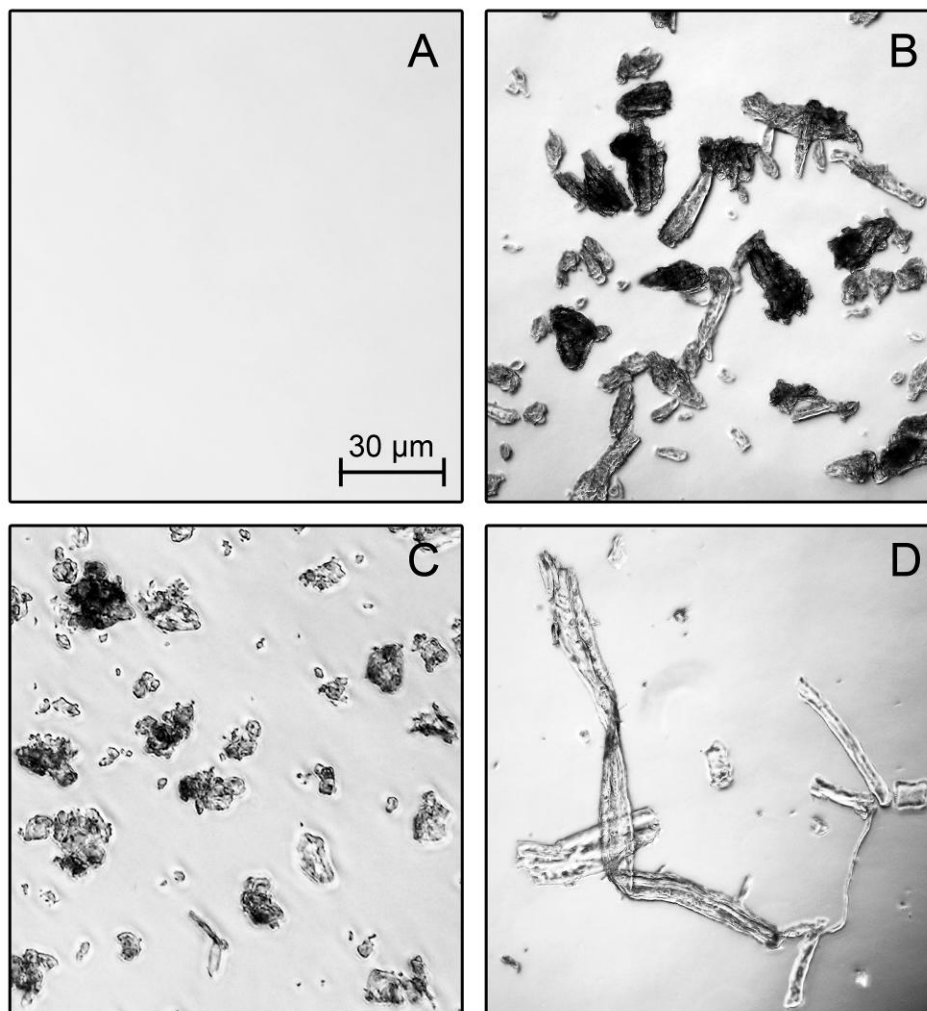
Figure 3-1:   Light microscopic pictures of the applied cellulosic substrates. (**A**) Carboxymethyl cellulose (water-soluble); (**B**) Avicel PH101; (**C**) Sigmacell 101; (**D**) α-cellulose; 10 g/L cellulose in 0.1 M sodium acetate buffer at pH 4.8; microscope: Eclipse E600 (Nikon, Tokyo, JP).

Few cellulase adsorption studies have been performed using α-cellulose or other fibrous substrates (Bansal et al., 2009), and these studies utilized complex cellulase systems (Gan et al., 2003; Moon et al., 2001; Peri et al., 2007; Shin et al., 2006); as yet, no purified cellulases have been analyzed with α-cellulose. As insoluble substrates are applied, attention has to be paid to hydrodynamics. Until now, cellulase adsorption and activity have not been investigated systematically by considering liquid mixing and particle suspension.

Besides the investigation of cellulase adsorption and activity, the kinetic modeling of cellulose hydrolysis is a powerful tool to quantitatively predict and understand the enzymatic hydrolysis of cellulose (Bansal et al., 2009; Zhang and Lynd, 2004). It allows the rapid study of a proposed hydrolysis process through the simple use of computational methods (Levine et al., 2010). By understanding the kinetics and mechanisms of the enzymatic cellulose hydrolysis, a rational design and optimization of the hydrolysis process can be achieved. Up to now, a large number of models have been developed to predict the enzymatic hydrolysis of cellulose (Bansal et al., 2009; Zhang and Lynd, 2004). These models can be divided into three categories: (1) empirical models, (2) semi-mechanistic models, and (3) mechanistic models. The development of fully mechanistic models is still ongoing due to the complexity of cellulose hydrolysis (Bansal et al., 2009; Engel et al., 2011). However, empirical and semi-mechanistic models have been successfully applied to predict initial hydrolysis rates and hydrolysis kinetics (Bailey, 1989; Engel et al., 2011; Zhang and Lynd, 2004). The semi-mechanistic models are particularly useful, since only few information are sufficient to describe the applied hydrolysis system (Bansal et al., 2009).

In Chapter 3.1, insoluble α-cellulose is proposed and applied as a more practical substrate to screen and characterize purified CBHs and EGs. Therefore, the adsorption and activity of these purified cellulases is analyzed in detail. Moreover, a semi-mechanistic model is developed to predict the kinetics of α-cellulose hydrolysis. In addition, the influence of various hydrolysis conditions (such as pH, temperature, and hydrodynamics) on the action of purified cellulases is elucidated. Here, this study investigates and correlates in detail cellulase adsorption and activity under different hydrodynamic conditions.

3.1.2   Materials and Methods

3.1.2.1   Cellulosic Substrates

The cellulosic substrates carboxymethyl cellulose (CMC), Avicel PH101, Sigmacell 101, and α-cellulose (Figure 3-1) were purchased from Sigma-Aldrich (St. Louis, USA). The physical properties and product information are presented in Table 3-1. The crystallinity index *CrI* of the cellulosic substrates was determined by powder X-ray diffraction (XRD) as described in Chapter 2.2.14. Different *CrI* values for Sigmacell 101 can be found in the literature (Dourado et al., 1999; Pala et al., 2002). In Chapter 2.3.4.3, other *CrI* values for

Sigmacell 101 were also determined. This may be explained by the varying quality of this cellulose type depending on batches and production location (Park et al., 2010). Nevertheless, Sigmacell 101 is typically chosen as a more amorphous cellulose (Dourado et al., 1999). The weight-average degree of polymerization DP_w was determined for all cellulosic substrates by gel permeation chromatography as described by Evans et al. (1989) – in cooperation with Roberto Rinaldi from the "Max-Planck-Institut für Kohlenforschung" (Mülheim an der Ruhr, DE). In addition, the geometric mean particle size d_P was analyzed by laser diffraction (Bowen, 2002) as described in Chapter 2.2.13.

Table 3-1:   Physical properties and product information of applied cellulosic substrates.

Substrate	Solubility in water	Impurities	CrI [%]	DP_w [AGU]	d_p [µm]	Brand	Product code
CMC	Soluble[a]	Pure[a]	-	400[c]	-	Fluka[d]	21900
Avicel PH101	Insoluble[a]	Pure[a]	82	200-240	43.82	Fluka[d]	11635
Sigmacell 101	Insoluble[a]	Pure[a]	Amorphous[e]	1590-1960	15.86	Sigma[d]	S6790
α-Cellulose	Insoluble[a]	Impure: 22% (w/w) xylan[b]	64	2140-2420	68.77	Sigma[d]	C8002

CMC, carboxymethyl cellulose; CrI, crystallinity index; DP_w, the weight-average degree of polymerization; d_P, geometric mean particle size.

[a] According to Zhang et al. (2006).

[b] According to Gupta and Lee (2009). The amount of xylan was verified for the α-cellulose batch, applied within this study, by complete enzymatic hydrolysis of α-cellulose and subsequent HPLC-analysis of glucose and xylose (data not shown).

[c] According to manufacture's data.

[d] Fluka and Sigma are subsidiaries of Sigma-Aldrich.

[e] In the case of Sigmacell 101, no clearly resolved X-ray diffraction profiles were detected. Instead, a smooth peak was detected which is typical for amorphous cellulose according to various authors (Bansal et al., 2010; Hall et al., 2010). Pala et al. (2002) found similar results for Sigmacell 101.

3.1.2.2 Purification of Cellulases

The commercial cellulase preparation Celluclast® 1.5L (Novozymes, Bagsværd, DK) was applied to purify the cellulases CBH I, CBH II, EG I, and EG II by using column chromatography, with an Äkta FPLC (GE Healthcare, Buckinghamshire, UK) which automatically measures conductivity and ultraviolet absorbance at 280 nm. All the columns were purchased from GE Healthcare. In addition, chromatographic experiments were carried

out at room temperature, and the automatically collected fractions were directly cooled at 4°C. For anion exchange chromatography, 7.5 mL Celluclast$^®$ was previously rebuffered using 0.05 M Tris-HCl buffer (pH 7) and Sephadex G-25 Fine (dimensions: 2.6 cm × 10 cm) at 110 cm/h. The rebuffered sample was loaded on DEAE-Sepharose (dimensions: 1.6 cm × 10 cm) at 60 cm/h using 0.05 M Tris-HCl (pH 7) as a running buffer. The bound proteins were eluted stepwise (35% v/v, 100% v/v) with 0.2 M sodium chloride in 0.05 M Tris-HCl buffer (pH 7). Furthermore, hydrophobic interaction chromatography was performed with 1 M ammonium acetate buffer (pH 5.5) and phenyl-Sepharose (dimensions: 1.6 cm × 2.5 cm) at 30 cm/h. No additional salts had to be added as ammonium effectively promotes ligand-protein interactions in hydrophobic interaction chromatography (Henrissat et al., 1985; Melander and Horvath, 1977). After loading of a rebuffered sample, the bound proteins were eluted with 0.05 M ammonium acetate buffer (pH 5.5). Moreover, cation exchange chromatography was performed with 0.02 M sodium acetate buffer (pH 3.6) and SP-Sepharose (dimensions: 1.6 cm × 2.5 cm) at 60 cm/h. The rebuffered sample was loaded, and bound proteins were eluted stepwise (15% v/v, 100% v/v) with 1 M sodium chloride in 0.02 M sodium acetate buffer (pH 3.6). Finally, when size exclusion chromatography was applied, a 0.6 mL sample was directly injected using 0.01 M sodium acetate buffer (pH 4.8) and Sephacryl S-200 HR (dimensions: 1.6 cm × 60 cm) at 15 cm/h.

3.1.2.3   SDS-Polyacrylamide Gel Electrophoresis of Cellulases

SDS-polyacrylamide gel electrophoresis (Laemmli, 1970) was applied to analyze the molecular mass (identity) and purity of single cellulases. The assay was performed as described in Chapter 2.2.5. In contrast to Chapter 2.2.5, the Prestained Protein Marker (New England Biolabs, Ipswich, USA) was used as a molecular mass marker (Appendix B).

3.1.2.4   Measurement of Cellulase Concentration

After cellulase purification, the cellulase concentrations of the final samples were analyzed by the bicinchoninic acid assay (Smith et al., 1985) as described in Chapter 2.2.7.

3.1.2.5   Qualitative Adsorption Study of Cellulases via Confocal Laser Scanning Microscopy

By applying confocal laser scanning microscopy, the adsorption of purified cellulases onto α-cellulose was qualitatively verified. As described in Chapter 2.2.9, purified cellulases were

labeled with fluorescein isothiocyanate (FITC), and FITC-labeled cellulases were subsequently dialyzed to remove excessive FITC. Two different blanks were labeled and dialyzed similarly: (1) without cellulase (= buffer) or (2) with BSA instead of cellulase. After labeling and dialysis, adsorption experiments were performed in 0.1 M sodium acetate buffer (pH 4.8) using 10 g/L α-cellulose and 1 g/L labeled cellulase. Solutions with α-cellulose and solutions with labeled cellulase were preincubated separately at 45°C for 10 min, and experiments were started by mixing both solutions. The final mixtures were incubated for 40 min as described in Chapter 2.2.9. To verify a specific adsorption of labeled cellulases, blanks without cellulases (= buffer) or with labeled BSA instead of labeled cellulases were incubated similarly. After incubation, the samples were put on ice and immediately analyzed by confocal laser scanning microscopy as described in Chapter 2.2.9.

3.1.2.6   Quantitative Adsorption Experiments with Cellulases

Quantitative adsorption experiments were performed in 0.1 M sodium acetate buffer (pH 4.8) using 10 g/L α-cellulose and various amounts (see below) of the particular cellulases CBH I and EG I. Solutions with α-cellulose and solutions with cellulases were preincubated separately at 45°C for 10 min, and experiments were started by mixing both solutions. The final mixtures were incubated as duplicates in 2 mL Eppendorf tubes with a filling volume $V_L = 1$ mL on a thermomixer MHR23 (HLC Biotech, Bovenden, DE) with a shaking diameter $d_0 = 3$ mm. Blanks, either without cellulase, neither substrate nor cellulase, or without substrate were incubated similarly. The incubation was stopped by centrifugation (8000 g, 1 min), and the supernatants were immediately analyzed for unbound cellulase using the bicinchoninic acid assay (Chapter 3.1.2.4). As single cellulases and short incubation times were applied, only small amounts of reducing sugars were produced and, therefore, cellulase adsorption could be analyzed by the bicinchoninic acid assay (Kumar and Wyman, 2008). The adsorbed cellulase concentration was calculated as the difference between initial (blanks) and unbound cellulase concentration.

In order to determine adsorption isotherms, the cellulase concentrations were varied between 0.01 g/L and 1.25 g/L. Preliminary adsorption kinetics showed that an incubation time of 40 min was needed to reach equilibrium. The shaking frequency was $n = 1000$ rpm to exclude mass transfer limitations. Adsorption isotherm parameters were determined using the Langmuir isotherm (Chapter 2.2.10 and Eq. 2-1).

In order to determine adsorption kinetics, the final cellulase concentration was 0.9 g/L, and the incubation time was varied between 0-100 min. Different shaking frequencies n = 0-1000 rpm were chosen to analyze hydrodynamic effects. Parameters for adsorption kinetics were determined using simple pseudo-first-order kinetics (Copeland, 2000):

$$A(t) = A_{EQ} \cdot (1 - e^{(-k_{ad} \cdot t)}) \tag{3-1}$$

In Eq. 3-1, $A(t)$ denotes the amount of adsorbed protein [$\mu mol_{protein}/g_{cellulose}$] at time t [s], A_{EQ}, the amount of adsorbed protein at equilibrium [$\mu mol_{protein}/g_{cellulose}$], and k_{ad}, the pseudo-first-order adsorption rate constant for approaching equilibrium [1/s]. To reach the complete saturation of α-cellulose, high cellulase concentrations were applied during kinetic adsorption studies. Consequently, A_{EQ} can be replaced by the maximum protein adsorption A_{max} [$\mu mol_{protein}/g_{cellulose}$].

$$A(t) = A_{max} \cdot (1 - e^{(-k_{ad} \cdot t)}) \tag{3-2}$$

3.1.2.7   Hydrolysis Experiments

Hydrolysis experiments with a final concentration of 10 g/L cellulose and 0.1 g/L cellulase were performed in 0.1 M sodium acetate buffer (pH 4.8). The mixtures were incubated as triplicates in 2 mL Eppendorf tubes with V_L = 1 mL on a thermomixer MHR23 at 45°C, n = 0-1000 rpm, and d_0 = 3 mm. Blanks, either without cellulase – neither substrate nor cellulase – or without substrate, were incubated similarly.

In case of kinetic experiments, samples were taken after defined time intervals, and the hydrolysis was stopped by boiling (10 min, 100°C). To determine initial cellulase activities, incubation times were fixed depending on the applied substrate: 10 min for CMC, 120 min for Avicel PH101, 30 min for Sigmacell 101, and 60 min for α-cellulose. Here, preliminary kinetic experiments showed that, during the fixed incubation times, the reducing sugar concentrations were linearly increasing, and inhibiting product concentrations were not reached. In addition, low enzyme concentrations were applied, so jamming of cellulases could

be neglected (Bommarius et al., 2008). The cellulase activities on Avicel and CMC were used to differentiate CBHs and EGs, respectively (Ghose, 1987; Zhang et al., 2006).

Finally, reducing sugars were quantified by applying the dinitrosalicylic acid assay (Chapter 3.1.2.8), and specific sugars (glucose, cellobiose, and cellotriose) were quantified via HPLC (Chapter 3.1.2.9).

3.1.2.8   Dinitrosalicylic Acid Assay and the Definition of Cellulase Activities

The amount of released reducing sugars was determined with the dinitrosalicylic acid assay (Miller, 1959) as described in Chapter 2.2.16. Product concentrations were calculated using glucose as a standard, and activities were expressed as the unit U (defined as $\mu mol_{glucose\ equivalents}$/min). As CBHs and EGs show different product profiles (Kim et al., 1994b), cellulase activities may be underestimated when glucose is used as a standard in reducing sugar assays (Zhang et al., 2006). Nevertheless, glucose is often applied (Ghose, 1987) when analyzing relative changes in single cellulase activities.

3.1.2.9   HPLC-Analysis of Soluble Sugars

Glucose, cellobiose, and cellotriose concentrations were measured with a Dionex HPLC Ultimate 3000 (Dionex, Sunnyvale, USA) – equipped with an organic acid-resin (300 mm x 8 mm, CS-Chromatographie, Langerwehe, DE) and a Shodex RI-101 detector (Showa Denko, Tokyo, JP). Sulphuric acid in a concentration of 5 mM was used as solvent at a flow rate of 0.6 mL/min and a temperature of 60°C.

3.1.2.10 Effect of pH and Temperature on Cellulase Activity

To analyze the influence of pH and temperature on cellulase activity, initial cellulase activities were determined at various incubation conditions while using α-cellulose as a substrate. Here, hydrolysis experiments were generally performed as described in Chapter 3.1.2.7. When analyzing the influence of pH, the hydrolysis experiments were conducted at a constant temperature of 45°C and in 0.1 M phosphate buffer at different pH values ranging from 2.1 to 8.6, adjusted with HCl and NaOH. Here, the phosphate buffer was used instead of sodium acetate buffer, since phosphate buffer exhibits a larger buffer capacity. However, when analyzing the influence of temperature, the hydrolysis experiments were conducted at different temperatures and in 0.1 M sodium acetate buffer at a constant pH value of 4.8.

Parameters describing the effect of the pH value on cellulase activity were determined using the following Eq. 3-3 (Copeland, 2000):

$$V = \frac{V_{pH,optimal}}{\left(\dfrac{[H^+]}{K_{a1}}\right) + \left(\dfrac{K_{a2}}{[H^+]}\right) + 1} \qquad (3\text{-}3)$$

where V denotes the cellulase activity [g/(L·h)] at a defined pH value, $V_{pH,optimal}$, the cellulase activity at optimal pH value [g/(L·h)], and K_{a1} and K_{a2} refer to the acid dissociation constants [mol/L] for the two hypothetical, relevant acid-base groups of the cellulase.

To describe the effect of temperature on cellulase activity, the Arrhenius equation was applied (Copeland, 2000):

$$k_{cat,app} = A_{pre} \cdot e^{\left(-\frac{E_A}{R} \cdot \frac{1}{T}\right)} \quad \Leftrightarrow \quad \ln(k_{cat,app}) = -\frac{E_A}{R} \cdot \frac{1}{T} + \ln A_{pre} \qquad (3\text{-}4)$$

In Eq. 3-4, $k_{cat,app}$ denotes the apparent turnover number [1/s] of the cellulase, A_{pre}, the pre-exponential factor [1/s], E_A, the activation energy of the reaction [kJ/mol], R, the ideal gas constant [8.314 J/(mol·K)], and T, the temperature [K]. At constant cellulase concentration and hydrolysis conditions, $k_{cat,app}$ can be replaced by the apparent maximum cellulase activity $V_{max,app}$ [g/(L·h)] (Copeland, 2000):

$$\ln(V_{max,app}) = -\frac{E_A}{R} \cdot \frac{1}{T} + \ln A_{pre} \qquad (3\text{-}5)$$

3.1.2.11 Determination of Hydrodynamics

In order to determine the hydrodynamics during the various adsorption and activity experiments, pictures of the liquid phase with immersed α-cellulose particles were taken at different shaking frequencies. A mixture of 10 g/L α-cellulose in 0.1 M sodium acetate buffer (pH 4.8) was shaken in a transparent 2 mL Eppendorf tube with an inner tube diameter $D_t = 1$ cm on an orbital shaking platform. The filling volume V_L and the shaking diameter d_0

were constant at V_L = 1 mL and d_0 = 3 mm. A miniature charged-coupled device camera XC-777AP (Sony, Tokyo, JP) was installed on the orbital shaking platform close to the Eppendorf tube, and video images were recorded. At all shaking frequencies, a pause of 5 min was given to allow the suspension to stabilize itself before the next shaking frequency was set. The critical shaking frequency n_{crit} [-] for liquid mixing, depending on the geometric (d_0, D_t, V_L) and physical parameters (liquid density ρ_L, surface tension σ) of the applied reaction system, was calculated according to Hermann et al. (2003):

$$n_{crit} = \sqrt{\frac{\sigma \cdot D_t}{4 \cdot \pi \cdot V_L \cdot \rho_L \cdot d_0}} \tag{3-6}$$

The critical shaking frequency n_{crit} is reached when the labor delivered by the centrifugal force is equal to the surface tension of the liquid. Since sodium acetate is capillary-inactive and cellulose loading was low, both their impacts were negligible.

3.1.2.12 Modeling of Cellulose Hydrolysis

A semi-mechanistic model was used to predict the kinetics of cellulose hydrolysis. The model was developed as described in Chapter 3.1.3.7.

3.1.2.13 Computational Methods

Parameters of the adsorption models (Chapter 3.1.2.6) and the activity models (Chapter 3.1.2.10) were calculated by nonlinear, least squares regression analysis using MATLAB version R2008b (The MathWorks, Natick, USA). The kinetics of cellulose hydrolysis (Chapter 3.1.2.12) was modeled with the software ModelMaker Version 3.0.4 (Cherwell Scientific Ltd, Oxford, UK). The model was solved with the Runge-Kutta method, and parameter estimation was performed by minimizing the sum of least squares using the simplex algorithm.

3.1.3   Results and Discussion

3.1.3.1   Purification of Cellulases

The enzyme mixture Celluclast[®], consisting of cellulolytic and xylanolytic enzymes produced by *Trichoderma reesei* (Gama et al., 1998; Henrissat et al., 1985; Herpoel-Gimbert et al., 2008), was used as the source material to purify the individual cellulases. According to their relative protein amount (Chapter 1.4.2.3), the main cellulases are CBH I, CBH II, EG I, and EG II (Goedegebuur et al., 2002; Nagendran et al., 2009; Rosgaard et al., 2007; Tolan and Foody, 1999). Figure 3-2 shows a flow diagram for the applied chromatographic purification of these various cellulases. After every purification step, the fractions were comprehensively analyzed by SDS-polyacrylamide gel electrophoresis and cellulase activity assays using Avicel and CMC to differentiate CBHs and EGs, respectively. The chromatograms and fraction analysis (including SDS-polyacrylamide gel electrophoresis and cellulase activity assay) of all purification steps are shown in Appendix A.

In order to determine the molecular mass and purity of the individual cellulases, SDS-polyacrylamide gel electrophoresis (Figure 3-3) and a densitometric analysis (Tan et al., 2007) were applied. By comparing the molecular masses with values reported in the literature (summarized in Table 1-2) (Gama et al., 1998; Henrissat et al., 1985; Herpoel-Gimbert et al., 2008; Jeoh et al., 2008; Schülein, 1988; Shoemaker et al., 1983; Tomme et al., 1988), the following cellulases were identified: CBH I (61 kDa), CBH II (54 kDa), EG I (55 kDa), and EG II (46 kDa). In addition, the amino acid sequence of each cellulase was determined by mass spectrometry (Schuchardt and Sickmann, 2007), and cellulase identities were checked using the Mascot database (Grosse-Coosmann et al., 2005) (data not shown). The final fractions showed cellulases with high purity (≥ 0.99), which is better or comparable with the results of other researchers (Ellouz et al., 1987; Henrissat et al., 1985; Medve et al., 1998b; Shoemaker et al., 1983). In other studies, only two or three of the major *T. reesei* cellulases could be purified (Medve et al., 1998b; Schülein, 1988; Shoemaker et al., 1983) or more purification steps were necessary (Gama et al., 1998).
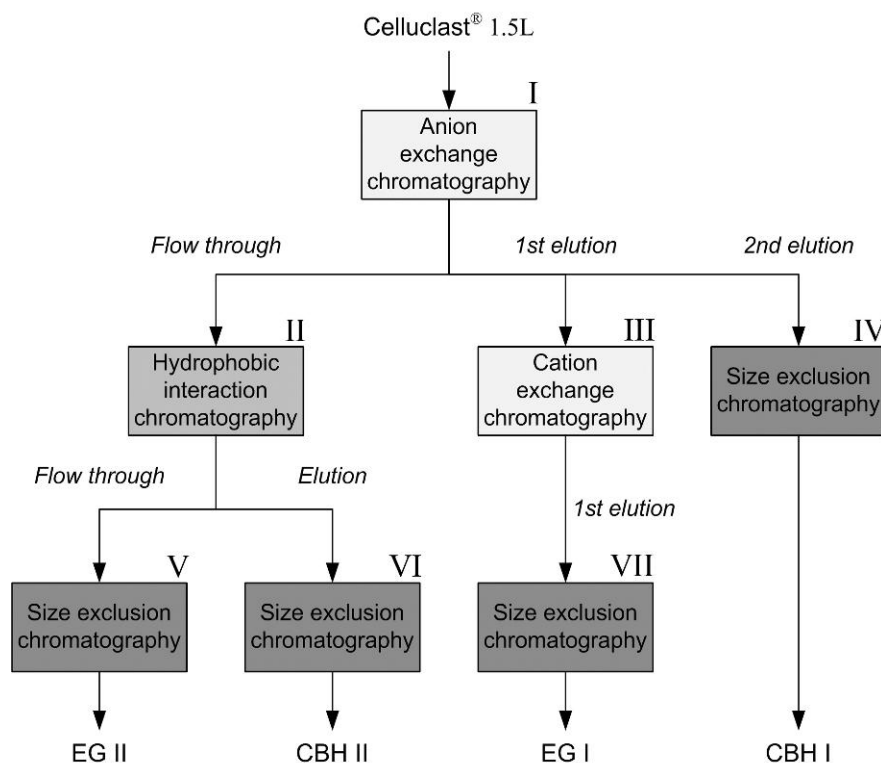
Figure 3-2:   Flow diagram for the applied chromatographic purification of the individual cellulases. Roman numbers indicate the different chromatographic purification steps. After every purification step, the fractions were analyzed by SDS-polyacrylamide gel electrophoresis and cellulase activity assays using Avicel and carboxymethyl cellulose (CMC) to differentiate cellobiohydrolases (CBH) and endoglucanases (EG), respectively. The chromatograms and fraction analysis (including SDS-polyacrylamide gel electrophoresis and cellulase activity assay) of all purification steps are shown in Appendix A.
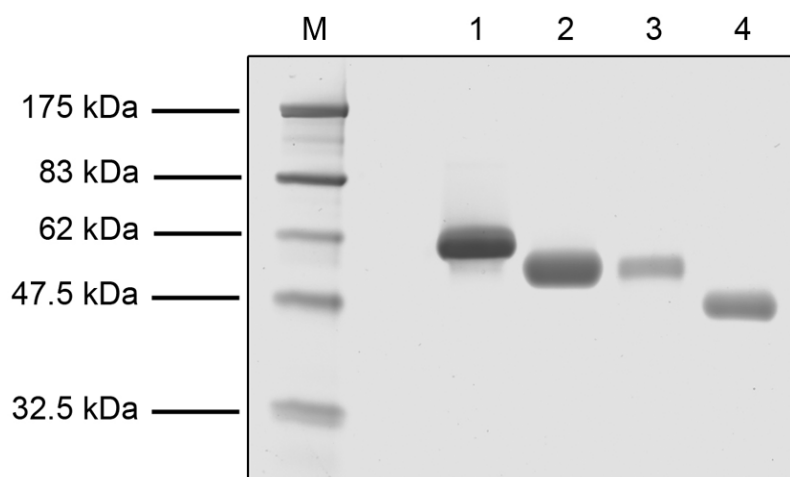
Figure 3-3:   SDS-polyacrylamide gel electrophoresis of the purified cellulases. (M) molecular mass marker, (1) cellobiohydrolase (CBH) I, (2) CBH II, (3) endoglucanase (EG) I, (4) EG II; 12% polyacrylamide gel, the same volume of the purified cellulase samples (15 µL) was loaded onto the particular slots.

3.1.3.2 Qualitative Adsorption Study of Cellulases via Confocal Laser Scanning Microscopy

Since the adsorption of cellulases is a prerequisite for cellulose hydrolysis, qualitative (Chapter 3.1.3.2) and quantitative adsorption studies (Chapters 3.1.3.3 and 3.1.3.4) were performed by the example of CBH I and EG I. After these were purified, their adsorption onto α-cellulose as a practical cellulosic substrate was analyzed.

For the initial qualitative analysis, CBH I and EG I were labeled with the fluorophore FITC and subsequently dialyzed to remove excessive FITC. Afterwards, the labeled cellulases were separately incubated with α-cellulose for 40 min. Finally, the resulting α-cellulose particles were analyzed by confocal laser scanning microscopy. Figure 3-4A shows that α-cellulose was fluorescent after incubation with FITC-labeled CBH I and FITC-labeled EG I. By contrast, after incubation with FITC-labeled BSA or buffer (negative controls), no fluorescent α-cellulose particles could be detected (data not shown). Therefore, the fluorescence was not caused by unspecific protein adsorption or direct labeling of α-cellulose by remaining FITC. Moreover, the reaction of FITC with amine and sulfhydryl groups of cellulases did not inhibit their adsorption onto cellulose. In accordance with the adsorption study of FITC-labeled swollenin onto filter paper (Figure 2-3A, Chapter 2.3.2), the fluorescence was not homogeneously distributed among a single α-cellulose particle (Figure 3-4A). Moreover, the fluorescence intensity varied between different particles. Here, the α-cellulose particles with a rough surface (black arrows, Figure 3-4) showed a slightly higher fluorescence than those particles with a smooth surface (white arrows, Figure 3-4). As already described in Chapter 2.3.2, this inhomogeneity may again be explained by different and partially inaccessible α-cellulose-binding sites (Carrard and Linder, 1999; Linder and Teeri, 1997) resulting from: (1) the inhomogeneous structure of α-cellulose (Figure 3-4B), (2) amorphous and crystalline regions of α-cellulose (Table 3-1), and (3) the general porosity of cellulose particles (Grethlein, 1985; Zhang and Lynd, 2004).

Cellobiohydrolase I   Endoglucanase I
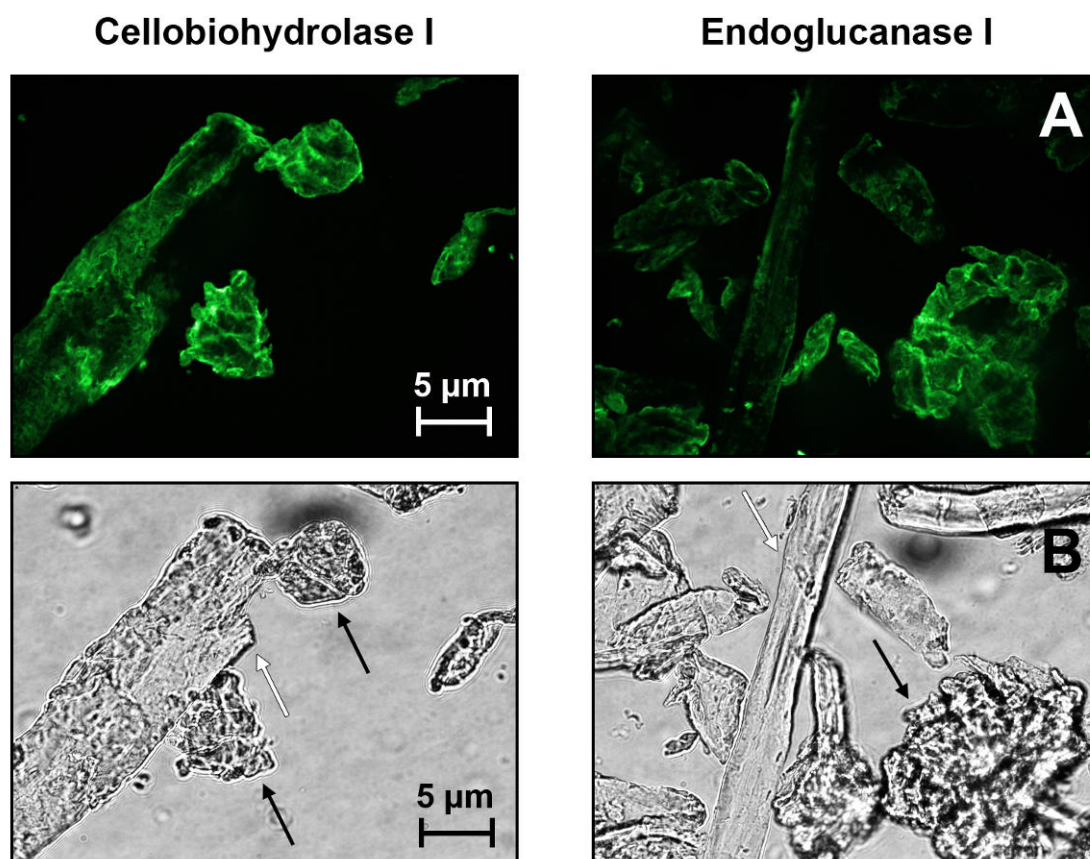
Figure 3-4: Confocal laser scanning microscopy of α-cellulose after incubation with fluorescein isothiocyanate (FITC)-labeled cellobiohydrolase (CBH) I or endoglucanase (EG) I. (**A**) Fluorescence microscopy at 521 nm; (**B**) light microscopy. Rough particle surfaces and smooth particle surfaces are indicated with black arrows and white arrows, respectively; labeling: FITC Labeling Kit (Merck, Darmstadt, DE) according to the manufacturer's protocol; incubation: 10 g/L α-cellulose in 0.1 M sodium acetate buffer (pH 4.8), 1 g/L FITC-labeled CBH I or 1 g/L EG I, $T = 45°C$, $V_L = 1$ mL, $n = 1000$ rpm, $d_0 = 3$ mm, incubation time 40 min; microscope: Opera system (PerkinElmer, Waltham, USA).

3.1.3.3   Adsorption Isotherms of Cellulases

After qualitatively verifying the adsorption of CBH I and EG I, the adsorption isotherms of these purified cellulases were determined by using α-cellulose. Preliminary adsorption kinetics showed that an incubation of 40 min was needed to reach equilibrium. As seen in Figure 3-5, isotherms of CBH I and EG I showed the adsorption to be a characteristic function of free cellulase concentration. After a sharp increase in adsorbed cellulase at low cellulase concentrations, a plateau was reached at higher concentrations (> 10 μmol/L). In addition, denatured CBH I and EG I, boiled for 10 min, showed no adsorption (data not shown). Therefore, cellulase adsorption was specific and required functional protein structures.

Figure 3-5: Adsorption isotherms of the purified cellulases onto α-cellulose. (●) Cellobiohydrolase (CBH) I, (○) endoglucanase (EG) I. Predicted Langmuir isotherms, according to Eq. 2-1, are shown as solid lines, and corresponding parameters are listed in Table 3-2; incubation: 10 g/L α-cellulose in 0.1 M sodium acetate buffer (pH 4.8), $T = 45°C$, $V_L = 1$ mL, $n = 1000$ rpm, $d_0 = 3$ mm, reaction time 40 min.

In this investigation, the Langmuir isotherm (Eq. 2-1) provided a good fit (Figure 3-5, Table 3-2). The dissociation constant K_D, as a reciprocal value for adsorption affinity, was lower for CBH I than for EG I. Different values for K_D have to be derived from differences in cellulose-binding domains or catalytic domains. According to Linder et al. (1995), the cellulose-binding domains of CBH I and EG I show single amino acid substitutions leading to differences in binding affinity. In addition, catalytic domains of cellulases are known to specifically adsorb to cellulose-binding sites independently of cellulose-binding domains (Lynd et al., 2002). The maximum cellulase adsorption A_{max} was higher for EG I than for CBH I, indicating more accessible cellulose-binding sites for EG I, which was also observed by other researchers (Beldman et al., 1987; Nidetzky et al., 1994b). Besides the aforementioned differences in cellulase structure and binding affinity, these maximum adsorption differences could be explained by the lower molecular mass of EG I (Chapter 3.1.3.1) and, therefore, a better access to internal binding sites as described for other proteins and materials (Hunter and Carta, 2002; Oberholzer and Lenhoff, 1999). Nidetzky et al. (1994b) found similar values of K_D and A_{max} by using filter paper as cellulosic substrate (CBH I: 0.71 μmol/L, 0.17 μmol/g; EG I: 1.79 μmol/L, 0.17 μmol/g). Filter paper shows similar CrI and DP_w values as α-cellulose (Kongruang et al., 2004; Zhang and Lynd, 2004; Zhang et al., 2006) and is used for the measurement of total cellulase activity (Ghose, 1987; Wood and Bhat, 1988).

However, the filter paper assay requires considerable effort and is error-prone (Coward-Kelly et al., 2003; Decker et al., 2003). Furthermore, many adsorption studies were performed at low temperatures (2-5°C) to prevent cellulose hydrolysis and, thus, cellulase desorption (Lee et al., 1982; Lu et al., 2002; Medve et al., 1997; Nidetzky and Steiner, 1993; Reinikainen et al., 1995; Srisodsuk et al., 1993). In this study, a more practical temperature of 45°C was selected similar to those temperatures in cellulose hydrolysis. Here, no decrease in adsorbed cellulase was observed.

Table 3-2:   Langmuir adsorption parameters of purified cellulases by using α-cellulose at $n = 1000$ rpm.

Cellulase	Langmuir adsorption parameters[a]		
	A_{max} [μmol/g]	K_D [μmol/L]	R^2 [-]
CBH I	0.155 ± 0.003	0.433 ± 0.039	0.93
EG I	0.212 ± 0.010	2.146 ± 0.216	0.90

Errors are given as standard deviations.

CBH, cellobiohydrolase; EG, endoglucanase; A_{max}, maximum cellulase adsorption; K_D, dissociation constant; R^2, coefficient of determination.

[a] According to Eq. 2-1.

3.1.3.4 Adsorption Kinetics of Cellulases

According to Figure 3-6, the adsorption kinetics of CBH I and EG I on α-cellulose were determined. For both cellulases, the respective adsorption rose quickly until a final plateau was reached. The final amount of adsorbed cellulase did not change with further incubation. Seemingly, α-cellulose does not contain many micropores (Lee et al., 1983) that can only be penetrated slowly by cellulases (Kim et al., 1994a). As shown in Table 3-3, the simple pseudo-first-order kinetic model (Eq. 3-2) provided a good fit. Taking experimental errors into account, similar values for A_{max} were determined as in adsorption isotherm experiments (Table 3-2), and, thus, the complete saturation of α-cellulose was reached in kinetic studies. The kinetic constant k_{ad} was higher for CBH I than for EG I (Table 3-3), and saturation was reached after 25 min and 40 min, respectively (Figure 3-6). As with filter paper, similar incubation times were found for CBH I and EG I (Nidetzky et al., 1994b). In general, cellulase adsorption is rapid compared to the time required for complete hydrolysis (Lynd et al., 2002; Zhang and Lynd, 2004). Depending on the applied cellulose, the adsorption equilibrium is normally reached after 30-90 min (Boussaid and Saddler, 1999; Kim et al., 1994b; 1994a; 1998; Kumar and Wyman, 2009b; Medve et al., 1998a; Singh et al., 1991).
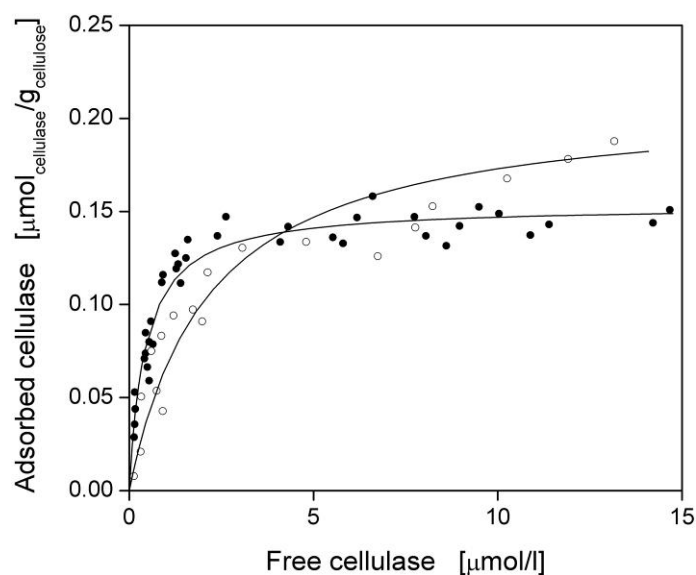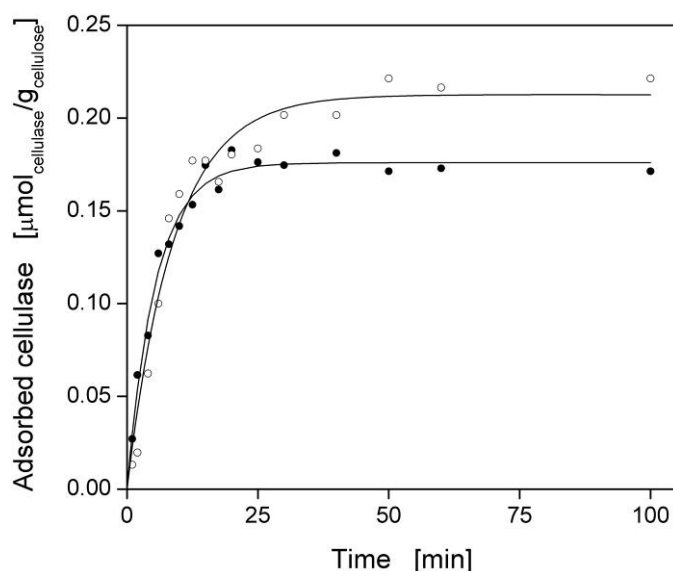
Figure 3-6: Adsorption kinetics of the purified cellulases onto α-cellulose. (●) Cellobiohydrolase (CBH) I, (○) endoglucanase (EG) I. Predicted adsorption kinetics, according to Eq. 3-2, are shown as solid lines, and corresponding parameters are listed in Table 3-3; incubation: 10 g/L α-cellulose in 0.1 M sodium acetate buffer (pH 4.8), 0.9 g/L cellulase, $T = 45°C$, $V_L = 1$ mL, $n = 1000$ rpm, $d_0 = 3$ mm.

Table 3-3: Kinetic adsorption parameters of purified cellulases by using α-cellulose at $n = 1000$ rpm.

Cellulase	Kinetic adsorption parameters[a]		
	A_{max} [μmol/g]	k_{ad} [1/s]	R^2 [-]
CBH I	0.170 ± 0.003	0.0031 ± 0.0002	0.98
EG I	0.213 ± 0.007	0.0019 ± 0.0002	0.96

Errors are given as standard deviations.

CBH, cellobiohydrolase; EG, endoglucanase; A_{max}, maximum cellulase adsorption; k_{ad}, pseudo-first-order adsorption rate constant; R^2, coefficient of determination.

[a] According to Eq. 3-2.

3.1.3.5 Sugar Production Patterns of Cellulases

After cellulase adsorption studies, the hydrolytic activities of CBHs and EGs towards α-cellulose were investigated. At first, the sugar production patterns of all purified cellulases were determined by HPLC analysis. As shown by Figure 3-7A-B, CBH I and CBH II mainly produced cellobiose during α-cellulose hydrolysis. This result is in good agreement with the literature, since CBHs release cellobiose from the ends of cellulose chains (Chapter 1.4.2.1) (Kim et al., 1994b; Lynd et al., 2002; Medve et al., 1998a). By contrast, EG I and EG II produced cellotriose, cellobiose, and glucose in a mass ratio of approximately 1.0:3.3:2.2

(Figure 3-7C-D), which fits to typical production profiles of EGs (Kim et al., 1994b; Medve et al., 1998a). In conclusion, the hydrolytic activity of all purified cellulases could be verified. Since the sugar production profiles are consistent with the typical profiles reported in the literature (Kim et al., 1994b; Medve et al., 1998a), these results provide an additional evidence for the high purity of the isolated cellulases (Chapter 3.1.3.1).
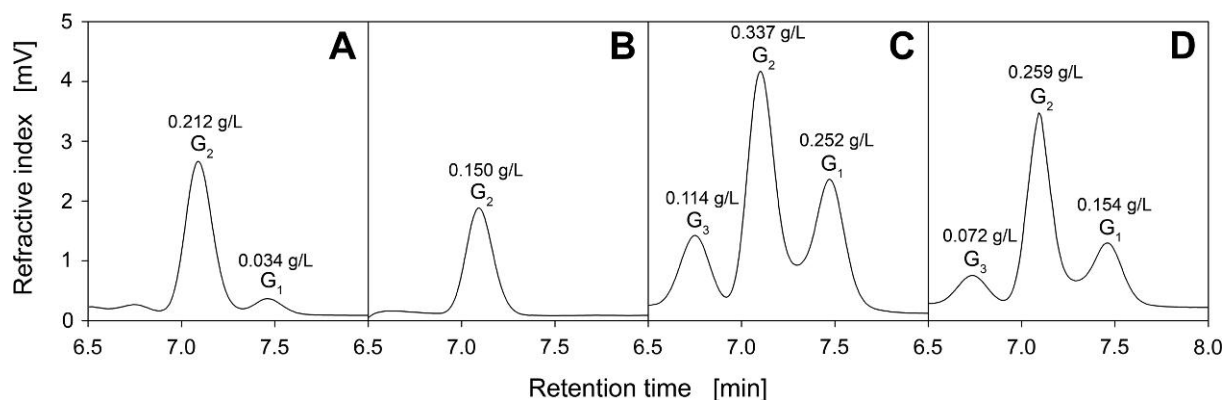
Figure 3-7:   Soluble sugars produced by enzymatic hydrolysis of α-cellulose. (**A**) Cellobiohydrolase (**CBH**) I; (**B**) CBH II; (**C**) endoglucanase (EG) I; (**D**) EG II. The concentrations of cellotriose (G_3), cellobiose (G_2), and glucose (G_1) are shown above the respective symbols; incubation: 10 g/L α-cellulose in 0.1 M sodium acetate buffer (pH 4.8), 0.1 g/L cellulase, $T = 45°C$, $V_L = 1$ mL, $n = 1000$ rpm, $d_0 = 3$ mm, reaction time: 60 min; high-performance liquid chromatography (HPLC) system: Dionex HPLC Ultimate 3000 (Dionex, Sunnyvale, USA).

3.1.3.6 Kinetics of Cellulose Hydrolysis Catalyzed by Cellulases

After analyzing the adsorption and sugar production patterns of purified cellulases, the enzymatic hydrolysis of α-cellulose was investigated in detail. Therefore, α-cellulose was hydrolyzed by different concentrations of CBH I and EG I, and the formation of reducing sugars was measured over time (Figure 3-8). At the start of all kinetic experiments, the reducing sugar concentration rose quickly and showed a linear increase. Depending on the applied cellulase concentration, this linear increase was detected from 0-2 h (0.1 g/L cellulase) or 0-1.5 h (0.25 g/L cellulase). When using the higher CBH I concentration of 0.25 g/L, the initial hydrolysis rate did not proportionally increase. This can be explained by the adsorption isotherm of CBH I, indicating that the saturation of cellulose-binding sides already started at a CBH I to cellulose ratio of 0.25 $g_{cellulase}$ per 10 $g_{cellulose}$ (equivalent to 0.41 $\mu mol_{cellulase}$ per 1 $g_{cellulose}$; Chapter 3.1.3.3). After the rapid increase in reducing sugar concentration, the hydrolysis rates declined for both cellulases. In case of CBH I, final plateaus were reached after 10 h whereas, in case of EG I, a slight increase in reducing sugars

was still detected from 5-10 h. Moreover, EG I led to significantly higher hydrolysis rates and yields than CBH I. This can be explained by the fact that α-cellulose contains amorphous and crystalline regions (Table 3-1, *CrI*: 64%). Since EGs more rapidly hydrolyze amorphous regions than CBHs, EGs generally show higher hydrolysis rates towards partially amorphous substrates such as α-cellulose (Gama et al., 1998; Zhang and Lynd, 2004; Zhang et al., 2006).
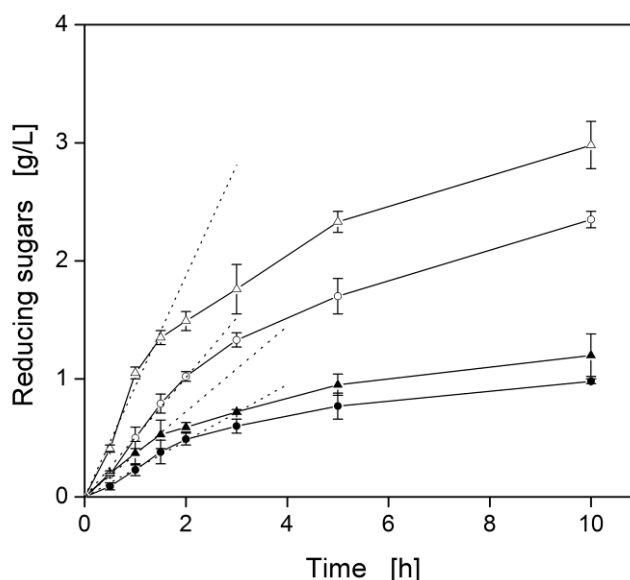
Figure 3-8:   Hydrolysis of α-cellulose by using purified cellulases. (●) 0.1 g/L cellobiohydrolase (CBH) I, (○) 0.1 g/L endoglucanase (EG) I, (▲) 0.25 g/L CBH I, (△) 0.25 g/L EG I. For each hydrolysis experiment, the initial linear increase in reducing sugar concentration is shown as a dotted line; incubation: 10 g/L α-cellulose in 0.1 M sodium acetate buffer (pH 4.8), $T = 45°C$, $V_L = 1$ mL, $n = 1000$ rpm, $d_0 = 3$ mm.

In general, the detected decline in cellulose hydrolysis rates (Figure 3-8) can be explained by the following four factors: cellulose depletion, cellulase inactivation, product inhibition, or alteration of the physical cellulose properties (Bansal et al., 2009; Bommarius et al., 2008; Zhang et al., 1999; Zhang and Lynd, 2004). According to Figure 3-8, only a small amount of 10 g/L α-cellulose was hydrolyzed after 10 h. Therefore, the depletion of cellulose was minimal and not the main factor leading to the detected decline in cellulose hydrolysis rates. Since cellulases from *T. reesei* are stable under the applied incubation conditions (residual activity after six days: > 90%; Engel et al., 2010; Engel et al., 2011), the inactivation of cellulases can be neglected. As shown by HPLC analysis (Chapter 3.1.3.5), glucose and cellobiose were the main products after the enzymatic hydrolysis of α-cellulose by CBH I and EG I. Since cellulases are severely inhibited by these sugars (Holtzapple et al., 1990), product inhibition is one possible explanation for the detected decline in cellulose hydrolysis rates

(Figure 3-8). Moreover, the alteration of physical cellulose properties can lead to a rapid decline in hydrolysis rates (Bansal et al., 2009; Väljamäe et al., 1999; Zhang and Lynd, 2004). Although several researchers have analyzed cellulose during its hydrolysis, the decline in hydrolysis rates has not been clearly elucidated so far (Zhang and Lynd, 2004). For example, a decrease in cellulose accessibility (Fan et al., 1980) and in maximum cellulase adsorption (= adsorption capacity) was detected (Bansal et al., 2009; Bommarius et al., 2008; Ooshima et al., 1983). The unproductive adsorption of cellulases onto prehydrolyzed cellulose was also described to block further hydrolysis (Ooshima et al., 1990; Zhang and Lynd, 2004). Moreover, cellulose reactivity can decrease during enzymatic hydrolysis (Bansal et al., 2009; Zhang and Lynd, 2004). According to Carrard et al. (2000), the fresh addition of non-hydrolyzed cellulose stimulated more soluble sugar formation, thereby indicating the loss of cellulose reactivity at the end of hydrolysis. Although various researchers have tried to analyze the decrease in cellulose reactivity (Carrard et al., 2000; Desai and Converse, 1997; Drissen et al., 2007; Hong et al., 2007; Yang et al., 2006; Zhang et al., 1999), there is no consensus regarding the incidence and reasons for declining cellulose reactivity (Bansal et al., 2009; Lynd et al., 2002).

3.1.3.7   Modeling of Cellulose Hydrolysis Catalyzed by Cellulases

As described in Chapter 3.1.1, kinetic modeling is a powerful tool to understand and eventually improve the enzymatic hydrolysis of cellulose (Bansal et al., 2009; Zhang and Lynd, 2004). Up to now, a large number of models have been developed to predict the enzymatic cellulose hydrolysis (Bansal et al., 2009; Zhang and Lynd, 2004). According to Chapter 3.1.1, semi-mechanistic models are particularly useful, since only few information are sufficient to describe the applied reaction system (Bansal et al., 2009).

In order to model the α-cellulose hydrolysis catalyzed by purified cellulases (Chapter 3.1.3.6, Figure 3-8), a semi-mechanistic model was developed within this chapter. The developed model is based on the Michaelis-Menten kinetics (Copeland, 2000) which often provide a good fit for the enzymatic hydrolysis of insoluble cellulose (Bansal et al., 2009; Zhang and Lynd, 2004):

$$\frac{dC}{dt} = -\frac{k_{cat,app} \cdot E_{ad} \cdot C}{K_{M,app} + C} \tag{3-7}$$

where C denotes the cellulose concentration [g/L], $k_{cat,app}$, the apparent turnover number [1/s] of the cellulases, E_{ad}, the adsorbed cellulase concentration [mg$_{protein}$/L], and $K_{M,app}$, the apparent Michaelis constant [g/L]. By incorporating the correction coefficient between molecular weights of glucose and glucan monomers (180/162), the increase in reducing sugar concentration P [g/L] can be calculated as follows:

$$\frac{dP}{dt} = -\frac{dC}{dt} \cdot \frac{180}{162} \tag{3-8}$$

To account for the detected decline in cellulose hydrolysis rates (Chapter 3.1.3.6, Figure 3-8), additional terms for the product inhibition of cellulases and the alteration of cellulose properties during hydrolysis (such as a decrease in cellulose accessibility and reactivity) were included. At first, the competitive inhibition by soluble reducing sugars was implemented. Since the structural information of cellulases and a large amount of experimental data indicate the competitive inhibition of single cellulases by cellobiose and glucose, competitive inhibition is the most common applied mechanism for modeling cellulase inhibition (Levine et al., 2010; Levine et al., 2011; Zhang and Lynd, 2004). According to various studies (Bansal et al., 2009; Kadam et al., 2004), the alteration of cellulose properties was addressed by using a linear decreasing hydrolysis rate with increasing cellulose conversion. By contrast, the sole Michaelis-Menten kinetics (Eq. 3-7) leads to a non-linear decreasing hydrolysis rate with increasing cellulose conversion. By combining the aforementioned linear term with the Michaelis-Menten kinetics, a disproportionately stronger decline in hydrolysis rates was achieved. Finally, Eq. 3-7 was changed as follows:

$$\frac{dC}{dt} = -\frac{k_{cat,app} \cdot E_{ad} \cdot C}{K_{M,app} \cdot \left(1 + \dfrac{P}{K_i}\right) + C} \cdot \frac{C}{C_0} \tag{3-9}$$

where K_i is the inhibition constant [g/L], and C_0 is the initial cellulose concentration [g/L].

To calculate the concentration of adsorbed cellulase E_{ad}, a cellulase mass balance (Eq. 3-10) was included, with E_0 denoting the initial cellulase concentration [g/L] and E denoting the free/unbound cellulase concentration in solution [g/L].

$$E_{ad} = E_0 - E \qquad (3\text{-}10)$$

Moreover, the cellulase adsorption kinetics was implemented as described in the Chapters 3.1.2.6 and 3.1.3.4:

$$\frac{dE_{ad}}{dt} = -\frac{dE}{dt} = k_{ad} \cdot E \qquad (3\text{-}11)$$

where k_{ad} is the pseudo-first-order adsorption rate constant for approaching equilibrium [1/s]. Here, it should be noted that Eq. 3-11 is not mechanistically sound. It assumes an adsorption rate which only depends on the free cellulase concentration. Consequently, Eq. 3-11 allows a complete adsorption of all cellulases. However, not all free cellulases can bind onto the cellulose due to limited cellulose-binding sites and an equilibrium condition between adsorbed and unbound cellulases. Therefore, a maximum permissible value for E_{ad} was included by using the Langmuir equation according to the Chapters 3.1.2.6 and 3.1.3.3:

$$E_{ad,EQ} = \frac{A_{max} \cdot C \cdot E}{K_D + E} \quad ; \quad E_{ad,EQ} = E_{ad}(t \to \infty) \qquad (3\text{-}12)$$

In Eq. 3-12, $E_{ad,EQ}$ denotes the adsorbed cellulase concentration at equilibrium [$mg_{protein}$/L], A_{max}, the maximum cellulase adsorption [$mg_{protein}$/$g_{cellulose}$], and K_D, the dissociation constant [$mg_{protein}$/L]. Within the final model, the total time period for approaching equilibrium ($t \to \infty$) was set to be 40 min, according to Chapter 3.1.3.4.

The experimental data and modeled hydrolysis curves are shown in Figure 3-9. The developed semi-mechanistic model provided a good fit for both CBH I and EG I at two different cellulase concentrations. The coefficients of determination for all modeled hydrolysis curves are listed in the legend of Figure 3-9. Only in the case of EG I at a concentration of 0.25 g/L, the applied model slightly underestimated the formation of

reducing sugars within the first 2 h. All applied model parameters are summarized in Table 3-4. The parameters A_{max}, k_{ad}, and K_D were experimentally determined within the previous Chapters 3.1.3.3 and 3.1.3.4, whereas the remaining parameters $k_{cat,app}$, K_i, and $K_{M,app}$ had to be fitted to the hydrolysis data presented in Figure 3-9.
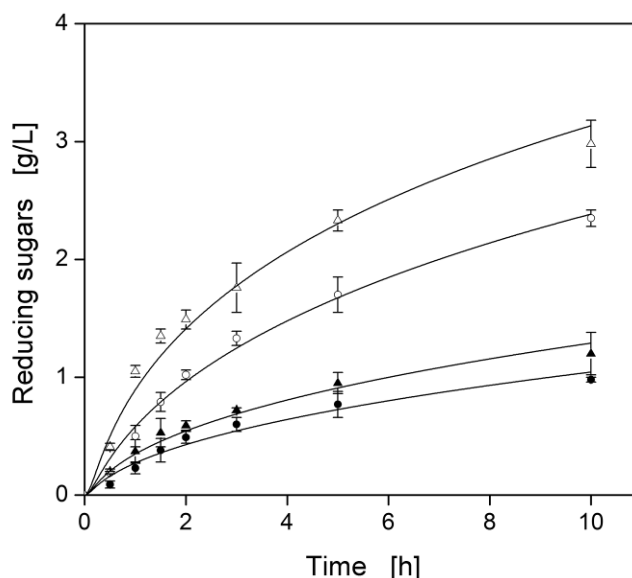
Figure 3-9:   Semi-mechanistic model for the hydrolysis of α-cellulose by using purified cellulases. (●) 0.1 g/L cellobiohydrolase (CBH) I, (○) 0.1 g/L endoglucanase (EG) I, (▲) 0.25 g/L CBH I, (△) 0.25 g/L EG I. Experimental data was obtained from Figure 3-8. Predicted hydrolysis kinetics, according to the model described in Chapter 3.1.3.7, are shown as solid lines, and corresponding parameters are listed in Table 3-4. The coefficients of determination are as follows: 0.1 g/L CBH I ($R^2 = 0.95$), 0.1 g/L EG I ($R^2 = 0.97$), 0.25 g/L CBH I ($R^2 = 0.96$), 0.25 g/L EG I ($R^2 = 0.91$); incubation: 10 g/L α-cellulose in 0.1 M sodium acetate buffer (pH 4.8), $T = 45°C$, $V_L = 1$ mL, $n = 1000$ rpm, $d_0 = 3$ mm.

The fitted K_i values of CBH I and EG I were 0.03 g/L and 0.08 g/L, respectively (Table 3-4). Consequently, CBH I was more inhibited by reducing sugars than EG I. Several studies analyzed the inhibitory effect of glucose, cellobiose, or reducing sugars (Holtzapple et al., 1990; Zhang and Lynd, 2004). In the case of CBH I from *Trichoderma* spec., similar K_i values were also determined: 0.032 g/L (Levine et al., 2010), 0.036 g/L (Halliwell and Griffin, 1973), 0.065 g/L (Levine et al., 2011), or 0.387 g/L (Maguire, 1977). In the case of EGs from *T. reesei*, a wide range of K_i values was reported by various authors: 0.003 g/L (Levine et al., 2010), 0.01 g/L (Levine et al., 2011), or 3.762 g/L (Gruno et al., 2004). This difference in K_i values may be explained by the different physical properties of the applied cellulosic substrate which strongly influence the inhibition of cellulases (Gruno et al., 2004). As shown by Table 3-4, the fitted $k_{cat,app}$ and $K_{M,app}$ values of CBH I and EG I were as follows:

CBH I: 0.0035 1/s, 2.83 g/L; EG I: 0.0073 1/s, 1.41 g/L. Huang (1975) reported similar values for $k_{cat,app}$ (0.02 1/s) and $K_{M,app}$ (1.68 g/L) when analyzing the hydrolysis of completely amorphous cellulose catalyzed by a cellulase mixture. Since completely amorphous cellulose leads to higher hydrolysis rates (Hall et al., 2010) and a cellulase mixture shows a synergistic interaction between the individual cellulases (Engel et al., 2011; Nidetzky et al., 1994a), the $k_{cat,app}$ value determined by Huang (1975) was higher than those values for CBH I and EG I of the current study. However, the developed model precisely described the hydrolysis of α-cellulose catalyzed by single CBHs or EGs (Figure 3-9).

Table 3-4: Model parameters for the hydrolysis of α-cellulose by using purified cellulases.

Cellulase	A_{max} [mg/g][a]	k_{ad} [1/s]	K_D [mg/L][a]	$k_{cat,app}$ [1/s]	K_i [g/L]	$K_{M,app}$ [g/L]
CBH I	10.370[c]	0.0031[c]	26.413[b]	0.0035	0.03	2.83
EG I	11.715[c]	0.0019[c]	118.03[b]	0.0073	0.08	1.41

Fitted model parameters are marked in grey. Other model parameters were experimentally determined.

CBH, cellobiohydrolase; EG, endoglucanase; A_{max}, maximum cellulase adsorption; k_{ad}, pseudo-first-order adsorption rate constant; $k_{cat,app}$, apparent turnover number; K_D, dissociation constant; K_i, inhibition constant; $K_{M,app}$, apparent Michaelis constant.

[a] Molar amounts were converted into masses by using the molecular masses of CBH I (61 kDa) and EG I (55 kDa) according to Chapter 3.1.3.1.

[b] According to Figure 3-5 and Table 3-2.

[c] According to Figure 3-6 and Table 3-3.

In general, the sole Michaelis-Menten model is not mechanistically sound for the enzymatic hydrolysis of insoluble cellulose because of the following reasons (Bansal et al., 2009; Lynd et al., 2002; Zhang and Lynd, 2004): (1) cellulases need to adsorb onto the cellulose, and hydrolysis occurs on the surface of cellulose fibers; (2) cellulose is not uniform and exhibits variable physical properties that are altered during hydrolysis; (3) the Michaelis-Menten condition – substrate being in excess relative to enzyme – is not achieved at high cellulase/cellulose ratios, since the fraction of cellulose accessible to cellulases is relatively low; (4) the Michaelis-Menten condition may not be retained during hydrolysis since cellulose is depleted at higher conversions; (5) cellulose hydrolysis represents a heterogeneous reaction system including mass transfer limitations. Within this study, some of the aforementioned limitations were already addressed by implementing simple terms for cellulase adsorption (Eq. 3-10 to Eq. 3-12) and the alteration of physical cellulose properties

(Eq. 3-9). Moreover, specific hydrolysis conditions were selected in order to avoid additional limitations. For example, low cellulase/cellulose ratios and single cellulases were applied to minimize cellulose conversion and, thus, cellulose depletion. Moreover, an appropriate hydrodynamic condition was chosen so that the cellulose surface was accessible to the cellulases and mass transfer limitation could be excluded (a detailed discussion about hydrodynamic conditions and their effects is given in the later Chapter 3.1.3.9).

In conclusion, the developed model was well suited to describe the hydrolysis of α-cellulose by purified cellulases, since the basic Michaelis-Menten model was extended by additional mathematical terms and specific hydrolysis conditions were chosen. By using this model, it could be clearly shown that the product inhibition of cellulases as well as the alteration of cellulose properties led to incomplete cellulose hydrolysis. However, in order to understand all aspects of cellulose hydrolysis, fully mechanistic models need to be established (Zhang and Lynd, 2004). Such models have to consider all phenomena during enzymatic hydrolysis and all physical properties of cellulose. Despite several advances in mechanistic modeling of the enzymatic cellulose hydrolysis (Levine et al., 2010; Levine et al., 2011), no fully mechanistic model has been developed which precisely predicts the kinetics of cellulose hydrolysis from low up to high conversions.

3.1.3.8   Effect of pH and Temperature on Cellulases

As shown in Chapter 3.1.3.6, reducing sugar concentrations were linearly increasing within the initial phase (0-2 h) of α-cellulose hydrolysis. Therefore, initial cellulase activities could be determined within 1 h when using 10 g/L α-cellulose and 0.1 g/L purified cellulase. To analyze the influence of pH and temperature on cellulase activity, initial activities of CBH I and EG I were determined at various incubation conditions.

When analyzing the influence of pH on cellulase activity, the hydrolysis experiments were conducted at a constant temperature of 45°C and in 0.1 M phosphate buffer at different pH values. As shown by Figure 3-10A, the activity of CBH I and EG I was a characteristic function of pH, and a typical bell-shaped profile was detected. Here, the applied model describing the pH dependency of enzymes (Eq. 3-3) provided a good fit, and the corresponding parameters (pK_{a1}, pK_{a2}, and $V_{pH,optimal}$) are listed in Table 3-5. The optimal activity of CBH I and EG I was achieved at pH values of 5.0 and 4.8, respectively. Several authors found similar optimal pH values ranging from 4.5 to 5 when using cellulases from

T. reesei (Becker et al., 2001; Boer and Koivula, 2003; Busto et al., 1996; Busto et al., 1998; Voutilainen et al., 2008). Moreover, Maguire (1977) determined almost identical pK_{a1} (3.8) and pK_{a2} values (6.5) when analyzing the hydrolysis of α-cellulose by CBH I.
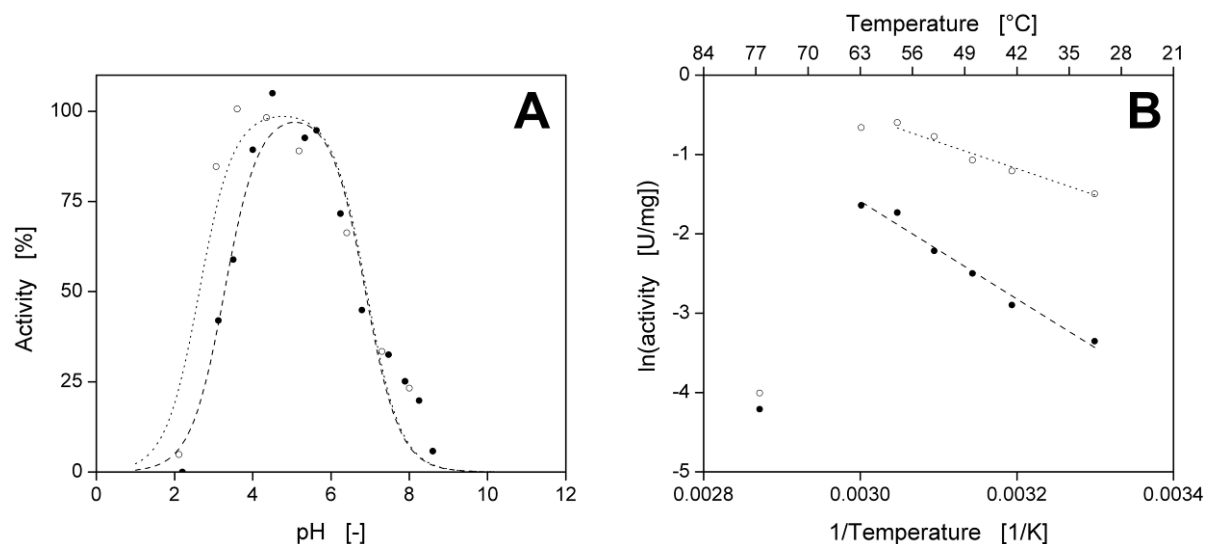
Figure 3-10:   Effects of pH and temperature on the activity of purified cellulases. (**A**) Effect of pH on the activity of cellobiohydrolase (CBH) I (●) and endoglucanase (EG) I (○). Relative values are standardized to maximum activities (CBH I: 0.20 U/mg; EG I: 0.54 U/mg). Predicted cellulase activities, according to Eq. 3-3, are shown as dashed line (CBH I) and dotted line (EG I), and corresponding parameters are listed in Table 3-5; incubation: 10 g/L α-cellulose in 0.1 M sodium phosphate buffer, $T = 45°C$, $V_L = 1$ mL, $n = 1000$ rpm, $d_0 = 3$ mm, 0.1 g/L cellulase, reaction time: 60 min; (**B**) Arrhenius plot of the activity of CBH I (●) and EG I (○). Predicted activities, according to Eq. 3-5, are shown as dashed line (CBH I) and dotted line (EG I), and corresponding parameters are listed in Table 3-5; incubation: 10 g/L α-cellulose in 0.1 M sodium acetate buffer (pH 4.8), $V_L = 1$ mL, $n = 1000$ rpm, $d_0 = 3$ mm, 0.1 g/L cellulase, reaction time: 60 min.

Table 3-5:   Parameters describing the effects of pH and temperature on the activity of purified cellulases.

Cellulase	Parameters (pH model)[a]				Parameters (Arrhenius model)[b]		
	$V_{pH,optimal}$ [g/(L·h)]	pK_{a1} [-]	pK_{a2} [-]	R^2 [-]	E_A [kJ/mol]	lnA_{pre} [-]	R^2 [-]
CBH I	0.20 ± 0.01	3.28 ± 0.16	6.88 ± 0.17	0.93	50.9 ± 4.2	16.8 ± 1.6	0.98
EG I	0.54 ± 0.06	2.63 ± 0.29	6.91 ± 0.28	0.90	29.9 ± 3.6	10.3 ± 1.4	0.97

Errors are given as standard deviations.

CBH, cellobiohydrolase; EG, endoglucanase; A_{pre}, pre-exponential factor; E_A, activation energy; K_a, acid dissociation constant; R^2, coefficient of determination; $V_{pH,optimal}$, cellulase activity at optimal pH value.

[a] According to Eq. 3-3.

[b] According to Eq. 3-5.

When analyzing the influence of temperature on cellulase activity, the hydrolysis experiments were conducted at different temperatures and in 0.1 M sodium acetate buffer at a constant pH value of 4.8. Figure 3-10B shows that the activities of purified CBH I and EG I increased up to temperatures of 58°C and 56°C, respectively. In case of higher temperatures, cellulase activities decreased due to enzyme denaturation (Copeland, 2000; Voutilainen et al., 2008). In the literature (Busto et al., 1996; Busto et al., 1998; Voutilainen et al., 2008), similar optimal temperatures (55-60°C) were reported when analyzing the initial activities of *T. reesei* cellulases. In addition, the Arrhenius equation (Eq. 3-5) provided a very good fit (Figure 3-10B), and activation energies could be determined (Table 3-5). When using α-cellulose as cellulosic substrate, the activation energies for CBH I and EG I were 50.9 kJ/mol and 29.9 kJ/mol, respectively. In the literature (Busto et al., 1998; He et al., 2000; Hu et al., 2009; Li et al., 1965; Maguire, 1977), similar activation energies ranging from 22-52 kJ/mol were determined when using cellulases from *Trichoderma* spec. and various cellulosic substrates (including α-cellulose). However, the difference in activation energies between CBH I and EG I may be explained by their different modes of action (Chapter 1.4.2.1): (1) CBHs hydrolyze amorphous and crystalline regions of cellulose, and they release soluble cellobiose as the major product (Lynd et al., 2002) (Chapter 3.1.3.5); (2) EGs primarily hydrolyze amorphous regions and release soluble sugars (such as cellotriose, cellobiose, and glucose; Chapter 3.1.3.5) as well as longer insoluble cellulose chains (Lynd et al., 2002). Here, it should be noted that, besides the applied cellulases, the physical properties of cellulose (especially cellulose crystallinity/reactivity) also affect the activation energies of the enzymatic cellulose hydrolysis (Lynd et al., 2002; Rautela and King, 1968).

3.1.3.9 Effect of Hydrodynamics on Cellulases

As α-cellulose is an insoluble substrate, the hydrodynamics of the reaction system have to be taken into account. Therefore, the impact of shaking frequency and the resulting hydrodynamics on the adsorption as well as on the activity of the cellulases were investigated in detail for the first time.

Adsorption kinetics of CBH I and EG I were determined for different shaking frequencies using simple pseudo-first-order kinetics (Figure 3-11A). This model provided a good fit at all shaking frequencies; in contrast to Nidetzky et al. (1994b), no biphasic adsorption kinetics with two different adsorption rates were observed. At all applied shaking frequencies and as seen in prior experiments (Tables 3-2 and 3-3), A_{max} (solid line) was higher for EG I, and k_{ad}

(dotted line) was higher for CBH I. Between 0 rpm and 300 rpm, A_{max} and k_{ad} were almost constant for both cellulases, whereas for both a sharp increase could be determined between 300 rpm and 800 rpm. Above 800 rpm, only a slight increase in k_{ad} was observed. Consequently, enhanced mixing improved the contact between cellulase and substrate (Ingesson et al., 2001), and, therefore, the mass transfer and the kinetic constant k_{ad} increased. However, also the maximum cellulase adsorption A_{max} rose with enhanced mixing, which was not observed for CBH I and EG I using filter paper as a cellulosic substrate (Nidetzky et al., 1994b). This increase in A_{max} may be explained by a better exposure of α-cellulose to the liquid and, therefore, a better cellulose surface accessibility for cellulase adsorption.

As seen in Figure 3-11B, the activities of CBH I and EG I were also investigated at different shaking frequencies using α-cellulose as a substrate. For both cellulases, the same trend in activity was observed, whereby a sharp increase occurred between 400 rpm and 800 rpm as in the adsorption kinetic experiments (Figure 3-11A). Consequently, higher shaking frequencies clearly improved the adsorption of cellulases, thereby bolstering their respective activity, because adsorption is a prerequisite for cellulose hydrolysis (Lynd et al., 2002; Tanaka et al., 1986; Zhang and Lynd, 2004). Thus, when short incubation times of cellulases are applied (for example, washing agent), catalyst optimization should also be focused on improving the cellulase binding properties. In other studies, the effect of agitation on cellulose hydrolysis was investigated without considering adsorption. These studies showed that enhanced agitation increases initial cellulose hydrolysis rates (Enayati and Parulekar, 1995; Ingesson et al., 2001; Tengborg et al., 2001). However, attention has to be paid to cellulase inactivation reducing the final yield of cellulose hydrolysis (Reese, 1980). This is especially important when using high solid concentrations (Mukataka et al., 1983) and shear force sensitive cellulases (Reese and Mandels, 1980). In this current study, however, low solid concentrations, short incubation times, and a shaken system were applied so that cellulase inactivation could be neglected. Moreover, upon using immobilized or displayed cellulases (Fujita et al., 2004; van Zyl et al., 2007; Yanase et al., 2010), lower shaking frequencies are beneficial to ensure sufficient surface contact between cellulase and solid substrate (Khaw et al., 2007). In comparison to the adsorption parameters, a disproportionate increase in cellulase activity was observed with enhanced agitation (Figure 3-11A-B). As CBHs and EGs are inhibited by soluble hydrolysis products, such as glucose and cellobiose (Gruno et al., 2004; Holtzapple et al., 1990; Kruus et al., 1995b), agitation may transport these inhibiting products

away from the cellulases, thus decreasing the local concentration of inhibiting products and improving the cellulase activity.

In order to understand the influence of shaking frequency on the adsorption and activity of cellulases, the hydrodynamics inside the respective reaction tube were investigated in detail. Pictures of the liquid phase with immersed α-cellulose particles were taken at different shaking frequencies (Figure 3-11C). For $n \leq 200$ rpm, the liquid surface remained horizontal, and no liquid mixing was observed. Once $n \geq 400$ rpm, liquid mixing started (white arrow; Figure 3-11C). According to Hermann et al. (2003), a critical shaking frequency n_{crit} is necessary for liquid mixing and can be calculated according to Eq. 3-6. In this current investigation, n_{crit} was 260 rpm (black arrows; Figure 3-11A-B), which fitted well to the start of liquid mixing between 200 rpm and 400 rpm (white arrow; Figure 3-11C). The boundary layer at the cellulose-liquid interface is relatively thick without mixing (Andrade and Hlady, 1986) and can decrease the rate of cellulase adsorption. However, mixing was increased by exceeding n_{crit}, thereby leading to a decrease in the width of the boundary layer at the cellulose-liquid interface. Since adsorption kinetics and cellulase activity did not significantly change between 0 rpm and 400 rpm, liquid mixing was not the rate limiting step.

A sharp increase in adsorption parameters and cellulase activities was observed once the suspension of cellulose particles began ($n = 600$ rpm; Figure 3-11C). As soon as the particles were completely suspended ($n = 800$ rpm), their whole surface was exposed to the liquid, and all external cellulose-binding sites were accessible to the cellulases. Hence, an optimal particle-liquid mass transfer was achieved (Pangarkar et al., 2002), and the parameters A_{max}, k_{ad} as well as cellulase activities reached their maximum values. Complete suspension is defined as the point when no particles are deposited on the tank bottom for longer than one second (Zwietering, 1958). This criterion is designated as the just suspending speed or off bottom speed. A correlation for calculating the just suspending speed in shaking vessels was developed by Kato et al. (1995). However, it can not be applied to cellulose particles because of their fibrous structure and wide particle size distribution. Complete suspension is known to be required for high cellulase activity (Huang, 1975). However, this current study shows for the first time the effect of suspension on cellulase adsorption as well as the correlation between the adsorption and the activity of cellulases at different hydrodynamic conditions.

Figure 3-11: Adsorption kinetics and activities of the purified cellulases onto α-cellulose at different hydrodynamic conditions. (**A**) Influence of shaking frequency on kinetic adsorption parameters (including standard deviations) – maximum cellulase adsorption (A_{max}; solid line) and pseudo-first-order adsorption rate constant (k_{ad}; dotted line) – according to Eq. 3-2: (■) A_{max} of cellobiohydrolase (CBH) I, (□) A_{max} of endoglucanase (EG) I, (▲) k_{ad} of CBH I, (△) k_{ad} of EG I. The critical shaking frequency (n_{crit}), calculated according to Eq. 3-6, is indicated with black arrows; (**B**) influence of shaking frequency on the activity of cellulases (dashed line): (●) CBH I, (○) EG I. Relative values (including standard deviations) are standardized to maximum activities (CBH I: 0.25 U/mg; EG I: 0.64 U/mg); (**C**) pictures of the liquid phase with immersed α-cellulose particles at different shaking frequencies. The white arrow indicates the start of liquid mixing. Images were obtained with a charged-coupled device camera installed on a shaking platform; incubation: 10 g/L α-cellulose in 0.1 M sodium acetate buffer (pH 4.8), $T = 45°C$, $V_L = 1$ mL, $n = 0$-1000 rpm, $d_0 = 3$ mm.

3.1.3.10 Cellulase Activity with α-Cellulose and Conventional Model Substrates

After the adsorption and activity of purified cellulases were studied with α-cellulose at various hydrolysis conditions, the cellulase activities on different artificial model substrates and on α-cellulose were finally compared (Figure 3-12). EG I and EG II showed high specific activities towards CMC and low activities towards Avicel. Regarding CBH I and CBH II, the opposite was observed. Since Avicel and CMC are model substrates to differentiate CBHs and EGs, these results are in good agreement with the literature (Ghose, 1987; Kruus et al., 1995a; Teeri, 1997; Zhang et al., 2006). However, when comparing CBHs and EGs, a common cellulosic substrate is necessary. In the case of Sigmacell, the activities of EGs were just six-times higher than the activities of CBHs. As Sigmacell is an insoluble and unsubstituted cellulose with low *CrI*, it can be hydrolyzed by CBHs and EGs (Lynd et al., 2002). Sigmacell, however, is an artificial substrate processed from α-cellulose (Sjöström and Alén, 1999; Zhang et al., 2006) and does not mirror the actual biomass present in a biorefinery. By using insoluble α-cellulose, the activities were very similar, and the ratio between EGs and CBHs was approximately 2.7:1. α-Cellulose is normally used for total cellulase activity measurements (Decker et al., 2003; Zhang et al., 2006). As α-cellulose mimics the alkaline-pretreated biomass used in biorefineries, α-cellulose is suggested as an excellent substrate in early experiments to screen for apt cellulases to process practical cellulosic substrates.
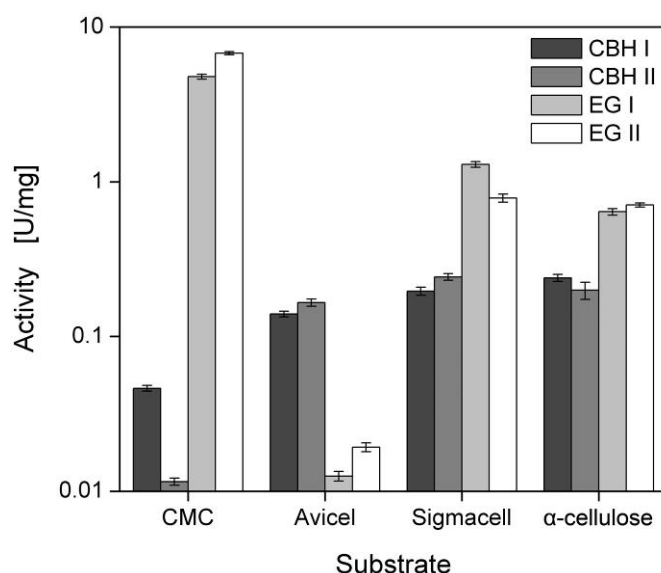
Figure 3-12:   Activities of the purified cellulases towards different cellulosic substrates. Incubation: 10 g/L cellulose in 0.1 M sodium acetate buffer (pH 4.8), 0.1 g/L cellulase, $T = 45°C$, $V_L = 1$ mL, $n = 1000$ rpm, $d_0 = 3$ mm, reaction time: 10 min (CMC), 120 min (Avicel), 30 min (Sigmacell), 60 min (α-cellulose).

3.1.4 Conclusions

In Chapter 3.1, insoluble α-cellulose was found to be an excellent practical substrate to characterize and screen for purified CBHs and EGs. First, a novel and reproducible purification method was established to prepare the major cellulases from *T. reesei* with high purity. Second, the adsorption isotherms and kinetics of the purified cellulases were analyzed for the first time by using α-cellulose as a cellulosic substrate. The calculated adsorption parameters (A_{max}, K_D, k_{ad}) of the studied cellulases were comparable to those for filter paper as an established model substrate. Third, the hydrolytic activities of all purified cellulases were analyzed in detail. Thereby, the sugar production patterns of all purified cellulases were investigated – proving cellobiose as major product of CBHs, and cellotriose, cellobiose, and glucose as major products of EGs. Furthermore, when analyzing the kinetics of α-cellulose hydrolysis, the hydrolysis rates were constant at the start of the experiment (rapid and linear increase in reducing sugar concentration) but declined afterwards due to product inhibition or the alteration of physical cellulose properties (such as a decrease in cellulose accessibility and reactivity). Here, a simple semi-mechanistic model was developed to predict the kinetics of α-cellulose hydrolysis. Additionally, the effects of pH and temperature on cellulase activity were analyzed and modeled by applying a simple pH-activity model and the Arrhenius equation (optimal pH value: 4.8-5, optimal temperature: 55-60°C). Fourth, the effects of different hydrodynamic conditions (including liquid mixing and cellulose suspension) on the adsorption and activity of the purified cellulases were investigated. Thereby, this investigation shows in detail, for the first time, the effect of hydrodynamics on cellulase adsorption as well as the correlation between the adsorption and the 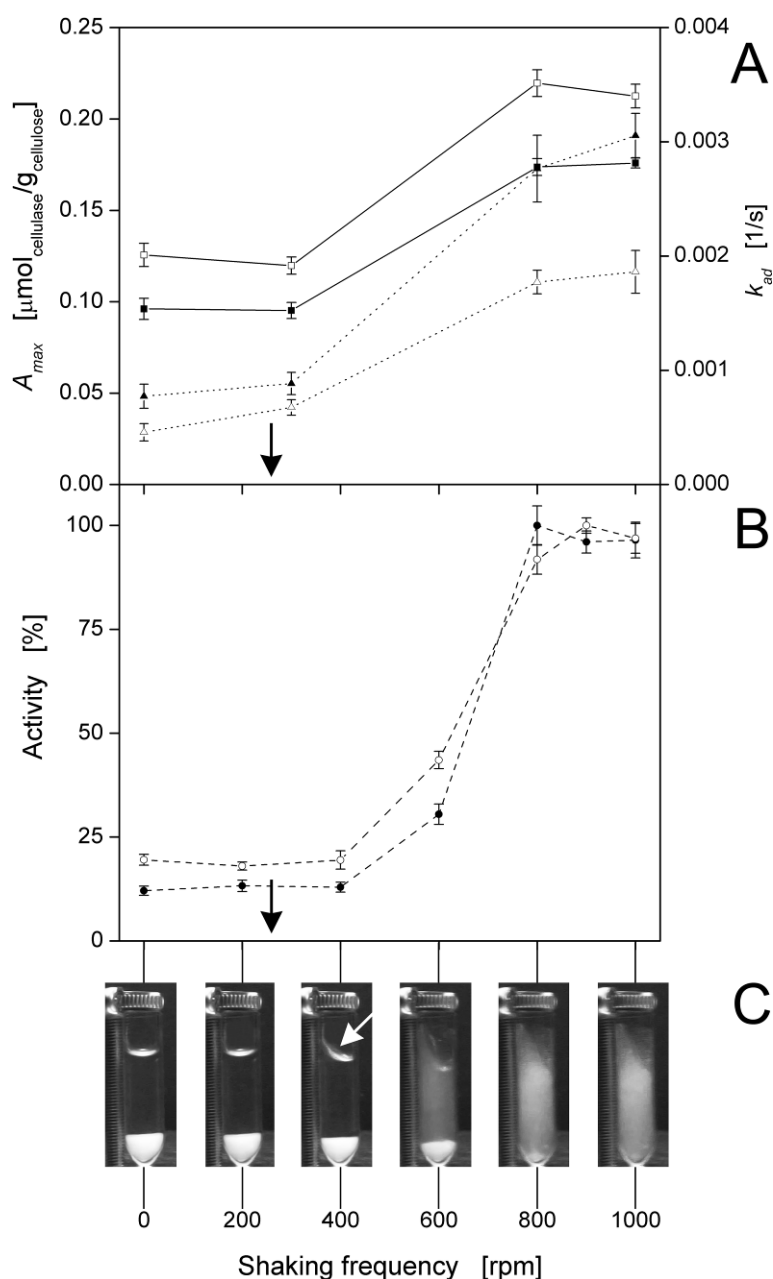activity of cellulases at different hydrodynamic conditions. Complete suspension of α-cellulose particles clearly enhanced the adsorption of cellulases thereby augmenting cellulase activity. Finally, by comparing conventional model substrates with α-cellulose, CBHs and EGs showed similar cellulase activities only on insoluble α-cellulose.

Even though other researchers use conventional pure cellulosic substrates, these are not suitable for characterizing purified CBHs and EGs. Instead, α-cellulose is ideal when alkaline pretreatment is considered as a previous pretreatment step. In the future, screening experiments should be conducted with α-cellulose so that proper cellulases are selected to best hydrolyze the real alkaline-pretreated biomass used in biorefineries. In addition, α-cellulose can be used in automated screening platforms (Decker et al., 2003) as suspensions of

α-cellulose particles can be handled by pipetting. Since lignocellulose pretreatment in biorefineries significantly alters the structure of cellulose, cellulases should be also characterized with other practical cellulosic substrates that represent other pretreatment techniques (such as ammonia fiber explosion, ionic liquid process, organosolv process, and steam explosion) (Kumar and Wyman, 2009a; Zhang et al., 2007).

Besides the application of practical cellulosic substrates such as α-cellulose, sophisticated cellulase assays are also essential when characterizing cellulases. Therefore, a new sophisticated cellulase assay is presented in Chapter 3.2.

3.2   Online Monitoring of the Enzymatic Hydrolysis of Insoluble Cellulose by Using High-Throughput Scattered Light Detection

3.2.1   Introduction

Since the cellulose hydrolysis catalyzed by cellulases is a rate-limiting and expensive processing step in biorefineries (Galbe et al., 2007; Zhang et al., 2006), the development of improved cellulases is especially important. During the last years, novel cellulases have been discovered, and known cellulases have been engineered through directed evolution and rational design approaches leading to an increasing number of improved cellulases (Fukumura et al., 1997; Kruus et al., 1995a; Liang et al., 2010; Liang et al., 2011; Morozova et al., 2010; Zhang et al., 2006). In order to screen these cellulase variants, methods for assaying cellulase activities are, in particular, relevant (Decker et al., 2009; Zhang et al., 2006).

Many cellulase assays are based on the hydrolysis of water-soluble substrates (Zhang et al., 2006). As shown in the Chapters 1.4.2.4 and 3.1, however, such hydrolysis data are not pertinent to the realistic hydrolysis of insoluble substrates (Zhang et al., 2006), because enzymatic hydrolysis proceeds on the surface of insoluble substrates and involves, beside the catalytic domain, also the cellulose-binding domain of cellulases (Lynd et al., 2002; Pristavka et al., 2000; Rabinovich et al., 1982; Yuldashev et al., 1993). Consequently, the use of insoluble cellulosic substrates would be an advantage in screening experiments so that the

most appropriate cellulases are selected for the hydrolysis of real insoluble lignocellulose (Chapter 3.1).

When insoluble cellulose with a high degree of polymerization is used, the majority of cellulase assays involves the detection of reducing sugars or total sugars (Zhang et al., 2006). The dinitrosalicylic acid assay is one of the most common reducing sugar assays and is often applied when analyzing the activity of cellobiohydrolases, endoglucanases, β-glucosidases, or cellulase mixtures (Zhang et al., 2006). However, the reducing sugar assays (such as Mandels-Weber filter paper assay; Mandels et al., 1976) are error-prone, and the respective high-throughput systems require considerable effort (Decker et al., 2003; Navarro et al., 2010). In addition, they do not allow the online measurement of cellulase activities, since the detection of reducing sugars often requires harsh conditions, as in the case of the dinitrosalicylic acid assay.

When using insoluble substrates, enzyme activities can be generally detected offline or online by measuring the degradation of substrate particles that lead to a clearing of the turbid particle suspension (Maurer and Gabler, 2004). The resulting decrease in turbidity can be quantified using spectrophotometry. The decrease in absorbance correlates to the applied enzyme concentration, which was verified by analyzing the soluble products of the respective enzyme reaction (Chen and Penner, 2007; Wang and Broda, 1992). Alternatively, the degradation of substrate particles can be measured using nephelometry. In this case, the decrease in the scattered light intensity of a particle suspension is measured during the enzymatic reaction (Enari and Nikupaavola, 1988). Nummi et al. (1981) detected cellulase activities using spectrophotometric and nephelometric methods. Both optical methods are sensitive, convenient, and non-invasive (Latimer, 1982), and they can be applied for online analysis. Up to now, however, they have not been implemented in high-throughput techniques for assaying cellulase activity.

In Chapter 3.2, the first cellulase assay combining high-throughput, online analysis, and insoluble cellulosic substrates is presented in detail. This assay is based on the BioLector technique, which allows the online monitoring of scattered light intensities in a continuously shaken microtiter plate (Kensy et al., 2009; Samorski et al., 2005). In preliminary studies, it was shown that the BioLector technique can be applied in general for measuring the enzymatic degradation of insoluble substrates (Huber et al., 2011). However, this chapter

focuses on proving the applicability of the BioLector technique for assaying, in particular, cellulase adsorption and activity. As described in Chapter 2, the cellulase-related protein swollenin leads to the non-hydrolytic deagglomeration of cellulose particles (Chapters 2.3.3 and 2.3.4.1). Therefore, the BioLector is additionally applied to analyze the non-hydrolytic effect of swollenin.

3.2.2   Materials and Methods

3.2.2.1   Cellulosic Substrates

The cellulosic substrates α-cellulose, Avicel PH101, and Sigmacell 101 were used. The physical properties (solubility; purity; crystallinity index, CrI; weight-average degree of polymerization, DP_w, geometric mean particle size, d_P) and product information are presented in Table 3-1 (Chapter 3.1.2.1).

3.2.2.2   Cellulase Preparation

The commercial cellulase preparation Celluclast[®] 1.5L (Novozymes, Bagsværd, DK) was used for the hydrolysis of the cellulosic substrates. The detailed enzyme composition of Celluclast[®] and additional information are given in Chapter 2.2.2. To remove salts, sugars, and other interfering components, Celluclast[®] was previously rebuffered by using column chromatography (as described in Chapter 2.2.2) and 0.1 M sodium acetate buffer (pH 4.8) as a running buffer. Specific filter paper activities (per g protein) of the off-the-shelf Celluclast[®] and the applied rebuffered Celluclast[®] were measured according to Ghose (1987): 182 U/g for off-the-shelf Celluclast[®], 244 U/g for rebuffered Celluclast[®].

3.2.2.3   Hydrolysis and Adsorption Experiments in the BioLector

Hydrolysis experiments were performed with varying concentrations of cellulosic substrate and cellulase depending on the experimental objective. The experiments were conducted in a continuously shaken microtiter plate under the following constant conditions: temperature $T = 37°C$, total filling volume $V_L = 200$ μL, shaking diameter $d_0 = 3$ mm, shaking frequency $n = 900$ rpm. Higher temperatures could not be applied, since the maximum incubation temperature of the utilized BioLector device was 37°C. The shaking frequency was chosen to ensure the complete suspension of cellulose particles (Kato et al., 2001) (Chapter 3.1.3.9). Therefore, mass transfer limitations were excluded, and the whole cellulose particle surface

was accessible to the cellulases, thereby optimizing cellulase adsorption and activity (Chapter 3.1.3.9). According to Engel et al. (2010), the rebuffered Celluclast® is stable under the applied incubation conditions, so the inactivation of cellulases could be neglected. The final mixtures were incubated as triplicates in black 96-well microtiter plates with transparent bottoms (μClear, Greiner Bio-One, Frickenhausen, DE). To avoid evaporation, the microtiter plates were sealed with adhesive foil (Cat. AB-0580, Abgene, Epsom, UK). Depending on the particular experimental objective, the experiments were conducted in 0.1 M sodium acetate buffer (pH 4.8) or in 0.1 M phosphate buffer at different pH values, adjusted with HCl and NaOH. Blanks (either without cellulase, without substrate and cellulase, or without substrate) were incubated similarly.

To analyze the non-hydrolytic effect of cellulases and swollenin on cellulose during scattered light measurements, 2.5 g/L α-cellulose was incubated with SDS, BSA, active cellulases, inhibited cellulases, or swollenin (each at 0.25 g/L) in 0.1 M sodium acetate buffer (pH 4.8). To inhibit cellulases, disodium hexachloropalladate (Na_2PdCl_6) was added to the mixture at a final concentration of 200 μM (Lassig et al., 1995). In addition, incubations with cellulases were performed at extreme pH values (1.70, 9.04, or 11.08) using 0.1 M phosphate buffer. All incubations were conducted in the BioLector under the aforementioned conditions.

Hydrolysis and adsorption experiments were performed using a commercial BioLector (m2p-labs GmbH, Aachen, DE) (Kensy et al., 2009), detecting the scattered light intensity in each of the 96 wells at 620 nm. The BioLector technique allows the online monitoring of scattered light and fluorescence intensities in a continuously shaken microtiter plate. Figure 3-13A shows a scheme of the applied BioLector technique. According to Samorski et al. (2005), the BioLector typically consists of an orbital shaker, an x-y positioning device with an attached optical fiber, a fluorescence spectrometer, and a computer. As shown in Figure 3-13B, the optical fiber is fixed at a tilting angle of approximately 30° to avoid the interference by light directly reflected from the well bottom. One measurement of the entire 96-well microtiter plate was adjusted to a time period ranging from 180 s to 400 s.
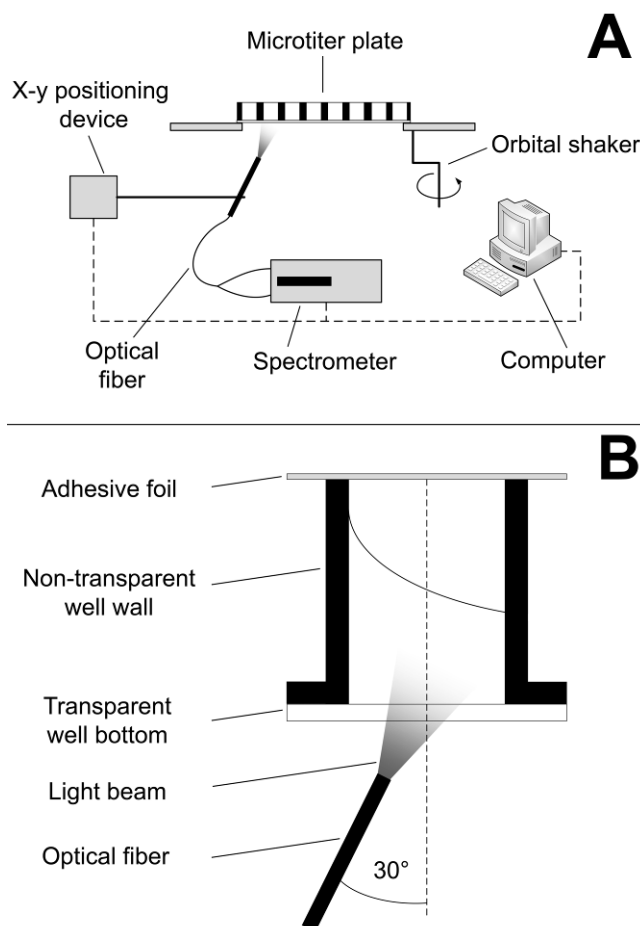
Figure 3-13: Scattered light detection using the BioLector technique. (**A**) Scheme of the technical equipment of the BioLector; (**B**) magnification of one well of the microtiter plate during scattered light measurement. The optical fiber is fixed at a tilting angle of approximately 30° to avoid the interference by light directly reflected from the well bottom.

3.2.2.4 Light Microscopy and Laser Diffraction

Light microscopy and laser diffraction (Bowen, 2002) were applied to visualize the hydrolysis of cellulosic substrates by cellulases. Therefore, hydrolysis experiments were conducted in the BioLector under the aforementioned conditions (Chapter 3.2.2.3). After defined time intervals, microscopic pictures were taken with an Eclipse E600 (Nikon, Tokyo, JP). Additionally, the cellulose particle size distributions were measured by laser diffraction (Bowen, 2002), and the geometric mean particle sizes d_P were calculated as described in Chapter 2.2.13.

3.2.2.5 Dinitrosalicylic Acid Assay

The dinitrosalicylic acid assay (Miller, 1959) was applied to determine the amount of reducing sugars released during cellulose hydrolysis and to validate cellulase activities

determined by using the BioLector-based cellulase assay (see later Chapter 3.2.2.7). Hydrolysis experiments were conducted by using the BioLector under the aforementioned conditions (Chapter 3.2.2.3). After defined time intervals, samples were taken, and the hydrolysis was stopped by boiling for 10 min. Finally, the samples were analyzed by applying the dinitrosalicylic acid assay as described in Chapter 2.2.16.

3.2.2.6   Calibration of Scattered Light Intensities

To calibrate scattered light intensities, suspensions with varying concentrations of untreated and prehydrolyzed cellulose (0-15 g/L in 0.1 M sodium acetate buffer, pH 4.8) were analyzed in the BioLector under the aforementioned conditions. To prepare prehydrolyzed cellulose, 2.5 g/L cellulosic substrate was previously incubated with varying concentrations of cellulase (2.5 g/L, 10 g/L, and 25 g/L) in 0.1 M sodium acetate buffer (pH 4.8). The mixtures were incubated in 1000-mL flasks with $V_L = 250$ mL on an orbital shaking platform at 37°C, $n = 300$ rpm, and $d_0 = 50$ mm. After incubation for 5 h or 10 h, the reaction was terminated by boiling for 10 min. To remove adsorbed cellulases, the mixtures were centrifuged (14 000 × g, 10 min), and the cellulose pellet was washed four times with 100 mL 0.05 M citrate buffer (pH 10) and once with 100 mL distilled water (Zhu et al., 2009). Finally, the washed cellulose was used for calibration. In addition, particle size distributions of untreated and prehydrolyzed cellulose were measured by laser diffraction as described in Chapter 2.2.13.

3.2.2.7   Determination of Cellulase Activity and Modeling

To calculate cellulase activities, an automatic software was programmed using the Java platform. First, the mean scattered light intensity of the cellulose blank was calculated. To exclude systematic errors resulting from variations in lamp intensity, the differences between the raw data of the cellulose blank and the mean value of the cellulose blank were calculated and subtracted from each scattered light curve. Second, the maximum of each curve was identified. Third, the initial reaction rate was determined as the linear decrease in scattered light intensity over time (see later Figure 3-15A). Therefore, a linear regression was applied to each curve, and the range of values with the highest coefficient of determination was determined (see later Figure 3-15A). As a boundary condition, the range of values had to start from the maximum of the scattered light curve and had to range over at least 2 h. Fourth, the calculated initial reaction rates (arbitrary units/h or a.u./h) were translated into cellulase activities [g/(L·h)] by using the slopes of the aforementioned calibration curves (Chapter

3.2.2.6). The resulting standard deviations of the calculated cellulase activities were on average below 4.5%.

Kinetic parameters were determined using the Michaelis-Menten model (Copeland, 2000) where $K_{M,app}$ denotes the apparent Michaelis constant [g/L] and $V_{max,app}$, the apparent maximum cellulase activity [g/(L·h)]. Parameters describing the effect of the pH value on cellulase activity were determined using the Eq. 3-3 (Chapter 3.1.2.10).

3.2.2.8 Computational Methods

All parameters were calculated by nonlinear, least squares regression analysis using MATLAB version R2008b (The MathWorks, Natick, USA).

3.2.3 Results and Discussion

3.2.3.1 Principle of the Cellulase Assay

In this study, an innovative method based on the BioLector technique was applied to assay, in particular, cellulase adsorption and activity. The BioLector allows the online monitoring of scattered light intensities in a continuously shaken microtiter plate (Kensy et al., 2009; Samorski et al., 2005). In contrast to spectrophotometers, it does not require the interruption of shaking, thereby avoiding, in particular, particle sedimentation and mass transfer limitations (Chapter 3.1.3.9) (Ingesson et al., 2001; Kato et al., 2001). To illustrate the basic principle of this method, the cellulosic substrate α-cellulose (Table 3-1) was hydrolyzed by using a complex cellulase preparation. Light microscopy and particle size measurements by using laser diffraction (Bowen, 2002) were applied to visualize the hydrolysis of the cellulosic substrate. As seen in Figure 3-14A (0 h), the initial α-cellulose suspension consisted of insoluble particles of different size and shape. During cellulose hydrolysis, the particles were degraded, and a decrease in particle size was observed (Figure 3-14A). According to Figure 3-14B, the initial cellulose suspension showed a broad and inhomogeneous particle size distribution with a geometric mean particle size d_P of 69 μm. After 24 h and 48 h, the particle size distribution shifted to lower values, and large cellulose particles were predominantly hydrolyzed to smaller particles.
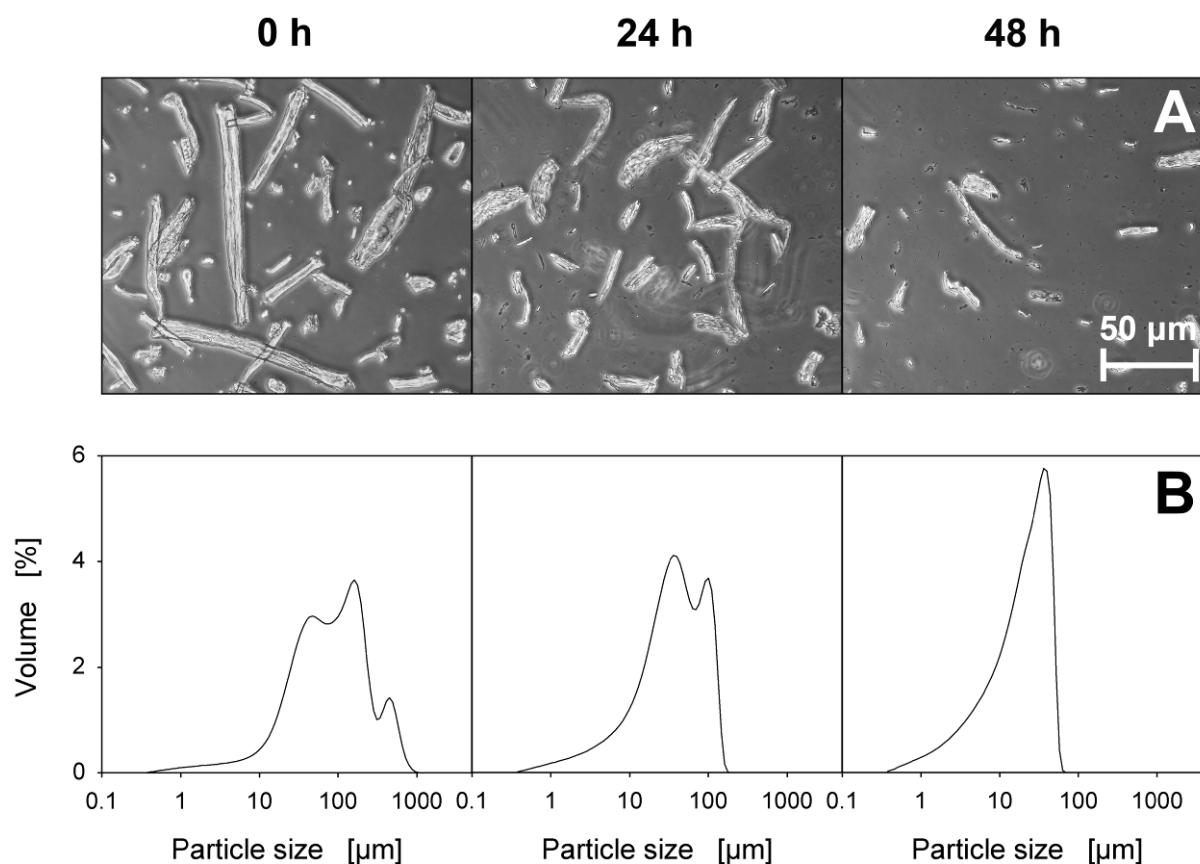
Figure 3-14: Degradation of cellulose particles by cellulases. (**A**) Light microscopic pictures of α-cellulose during hydrolysis (0 h, 24 h, and 48 h); (**B**) particle size distribution of α-cellulose during hydrolysis (0 h, 24 h, and 48 h); incubation: BioLector, 2.5 g/L α-cellulose in 0.1 M sodium acetate buffer (pH 4.8), 0.25 g/L rebuffered Celluclast®, $T = 37°C$, $V_L = 200$ μL, $n = 900$ rpm, $d_0 = 3$ mm, 96-well plate; microscope: Eclipse E600 (Nikon, Tokyo, JP); particle size analyzer: LS13320 (Beckman Coulter, Brea, USA).

Figure 3-15A summarizes the course of the geometric mean particle size d_P over time for the aforementioned experiment. Here, the geometric mean particle size (black circles) fell rapidly from 69 μm to 55 μm after the addition of cellulases and, then, gradually decreased to 16 μm after an incubation of 48 h. In addition, Figure 3-15A shows the typical course of scattered light intensity during cellulose hydrolysis in the BioLector. The initial cellulose suspension was turbid and led to a high scattered light intensity (dotted line). After the cellulase was added to this cellulose suspension at the start of the experiment, an initial increase in the scattered light intensity was observed. This may be explained by a non-hydrolytic deagglomeration of cellulose particles due to the interaction with the cellulose-binding domain of the cellulases (Arantes and Saddler, 2010; Din et al., 1991). After this initial increase, a reduction in scattered light intensity was observed as a result of the aforementioned hydrolytic degradation of cellulose particles. In this case, the respective

scattered light intensity showed an extended period of linearity (dashed line). At the end of the reaction, the scattered light intensity tended towards a constant value.

To compare this prospective method with an established cellulase assay, a dinitrosalicylic acid assay was conducted in parallel to the scattered light measurements (Figure 3-15B). The dinitrosalicylic acid assay is one of the most common reducing sugar assays and often applied when analyzing the activity of cellulases (Zhang et al., 2006). As shown by the comparison of Figure 3-15A and B, the decrease in scattered light intensity and the accumulation of reducing sugars proceeded simultaneously. Therefore, the gradual reduction in mean particle size (Figure 3-15A) was mostly based on the hydrolytic degradation of insoluble cellulosic particles and not on their non-hydrolytic deagglomeration. Moreover, it is striking that the period of linearity in the accumulation of reducing sugars (Figure 3-15B, dashed line) was the same as in the scattered light measurements (Figure 3-15A, dashed line), thereby validating the new prospective cellulase assay based on the BioLector technique. Here, the initial reaction rates, obtained from calibrated scattered light intensities (see later Chapter 3.2.3.4) and from the accumulation of reducing sugars, were close to each other: 0.06 g/(L·h) for the BioLector technique, 0.05 g/(L·h) for the dinitrosalicylic acid assay. Consequently, the linear decrease in scattered light intensity could be used to determine the initial reaction rate (Chen and Penner, 2007; Wang and Broda, 1992) and, finally, the activity of cellulases during the hydrolysis of insoluble cellulosic substrates. In comparison to the hydrolysis kinetics of purified cellulases at 45°C (Chapter 3.1.3.6, Figure 3-8), a longer period of linearity was detected (Figure 3-15B). This can be explained as follows: (1) a cellulase mixture containing β-glucosidase was used, thereby reducing the product inhibition of cellulases by cellobiose and delaying the decline in hydrolysis rates; (2) the activity of the cellulase mixture was relatively low, since a lower temperature of 37°C was applied. This lower temperature is attributed to the fact that the utilized BioLector device could not maintain incubation temperatures above 37°C. For future studies, the BioLector device should be modified in order to allow higher incubation temperatures which are closer to the temperature optimum of cellulases.
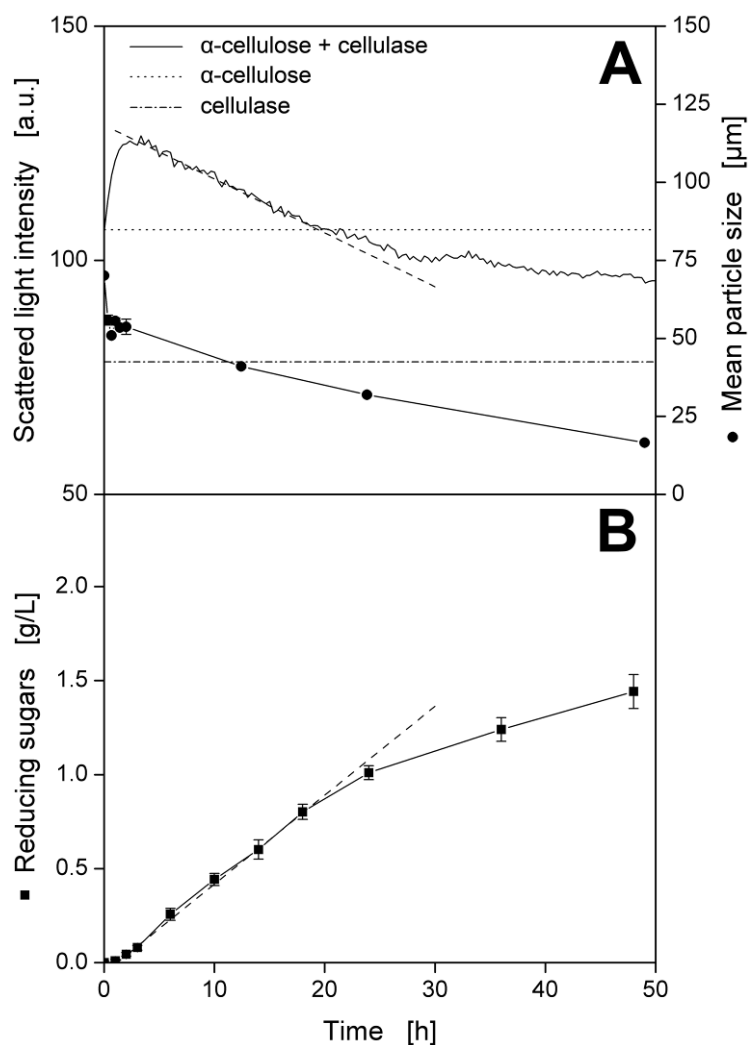
Figure 3-15:   Principle of the prospective cellulase assay. (**A**) Course of scattered light intensity and mean particle size during the hydrolysis of α-cellulose. The linear decrease in scattered light intensity is shown as a dashed line. Mean particle sizes were measured for the incubation of α-cellulose with cellulase; (**B**) production of reducing sugars during the hydrolysis of α-cellulose. The linear increase in reducing sugar concentration is shown as a dashed line. Errors are given as standard deviations; incubation: BioLector, 2.5 g/L α-cellulose in 0.1 M sodium acetate buffer (pH 4.8), 0.25 g/L rebuffered Celluclast®, $T = 37°C$, $V_L = 200$ μL, $n = 900$ rpm, $d_0 = 3$ mm, 96-well plate; particle size analyzer: LS13320 (Beckman Coulter, Brea, USA).

3.2.3.2 Non-hydrolytic Effect of Cellulases during Scattered Light Measurements

To understand the non-hydrolytic effect of cellulases on cellulose during scattered light measurements, α-cellulose was incubated with active cellulases, inhibited cellulases, SDS, or BSA. As seen in Figure 3-16A, the typical course of scattered light intensity was observed during the incubation of α-cellulose and active cellulases. An initial increase in scattered light intensity within 2.5 h was followed by a linear decrease. In contrast, the incubations with the

detergent SDS or the protein BSA showed no increase in scattered light intensity. Consequently, the initial increase resulted from a specific effect of cellulases which can be attributed to the adsorption of cellulases onto the substrate. It is known that cellulase adsorption leads to a non-hydrolytic deagglomeration of cellulose particles (Arantes and Saddler, 2010; Din et al., 1991). Therefore, an increased scattered light intensity of the cellulose suspension might be addressed to this non-hydrolytic effect. Furthermore, cellulase adsorption is rapid compared to the time required for complete hydrolysis (Lynd et al., 2002). Depending on the applied cellulose and incubation conditions, the adsorption equilibrium is usually reached within 90 min (Chapter 3.1.3.4) (Lynd et al., 2002). Therefore, the observed increase in scattered light intensity is consistent with the time periods required for cellulase adsorption.

As seen in Figure 3-16B, the incubations with inactive cellulases were also investigated by using the BioLector technique. After adding the cellulase inhibitor Na_2PdCl_6 to the mixture, only an increase and no decrease in scattered light intensity were observed. These results with inactive cellulases confirmed the assumption that the initial increase in scattered light intensity is based on a non-hydrolytic effect of cellulases. Since palladium complexes inhibit the catalytic domain of *T. reesei* cellulases without affecting the cellulose-binding domain (Lassig et al., 1995), the cellulases retained their ability for adsorption onto the α-cellulose without it being degraded. Therefore, the initial increase in scattered light intensity can be attributed to the effect of cellulose-binding domains (Lynd et al., 2002; Pristavka et al., 2000; Rabinovich et al., 1982; Yuldashev et al., 1993). In addition, cellulases led to no increase in scattered light intensity when incubated at extreme pH values (1.7 or > 9) (Figure 3-16B). This is an additional evidence for the relationship between the initial increase in scattered light intensity and cellulase adsorption, since the affinity of cellulose-binding domains for cellulose is dramatically decreased at extreme pH values (Rabinovich et al., 1982; Rabinovich, 1988; Reinikainen et al., 1995). Consequently, conditions preventing the adsorption of cellulose-binding domains onto cellulose abolished the corresponding increase in scattered light intensity (Figure 3-16B).
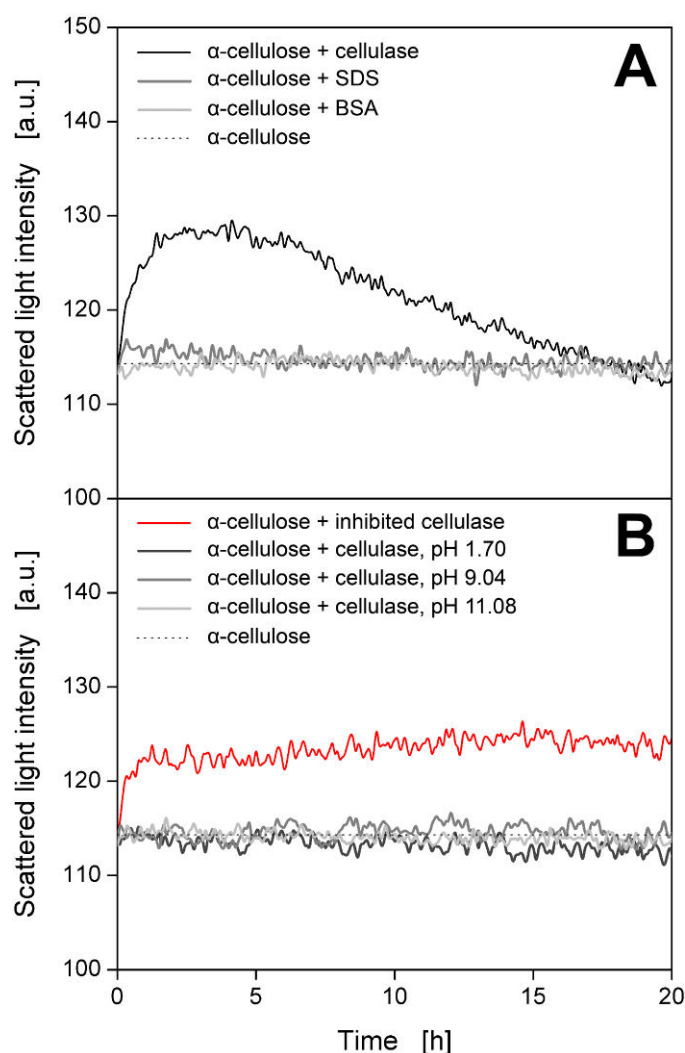
Figure 3-16:   Non-hydrolytic effect of cellulases on α-cellulose during scattered light measurements. (**A**) Incubation of α-cellulose with cellulase, SDS, or BSA; (**B**) incubation of α-cellulose with inhibited cellulase and at extreme pH values; incubation: BioLector, 2.5 g/L α-cellulose in 0.1 M sodium acetate buffer (pH 4.8) or in 0.1 M phosphate buffer (pH 1.70, 9.04, or 11.08), 0.25 g/L rebuffered Celluclast$^{\circledR}$ / 0.25 g/L rebuffered Celluclast$^{\circledR}$ + 200 μM inhibitor Na$_2$PdCl$_6$ / 0.25 g/L SDS / 0.25 g/L BSA, T = 37°C, V_L = 200 μL, n = 900 rpm, d_0 = 3 mm, 96-well plate.

3.2.3.3   Non-hydrolytic Effect of Swollenin during Scattered Light Measurements

As described in Chapter 2, the protein swollenin lacks a catalytic domain but consists of a cellulose-binding domain and an expansin-homologous domain. Like cellulases (Chapters 3.2.3.1 and 3.2.3.2), swollenin also led to the non-hydrolytic deagglomeration of cellulosic substrates (Chapters 2.3.3 and 2.3.4.1). To validate the non-hydrolytic effect of swollenin, it was also analyzed by applying the BioLector technique. As seen in Figure 3-17, the incubation of swollenin with α-cellulose led to an increase in scattered light intensity. In

contrast, the incubation with the protein BSA showed no increase in scattered light intensity – thereby proving a specific effect of swollenin. Since swollenin exhibits no catalytic domain (Saloheimo et al., 2002), this increase in scattered light intensity can be attributed to the adsorption of swollenin onto cellulose (Chapter 2.3.2) and the non-hydrolytic deagglomeration (Chapter 2.3.3). As described in Chapter 2.3.4.1, the incubation with swollenin led to a decrease in the geometric mean particle size of cellulose. Since cellulose was not hydrolyzed by swollenin and the total amount of cellulose remained constant (Chapter 2.3.3), this decrease in particle size was accompanied by an increase in particle number. Consequently, the cellulose suspension became more turbid, and an increase in scattered light intensity could be detected (Figure 3-17).

In comparison to the incubation of α-cellulose with inactive cellulases (Figure 3-16B), the incubation with swollenin (Figure 3-17) showed a similar course in scattered light intensity. However, the time period for a constant scattered light signal was different: 1.5 h for the incubation with inactive cellulases (Figure 3-16B) and 4-5 h for the incubation with swollenin (Figure 3-17). Since the time periods to reach adsorption equilibrium are very similar for cellulases (< 1.5 h; Lynd et al., 2002) (Chapter 3.1.3.4) and swollenin (≤ 2 h, Chapter 2.3.2), this difference may be explained by additional phenomena taking place after swollenin adsorption. Here, it should be noted that the total increase in scattered light intensity was higher for the incubation with swollenin (Figure 3-17) than for the incubation with inactive cellulases (Figure 3-16B). This difference indicates that swollenin may show an additional action on the cellulose surface. Since cellulases as well as swollenin contain a cellulose-binding domain, this difference can be attributed to the expansin-homologous domain of swollenin. Saloheimo et al. (2002) already hypothesized that the expansin-homologous domain may be important for the action of swollenin and primarily lead to the non-hydrolytic deagglomeration of cellulosic substrates. To finally understand the effect of cellulases and swollenin on cellulosic substrates, additional experiments with single domains (cellulose-binding domain, catalytic domain, and expansin-homologous domain) and fusion proteins of these domains need to be performed. These experiments may elucidate to what extend the single domains contribute to the induced deagglomeration of cellulosic substrates. Nevertheless, the BioLector technique is the first assay for non-hydrolytic proteins (such as swollenin) that simultaneously combines high-throughput and online analysis.
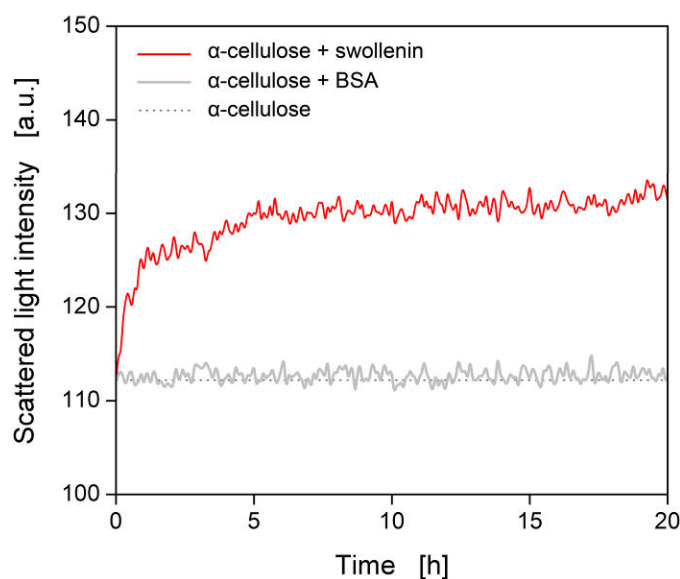
Figure 3-17:   Non-hydrolytic effect of swollenin on α-cellulose during scattered light measurements; incubation: BioLector, 2.5 g/L α-cellulose in 0.1 M sodium acetate buffer (pH 4.8), 0.25 g/L BSA or 0.25 g/L swollenin, $T = 37°C$, $V_L = 200$ μL, $n = 900$ rpm, $d_0 = 3$ mm, 96-well plate.

3.2.3.4   Calibration of Scattered Light Intensities

To calibrate scattered light intensities, suspensions of untreated and prehydrolyzed cellulose (Avicel PH101, α-cellulose, Sigmacell 101) were measured via the BioLector (Figure 3-18). For all cellulosic substrates, the scattered light intensity was a linear function of cellulose concentration up to 15 g/L (Figure 3-18A-C). In addition, the calibration curves of untreated and prehydrolyzed cellulose were almost identical when considering the same cellulose type. However, when Avicel and α-cellulose were prehydrolyzed by applying high cellulase concentrations and long incubation times (25 g/L, 10 h), the slope of the respective calibration curves increased (Figure 3-18A-B). As seen in Figure 3-18D-E, the shape of the particle size distributions of Avicel and α-cellulose changed significantly during prehydrolysis (25 g/L, 10 h), and particle sizes shifted to lower values. In comparison to untreated or less prehydrolyzed cellulose, these smaller particles led to a cellulose suspension with higher scattered light intensity and, therefore, changes in the respective calibration curves (Figure 3-18A-B). Nevertheless, as initial reaction rates were investigated within this study, and screening experiments are normally conducted with lower cellulase concentrations, these changes in calibration curves could be neglected. In the case of Sigmacell 101, all calibration curves were almost identical (Figure 3-18C), and the particle size distributions did not change significantly during prehydrolysis (Figure 3-18F). This may be explained by the small initial particle size and the low *CrI* of Sigmacell 101 (Table 3-1) and, therefore, by a direct hydrolytic degradation of Sigmacell 101 with almost no formation of smaller particles.
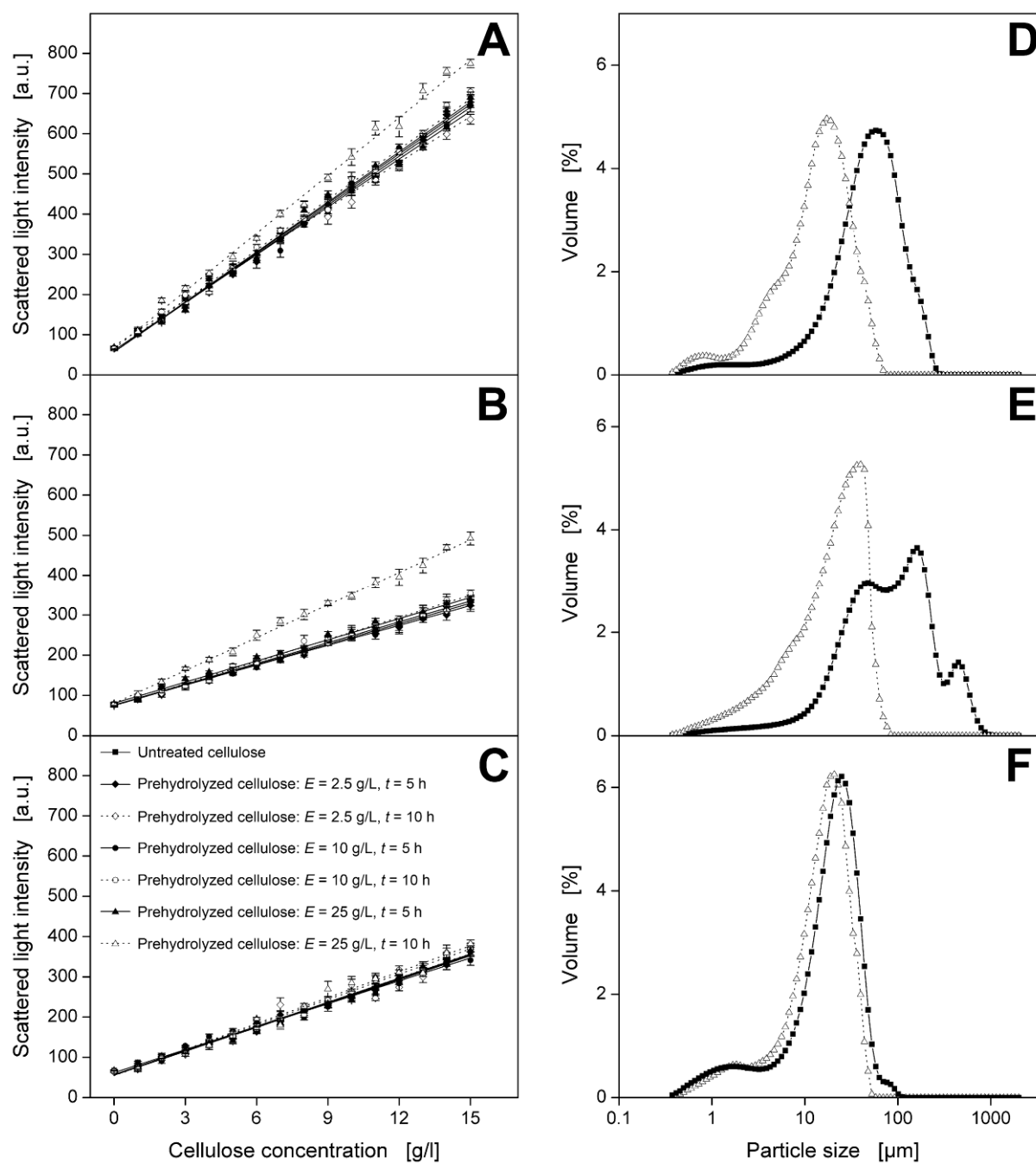
Figure 3-18:   Calibration of scattered light intensity with untreated and prehydrolyzed cellulosic substrates. (**A, B, C**) Calibration curves using the BioLector device: (**A**) Avicel PH101, (**B**) α-cellulose, (**C**) Sigmacell 101. Errors are given as standard deviations. Predicted linear calibration curves are shown as solid and dotted lines; (**D, E, F**) particle size distributions of untreated and prehydrolyzed (25 g/L Celluclast® for 10 h) cellulose: (**D**) Avicel PH101, (**E**) α-cellulose, (**F**) Sigmacell 101; prehydrolysis: 2.5 g/L cellulosic substrate in 0.1 M sodium acetate buffer (pH 4.8) was prehydrolyzed with 2.5 g/L / 10 g/L / 25 g/L rebuffered Celluclast® for 5 or 10 h; calibration: BioLector, 0-15 g/L cellulose in 0.1 M sodium acetate buffer (pH 4.8), $T = 37°C$, $V_L = 200$ μL, $n = 900$ rpm, $d_0 = 3$ mm, 96-well plate; particle size analyzer: LS13320 (Beckman Coulter, Brea, USA).

3.2.3.5 Determination of Kinetic Parameters

The basic enzyme characterization is achieved by determining initial enzyme activities. Since the calibration curves of untreated cellulose were valid during the initial phase of hydrolysis, they could be used to translate initial reaction rates (arbitrary units/h) into initial cellulase activities [g/(L·h)]. To investigate the effect of cellulose concentration on the initial cellulase activity, varying concentrations of different cellulosic substrates (0-15 g/L) were incubated with a fixed cellulase concentration. Figure 3-19A shows exemplarily the results for the hydrolysis of Sigmacell 101. By using the new cellulase assay presented within this study, a large amount of information for different incubation conditions can be obtained. As seen in Figure 3-19A, all curves showed the typical course of scattered light intensity over time as in the aforementioned experiments (Figure 3-15A): (1) initial increase in scattered light intensity, (2) subsequent linear decrease in scattered light intensity, and (3) tendency towards a constant scattered light intensity at the end of cellulose hydrolysis. As shown in Figure 3-19A, the absolute slope of the linearly decreasing scattered light intensities and, therefore, the cellulase activity rose with increasing cellulose concentration.

As seen in Figure 3-19B, the cellulase activity was a characteristic function of cellulose concentration. For all cellulosic substrates, the Michaelis-Menten model (Copeland, 2000) provided a good fit, and the apparent kinetic parameters $K_{M,app}$ and $V_{max,app}$ could be determined (Table 3-6). As described in Chapter 3.1.3.7, the Michaelis-Menten model is not mechanistically sound for the enzymatic cellulose hydrolysis because of some concerns such as mass transfer limitations, low cellulose accessibility, or cellulose depletion. In this study, however, the complete suspension of cellulose particles was ensured so that mass transfer limitations could be excluded and the whole cellulose surface was accessible to the cellulases (Chapter 3.1.3.9). Moreover, the depletion of cellulose was minimal due to the following reasons: (1) the applied cellulases exhibited relatively low activities at 37°C; (2) initial hydrolysis rates were determined; (3) high cellulose/cellulase ratios were applied (Figure 3-19). Consequently, the limitations of the Michaelis-Menten model were addressed within this study by applying appropriate hydrolysis conditions.

Figure 3-19:   Influence of cellulose concentration on the cellulase activity. (**A**) Scattered light intensity during the hydrolysis of varying Sigmacell 101 concentrations; (**B**) Michaelis-Menten-Plot using different cellulosic substrates (Sigmacell 101, α-cellulose, Avicel PH101). Predicted cellulase activities, according to the Michaelis-Menten model (Copeland, 2000), are shown as dashed lines, and corresponding parameters are listed in Table 3-6; incubation: BioLector, 0-15 g/L cellulose in 0.1 M sodium acetate buffer (pH 4.8), 0.25 g/L rebuffered Celluclast[®], $T = 37°C$, $V_L = 200$ μL, $n = 900$ rpm, $d_0 = 3$ mm, 96-well plate.

Although the apparent kinetic parameters $K_{M,app}$ and $V_{max,app}$ are not mechanistically sound for enzymatic reactions on suspended substrates, these parameters allow the rapid characterization and comparison of different cellulases or substrates under given suspension conditions. According to Table 3-6, the apparent Michaelis constant $K_{M,app}$, as a reciprocal indicator for the adsorption and affinity of cellulase onto the substrate, was lower for Sigmacell 101 than for α-cellulose and Avicel. In addition, the apparent maximum cellulase

activity $V_{max,app}$ was higher for Sigmacell 101 than for α-cellulose and Avicel. The different values for $K_{M,app}$ and $V_{max,app}$ derive from differences in the physical properties of the applied cellulosic substrates (Table 3-6). According to Hall et al. (2010), the *CrI* is a key predictor of cellulose hydrolysis, and initial cellulase activities decrease with increasing *CrI*. Since $K_{M,app}$ values increased and $V_{max,app}$ values decreased with increasing *CrI* (Table 3-6), these results are in good agreement with the literature (Hall et al., 2010).

Table 3-6: Physical properties of applied cellulosic substrates and determined Michaelis-Menten parameters of rebuffered Celluclast® using different cellulosic substrates; incubation: BioLector, 0.1 M sodium acetate buffer (pH 4.8), 0.25 g/L Celluclast®, $T = 37°C$, $V_L = 200$ μL, $n = 900$ rpm, $d_0 = 3$ mm, 96-well plate).

Cellulose	CrI [%]	d_P [μm]	$K_{M,app}$ [g/L]	$V_{max,app}$ [g/(L·h)]
α-Cellulose	64[a]	68.77[a]	6.30 ± 1.41	0.338 ± 0.032
Avicel PH101	82[a]	43.82[a]	6.53 ± 1.70	0.190 ± 0.021
Sigmacell 101	Amorphous[a]	15.86[a]	5.22 ± 1.59	0.596 ± 0.071

Errors are given as standard deviations.

CrI, crystallinity index; d_P, geometric mean particle size; $K_{M,app}$, apparent Michaelis constant; $V_{max,app}$, apparent maximum cellulase activity.

[a] According to Table 3-1. Physical properties (crystallinity index and geometric mean particle size) are repeated to allow a direct comparison of these properties with the determined Michaelis-Menten parameters.

To investigate the effect of cellulase concentration on the course of cellulose hydrolysis, a defined amount of cellulose was hydrolyzed using varying concentrations of cellulase (0-25 g/L). Figure 3-20A shows that the curves differed depending on the applied cellulase concentration. The absolute slope of the linearly decreasing scattered light intensities rose with increasing cellulase concentration. In addition, the period of linearity was shortened by using higher cellulase concentrations. Consequently, the aforementioned differences in the calibration curves of weakly and strongly prehydrolyzed cellulose could be neglected (Figure 3-18A-B), because only short incubation times were necessary to determine the initial activity of highly concentrated cellulase mixtures.

As seen in Figure 3-20B, a linear dependency of the cellulase activity on the cellulase concentration was observed up to a concentration of 1 g/L (dotted, dashed, and dash-dotted lines), which corresponds to a cellulase/cellulose mass ratio of 1/2.5. Since the new cellulase assay is applicable to cellulosic substrate concentrations of up to 15 g/L (Figure 3-18A-C), this linear dependency of the cellulase activity might be extended up to a cellulase concentration of 6 g/L by just using higher substrate concentrations. However, at higher cellulase concentrations (> 15 g/L, Figure 3-20B), a saturation was reached, indicating either diffusion limitations or limited surface area of the substrate. Here, the maximum cellulase activities (> 15 g/L cellulase) increased with decreasing particle size d_P of the applied cellulosic substrates (Table 3-6). Since a smaller particle size and, therefore, a larger external surface area accessible to the cellulases increase cellulase activity, these results concur well with the literature (Dasari and Berson, 2007; Gama et al., 1994; Huang et al., 2010). Moreover, the differences in maximum cellulase activity could be explained by the different porosities of the applied cellulosic substrates (Gama et al., 1994; Huang et al., 2010). However, at low cellulase concentrations, the cellulase activity showed a different correlation, and the curves of α-cellulose and Avicel intersected (arrow; Figure 3-20B). In this case, the cellulase activity increased with decreasing crystallinity index CrI of the applied cellulosic substrate, which was already shown in the prior experiment (Figure 3-19B). Thus, when low cellulase concentrations are applied, the crystallinity index is one of the main factors influencing cellulose hydrolysis rates (Hall et al., 2010). However, in the case of high cellulase concentrations, the mean particle size is one of the key predictors for cellulose hydrolysis.
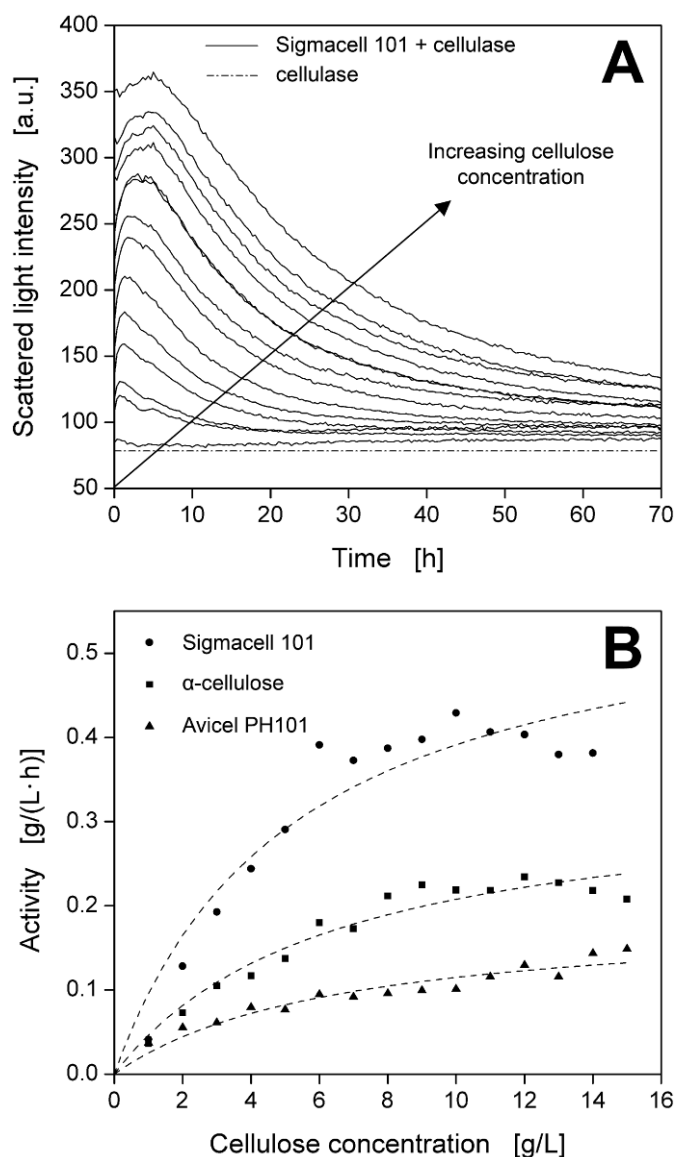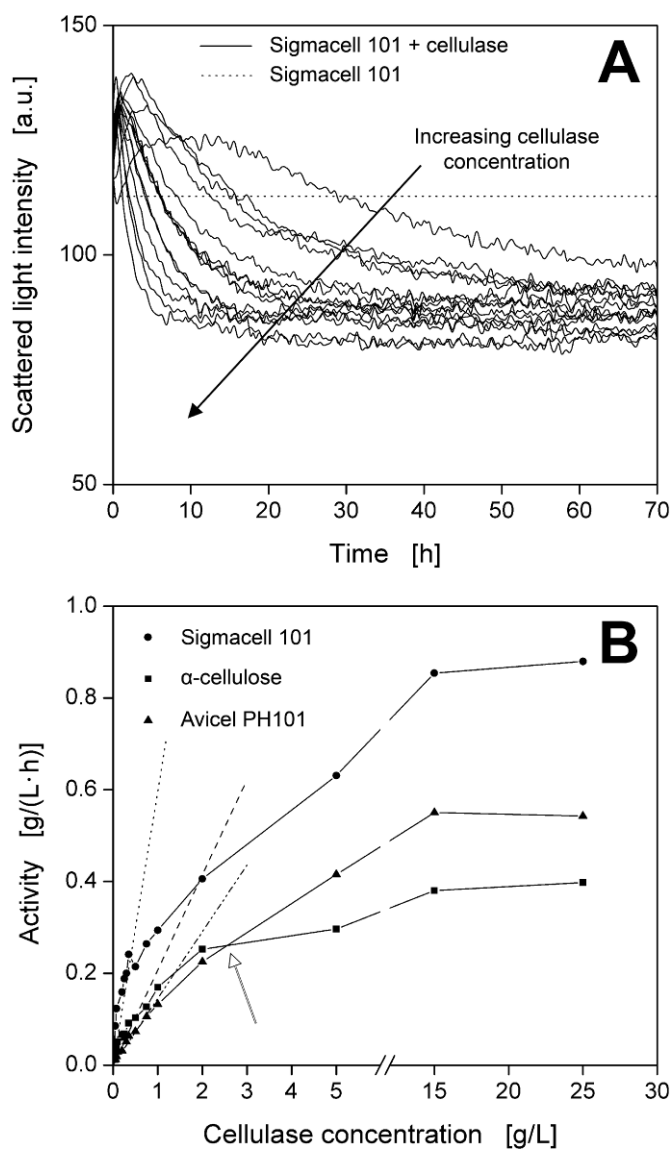
Figure 3-20: Influence of cellulase concentration on the cellulase activity. (**A**) Scattered light intensity during the hydrolysis of Sigmacell 101 by using varying cellulase concentrations; (**B**) influence of cellulase concentration on the cellulase activity using different cellulosic substrates (Sigmacell 101, α-cellulose, Avicel PH101; Table 3-6). Estimated cellulase activities, as a linear function of cellulase concentration, are shown as dotted (Sigmacell 101), dashed (α-cellulose), and dash-dotted (Avicel PH101) lines. The white arrow indicates the intersection of the curves for α-cellulose and Avicel PH101; incubation: BioLector, 2.5 g/L cellulose in 0.1 M sodium acetate buffer (pH 4.8), 0-25 g/L rebuffered Celluclast®, $T = 37$°C, $V_L = 200$ µL, $n = 900$ rpm, $d_0 = 3$ mm, 96-well plate.

3.2.3.6 pH-Dependency of Cellulase Activity

To analyze the effect of pH on the course of cellulose hydrolysis, α-cellulose was hydrolyzed under identical conditions, except that the pH of the mixtures was varied (Figure 3-21).
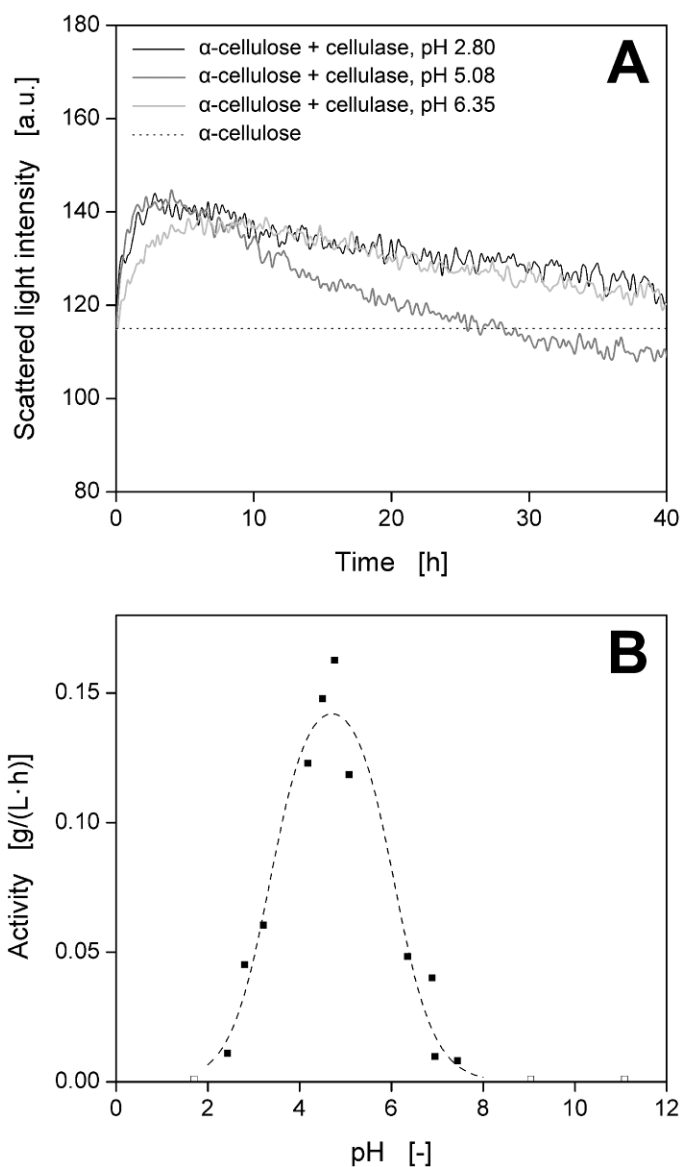
Figure 3-21:   Influence of pH on the cellulase activity. (**A**) Scattered light intensity during the hydrolysis of α-cellulose at different pH; (**B**) influence of pH on the cellulase activity using α-cellulose as cellulosic substrate. Open symbols (□) indicate no changes in scattered light intensity (Figure 3-16B), and, therefore, no cellulase activities were observed. Predicted cellulase activities, according to Eq. 3-3, are shown as a dashed line (R^2 = 0.96), and corresponding parameters (± standard deviations) are: $V_{pH,optimal}$ = 0.154 ± 0.009 g/(L·h), pK_{a1} = 3.351 ± 0.131, pK_{a2} = 6.06 ± 0.146; incubation: BioLector, 2.5 g/L α-cellulose in 0.1 M phosphate buffer, 0.25 g/L Celluclast®, T = 37°C, V_L = 200 µL, n = 900 rpm, d_0 = 3 mm, 96-well plate.

Figure 3-21A shows, exemplarily, the results at three different pH values. Here, the slope of the linearly decreasing scattered light intensity varied depending on the applied pH. As shown in the prior adsorption experiments (Figure 3-16B), no significant changes in scattered light intensity were observed when using very low or high pH values (open symbols, Figure 3-21B). As seen in Figure 3-21B, the cellulase activity was a characteristic function of pH, and a typical bell-shaped profile was detected. The applied model describing the pH dependency of enzymes (Eq. 3-3) (Copeland, 2000) provided a good fit, and the corresponding parameters (pK_{a1}, pK_{a2}, and $V_{pH,optimal}$) are listed in the legend of Figure 3-21. The optimal cellulase activity was achieved at a pH of approximately 4.7. When analyzing the effect of pH on purified cellulases by using the conventional dinitrosalicylic acid assay (Chapter 3.1.3.8), almost identical optimal pH values (Figure 3-10A) and model parameters were determined (Table 3-5). Moreover, various authors (Becker et al., 2001; Boer and Koivula, 2003; Busto et al., 1996; Busto et al., 1998) found similar optimal pH values ranging from 4.5 to 5 when using cellulases from *T. reesei*. These similar results additionally proof the applicability of the BioLector technique for screening and characterizing cellulases.

3.2.4   Conclusions

Chapter 3.2 demonstrates an innovative method for assaying cellulase adsorption and activity. This assay is based on the BioLector technique, which allows the online monitoring of scattered light intensities in a continuously shaken microtiter plate. By monitoring cellulose hydrolysis in the BioLector, a typical course of scattered light intensity was detected, which could be clearly verified using a conventional reducing sugar assay. It was shown that this innovative cellulase assay can be easily applied for assaying cellulase activities. In addition, this study shows for the first time that high-throughput scattered light measurements can be used for monitoring the non-hydrolytic effect of cellulases or non-hydrolytic proteins (such as swollenin) on insoluble cellulose.

Even though a large number of cellulase assays exist at the moment, they are not ideal for analyzing cellulases, because they are slow, tedious, or based on soluble cellulosic substrates that do not reflect real insoluble biomass in biorefineries. The presented BioLector technique is an ideal alternative for measuring cellulase adsorption and activity, because it links high-throughput, online analysis, and realistic insoluble cellulosic substrates in one simple system. Using a 96-well microtiter plate, the BioLector technique allows the complete

characterization of cellulases within one experiment, thereby, analyzing the influence of pH value, cellulose, and cellulase concentration. Finally, the presented technique can substantially accelerate screening experiments with novel cellulases or optimized cellulase mixtures while using a variety of insoluble cellulosic substrates and incubation conditions.

In the future, screening experiments should be conducted with the presented BioLector technique so that most appropriate cellulases and incubation parameters can be selected for the hydrolysis of real insoluble biomass used in biorefineries. Moreover, it yields a large amount of measurements that are needed for mathematical models and respective parameters correlating characteristics of both insoluble cellulose and cellulases. Due to this large amount of measurements, the BioLector technique also allows a very accurate determination of kinetic parameters; in contrast to conventional offline assays yielding only a small amount of data points. Nevertheless, further investigations are needed to gain a better understanding of the mechanism of cellulose hydrolysis and to establish kinetic models. It should be noted that, up to now, initial reaction rates were determined using the BioLector technique. However, once detailed kinetic models are established, progress curve analysis should be performed (Zavrel et al., 2008), analyzing cellulase kinetics and enzyme inactivation from one BioLector curve. Moreover, the actual BioLector device should be modified in order to allow incubation temperatures which are above 37°C and closer to the temperature optimum of cellulases. In addition, purified cellobiohydrolases, purified endoglucanases, and mixtures of cellulases and swollenin should be investigated using this prospective method.

4   Simultaneous Saccharification and Fermentation for Itaconic Acid Production

4.1 Introduction

In case of the biocatalytic conversion of lignocellulose (Figures 1-4 and 1-9), the hydrolysis is followed by the fermentation of the released sugars to platform chemicals or fuels. In 2004, the U.S. Department of Energy published a study about the top twelve value-added platform chemicals from biomass (Table 1-1) (Werpy and Petersen, 2004). One of these twelve candidates is itaconic acid (methylene butanedioic acid) – a white crystalline unsaturated dicarboxylic acid (Willke and Vorlop, 2001). It is applied as an additional monomer in styrene-butadiene heteropolymers (synthetic rubber) which can be used in detergents and emulsion paints as well as in the fiber, pharmaceutical, and herbicide industries (Bressler and Braun, 2000; Werpy and Petersen, 2004). Furthermore, itaconic acid can be transformed to the potential biofuel 3-methyltetrahydrofuran (3-MTHF) (Geilen et al., 2010; Marquardt et al., 2010). Various fungi, such as *Aspergillus terreus* (Lockwood and Reeves, 1945) and *Ustilago maydis* (Guevarra and Tabuchi, 1990; Haskins et al., 1955), produce itaconic acid. In case of *A. terreus,* it has been shown that itaconic acid is derived from the tricarboxylic acid cycle via cis-aconitate (Bonnarme et al., 1995). This reaction is catalyzed by cis-aconitate decarboxylase (Bonnarme et al., 1995; Kanamasa et al., 2008).

Cellulosic biomass can be biocatalytically converted to platform chemicals via different process configurations (Chapter 1.4.4). Such configuration is the so-called separate hydrolysis and fermentation (SHF). Thereby, cellulose is enzymatically hydrolyzed to glucose, and the produced glucose is subsequently fermented to the desired product in a second reaction vessel. The main disadvantages of such SHF processes are as follows: (1) the applied cellulases are inhibited by a high glucose concentration at the end of the hydrolysis (Holtzapple et al., 1990); (2) SHF processes require high investment costs due to two separate reaction vessels for hydrolysis and fermentation (Wyman, 1994). In contrast, simultaneous saccharification and fermentation (SSF) processes integrate cellulose hydrolysis and fermentation in one single reaction vessel (Chapter 1.4.4). This remarkably reduces the

investment costs (Wyman, 1994). Moreover, the glucose produced during the hydrolysis is directly consumed by the microorganisms, thereby preventing the product inhibition of the cellulases (Wyman, 1994). Up to now, SSF processes have been applied to convert cellulosic biomass to the following chemicals: ethanol (Olofsson et al., 2008), lactic acid (Abe and Takagi, 1991; Romani et al., 2008; Wee et al., 2006; Yáñez et al., 2003), acetic acid (Borden et al., 2000), citric acid (Asenjo and Jew, 1983), and succinic acid (Chen et al., 2011). As yet, no SSF process for itaconic acid production has been established.

For producing itaconic acid via SSF, it is necessary to find suitable process conditions (e.g. temperature, pH) for both the applied cellulases (hydrolysis) and microorganisms (fermentation). The microorganism typically applied to produce itaconic acid is *A. terreus*, a filamentous fungus. It produces itaconic acid only at pH values between 1.8 and 3.5 (Riscaldati et al., 2000; Rychtera and Wase, 1981). In this highly acidic pH range, however, the conventional and industrially applied cellulase mixtures from *Trichoderma reesei* show very low stabilities and are almost inactive (Nagieb et al., 1985). For example, Celluclast$^{®}$ demonstrates a pH optimum of about 4.7 and is active in a pH range of 2.5 to 7 (Chapter 3.2.3.6). In contrast to *A. terreus*, the smut fungus *U. maydis* mainly produces itaconic acid in a less acidic pH range of approximately 5 to 6 (Guevarra and Tabuchi, 1990) which is closer to the pH optimum of cellulases from *T. reesei*. In addition, *U. maydis* grows as single cells (yeast-like) in liquid cultures and is less sensitive to shear stress than *A. terreus* mycelia. Consequently, *U. maydis* may be generally a more promising candidate for itaconic acid production via SSF processes.

Chapter 4 proposes a SSF process for itaconic acid production. In just one step, the cellulosic substrate α-cellulose should be hydrolyzed by cellulases, and the resulting glucose should be simultaneously converted to itaconic acid by a not yet optimized *U. maydis* wild type strain. The separate hydrolysis of α-cellulose is investigated under SSF conditions and compared with the conventional hydrolysis using SHF conditions. A potential inhibitory effect of the final SSF product (itaconic acid) on the cellulases is also investigated. Finally, a SSF process with α-cellulose as sole carbon source is analyzed in detail and compared with a batch cultivation using glucose as sole carbon source.

4.2   Materials and Methods

4.2.1   Cellulosic Substrates

The cellulosic substrates α-cellulose and Whatman filter paper No.1 were purchased from Sigma-Aldrich (St. Louis, USA). The physical properties of filter paper were summarized by Zhang and Lynd (2004). Physical properties (solubility; purity; crystallinity index, *CrI*; weight-average degree of polymerization, DP_w; geometric mean particle size, d_P) and product information of α-cellulose are given in Chapter 3.1.2.1. Here, it should be noted that α-cellulose is impure and can contain up to 22% (w/w) xylan (Table 3-1).

4.2.2   Cellulase Preparation

The commercial cellulase mixture Celluclast[®] 1.5L (Novozymes, Bagsværd, DK) was applied for hydrolysis and SSF experiments. Celluclast[®] contains a complete cellulase system which consists of cellobiohydrolases, endoglucanases, and β-glucosidases (Chapter 2.2.2). To remove salts, sugars, and other interfering components, Celluclast[®] was previously rebuffered by using column chromatography (as described in Chapter 2.2.2). To determine specific filter paper activities, different dilutions of Celluclast[®] and the rebuffered Celluclast[®] were tested according to Ghose (1987). The following specific filter paper activities (per g protein) were measured: 210 U/g (Celluclast[®]) and 261 U/g (rebuffered Celluclast[®]).

4.2.3   Microorganisms

The smut fungus *Ustilago maydis* MB215 (Hewald et al., 2005) was used as the itaconic acid-producing microorganism. This wild type strain was kindly provided by Michael Bölker, Philipps-Universität (Marburg, DE). The strain is available at the German Collection of Microorganisms and Cell Cultures (DSMZ) under accession number DSM17144 [MB215]. Cryocultures were maintained in 20% (v/v) glycerol at -80°C in Tabuchi medium. Figure 4-1 shows a light microscopic picture of *U. maydis* MB215 in Tabuchi medium.
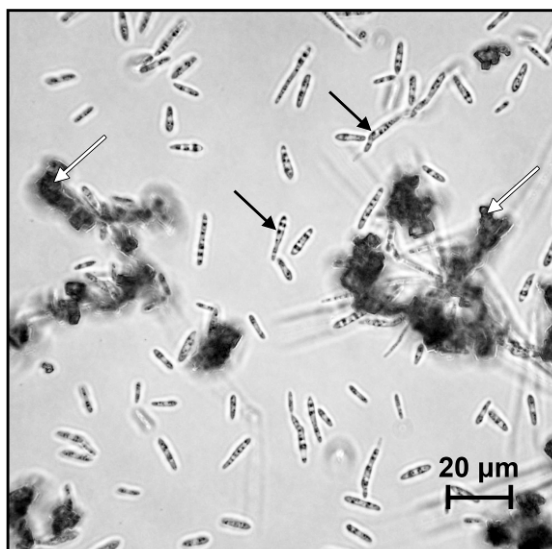
Figure 4-1:   Light microscopic picture of *Ustilago maydis* MB215 in Tabuchi medium. Lipid droplets (inside cells) and $CaCO_3$ particles are indicated with black arrows and white arrows, respectively; microscope: Eclipse E600 (Nikon, Tokyo, JP).

4.2.4   Media and Solutions

Tabuchi medium was used for *U. maydis* cultivations (Guevarra and Tabuchi, 1990). The medium consists of 0.5 g/L KH_2PO_4, 0.2 g/L $MgSO_4 \cdot 7H_2O$, 1 g/L yeast extract (dry chemical for bacteriology; Roth, Karlsruhe, DE), and 10 mg/L $FeSO_4 \cdot 7H_2O$. For precultures, 120 g/L glucose, 1.6 g/L NH_4Cl, and 33 g/L $CaCO_3$ (lime) were added to the medium. For main cultures, 0.267 g/L NH_4Cl and 20 g/L $CaCO_3$ were added. The glucose batch culture contained 60 g/L glucose, whereas for the SSF 60 g/L α-cellulose was used as sole carbon source. The $FeSO_4$ solution and the $CaCO_3$ buffer were sterilized separately and added after autoclaving. An initial pH value of 6.1 was adjusted.

The media composition of the glucose batch and the SSF cultivation was preliminarily optimized using the first step of a factorial "Design of Experiments" approach. For these experiments, four parameters (glucose, ammonium, α-cellulose, and calcium carbonate concentrations) were varied (results not shown). The "Design of Experiments" was performed with the program Design-Expert V8 by Stat-Ease (Minneapolis, USA). With the results from the "Design of Experiments", the aforementioned media compositions for the glucose batch and the SSF process were finally chosen.

4.2.5   Hydrolysis Experiments under SSF Conditions

Hydrolysis experiments with 60 g/L α-cellulose and 6 g/L rebuffered Celluclast[®] were conducted in four different buffers: (1) 0.1 M sodium acetate buffer, pH 4.8 (reference); (2) Tabuchi medium without $CaCO_3$, pH 4.8; (3) Tabuchi medium without $CaCO_3$, pH 6.1; (4) Tabuchi medium with 20 g/L $CaCO_3$, pH 6.1. The hydrolysis experiments were incubated as triplicates in 250 mL Erlenmeyer flasks under the following constant conditions: temperature T = 30 °C, total filling volume V_L = 20 mL, shaking diameter d_0 = 50 mm, shaking frequency n = 300 rpm. The shaking frequency was chosen to ensure sufficient oxygen supply in the cultivation experiments as well as the complete suspension of cellulose particles (Kato et al., 2001) (Chapter 3.1.3.9). Thus, mass transfer limitations were excluded, and the whole cellulose particle surface became accessible to the cellulases, thereby optimizing cellulase adsorption and activity (Chapter 3.1.3.9). Three different blanks were incubated similarly: (1) without cellulase, (2) without substrate, or (3) without substrate and without cellulase. After defined time intervals, samples were taken and centrifuged (825 × g, 3 min, 4°C). The resulting supernatants were heated (10 min, 100°C) to inactivate cellulases, and the supernatants were subsequently analyzed for reducing sugar concentration with the dinitrosalicylic acid assay (Chapter 4.2.7.1) and for glucose concentration with HPLC (Chapter 4.2.7.3). Initial cellulase activities during hydrolysis experiments were calculated by applying a linear fit to reducing sugar concentration data from 0-2 h.

4.2.6   Cultivation (Glucose-Batch, SSF)

In order to monitor the oxygen transfer rates (OTR) during cultivation experiments, a respiration activity monitoring system (RAMOS) was used. The applied RAMOS device was fabricated in-house and described by various studies (Anderlei and Büchs, 2001; Anderlei et al., 2004). A commercial version of this device is available from HiTec Zang GmbH (Herzogenrath, DE) or Kühner AG (Birsfelden, CH). Precultures were inoculated from cryo-cultures. Main cultures were inoculated with 200 µL from a 24 h-old preculture. All cultivations were performed in 250 mL RAMOS shake flasks under the following constant conditions: temperature T = 30 °C, total filling volume V_L = 20 mL, shaking diameter d_0 = 50 mm, shaking frequency n = 300 rpm.

4.2.7   Analytical Methods

To obtain offline data of the cultivation experiments, additional Erlenmeyer flasks were used for sampling. The investigated *U. maydis* strain was cultivated in parallel in these flasks under the same conditions as the cultivations (batch, SSF) in the RAMOS device (Chapter 4.2.6). Each flask was only applied for one sampling step. One part of the flask was directly used for measuring ammonium, pH, non-hydrolyzed cellulose, and residual cellulase activity. The second part was centrifuged (825 × g, 3 min, 4°C), and the resulting supernatant was subsequently inactivated (10 min, 100°C) and used for the dinitrosalicylic acid assay and HPLC-analysis. Evaporation effects during the cultivation were considered in the determination and calculation of the offline measured concentration values.

4.2.7.1   Dinitrosalicylic Acid Assay during Hydrolysis and SSF Experiments

The dinitrosalicylic acid assay (Miller, 1959) was applied to quantify the reducing sugars released during hydrolysis and SSF experiments. Here, the dinitrosalicylic acid assay was performed as described in Chapter 2.2.16. Preliminary experiments showed that the assay was not influenced by itaconic acid concentrations of ≤ 70 g/L (= concentration within the analyzed sample).

4.2.7.2   Determination of Non-Hydrolyzed Cellulose

To quantify the amount of non-hydrolyzed cellulose during SSF experiments, cultivation broth was directly inactivated (10 min, 100°C) and applied as substrate solution in a subsequent hydrolysis step. To achieve a complete saccharification of non-hydrolyzed cellulose, this subsequent hydrolysis was conducted with 0.75 mL of the inactivated cultivation broth and an excess of fresh rebuffered Celluclast® (30 g/L) in 0.1 M sodium acetate buffer (pH 4.8). The mixtures were incubated in 2 mL Eppendorf tubes on a thermomixer MHR23 (HLC Biotech, Bovenden, DE) for 96 h under the following constant conditions: temperature $T = 45$ °C, total filling volume $V_L = 1.5$ mL, shaking diameter $d_0 = 3$ mm, shaking frequency $n = 1000$ rpm. Three different blanks were incubated similarly: (1) without cellulase, (2) without substrate, or (3) without substrate and without cellulase. Finally, the amount of glucose was determined via HPLC-analysis (Chapter 4.2.7.3) – dilution effects were accounted for – and the amount of non-hydrolyzed cellulose was calculated using the following equation:

$$C = P_{glucose} \cdot \frac{162}{180} \qquad\qquad (4\text{-}1)$$

with C denoting the residual concentration of cellulose [g/L] during SSF, $P_{glucose}$ denoting the glucose concentration [g/L] resulting from complete saccharification of cellulose sampled from SSF, and 162/180 denoting the correction coefficient between molecular weights of glucan monomers and glucose. Since no cellobiose and cellotriose were detected, complete saccharification of the cellulose was verified.

4.2.7.3   HPLC-Analysis of Soluble Sugars and Itaconic Acid

Glucose, cellobiose, xylose, and itaconic acid concentrations were measured via HPLC-analysis. The detailed procedure is described in Chapter 3.1.2.9.

4.2.7.4   Measurement of Ammonium Concentration

To measure ammonium concentrations in the culture broth, an ammonium cell test (Merck KGaA, Darmstadt, DE) was applied. The extinction at 690 nm was measured with a Spectroquant Nova 60 spectrophotometer (Merck KGaA, Darmstadt, DE).

4.2.7.5   Measurement of pH

The pH values were measured with a CyberScan pH 510 (Eutech, Nijkerk, NL) and with a Titroline alpha device (Schott Instruments, Mainz, DE).

4.2.7.6   Determination of Residual Cellulase Activity

Samples of SSF cultivations were centrifuged (825 $\times$ g, 3 min, 4°C), and the resulting supernatants were analyzed with respect to residual cellulase activities. To determine filter paper activities [FPU/mL], different dilutions of the supernatants were tested according to Ghose (1987). Moreover, cellulase activities on α-cellulose [U/mL] were tested according to Chapter 3.1.2.7.

4.3   Results and Discussion

4.3.1   Separate Enzymatic Hydrolysis of α-Cellulose under SSF Conditions

To investigate the separate cellulose hydrolysis under the SSF conditions needed for *U. maydis*, kinetic experiments were performed under varying conditions (pH and media composition). Figure 4-2 depicts the reducing sugars formed during the hydrolysis of α-cellulose by rebuffered Celluclast® at 30°C. Based on Figure 4-2, initial cellulase activities were calculated (Table 4-1) by applying a linear fit to reducing sugar concentration data from 0 h to 2 h. The reference experiment with optimal pH and media conditions for the cellulases – 0.1 M sodium acetate buffer (pH 4.8), according to the manufacturers protocol of Celluclast® – was compared to hydrolysis experiments in three different cultivation media: (1) Tabuchi medium without $CaCO_3$ at pH 4.8, (2) Tabuchi medium without $CaCO_3$ at pH 6.1, and (3) Tabuchi medium including 20 g/L $CaCO_3$ at pH 6.1.
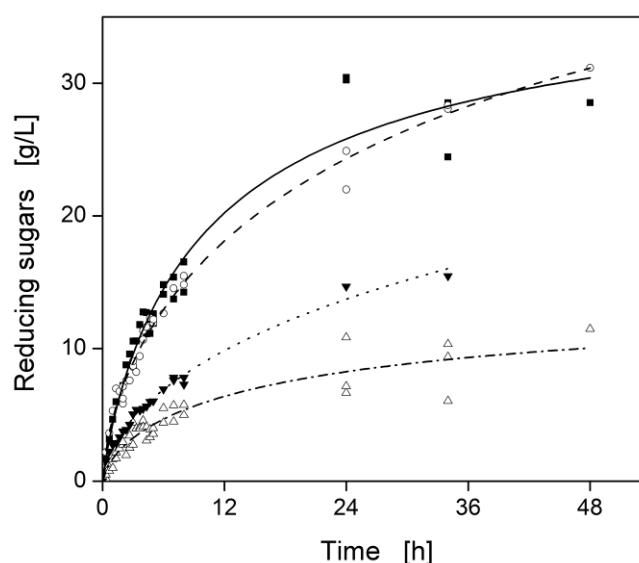
Figure 4-2:   Enzymatic hydrolysis of α-cellulose under conditions applied in SSF cultivations. Varying buffers/media: (■, solid line) 0.1 M sodium acetate buffer (pH 4.8) (reference), (○, dashed line) Tabuchi medium without $CaCO_3$ (pH 4.8), (▼, dotted line) Tabuchi medium without $CaCO_3$ (pH 6.1), (△, dashed-dotted line) Tabuchi medium with 20 g/L $CaCO_3$ (pH 6.1); incubation: 60 g/L α-cellulose in the aforementioned buffers/media, 6 g/L rebuffered Celluclast®, $T = 30°C$, $V_L = 20$ mL, $n = 300$ rpm, $d_0 = 50$ mm, 250 mL Erlenmeyer flask.

Table 4-1:   Initial cellulase activities under conditions applied in SSF cultivations.

Conditions	Initial cellulase activity [U/mg]	R^2 [-]
0.1 M sodium acetate buffer, reference (pH 4.8)	0.071 ± 0.0009	0.999
Tabuchi medium without $CaCO_3$ (pH 4.8)	0.082 ± 0.0018	0.997
Tabuchi medium without $CaCO_3$ (pH 6.1)	0.030 ± 0.0010	0.996
Tabuchi medium including 20 g/L $CaCO_3$ (pH 6.1)	0.026 ± 0.0004	0.998

Errors are given as standard deviations. Initial cellulase activities were calculated by applying a linear fit to reducing sugar concentration data from 0 h to 2 h (Figure 4-2).

R^2, coefficient of determination.

The hydrolysis under reference conditions (0.1 M sodium acetate buffer, pH 4.8) started with an initial α-cellulase activity of 0.071 U/mg (Table 4-1) and almost reached saturation at a reducing sugar concentration of ca. 28.5 g/L after 48 h (Figure 4-2). The saturation is most probably reached due to high glucose concentrations (20.9 g/L) and the resulting product inhibition of the cellulases (Holtzapple et al., 1990). The hydrolysis performed in Tabuchi medium including $CaCO_3$ at a pH 6.1 (final SSF medium) had an initial cellulase activity of only 0.026 U/mg. Moreover, the reducing sugar concentration was 11.5 g/L after 48 h, which corresponds to a final saccharification degree (Eq. 2-3) of only ca. 25% (with respect to the 78% cellulose content in α-cellulose). These diminished activity values are caused either by the high pH value, a specific medium component, or both. To investigate the influence of $CaCO_3$ and of the less acidic pH value in the Tabuchi medium, hydrolysis experiments in Tabuchi medium without $CaCO_3$ were performed at pH values of 6.1 and 4.8. In Tabuchi medium without $CaCO_3$ (pH 6.1), an initial cellulase activity of 0.03 U/mg (Table 4-1) and a reducing sugar concentration of 15.5 g/L (after 34 h) were measured (Figure 4-2). Since these results are similar to those with Tabuchi medium including $CaCO_3$ (pH 6.1), the $CaCO_3$ buffer had only a slightly adverse effect on the cellulase activity at pH 6.1. The slightly reduced cellulase activity may be explained by the adsorption of cellulases on the surface of the $CaCO_3$ crystals. By contrast, the hydrolysis curve for Tabuchi medium at pH 4.8 was nearly the same as the reference hydrolysis curve, and showed even slightly higher initial cellulase activities (0.082 U/mg) and a reducing sugar concentration of 31.2 g/L after 48 h. Consequently, the pH value of 6.1 could be identified as the major factor reducing the cellulase activity under SSF conditions. These results also indicated that, besides the $CaCO_3$ buffer, the other medium components did not significantly affect the cellulase activity. Since

xylose was not detected during all hydrolysis experiments, xylan (contained to 22% in α-cellulose, Table 3-1) was not hydrolyzed by Celluclast®.

As shown in Figure 4-2, the Tabuchi medium (SSF medium) leads to a reduction in cellulase activity due to the increased pH value. According to Olofsson et al. (2008), however, there is always a compromise needed to find favorable SSF conditions (e.g. temperature and pH) for both cellulases and microorganisms. Thus, in most SSF processes, the temperature is normally kept below 37°C (cellulase optimum at 55°C; Olofsson et al., 2008), and a pH value of 5.0 or 5.5 is chosen (cellulase optimum at pH 4.8; Mandels and Sternberg (1976) or Chapter 3.2.3.6). To finally solve this problem, new cellulases have to be screened or known cellulases have to be genetically engineered, thereby generating cellulases with temperature and pH optima comparable to those of the applied SSF microorganism. For example, Liang et al. (2011) have recently found a cellulase with an expanded temperature profile, retaining reasonably high activities at reduced temperatures. Alternatively, common SSF microorganisms may be replaced by suitable thermophilic ones (Prasetyo et al., 2011) growing at a pH of 4.8 and at temperatures closer to the optimum of cellulases (55°C). Despite the challenge to develop cellulases and microorganisms with similar temperature and pH optima, one principal advantage of a SSF process is that the cellulases are less inhibited by the end-product glucose, since the glucose released during hydrolysis is directly consumed by the applied microorganism (Olofsson et al., 2008).

4.3.2   Influence of Itaconic Acid on Cellulase Activity

During SSF processes, cellulases are exposed to high concentrations of the fermentation products (such as ethanol, lactic acid, or itaconic acid). Therefore, it is important to study if the applied cellulases are inhibited by these products (Takagi, 1984). Figure 4-3 shows the enzymatic hydrolysis of α-cellulose (Figure 4-3A) as well as the derived cellulase activities (Figure 4-3B) in the presence of different itaconic acid concentrations (0-70 g/L) under SSF conditions.

The specific cellulase activities varied only slightly (standard deviation: 0.003 U/mg) with respect to the arithmetic mean value of all hydrolysis experiments (ca. 0.019 U/mg) (Figure 4-3B). All experiments with itaconic acid reached slightly higher specific cellulase activities (0.016 U/mg to 0.025 U/mg) compared to the hydrolysis experiment without itaconic acid

(0.015 U/mg). Therefore, no negative influence of itaconic acid on the specific activity of Celluclast® could be identified under the applied SSF conditions. Here, it should be noted that almost saturating concentrations of itaconic acid were applied, since the solubility of itaconic acid in pure water is 83 g/L at 20°C (Willke and Vorlop, 2001). According to Tagaki (1984), several acids (such as acetic acid, citric acid, itaconic acid, α-ketoglutaric acid, lactic acid, and succinic acid) scarcely inhibit cellulases. By contrast, ethanol as well as butanol are quite strong inhibitors of cellulases (Takagi, 1984). Consequently, the results from this current study as well as Tagaki`s study confirm the applicability of Celluclast® in SSF processes for itaconic acid production.
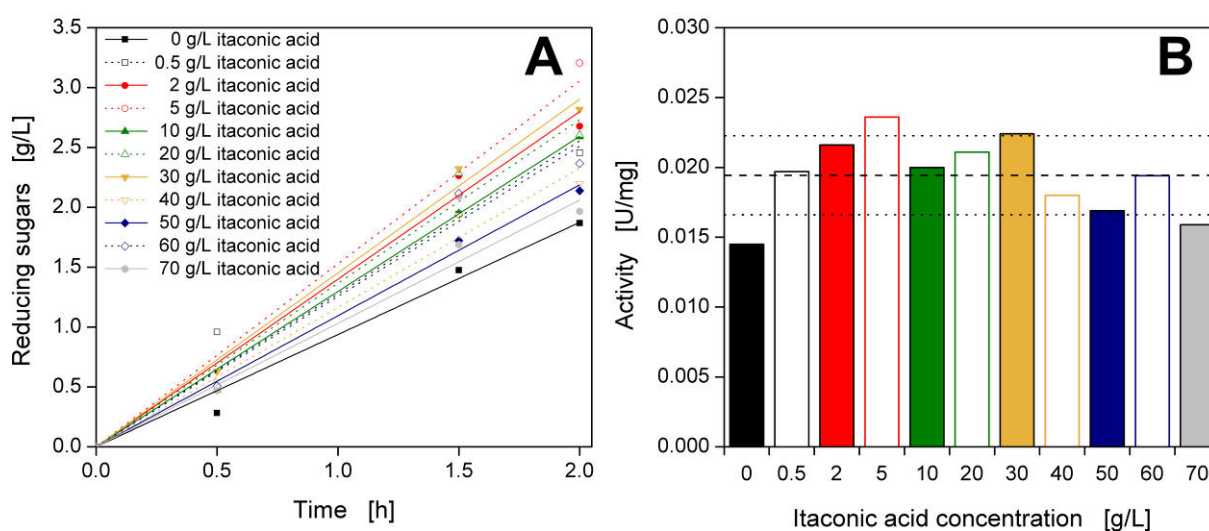
Figure 4-3:   Influence of itaconic acid concentration on the cellulase activity. (**A**) Hydrolysis kinetics in the presence of different itaconic acid concentrations; (**B**) cellulase activity at different itaconic acid concentrations. Initial cellulase activities during hydrolysis experiments were calculated by applying a linear fit to reducing sugar concentration data (Figure 4-3A) from 0 h to 2 h. Here, the coefficients of determination were > 0.90 for each fit, and the coefficients of variation were < 6% for each activity value. Dashed line: arithmetic mean value for all measured activities. Black dotted lines: arithmetic mean value ± standard deviation for all measured activities; incubation: 60 g/L α-cellulose in Tabuchi medium with 20 g/L $CaCO_3$ (pH 6.1), 6 g/L rebuffered Celluclast®, T = 30°C, V_L = 20 mL, n = 300 rpm, d_0 = 50 mm, 250 mL Erlenmeyer flasks.

4.3.3   SSF for Itaconic Acid Production

To prove the general feasibility of a SSF process producing itaconic acid, the wild type strain *U. maydis* MB215 was used. A batch cultivation with glucose as well as a SSF with α-cellulose as sole carbon source were analyzed in detail and compared (Figure 4-4).

The oxygen transfer rate (OTR) of the glucose batch (Figure 4-4A) increased sharply and peaked at 8.7 mmol/(L·h) after 13.5 h. Subsequently, it dropped until 24 h and then gradually declined until 96 h. After 96 h, the OTR finally dropped down to a value of 1.5 mmol/(L·h). As confirmed by HPLC measurement (Figure 4-4B), the glucose was depleted at this final point (96 h). There was a distinct break in the OTR curve at the time point of 12 h (Figure 4-4A, black arrow) when the ammonium was exhausted (Figure 4-4C). The itaconic acid production started directly after this ammonium depletion. No further increase in itaconic acid could be detected after 132 h. Finally, an itaconic acid concentration of about 9.1 g/L was reached in this experiment. Once the ammonium was depleted and the itaconic acid production started, the pH of the culture (Figure 4-4C) decreased to a minimum of 5.5 after approximately 47.5 h. By contrast, when glucose was completely consumed after 96 h, the pH value increased again due to cell lysis (proven by light microscopy, data not shown).
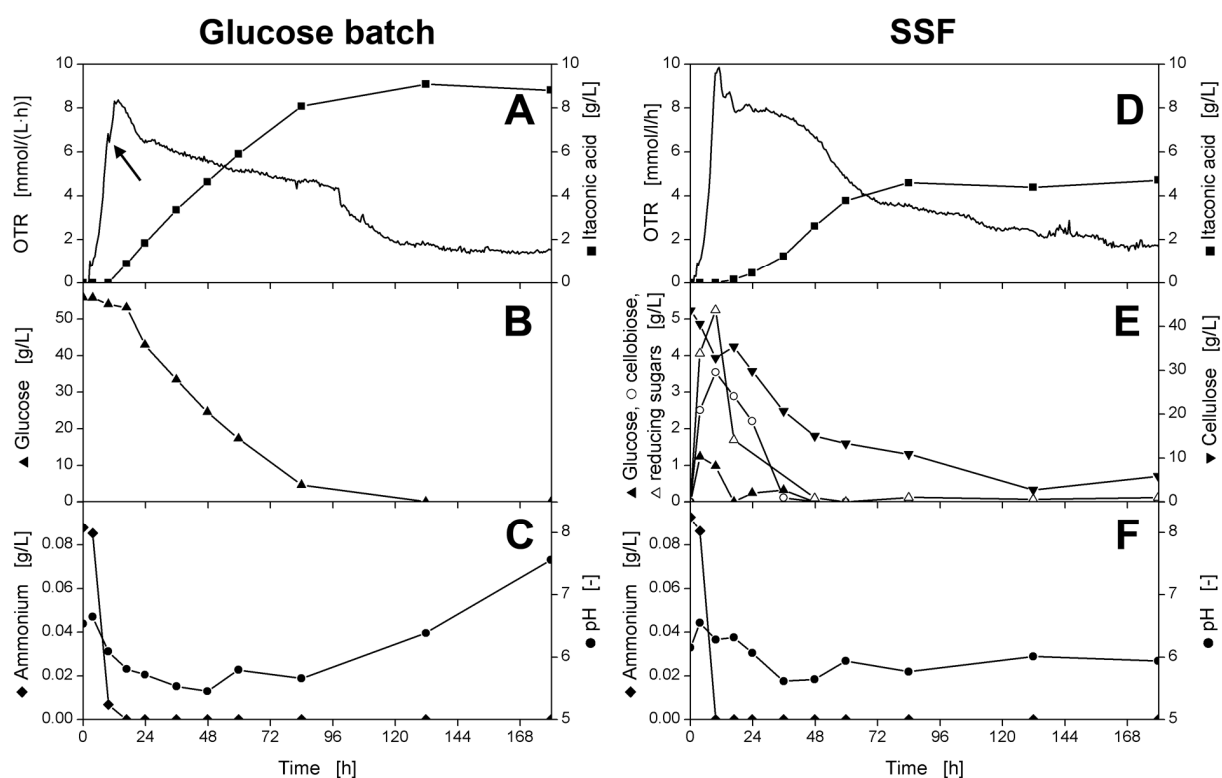
Figure 4-4:   Glucose batch vs. simultaneous saccharification and fermentation (SSF) for itaconic acid production by using the *U. maydis* wild type strain MB215. (**A**, **B**, **C**) Batch cultivation with 60 g/L glucose as sole carbon source (reference). The black arrow (**A**) indicates a distinct break in the OTR curve at the time point of 12 h when the ammonium was exhausted (**C**); (**D**, **E**, **F**) SSF with 60 g/L α-cellulose as sole carbon source and 6 g/L rebuffered Celluclast®; incubation: Tabuchi medium with 20 g/L $CaCO_3$ (pH 6.1) and 0.267 g/L NH_4Cl, $T = 30°C$, $V_L = 20$ mL, $n = 300$ rpm, $d_0 = 50$ mm, 250 mL Erlenmeyer flasks.

The final itaconic acid concentration of 9.1 g/L (produced with 60 g/L glucose, itaconic acid yield ($Y_{P/S}$) of 0.15 g/g) was relatively low compared to an established *A. terreus* production strain with 82.3 g/L itaconic acid (produced with 160 g/L glucose, $Y_{P/S}$ of 0.51 g/g) (Yahiro et al., 1995). However, the aim of this study is to demonstrate the first proof-of-concept for the itaconic acid production in a SSF process. In this study, *A. terreus* could not be used as production host, since the applied cellulases are instable (Nagieb et al., 1985) and almost inactive (Chapter 3.2.3.6) at the low pH range required for itaconic acid production by *A. terreus* (pH 1.8-3.5, Riscaldati et al., 2000; Rychtera and Wase, 1981).

In comparison to the glucose batch, the OTR curve of the SSF also rose sharply initially, showing a peak of 9.9 mmol/(L·h) after 11 h (Figure 4-4D). During this time period of up to 11 h, the products resulting from cellulose hydrolysis (glucose, cellobiose, or all reducing sugars) accumulated (Figure 4-4E). The glucose concentration increased to 1.2 g/L after 7 h, because the initial cell concentration of *U. maydis* was too low to allow the direct consumption of all the released glucose. After 7 h, however, the total glucose uptake rate of the cells was sufficient for the complete consumption of the released glucose. Hence, the glucose concentration decreased and reached almost 0 g/L after 20 h; this decrease in glucose concentration was checked and reproduced in two additional SSF experiments (data not shown). In comparison, cellobiose accumulated (3.6 g/L after ca. 9.5 h) due to the low β-glucosidase activity in the applied cellulase mixture from *T. reesei* (Chapter 1.4.2.3). However, after 20 h, cellobiose was more rapidly converted to glucose, and the cellobiose concentration equaled 0 g/L after 36 h. In this time period (20-36 h), the glucose production exceeded meanwhile again the glucose consumption by *U. maydis*. This may be explained by the following reasons: (1) Due to the low glucose concentration after 20 h, the β-glucosidase was less inhibited by glucose (Holtzapple et al., 1990) and led to higher glucose production rates; (2) the interim glucose consumption by *U. maydis* was relatively low from 20-36 h, since ammonium was already depleted and the cells needed to adapt their metabolism. After 47.5 h, the glucose was simultaneously consumed as soon it was produced. From this time point, the culture was carbon source-limited and exhibited a constant OTR (2-4 mmol/(L·h)) which is typical for fed-batch mode. The reducing sugar concentration was a sum of all sugar molecules (glucose, cellobiose, and oligosaccharides). The overall reducing sugar concentration peaked at 9.5 h at a concentration of 5.3 g/L. After 47.5 h, it was approximately 0.1 g/L due to the presence of oligosaccharides produced during the hydrolysis of α-cellulose.

As a result of the enzymatic hydrolysis, the α-cellulose concentration decreased during the SSF experiment (27 g/L after 48 h) and reached a minimum of 2.7 g/L at 127 h (Figure 4-4E). This corresponded to saccharification degrees of 65% (48 h) and 95% (127 h), respectively. By contrast, in the separate hydrolysis experiment (Figure 4-2), a stagnant and significantly lower saccharification degree of 25% was reached after 48 h. This difference in saccharification clearly demonstrated that the cellulases were less inhibited during SSF because of the immediate consumption of glucose by *U. maydis*. This is one of the major benefits of SSF and leads to significantly increased saccharification degrees (Olofsson et al., 2008). However, a small amount of cellulose remained unhydrolyzed (Figure 4-4E). Olofsson et al. (2008) listed the following reasons for incomplete cellulose hydrolysis in SSF processes: (1) inhibition of cellulases by the main products or by-products of the applied microorganisms, (2) enzyme inactivation, (3) unproductive enzyme adsorption, (4) decreasing availability of cellulose chain ends, and (5) increasing crystallinity with proceeding cellulose conversion. Since high residual cellulase activities of 72% or 69% were measured at the end of the SSF experiment (after 180 h) by using α-cellulose or filter paper as a substrate, cellulase inactivation could be ruled out. In addition, it should be noted that xylan – found up to 22% in α-cellulose (Table 3-1) – was not hydrolyzed by Celluclast®, and xylose was not detected via HPLC during separate hydrolysis and SSF experiments (data not shown). Consequently, the cellulose contained in α-cellulose was the sole carbon source during SSF. Moreover, xylan may cover the residual unhydrolyzed cellulose and render it inaccessible for a further enzymatic attack (Mosier et al., 2005). Therefore, xylan may be an additional reason for the small residual amount of cellulose at the end of the presented SSF experiment.

Figure 4-4F depicts the pH course during the SSF experiment. The pH value decreased to 5.6 until 36 h and then remained at a constant value of approximately 5.9. In contrast to the glucose batch (Figure 4-4C), no final increase in the pH value was detected. This indicates that no cell lysis occurred during SSF; due to the constant supply of glucose to the microorganisms. After the ammonium limitation (ca. 9.5 h, Figure 4-4F), the cells began to produce itaconic acid (Figure 4-4D). After 180 h, a maximum itaconic acid concentration of 4.71 g/L was achieved via SSF.

The reference batch cultivation reached an itaconic acid yield of 0.15 g/g (maximum theoretical yield: 0.72 g per g glucose). The SSF cultivation had a similar itaconic acid yield of 0.12 g/g (maximum theoretical yield: 0.8 g per g cellulose) with respect to the actual

cellulose content of α-cellulose. Within this study, an *U. maydis* wild type strain was used that was not particularly screened and optimized for itaconic acid production. Therefore, the itaconic acid yields of both *U. maydis* processes were relatively low compared to processes with optimized *A. terreus* production strains (itaconic acid yield of 0.51 g/g) (Yahiro et al., 1995). As explained above, however, *A. terreus* can not be applied in SSF processes with cellulases from *T. reesei*, since *A. terreus* produces itaconic acid only in a pH range between 1.8 and 3.5 (Riscaldati et al., 2000; Rychtera and Wase, 1981). At these highly acidic pH values, the industrially applied cellulase mixtures from *T. reesei* are almost inactive (Chapter 3.2.3.6) and show very low stabilities (Nagieb et al., 1985). In conclusion, this study shows for the first time that cellulose can be directly converted to itaconic acid in just one step via SSF. Therefore, this study can be considered as the first proof-of-concept for a SSF process producing itaconic acid.

4.4 Conclusions

Chapter 4 presents for the first time a SSF process for itaconic acid production. In just one step, α-cellulose was hydrolyzed via cellulases, and the resulting glucose was simultaneously converted to itaconic acid by a not yet optimized *U. maydis* wild type strain. The proposed SSF is a promising integrated process allowing the production of itaconic acid from cellulosic biomass without the need of a separate hydrolysis step.

In order to improve the overall productivity of the whole process, the applied cellulase mixture and the itaconic acid producing microorganism *U. maydis* need to be adapted to the requirements of the SSF. The applied cellulase mixture should be improved in such a way that the process optima of the cellulases (such as pH and temperature) are closer to the process optima of *U. maydis* (see discussion in Chapter 4.3.1). As mentioned before, a cellulase with an expanded temperature profile – retaining reasonably high activities at reduced temperatures – has already been found by Liang et al. (2011). Alternatively, a thermophilic strain of *U. maydis* – growing at temperatures closer to the optimum of cellulases (Prasetyo et al., 2011) – needs to be screened and applied. Furthermore, the process conditions should be further balanced to find a good compromise for both hydrolysis and fermentation. Since Celluclast® is intended for SHF processes, changing the cellulase composition of Celluclast® for SSF processes would also be beneficial. To improve the itaconic acid yield of the SSF, it

would be important to genetically engineer *U. maydis*. For example, genes/enzymes leading to the formation of undesired by-products, such as lipids (Klement et al., 2011), should be deleted. In the case of *A. terreus*, the biosynthesis of itaconic acid was already elucidated (Bonnarme et al., 1995; Kanamasa et al., 2008), and itaconic acid yields could be significantly increased (Yahiro et al., 1995). Equivalent research activities and improvements also need to be achieved with *U. maydis.* In addition, higher cellulose concentrations should be applied during SSF so that higher product concentrations are reached and the subsequent recovery of itaconic acid is more efficient. Finally, the whole process should be modeled to find an overall process optimum.

In future studies, the developed SSF process need to be compared with a SHF process in which hydrolysis and fermentation are performed under independent optimal conditions. In order to combine the advantages of SHF and SSF, a hybrid process should be also investigated. Such process would consist of two conversion steps. First, cellulose is partially hydrolyzed to cellooligomers under optimal hydrolysis conditions – without the formation of inhibiting glucose or cellobiose concentrations. Second, *U. maydis* is added to perform a SSF process. During this SSF, the cellooligomers are hydrolyzed to glucose by cellulases, and the glucose is directly converted to itaconic acid by *U. maydis*, thereby avoiding the product inhibition of cellulases.

5   Summary, Conclusions, and Outlook

Cellulose is an abundant and renewable resource which can be used for the sustainable production of platform chemicals such as itaconic acid. Because of its high number of functional groups, itaconic acid has a significant market potential and can be utilized for the production of established or novel products (such as synthetic rubber or the biofuel 3-methyltetrahydrofuran). In contrast to non-selective approaches necessitating previous gasification, the biocatalytic conversion of cellulose to itaconic acid is a very promising approach due to its high selectivity, mild conditions, and low exergy loss. However, such biocatalytic processes are seldom applied at industrial scale since their single conversion steps exhibit low efficiencies or high costs. In general, these conversion steps are: pretreatment, hydrolysis, and fermentation. In order to allow a knowledge-based optimization of the biocatalytic process, an in-depth understanding of the individual conversion steps was generated within this thesis. In addition, new approaches as well as screening technologies were established, and the possibility of integrated process configurations was validated.

In Chapter 2, cellulose was pretreated under mild conditions by applying the non-hydrolyzing protein swollenin – naturally produced in low yields by the fungus *T. reesei*. To yield sufficient swollenin for industrial applications, a new way of producing recombinant swollenin was presented. After expression in the yeast *K. lactis*, the resulting swollenin was purified. The adsorption parameters of the recombinant swollenin onto cellulose were quantified for the first time and were comparable to those of individual cellulases from *T. reesei*. Afterwards, four different insoluble cellulosic substrates were pretreated with swollenin. At first, it could be qualitatively shown by macroscopic evaluation, light microscopy and scanning electron microscopy that swollenin caused deagglomeration of cellulose agglomerates as well as dispersion of cellulose microfibrils (amorphogenesis/ decrystallization). Afterwards, the effects of swollenin on cellulose particle size, maximum cellulase adsorption (accessibility), and cellulose crystallinity were quantified. The pretreatment with swollenin resulted in a significant decrease in particle size of the cellulosic substrates as well as in their crystallinity, thereby substantially increasing maximum cellulase adsorption onto these substrates. Subsequently, the pretreated cellulosic substrates were hydrolyzed with cellulases. Here, pretreatment of cellulosic substrates with swollenin – even in non-saturating concentrations – significantly accelerated the hydrolysis. By correlating

particle size and crystallinity of the cellulosic substrates with initial hydrolysis rates, it could be shown that the swollenin-induced reduction in particle size and crystallinity resulted in high cellulose hydrolysis rates. In conclusion, recombinant swollenin was easily produced with the robust yeast *K. lactis*. For the first time, it was quantified and elucidated in detail how swollenin affects different cellulosic substrates and how it improves their subsequent hydrolysis. Since standard assays are missing for deagglomeration, amorphogenesis, and the comparison of different non-hydrolyzing proteins, the presented results may serve as an initial means to establish such assays for future studies. Moreover, a safe and environmentally friendly pretreatment can be achieved by simply incubating cellulosic substrates with swollenin under mild conditions. Depending on the applied feedstock, swollenin pretreatment may be a promising additional pretreatment step to open up the recalcitrant structure of cellulose.

Besides the application of proper pretreatment techniques, the efficiency of the subsequent cellulose hydrolysis substantially depends on selecting the best performing cellulases and the optimal hydrolysis conditions. In order to screen these optimal parameters, practical cellulosic substrates and sophisticated cellulase assays are essential. Within Chapter 3, both requirements were addressed.

In Chapter 3.1, insoluble α-cellulose was found to be an excellent practical substrate to screen and characterize the adsorption and the activity of cellobiohydrolases (CBH) and endoglucanases (EG). First, a novel and reproducible purification method was established to prepare the major cellulases from *T. reesei* (CBH I, CBH II, EG I, and EG II) with high purity. Second, CBH I and EG I were utilized in order to study and model the adsorption isotherms (Langmuir) and kinetics (pseudo-first-order). It was found that, using α-cellulose, the adsorption models fitted to the experimental data and yielded adsorption parameters (A_{max}, K_D, k_{ad}) comparable to those for filter paper as an established model substrate. Third, the hydrolytic activities of the purified cellulases were analyzed in detail. Thereby, the sugar production patterns were determined – proving cellobiose as the major product of CBHs, and cellotriose, cellobiose, and glucose as the major products of EGs. When analyzing the kinetics of α-cellulose hydrolysis, the hydrolysis rates were constant at the start of the experiment but declined afterwards due to product inhibition or the alteration of physical cellulose properties (such as a decrease in cellulose accessibility and reactivity). Here, a simple semi-mechanistic model could be developed to precisely predict the kinetics of α-cellulose hydrolysis.

Moreover, the effects of pH and temperature on cellulase activity were analyzed and modeled, and optimal hydrolysis conditions were determined (pH: 4.8-5, temperature: 55-60°C). Fourth, the adsorption and the activity of cellulases were investigated under different hydrodynamic conditions (including liquid mixing and cellulose suspension). Here, the complete suspension of cellulose particles had to be ensured in order to optimize cellulase adsorption and activity. Finally, in order to compare α-cellulose with three typically used model substrates, the exact cellulase activities towards all four substrates were measured. Here, all purified CBHs and EGs displayed comparable activities only on insoluble α-cellulose. In conclusion, Chapter 3.1 showed in detail, for the first time, the effect of hydrodynamics on cellulase adsorption as well as the correlation between the adsorption and the activity of cellulases at different hydrodynamic conditions. Moreover, it was proven that α-cellulose is an excellent insoluble substrate to screen both CBHs and EGs. The presented results and models already allow an optimization of the enzymatic cellulose hydrolysis. However, further investigations are needed to gain a deeper understanding of cellulose hydrolysis and to establish fully mechanistic models accounting for all inherent actions during cellulose hydrolysis and for all physical properties of heterogeneous cellulose. These mechanistic models may also supply valuable information to optimize cellulose pretreatment, since the physical cellulose properties limiting subsequent hydrolysis may be specified by using such models.

Despite the high number of cellulase assays, no assay has been developed so far that incorporates high-throughput, online analysis, and insoluble cellulosic substrates. In Chapter 3.2, a sophisticated cellulase assay was developed that links all these relevant aspects. This assay is based on the BioLector technique – allowing online monitoring of scattered light intensities in a continuously shaken microtiter plate. At first, the hydrolysis of different insoluble cellulosic substrates, catalyzed by a cellulase mixture from *T. reesei*, was monitored using the BioLector. Thereby, the initial hydrolysis rates, obtained from the course of calibrated scattered light intensities, could be clearly verified by using a conventional reducing sugar assay. Thus, it was proven that cellulase activities could be quantitatively assayed via the BioLector. At low cellulase/cellulose ratios, the determined cellulase activities and Michaelis-Menten parameters were mainly affected by the crystallinity of the cellulose. Here, the apparent maximum cellulase activities inversely correlated with the crystallinity. At high cellulase/cellulose ratios, the particle size of the cellulose – defining the external surface area accessible to the cellulases – was the key determining factor for cellulase activity.

Additionally, the developed technique was successfully applied to evaluate and model the effect of pH value on cellulase activity. Finally, cellulase adsorption as well as the non-hydrolytic effect (cellulose deagglomeration) of cellulases and swollenin could be analyzed by using scattered light detection. In conclusion, the first sophisticated cellulase assay was presented which simultaneously combines high-throughput, online analysis, and insoluble cellulosic substrates in one simple system. The developed technique can be used for assaying cellulase adsorption as well as cellulase activity. By using microtiter plates, it allows a comprehensive characterization of cellulases within one single experiment, thereby, analyzing the influence of pH value, cellulose, and cellulase concentration. Moreover, it yields a large amount of measurements that are needed for mechanistic models of cellulose hydrolysis. Consequently, the presented technique may substantially accelerate fundamental research on cellulase screening. However, it should be noted that, up to now, initial cellulase activities were determined by using the BioLector. Once detailed mechanistic models are established, progress curve analysis should be applied in order to analyze cellulase kinetics and further phenomena such as enzyme inactivation from one BioLector curve.

Up to now, itaconic acid has solely been produced via conventional fermentations using directly fermentable carbon sources such as glucose. In Chapter 4, the first integrated process was developed to directly convert cellulose to itaconic acid via simultaneous saccharification and fermentation (SSF). At first, the separate enzymatic hydrolysis of α-cellulose was investigated under SSF conditions and compared with conventional hydrolysis conditions. Here, cellulase activities diminished in the applied Tabuchi medium due to its inappropriate pH value of 6.1. After 48 h, only 25% of cellulose was hydrolyzed because of the reduced cellulase activities and the strong product inhibition by the released sugars. Additionally, a potential inhibitory effect of itaconic acid was investigated. However, itaconic acid concentrations of up to 70 g/L did not inhibit the applied cellulases. During the SSF, α-cellulose was hydrolyzed by cellulases, and the released glucose was simultaneously converted to itaconic acid by a not yet optimized *U. maydis* wild type strain. The SSF process was comprehensively analyzed and compared with an ordinary batch fermentation using glucose as sole carbon source. During SSF, over 95% of cellulose was hydrolyzed which is significantly higher than the yield of separate hydrolysis under SSF conditions. This increase in hydrolysis yield illustrated that the cellulases were less inhibited during SSF due to the direct consumption of glucose by *U. maydis*. After the depletion of ammonium, *U. maydis* converted the consumed glucose to itaconic acid. The final itaconic acid yield of the SSF

(0.12 g/g) was comparable to that of the glucose batch fermentation (0.15 g/g). In conclusion, Chapter 4 showed for the first time that itaconic acid can be produced in just one step via SSF. This integrated process configuration will allow the production of itaconic acid from cellulose without the need of a separate hydrolysis step. Consequently, the SSF will prevent the product inhibition of cellulases and will remarkably reduce the investment costs of biocatalytic processes. In order to increase the yield and productivity of the SSF, the applied cellulases and the *U. maydis* strain need to be improved in such a way that the process optima of both biocatalysts are closer to each other. Moreover, the formation of undesired by-products (such as lipids) needs to be eliminated by genetic engineering of *U. maydis*. Furthermore, the whole process should be modeled to find an overall process optimum.

Within this thesis, a detailed understanding of the biocatalytic conversion of cellulose to itaconic acid was generated. Not only all essential conversion steps (pretreatment, hydrolysis, and fermentation) were investigated in detail, but also novel approaches as well as technologies could be developed. Rather than establishing the complete conversion process, the limiting factors of the single conversion steps were determined. Furthermore, this work highlighted that integrated process configurations are promising alternatives to sequentially performed unit operations. Based on the presented results, a knowledge-based improvement of the whole biocatalytic process can be achieved. Thereby, the newly developed (integrated) approaches and technologies may contribute to the optimization procedure.

Nevertheless, further investigations are needed to gain a deeper understanding of the single conversion steps and to establish mechanistic models, especially in the case of cellulose hydrolysis. In order to perform the biocatalytic conversion of cellulose to itaconic acid at industrial scale, further aspects need to be addressed. At first, the biocatalysts have to be improved so that higher yields and productivities can be achieved. Moreover, product recovery and the recycling of water as well as biocatalysts have to be considered, since both aspects are essential for industrial processes. For example, (*in-situ*) ultrafiltration should be implemented in a continuous SSF process, thereby allowing the retention of cellulases, microorganisms, and unconverted cellulose. Furthermore, the aspects analyzed here for cellulosic substrates should be transferred to real lignocellulose also containing hemicellulose, lignin, and additional impurities. Thereby, even higher levels of process integration, such as simultaneous saccharification and co-fermentation (SSCF) or consolidated bioprocessing (CBP) should be addressed. Ultimately, the evaluation and model-based synthesis of the

complete process chain needs to be performed, since pretreatment, hydrolysis, fermentation, product recovery as well as recycling steps are strongly associated and need to be harmonized.

In conclusion, an in-depth understanding of the biocatalytic conversion of cellulose to itaconic acid was established within this thesis by analyzing all essential conversion steps (pretreatment, hydrolysis, and fermentation). This understanding is the fundamental basis for further improvements and paves the way for economically feasible production processes converting cellulose to platform chemicals such as itaconic acid.

Bibliography

Abe S, Takagi M. 1991. Simultaneous saccharification and fermentation of cellulose to lactic acid. Biotechnol Bioeng 37(1):93-96.

Adams GA, Bishop CT. 1953. Polysaccharides associated with alpha-cellulose. Nature 172(4366):28-29.

Alvira P, Tomas-Pejo E, Ballesteros M, Negro MJ. 2010. Pretreatment technologies for an efficient bioethanol production process based on enzymatic hydrolysis: A review. Bioresour Technol 101(13):4851-4861.

Anderlei T, Büchs J. 2001. Device for sterile online measurement of the oxygen transfer rate in shaking flasks. Biochem Eng J 7(2):157-162.

Anderlei T, Zang W, Papaspyrou M, Büchs J. 2004. Online respiration activity measurement (OTR, CTR, RQ) in shake flasks. Biochem Eng J 17(3):187-194.

Andrade JD, Hlady V. 1986. Protein adsorption and materials biocompatibility - a tutorial review and suggested hypotheses. Adv Polym Sci 79:1-63.

Arantes V, Saddler J. 2010. Access to cellulose limits the efficiency of enzymatic hydrolysis: the role of amorphogenesis. Biotechnol Biofuels 3:11.

Arantes V, Saddler J. 2011. Cellulose accessibility limits the effectiveness of minimum cellulase loading on the efficient hydrolysis of pretreated lignocellulosic substrates. Biotechnol Biofuels 4:3.

Arora DS, Chander M, Gill PK. 2002. Involvement of lignin peroxidase, manganese peroxidase and laccase in degradation and selective ligninolysis of wheat straw. Int Biodeterior Biodegrad 50(2):115-120.

Asenjo JA, Jew C. 1983. Primary metabolite or microbial protein from cellulose: conditions, kinetics, and modeling of the simultaneous saccharification and fermentation to citric acid. Ann N Y Acad Sci 413:211-217.

Bailey CJ. 1989. Enzyme-kinetics of cellulose hydrolysis. Biochem J 262(3):1001-1001.

Baker J, King M, Adney W, Decker S, Vinzant T, Lantz S, Nieves R, Thomas S, Li L-C, Cosgrove D and others. 2000. Investigation of the cell-wall loosening protein expansin as a possible additive in the enzymatic saccharification of lignocellulosic biomass. Appl Biochem Biotechnol 84-86(1):217-223.

Banerjee G, Car S, Scott-Craig JS, Borrusch MS, Aslam N, Walton JD. 2010. Synthetic enzyme mixtures for biomass deconstruction: Production and optimization of a core set. Biotechnol Bioeng 106(5):707-720.

Bansal P, Hall M, Realff MJ, Lee JH, Bommarius AS. 2009. Modeling cellulase kinetics on lignocellulosic substrates. Biotechnol Adv 27(6):833-848.

Bansal P, Hall M, Realff MJ, Lee JH, Bommarius AS. 2010. Multivariate statistical analysis of X-ray data from cellulose: A new method to determine degree of crystallinity and predict hydrolysis rates. Bioresour Technol 101(12):4461-4471.

Becker D, Braet C, Brumer H, Claeyssens M, Divne C, Fagerstrom BR, Harris M, Jones TA, Kleywegt GJ, Koivula A and others. 2001. Engineering of a glycosidase Family 7 cellobiohydrolase to more alkaline pH optimum: the pH behaviour of *Trichoderma reesei* CeI7A and its E223S/A224H/L225V/T226A/D262G mutant. Biochem J 356:19-30.

Beldman G, Voragen AGJ, Rombouts FM, Searlevanleeuwen MF, Pilnik W. 1987. Adsorption and kinetic behavior of purified endoglucanases and exoglucanases from *Trichoderma viride*. Biotechnol Bioeng 30(2):251-257.

Bengtsson O, Hahn-Hagerdal B, Gorwa-Grauslund M. 2009. Xylose reductase from *Pichia stipitis* with altered coenzyme preference improves ethanolic xylose fermentation by recombinant *Saccharomyces cerevisiae*. Biotechnol Biofuels 2:9.

Bhat MK, Bhat S. 1997. Cellulose degrading enzymes and their potential industrial applications. Biotechnol Adv 15(3-4):583-620.

Bidlack J, Malone M, Benson R. 1992. Molecular structure and component integration of secondary cell walls in plants. Proc Okla Acad Sci 72:51-56.

Boer H, Koivula A. 2003. The relationship between thermal stability and pH optimum studied with wild-type and mutant *Trichoderma reesei* cellobiohydrolase Cel7A. Eur J Biochem 270(5):841-848.

Bommarius AS, Katona A, Cheben SE, Patel AS, Ragauskas AJ, Knudson K, Pu Y. 2008. Cellulase kinetics as a function of cellulose pretreatment. Metab Eng 10(6):370-381.

Bonnarme P, Gillet B, Sepulchre AM, Role C, Beloeil JC, Ducrocq C. 1995. Itaconate biosynthesis in *Aspergillus terreus*. J Bacteriol 177(12):3573-3578.

Borden JR, Lee YY, Yoon HH. 2000. Simultaneous saccharification and fermentation of cellulosic biomass to acetic acid. Appl Biochem Biotechnol 84-86:963-970.

Boussaid A, Saddler JN. 1999. Adsorption and activity profiles of cellulases during the hydrolysis of two Douglas fir pulps. Enzyme Microb Technol 24(3-4):138-143.

Bowen P. 2002. Particle size distribution measurement from millimeters to nanometers, and from rods to platelets. J Disper Sci Technol 23(5):631-662.

Bozell JJ, Holladay JE, Johnson D, White JF. 2007. Top value-added chemicals from biomass. Volume II: results of screening for potential candidates from biorefinery lignin. Oak Ridge: U.S. Department of Energy, National Renewable Energy Laboratory (NREL).

Bresinsky A, Körner C, Kadereit JW, Neuhaus G, Sonnewald U. 2008. Strasburger - Lehrbuch der Botanik. Heidelberg: Spektrum Akademischer Verlag.

Bressler E, Braun S. 2000. Conversion of citric acid to itaconic acid in a novel liquid membrane bioreactor. J Chem Tech Biotech 75:66-72.

Busto MD, Ortega N, Perez-Mateos M. 1996. Location, kinetics and stability of cellulases induced in *Trichoderma reesei* cultures. Bioresour Technol 57(2):187-192.

Busto MD, Ortega N, Perez-Mateos M. 1998. Characterization of microbial endo-beta-glucanase immobilized in alginate beads. Acta Biotechnol 18(3):189-200.

Cao Y, Tan H. 2005. Study on crystal structures of enzyme-hydrolyzed cellulosic materials by X-ray diffraction. Enzyme Microb Technol 36(2-3):314-317.

Carrard G, Linder M. 1999. Widely different off rates of two closely related cellulose-binding domains from *Trichoderma reesei*. Eur J Biochem 262(3):637-643.

Carrard G, Koivula A, Soderlund H, Beguin P. 2000. Cellulose-binding domains promote hydrolysis of different sites on crystalline cellulose. PNAS 97(19):10342-10347.

Chandra R, Ewanick S, Hsieh C, Saddler JN. 2008. The characterization of pretreated lignocellulosic substrates prior to enzymatic hydrolysis, part 1: A modified Simons' staining technique. Biotechnol Progr 24(5):1178-1185.

Chandra RP, Bura R, Mabee WE, Berlin A, Pan X, Saddler JN. 2007. Substrate pretreatment: The key to effective enzymatic hydrolysis of lignocellulosics? Adv Biochem Engin Biotechnol 108:67-93.

Chen CS, Penner MH. 2007. Turbidity-based assay for polygalacturonic acid depolymerase activity. J Agric Food Chem 55(15):5907-5911.

Chen H, Hayn M, Esterbauer H. 1992. Purification and characterization of two extracellular beta-glucosidases from *Trichoderma reesei*. Biochim Biophys Acta 1121(1-2):54-60.

Chen K, Zhang H, Miao Y, Wei P, Chen J. 2011. Simultaneous saccharification and fermentation of acid-pretreated rapeseed meal for succinic acid production using *Actinobacillus succinogenes*. Enzyme Microb Technol 48(4-5):339-344.

Chen XA, Ishida N, Todaka N, Nakamura R, Maruyama JI, Takahashi H, Kitamoto K. 2010. Promotion of efficient saccharification of crystalline cellulose by *Aspergillus fumigatus* Swo1. Appl Environ Microbiol 76(8):2556-2561.

Chmiel H, Friedle J, Schroeder T, Schuldt S, Winkelnkemper T, Schembecker G. 2011. Aufarbeitung (Downstream Processing). Bioprozesstechnik: Spektrum Akademischer Verlag. p 295-372.

Colussi PA, Taron CH. 2005. *Kluyveromyces lactis* LAC4 promoter variants that lack function in bacteria but retain full function in *K. lactis*. Appl Environ Microbiol 71(11):7092-7098.

Copeland RA. 2000. Enzymes. New York, Chichester, Weinheim, Brisbane, Singapore, Toronto: John Wiley & Sons.

Cosgrove DJ. 2000. Loosening of plant cell walls by expansins. Nature 407(6802):321-326.

Coughlan MP. 1985. The properties of fungal and bacterial cellulases with comment on their production and application. Biotechnol Genet Eng Rev 3:39-109.

Coward-Kelly G, Aiello-Mazzari C, Kim S, Granda C, Holtzapple M. 2003. Suggested improvements to the standard filter paper assay used to measure cellulase activity. Biotechnol Bioeng 82(6):745-749.

Dasari RK, Berson RE. 2007. The effect of particle size on hydrolysis reaction rates and rheological properties in cellulosic slurries. Appl Biochem Biotechnol 137:289-299.

Dashtban M, Schraft H, Syed TA, Qin W. 2010. Fungal biodegradation and enzymatic modification of lignin. Int J Biochem Mol Biol 1(1):36-50.

Decker S, Brunecky R, Tucker M, Himmel M, Selig M. 2009. High-throughput screening techniques for biomass conversion. Bioenerg Res 2(4):179-192.

Decker SR, Adney WS, Jennings E, Vinzant TB, Himmel ME. 2003. Automated filter paper assay for determination of cellulase activity. Appl Biochem Biotech 105:689-703.

Desai SG, Converse AO. 1997. Substrate reactivity as a function of the extent of reaction in the enzymatic hydrolysis of lignocellulose. Biotechnol Bioeng 56(6):650-655.

Din N, Gilkes NR, Tekant B, Miller RC, Warren RAJ, Kilburn DG. 1991. Non-hydrolytic disruption of cellulose fibres by the binding domain of a bacterial cellulase. Nat Biotechnol 9(11):1096-1099.

Dourado F, Mota M, Pala H, Gama FM. 1999. Effect of cellulase adsorption on the surface and interfacial properties of cellulose. Cellulose 6(4):265-282.

Drissen RET, Maas RHW, Van Der Maarel MJEC, Kabel MA, Schols HA, Tramper J, Beeftink HH. 2007. A generic model for glucose production from various cellulose sources by a commercial cellulase complex. Biocatal Biotransform 25(6):419-429.

Du F, Wolger E, Wallace L, Liu A, Kaper T, Kelemen B. 2010. Determination of product inhibition of CBH1, CBH2, and EG1 using a novel cellulase activity assay. Appl Biochem Biotechnol 161(1):313-317.

Eisenbeiß G, Wagner G. 2006. Biomasse im System moderner Energieversorgung. Informationen zur Raumentwicklung 1:1-5.

Ellouz S, Durand H, Tiraby G. 1987. Analytical separation of *Trichoderma reesei* cellulases by ion-exchange fast protein liquid-chromatography. J Chromatogr 396:307-317.

Enari TM, Nikupaavola ML. 1988. Nephelometric and turbidometric assay for cellulase. Methods Enzymol 160:117-126.

Enayati N, Parulekar SJ. 1995. Enzymatic saccharification of soybean hull-based materials. Biotechnol Progr 11(6):708-711.

Engel P, Mladenov R, Wulfhorst H, Jäger G, Spiess AC. 2010. Point by point analysis: how ionic liquid affects the enzymatic hydrolysis of native and modified cellulose. Green Chem 12(11):1959-1966.

Engel P, Krull S, Seiferheld B, Spiess A. 2011. Rational approach to optimize cellulase mixtures for hydrolysis of regenerated cellulose containing residual ionic liquid. Bioresour Technol: accepted.

Esterbauer H, Steiner W, Labudova I, Hermann A, Hayn M. 1991. Production of *Trichoderma* cellulase in laboratory and pilot scale. Bioresour Technol 36(1):51-65.

Evans R, Wearne RH, Wallis AFA. 1989. Molecular-weight distribution of cellulose as its tricarbanilate by high-performance size exclusion chromatography. J Appl Polym Sci 37(12):3291-3303.

Fan LT, Lee YH, Beardmore DH. 1980. Mechanism of the enzymatic hydrolysis of cellulose: effects of major structural features of cellulose on enzymatic hydrolysis. Biotechnol Bioeng 22(1):177-199.

Fujita Y, Ito J, Ueda M, Fukuda H, Kondo A. 2004. Synergistic saccharification, and direct fermentation to ethanol, of amorphous cellulose by use of an engineered yeast strain codisplaying three types of cellulolytic enzyme. Appl Environ Microbiol 70(2):1207-1212.

Fukuda H, Kondo A, Tamalampudi S. 2009. Bioenergy: Sustainable fuels from biomass by yeast and fungal whole-cell biocatalysts. Biochem Eng J 44(1):2-12.

Fukumura M, Begum A, Kruus K, Wu JHD. 1997. Interactions and synergism between the recombinant CelD, an endoglucanase, and the cellulosome-integrating protein (CipA) of *Clostridium thermocellum*. J Ferment Bioeng 83(2):146-151.

Galbe M, Zacchi G. 2007. Pretreatment of lignocellulosic materials for efficient bioethanol production. Adv Biochem Engin Biotechnol 108:41-65.

Galbe M, Sassner P, Wingren A, Zacchi G. 2007. Process engineering economics of bioethanol production. Adv Biochem Engin Biotechnol 108:303-327.

Gama FM, Teixeira JA, Mota M. 1994. Cellulose morphology and enzymatic reactivity - a modified solute exclusion technique. Biotechnol Bioeng 43(5):381-387.

Gama FM, Vilanova M, Mota M. 1998. Exo- and endo-glucanolytic activity of cellulases purified from *Trichoderma reesei*. Biotechnol Tech 12(9):677-681.

Gan Q, Allen SJ, Taylor G. 2003. Kinetic dynamics in heterogeneous enzymatic hydrolysis of cellulose: an overview, an experimental study and mathematical modelling. Process Biochem 38(7):1003-1018.

Ganan P, Zuluaga R, Cruz J, Velez JM, Retegi A, Mondragon I. 2008. Elucidation of the fibrous structure of *Musaceae* maturate rachis. Cellulose 15(1):131-139.

Gao P-J, Chen G-J, Wang T-H, Zhang Y-S, Liu J. 2001. Non-hydrolytic disruption of crystalline structure of cellulose by cellulose binding domain and linker sequence of cellobiohydrolase I from *Penicillium janthinellum*. Acta Biochim Biophys Sin 33(1):13-18.

Garcia-Sanchez R, Karhumaa K, Fonseca C, Sanchez Nogue V, Almeida J, Larsson C, Bengtsson O, Bettiga M, Hahn-Hagerdal B, Gorwa-Grauslund M. 2010. Improved xylose and arabinose utilization by an industrial recombinant *Saccharomyces cerevisiae* strain using evolutionary engineering. Biotechnol Biofuels 3:13.

Geddes CC, Nieves IU, Ingram LO. 2011. Advances in ethanol production. Curr Opin Biotechnol 22(3):312-319.

Geilen FMA, Engendahl B, Harwardt A, Marquardt W, Klankermayer J, Leitner W. 2010. Selective and flexible transformation of biomass-derived platform chemicals by a multifunctional catalytic system. Angew Chem Int Ed 49(32):5510-5514.

Ghose TK. 1987. Measurement of cellulase activities. Pure Appl Chem 59(2):257-268.

Goedegebuur F, Fowler T, Phillips J, van der Kley P, van Solingen P, Dankmeyer L, Power S. 2002. Cloning and relational analysis of 15 novel fungal endoglucanases from family 12 glycosyl hydrolase. Curr Genet 41(2):89-98.

Graziani M, Fornasiero P. 2006. Renewable resources and renewable energy: A global challenge. Boca Raton: CRC Press, Taylor & Francis Group.

Green JW. 1963. Wood cellulose. Methods Carbohydr Chem 3:9-21.

Grethlein HE. 1985. The effect of pore size distribution on the rate of enzymatic hydrolysis of cellulosic substrates. Nat Biotechnol 3(2):155-160.

Grosse-Coosmann F, Boehm AM, Sickmann A. 2005. Efficient analysis and extraction of MS/MS result data from Mascot result files. BMC Bioinf 6(1):290.

Gruno M, Valjamae P, Pettersson G, Johansson G. 2004. Inhibition of the *Trichoderma reesei* cellulases by cellobiose is strongly dependent on the nature of the substrate. Biotechnol Bioeng 86(5):503-511.

Guevarra ED, Tabuchi T. 1990. Accumulation of itaconic, 2-hydroxyparaconic, itatartaric, and malic acids by strains of the genus *Ustilago*. Agric Biol Chem 54(9):2353-2358.

Gupta R, Lee YY. 2009. Mechanism of cellulase reaction on pure cellulosic substrates. Biotechnol Bioeng 102(6):1570-1581.

Hall M, Bansal P, Lee JH, Realff MJ, Bommarius AS. 2010. Cellulose crystallinity - a key predictor of the enzymatic hydrolysis rate. FEBS J 277(6):1571-1582.

Hall M, Bansal P, Lee JH, Realff MJ, Bommarius AS. 2011. Biological pretreatment of cellulose: Enhancing enzymatic hydrolysis rate using cellulose-binding domains from cellulases. Bioresour Technol 102(3):2910-2915.

Halliwell G, Griffin M. 1973. The nature and mode of action of the cellulolytic component C1 of *Trichoderma koningii* on native cellulose. Biochem J 135(4):587-594.

Hamelinck CN, van Hooijdonk G, Faaij APC. 2005. Ethanol from lignocellulosic biomass: techno-economic performance in short-, middle- and long-term. Biomass Bioenergy 28(4):384-410.

Han YJ, Chen HZ. 2007. Synergism between corn stover protein and cellulase. Enzyme Microb Technol 41(5):638-645.

Haskins RH, Thorn JA, Boothroyd B. 1955. Biochemistry of the Ustilaginales. XI. Metabolic products of *Ustilago zeae* in submerged culture. Can J Microbiol 1(9):749-756.

He DL, Bao LL, Long YM, Wei WZ, Yao SZ. 2000. A new study of the enzymatic hydrolysis of carboxymethyl cellulose with a bulk acoustic wave sensor. Talanta 50(6):1267-1273.

Henrissat B, Driguez H, Viet C, Schulein M. 1985. Synergism of cellulases from *Trichoderma reesei* in the degradation of cellulose. Nat Biotechnol 3(8):722-726.

Hermann R, Lehmann M, Büchs J. 2003. Characterization of gas-liquid mass transfer phenomena in microtiter plates. Biotechnol Bioeng 81(2):178-186.

Herpoel-Gimbert I, Margeot A, Dolla A, Jan G, Molle D, Lignon S, Mathis H, Sigoillot J-C, Monot F, Asther M. 2008. Comparative secretome analyses of two *Trichoderma reesei* RUT-C30 and CL847 hypersecretory strains. Biotechnol Biofuels 1:18.

Hewald S, Josephs K, Bolker M. 2005. Genetic analysis of biosurfactant production in *Ustilago maydis*. Appl Environ Microbiol 71(6):3033-3040.

Himmel ME, Ruth MF, Wyman CE. 1999. Cellulase for commodity products from cellulosic biomass. Curr Opin Biotechnol 10(4):358-364.

Himmel ME, Ding SY, Johnson DK, Adney WS, Nimlos MR, Brady JW, Foust TD. 2007. Biomass recalcitrance: Engineering plants and enzymes for biofuels production. Science 315(5813):804-807.

Himmel ME, Bayer EA. 2009. Lignocellulose conversion to biofuels: current challenges, global perspectives. Curr Opin Biotechnol 20(3):316-317.

Holtzapple M, Cognata M, Shu Y, Hendrickson C. 1990. Inhibition of *Trichoderma reesei* cellulase by sugars and solvents. Biotechnol Bioeng 36(3):275-287.

Hong J, Ye XH, Zhang YHP. 2007. Quantitative determination of cellulose accessibility to cellulase based on adsorption of a nonhydrolytic fusion protein containing CBM and GFP with its applications. Langmuir 23(25):12535-12540.

Hoshino E, Kanda T, Sasaki Y, Nisizawa K. 1992. Adsorption mode of exo- and endo-cellulases from *Irpex lacteus* (*Polyporus tulipiferae*) on cellulose with different crystallinities. J Biochem 111(5):600-605.

Hu G, Heitmann JA, Rojas OJ. 2009. In situ monitoring of cellulase activity by microgravimetry with a quartz crystal microbalance. J Phys Chem B 113(44):14761-14768.

Huang AA. 1975. Kinetic studies on insoluble cellulose-cellulase system. Biotechnol Bioeng 17(10):1421-1433.

Huang R, Su R, Qi W, He Z. 2010. Understanding the key factors for enzymatic conversion of pretreated lignocellulose by partial least square analysis. Biotechnol Progr 26(2):384-392.

Huber GW, Dumesic JA. 2006. An overview of aqueous-phase catalytic processes for production of hydrogen and alkanes in a biorefinery. Catal Today 111(1-2):119-132.

Huber GW, Iborra S, Corma A. 2006. Synthesis of transportation fuels from biomass: chemistry, catalysts, and engineering. Chem Rev 106(9):4044-4098.

Huber R, Wulfhorst H, Maksym L, Stehr R, Pöhnlein M, Jäger G, Spieß AC, Büchs J. 2011. Screening for enzyme activity in turbid suspensions with scattered light. Biotechnol Progr 27(2):555-561.

Hunter AK, Carta G. 2002. Protein adsorption on novel acrylamido-based polymeric ion-exchangers. IV. Effects of protein size on adsorption capacity and rate. J Chromatogr A 971(1-2):105-116.

Ingesson H, Zacchi G, Yang B, Esteghlalian AR, Saddler JN. 2001. The effect of shaking regime on the rate and extent of enzymatic hydrolysis of cellulose. J Biotechnol 88(2):177-182.

Ingram LO, Gomez PF, Lai X, Moniruzzaman M, Wood BE, Yomano LP, York SW. 1998. Metabolic engineering of bacteria for ethanol production. Biotechnol Bioeng 58(2-3):204-214.

Ingram LO, Aldrich HC, Borges ACC, Causey TB, Martinez A, Morales F, Saleh A, Underwood SA, Yomano LP, York SW and others. 1999. Enteric bacterial catalysts for fuel ethanol production. Biotechnol Progr 15(5):855-866.

Janssen A, Jakob M, Muether M, Pischinger S. 2010. Tailor-made fuels from biomass - potential of biogenic fuels for reducing emissions. MTZ 71:54-60.

Jeoh T, Wilson DB, Walker LP. 2002. Cooperative and competitive binding in synergistic mixtures of *Thermobifida fusca* cellulases Ce15A, Ce16B, and Ce19A. Biotechnol Progr 18(4):760-769.

Jeoh T, Ishizawa CI, Davis MF, Himmel ME, Adney WS, Johnson DK. 2007. Cellulase digestibility of pretreated biomass is limited by cellulose accessibility. Biotechnol Bioeng 98(1):112-122.

Jeoh T, Michener W, Himmel ME, Decker SR, Adney WS. 2008. Implications of cellobiohydrolase glycosylation for use in biomass conversion. Biotechnol Biofuels 1:10.

Jorgensen H, Kristensen JB, Felby C. 2007. Enzymatic conversion of lignocellulose into fermentable sugars: challenges and opportunities. Biofuels Bioprod Bioref 1(2):119-134.

Julenius K, Molgaard A, Gupta R, Brunak S. 2005. Prediction, conservation analysis, and structural characterization of mammalian mucin-type O-glycosylation sites. Glycobiology 15(2):153-164.

Kadam KL, Rydholm EC, McMillan JD. 2004. Development and validation of a kinetic model for enzymatic saccharification of lignocellulosic biomass. Biotechnol Prog 20(3):698-705.

Kaltschmitt M, Hofbauer H, Hartmann H. 2009. Energie aus Biomasse. Berlin: Springer Berlin Heidelberg.

Kanamasa S, Dwiarti L, Okabe M, Park EY. 2008. Cloning and functional characterization of the *cis*-aconitic acid decarboxylase (CAD) gene from *Aspergillus terreus*. Appl Microbiol Biotechnol 80(2):223-229.

Karlsson J, Saloheimo M, Siika-aho M, Tenkanen M, Penttilä M, Tjerneld F. 2001. Homologous expression and characterization of Cel61A (EG IV) of *Trichoderma reesei*. Eur J Biochem 268(24):6498-6507.

Karlsson J, Siika-aho M, Tenkanen M, Tjerneld F. 2002. Enzymatic properties of the low molecular mass endoglucanases Cel12A (EG III) and Cel45A (EG V) of *Trichoderma reesei*. J Biotechnol 99(1):63-78.

Kato Y, Hiraoka S, Tada Y, Shirota T, Koh ST, Lee YS, Yamaguchi T. 1995. Complete suspension of solid particles in a shaking vessel. Kagaku Kogaku Ronbun 21(5):948-952.

Kato Y, Hiraoka S, Tada Y, Nomura T. 2001. Performance of a shaking vessel with current pole. Biochem Eng J 7(2):143-151.

Kautola H, Vahvaselka M, Linko YY, Linko P. 1985. Itaconic acid production by immobilized *Aspergillus terreus* from xylose and glucose. Biotechnol Lett 7(3):167-172.

Kensy F, Zang E, Faulhammer C, Tan RK, Büchs J. 2009. Validation of a high-throughput fermentation system based on online monitoring of biomass and fluorescence in continuously shaken microtiter plates. Microb Cell Fact 8:31.

Khaw TS, Katakura Y, Ninomiya K, Moukamnerd C, Kondo A, Ueda M, Shioya S. 2007. Enhancement of ethanol production by promoting surface contact between starch granules and arming yeast in direct ethanol fermentation. J Biosci Bioeng 103(1):95-97.

Kim DW, Yang JH, Jeong YK. 1988. Adsorption of cellulase from *Trichoderma viride* on microcrystalline cellulose. Appl Microbiol Biotechnol 28(2):148-154.

Kim DW, Kim TS, Jeong YK, Lee JK. 1992. Adsorption kinetics and behaviors of cellulase components on microcrystalline cellulose. J Ferment Bioeng 73(6):461-466.

Kim DW, Jeong YK, Lee JK. 1994a. Adsorption kinetics of exoglucanase in combination with endoglucanase from *Trichoderma viride* on microcrystalline cellulose and its influence on synergistic degradation. Enzyme Microb Technol 16(8):649-658.

Kim DW, Jeong YK, Jang YH, Lee JK. 1994b. Purification and characterization of endoglucanase and exoglucanase components from *Trichoderma viride*. J Ferment Bioeng 77(4):363-369.

Kim DW, Jang YH, Jeong YK. 1998. Adsorption kinetics and behaviour of two cellobiohydrolases from *Trichoderma reesei* on microcrystalline cellulose. Biotechnol Appl Biochem 27:97-102.

Kim ES, Lee HJ, Bang WG, Choi IG, Kim KH. 2009. Functional characterization of a bacterial expansin from *Bacillus subtilis* for enhanced enzymatic hydrolysis of cellulose. Biotechnol Bioeng 102(5):1342-1353.

Klement T, Milker S, Jäger G, Grande PM, Dominguez de Maria P, Büchs J. 2011. Biomass pretreatment affects *Ustilago maydis* in producing itaconic acid. Microb Cell Fact: submitted.

Klemm D, Heublein B, Fink HP, Bohn A. 2005. Cellulose: Fascinating biopolymer and sustainable raw material. Angew Chem Int Ed 44(22):3358-3393.

Klosowski G, Mikulski D, Czuprynski B, Kotarska K. 2010. Characterisation of fermentation of high-gravity maize mashes with the application of pullulanase, proteolytic enzymes and enzymes degrading non-starch polysaccharides. J Biosci Bioeng 109(5):466-471.

Klyosov AA. 1990. Trends in biochemistry and enzymology of cellulose degradation. Biochemistry 29(47):10577-85.

Kobayashi T. 1978. Production of itaconic acid from wood waste. Proc Biochem 13(5):15-22.

Kongruang S, Han M, Breton C, Penner M. 2004. Quantitative analysis of cellulose-reducing ends. Appl Biochem Biotechnol 113(1):213-231.

Kruus K, Wang WK, Ching JT, Wu JHD. 1995a. Exoglucanase activities of the recombinant *Clostridium thermocellum* CelS, a major cellulosome component. J Bacteriol 177(6):1641-1644.

Kruus K, Andreacchi A, Wang WK, Wu JHD. 1995b. Product inhibition of the recombinant CelS, an exoglucanase component of the *Clostridium thermocellum* cellulosome. Appl Microbiol Biotechnol 44(3-4):399-404.

Kubicek CP. 1992. The cellulase proteins of *Trichoderma reesei*: structure, multiplicity, mode of action and regulation of formation. Adv Biochem Engin Biotechnol 45:1-27.

Kumar P, Barrett DM, Delwiche MJ, Stroeve P. 2009. Methods for pretreatment of lignocellulosic biomass for efficient hydrolysis and biofuel production. Ind Eng Chem Res 48(8):3713-3729.

Kumar R, Wyman CE. 2008. An improved method to directly estimate cellulase adsorption on biomass solids. Enzyme Microb Technol 42(5):426-433.

Kumar R, Wyman CE. 2009a. Access of cellulase to cellulose and lignin for poplar solids produced by leading pretreatment technologies. Biotechnol Progr 25(3):807-819.

Kumar R, Wyman CE. 2009b. Cellulase adsorption and relationship to features of corn stover solids produced by leading pretreatments. Biotechnol Bioeng 103(2):252-267.

Kumar R, Wyman CE. 2009c. Does change in accessibility with conversion depend on both the substrate and pretreatment technology? Bioresour Technol 100(18):4193-4202.

Kurz WG, Ericson LE. 1962. Microbial production of amino acids. II. The influence of carbon and nitrogen sources and metal ions on growth of *Ustilago maydis* (DC.) Cda. and on lysine and threonine production. Biotechnol Bioeng 4:37-52.

Kyriacou A, Neufeld RJ, Mackenzie CR. 1989. Reversibility and competition in the adsorption of *Trichoderma reesei* cellulase components. Biotechnol Bioeng 33(5):631-637.

Laemmli UK. 1970. Cleavage of structural proteins during the assembly of the head of bacteriophage T4. Nature 227(5259):680-685.

Lassig JP, Shultz MD, Gooch MG, Evans BR, Woodward J. 1995. Inhibition of cellobiohydrolase I from *Trichoderma reesei* by palladium. Arch Biochem Biophys 322(1):119-126.

Latimer P. 1982. Light scattering and absorption as methods of studying cell population parameters. Annu Rev Biophys Bioeng 11(1):129-150.

Lee SB, Shin HS, Ryu DDY, Mandels M. 1982. Adsorption of cellulase on cellulose: effect of physicochemical properties of cellulose on adsorption and rate of hydrolysis. Biotechnol Bioeng 24(10):2137-2153.

Lee SB, Kim IH, Ryu DD, Taguchi H. 1983. Structural properties of cellulose and cellulase reaction mechanism. Biotechnol Bioeng 25(1):33-51.

Lee TK, Kim CH. 1999. Molecular cloning and expression of an endo-beta-1,4-D-glucanase I (Avicelase I) gene from *Bacillus cellulyticus* K-12 and characterization of the recombinant enzyme. Appl Biochem Biotechnol 80(2):121-140.

Lever M. 1972. New reaction for colorimetric determination of carbohydrates. Anal Biochem 47(1):273-279.

Levine SE, Fox JM, Blanch HW, Clark DS. 2010. A mechanistic model of the enzymatic hydrolysis of cellulose. Biotechnol Bioeng 107(1):37-51.

Levine SE, Fox JM, Clark DS, Blanch HW. 2011. A mechanistic model for rational design of optimal cellulase mixtures. Biotechnol Bioeng 108(11):2561-2570.

Li LH, Flora RM, King KW. 1965. Individual roles of cellulase components derived from *Trichoderma viride*. Arch Biochem Biophys 111(2):439-447.

Liang C, Xue Y, Fioroni M, Rodríguez-Ropero F, Zhou C, Schwaneberg U, Ma Y. 2010. Cloning and characterization of a thermostable and halo-tolerant endoglucanase from *Thermoanaerobacter tengcongensis* MB4. Appl Microbiol Biotechnol 89:315-326.

Liang C, Fioroni M, Rodríguez-Ropero F, Xue Y, Schwaneberg U, Ma Y. 2011. Directed evolution of a thermophilic endoglucanase (Cel5A) into highly active Cel5A variants with an expanded temperature profile. J Biotechnol 154:46-53.

Linder M, Lindeberg G, Reinikainen T, Teeri TT, Pettersson G. 1995. The difference in affinity between 2 fungal cellulose-binding domains is dominated by a single amino-acid substitution. FEBS Lett 372(1):96-98.

Linder M, Teeri TT. 1996. The cellulose-binding domain of the major cellobiohydrolase of *Trichoderma reesei* exhibits true reversibility and a high exchange rate on crystalline cellulose. PNAS 93(22):12251-12255.

Linder M, Teeri TT. 1997. The roles and function of cellulose-binding domains. J Biotechnol 57:15-28.

Lockwood LB, Reeves MD. 1945. Some factors affecting the production of itaconic acid by *Aspergillus terreus*. Arch Biochem 6:455-469.

Lodi T, Neglia B, Donnini C. 2005. Secretion of human serum albumin by *Kluyveromyces lactis* overexpressing KlPDI1 and KlERO1. Appl Environ Microbiol 71(8):4359-4363.

Lu Y, Yang B, Gregg D, Saddler JN, Mansfield SD. 2002. Cellulase adsorption and an evaluation of enzyme recycle during hydrolysis of steam-exploded softwood residues. Appl Biochem Biotechnol 99:641-654.

Lynd LR, Wyman CE, Gerngross TU. 1999. Biocommodity engineering. Biotechnol Progr 15(5):777-793.

Lynd LR, Weimer PJ, van Zyl WH, Pretorius IS. 2002. Microbial cellulose utilization: fundamentals and biotechnology. Microbiol Mol Biol Rev 66(3):506-577.

Ma AZ, Hu Q, Qu YB, Bai ZH, Liu WF, Zhuang GQ. 2008. The enzymatic hydrolysis rate of cellulose decreases with irreversible adsorption of cellobiohydrolase I. Enzyme Microb Technol 42(7):543-547.

Maguire RJ. 1977. Kinetics of hydrolysis of cellulose by beta-1,4-glucan cellobiohydrolase of *Trichoderma viride*. Can J Biochem 55(6):644-650.

Mandels M, Andreotti R, Roche C. 1976. Measurement of saccharifying cellulase. Biotechnol Bioeng Symp 6:21-33.

Mandels M, Sternberg D. 1976. Recent advances in cellulase technology. J Ferment Technol 54(4):267-286.

Mansfield SD, Mooney C, Saddler JN. 1999. Substrate and enzyme characteristics that limit cellulose hydrolysis. Biotechnol Progr 15(5):804-816.

Marquardt W, Harwardt A, Hechinger M, Kraemer K, Viell J, Voll A. 2010. The biorenewables opportunity - toward next generation process and product systems. AIChE J 56(9):2228-2235.

Martinez D, Berka RM, Henrissat B, Saloheimo M, Arvas M, Baker SE, Chapman J, Chertkov O, Coutinho PM, Cullen D and others. 2008. Genome sequencing and analysis of the biomass-degrading fungus *Trichoderma reesei* (syn. *Hypocrea jecorina*). Nat Biotechnol 26(5):553-560.

Matsushika A, Inoue H, Murakami K, Takimura O, Sawayama S. 2009a. Bioethanol production performance of five recombinant strains of laboratory and industrial xylose-fermenting *Saccharomyces cerevisiae*. Bioresour Technol 100(8):2392-2398.

Matsushika A, Inoue H, Kodaki T, Sawayama S. 2009b. Ethanol production from xylose in engineered *Saccharomyces cerevisiae* strains: current state and perspectives. Appl Microbiol Biotechnol 84(1):37-53.

Matsushima T, Klug RJ. 1958. Utilization of L-sorbose by monosporidial lines and mutants of *Ustilago maydis*. Am J Bot 45(3):165-168.

Maurer K-H, Gabler M. 2004. Analysis of detergent enzymes. In: Waldhoff H, Spilker R, editors. Handbook of Detergents, Part C: CRC Press. p 471-485.

Medve J, Stahlberg J, Tjerneld F. 1994. Adsorption and synergism of cellobiohydrolase I and II of *Trichoderma reesei* during hydrolysis of microcrystalline cellulose. Biotechnol Bioeng 44(9):1064-1073.

Medve J, Ståhlberg J, Tjerneld F. 1997. Isotherms for adsorption of cellobiohydrolase I and II from *Trichoderma reesei* on microcrystalline cellulose. Appl Biochem Biotechnol 66(1):39-56.

Medve J, Karlsson J, Lee D, Tjerneld F. 1998a. Hydrolysis of microcrystalline cellulose by cellobiohydrolase I and endoglucanase II from *Trichoderma reesei*: adsorption, sugar production pattern, and synergism of the enzymes. Biotechnol Bioeng 59(5):621-634.

Medve J, Lee D, Tjerneld F. 1998b. Ion-exchange chromatographic purification and quantitative analysis of *Trichoderma reesei* cellulases cellobiohydrolase I, II and endoglucanase II by fast protein liquid chromatography. J Chromatogr A 808(1-2):153-165.

Melander W, Horvath C. 1977. Salt effects on hydrophobic interactions in precipitation and chromatography of proteins - interpretation of lyotropic series. Arch Biochem Biophys 183(1):200-215.

Michels J, Wagemann K. 2010. The german lignocellulose feedstock biorefinery project. Biofuels Bioprod Biorefin 4(3):263-267.

Mielenz JR. 2001. Ethanol production from biomass: technology and commercialization status. Curr Opin Microbiol 4(3):324-329.

Miller GL. 1959. Use of dinitrosalicylic acid reagent for determination of reducing sugar. Anal Chem 31(3):426-428.

Miller GL, Blum R, Glennon WE, Burton AL. 1960. Measurement of carboxymethylcellulase activity. Anal Biochem 1(2):127-132.

Moon H, Kim JS, Oh KK, Kim SW, Hong SI. 2001. Kinetic modeling of simultaneous saccharification and fermentation for ethanol production using steam-exploded wood with glucose- and cellobiose-fermenting yeast, *Brettanomyces custersii*. J Microbiol Biotechnol 11(4):598-606.

Morozova VV, Gusakov AV, Andrianov RM, Pravilnikov AG, Osipov DO, Sinitsyn AP. 2010. Cellulases of *Penicillium verruculosum*. Biotechnol J 5:871-880.

Mosier N, Wyman C, Dale B, Elander R, Lee YY, Holtzapple M, Ladisch M. 2005. Features of promising technologies for pretreatment of lignocellulosic biomass. Bioresour Technol 96(6):673-686.

Mosier NS, Hall P, Ladisch CM, Ladisch MR. 1999. Reaction kinetics, molecular action, and mechanisms of cellulolytic proteins. Adv Biochem Engin Biotechnol 65:23-40.

Mukataka S, Tada M, Takahashi J. 1983. Effects of agitation on enzymatic hydrolysis of cellulose in a stirred-tank reactor. J Ferment Technol 61(6):615-621.

Nagendran S, Hallen-Adams HE, Paper JM, Aslam N, Walton JD. 2009. Reduced genomic potential for secreted plant cell-wall-degrading enzymes in the ectomycorrhizal fungus *Amanita bisporigera*, based on the secretome of *Trichoderma reesei*. Fungal Genet Biol 46(5):427-435.

Nagieb ZA, Ghazi IM, Kassim EA. 1985. Studies on cellulase from *Trichoderma reesei* and its effect on pretreated cellulosic materials. J Appl Polym Sci 30(12):4653-4658.

Navarro D, Couturier M, da Silva G, Berrin J-G, Rouau X, Asther M, Bignon C. 2010. Automated assay for screening the enzymatic release of reducing sugars from micronized biomass. Microb Cell Fact 9(1):58.

Nidetzky B, Steiner W. 1993. A new approach for modeling cellulase-cellulose adsorption and the kinetics of the enzymatic hydrolysis of microcrystalline cellulose. Biotechnol Bioeng 42(4):469-479.

Nidetzky B, Steiner W, Hayn M, Claeyssens M. 1994a. Cellulose hydrolysis by the cellulases from *Trichoderma reesei*: a new model for synergistic interaction. Biochem J 298:705-710.

Nidetzky B, Steiner W, Claeyssens M. 1994b. Cellulose hydrolysis by the cellulases from *Trichoderma reesei*: adsorptions of two cellobiohydrolases, two endocellulases and their core proteins on filter paper and their relation to hydrolysis. Biochem J 303(3):817-823.

Nummi M, Fox PC, Nikupaavola ML, Enari TM. 1981. Nephelometric and turbidometric assays of cellulase activity. Anal Biochem 116(1):133-136.

Oberholzer MR, Lenhoff AM. 1999. Protein adsorption isotherms through colloidal energetics. Langmuir 15(11):3905-3914.

Okano K, Tanaka T, Ogino C, Fukuda H, Kondo A. 2010. Biotechnological production of enantiomeric pure lactic acid from renewable resources: recent achievements, perspectives, and limits. Appl Microbiol Biotechnol 85(3):413-423.

Olofsson K, Bertilsson M, Liden G. 2008. A short review on SSF - an interesting process option for ethanol production from lignocellulosic feedstocks. Biotechnol Biofuels 1(1):7.

Ooshima H, Sakata M, Harano Y. 1983. Adsorption of cellulase from *Trichoderma viride* on cellulose. Biotechnol Bioeng 25(12):3103-3114.

Ooshima H, Burns DS, Converse AO. 1990. Adsorption of cellulase from *Trichoderma reesei* on cellulose and lignacious residue in wood pretreated by dilute sulfuric acid with explosive decompression. Biotechnol Bioeng 36(5):446-452.

Ouajai S, Shanks RA. 2006. Solvent and enzyme induced recrystallization of mechanically degraded hemp cellulose. Cellulose 13(1):31-44.

Ouyang J, Yan M, Kong D, Xu L. 2006. A complete protein pattern of cellulase and hemicellulase genes in the filamentous fungus *Trichoderma reesei*. Biotechnol J 1(11):1266-1274.

Paiva AT, Sequeira SM, Evtuguin DV. 2007. Nanoscale structure of cellulosic materials: challenges and opportunities for AFM. In: Mendez-Vilas A, Diaz J, editors. Modern research and educational topics in microscopy. Badajoz: Formatex. p 726-733.

Pala H, Mota M, Gama FM. 2002. Enzymatic modification of paper fibres. Biocatal Biotransform 20(5):353-361.

Palatinus A, Giovannini AA, Huber MB. 2007. Scenarios for ethanol production from lignocellulose raw materials. Chem Ing Tech 79(5):657-662.

Palonen H, Tenkanen M, Linder M. 1999. Dynamic interaction of *Trichoderma reesei* cellobiohydrolases Cel6A and Cel7A and cellulose at equilibrium and during hydrolysis. Appl Environ Microbiol 65(12):5229-5233.

Pangarkar VG, Yawalkar AA, Sharma MM, Beenackers AACM. 2002. Particle-liquid mass transfer coefficient in two-/three-phase stirred tank reactors. Ind Eng Chem Res 41(17):4141-4167.

Park S, Baker JO, Himmel ME, Parilla PA, Johnson DK. 2010. Cellulose crystallinity index: measurement techniques and their impact on interpreting cellulase performance. Biotechnol Biofuels 3:10.

Peralta-Yahya PP, Keasling JD. 2010. Advanced biofuel production in microbes. Biotechnol J 5:147-162.

Peri S, Karra S, Lee YY, Karim MN. 2007. Modeling intrinsic kinetics of enzymatic cellulose hydrolysis. Biotechnol Progr 23(3):626-637.

Pfennig A. 2007. Supporting debottlenecking of global human processes by applying appropriate balances. Biotechnol J 2(12):1485-1496.

Pischinger S. 2009. Brochure: cluster of excellence tailor-made fuels from biomass. http://www.fuelcenter.rwth-aachen.de.

Prasetyo J, Naruse K, Kato T, Boonchird C, Harashima S, Park EY. 2011. Bio-conversion of paper sludge to biofuel by simultaneous saccharification and fermentation using a cellulase of paper sludge origin and thermotolerant *Saccharomyces cerevisiae* TJ14. Biotechnol Biofuels 4:35.

Pristavka AA, Salovarova VP, Zacchi G, Berezin IV, Rabinovich ML. 2000. Enzyme recovery in high-solids enzymatic hydrolysis of steam-pretreated willow: Requirements for the enzyme composition. Appl Biochem Microbiol 36:237-244.

Quiroz-Castaneda R, Martinez-Anaya C, Cuervo-Soto L, Segovia L, Folch-Mallol J. 2011a. Loosenin, a novel protein with cellulose-disrupting activity from *Bjerkandera adusta*. Microb Cell Fact 10(1):8.

Quiroz-Castaneda RE, Balcazar-Lopez E, Dantan-Gonzalez E, Martinez A, Folch-Mallol J, Martinez-Anaya C. 2009. Characterization of cellulolytic activities of *Bjerkandera adusta* and *Pycnoporus sanguineus* on solid wheat straw medium. Electron J Biotechnol 12(4):1-8.

Quiroz-Castaneda RE, Perez-Mejia N, Martinez-Anaya C, Acosta-Urdapilleta L, Folch-Mallol J. 2011b. Evaluation of different lignocellulosic substrates for the production of cellulases and xylanases by the basidiomycete fungi *Bjerkandera adusta* and *Pycnoporus sanguineus*. Biodegradation 22(3):565-572.

Rabinovich ML, Vanviet N, Klyosov AA. 1982. Adsorption of cellulolytic enzymes on cellulose and kinetics of the action of adsorbed enzymes. Two types of interaction of the enzymes with an insoluble substrate. Biochemistry Moscow 47(3):369-377.

Rabinovich ML. 1988. Mechanisms of enzymatic degradation of cellulose. In: Skryabin GK, Golovlev EL, Klyosov AA, editors. Microbiology and Biochemistry of Degradation of Plant Raw Materials: Nauka. p 70–108.

Ramos-Fernandez A, Paradela A, Navajas R, Albar JP. 2008. Generalized method for probability-based peptide and protein identification from tandem mass spectrometry data and sequence database searching. Mol Cell Proteomics 7(9):1748-1754.

Ramos LP, Nazhad MM, Saddler JN. 1993. Effect of enzymatic-hydrolysis on the morphology and fine-structure of pretreated cellulosic residues. Enzyme Microb Technol 15(10):821-831.

Rautela GS, King KW. 1968. Significance of crystal structure of cellulose in production and action of cellulase. Arch Biochem Biophys 123(3):589-601.

Reese ET. 1980. Shear inactivation of cellulases of *Trichoderma reesei*. Enzyme Microb Technol 2:239-240.

Reese ET, Mandels M. 1980. Stability of the cellulase of *Trichoderma reesei* under use conditions. Biotechnol Bioeng 22(2):323-335.

Reinikainen T, Teleman O, Teeri TT. 1995. Effects of pH and high ionic strength on the adsorption and activity of native and mutated cellobiohydrolase I from *Trichoderma reesei*. Proteins 22(4):392-403.

Rinaldi R, Palkovits R, Schueth F. 2008. Depolymerization of cellulose using solid catalysts in ionic liquids. Angew Chem Int Ed 120:8167-8170.

Rinaldi R, Engel P, Büchs J, Spiess AC, Schüth F. 2010. An integrated catalytic approach to fermentable sugars from cellulose. ChemSusChem 3(10):1151-1153.

Riscaldati E, Moresi M, Federici F, Petruccioli M. 2000. Effect of pH and stirring rate on itaconate production by *Aspergillus terreus*. J Biotechnol 83(3):219-230.

Rollin JA, Zhu Z, Sathitsuksanoh N, Zhang YHP. 2011. Increasing cellulose accessibility is more important than removing lignin: a comparison of cellulose solvent-based lignocellulose fractionation and soaking in aqueous ammonia. Biotechnol Bioeng 108:22-30.

Romani A, Yanez R, Garrote G, Alonso JL. 2008. SSF production of lactic acid from cellulosic biosludges. Bioresour Technol 99(10):4247-4254.

Rosgaard L, Pedersen S, Langston J, Akerhielm D, Cherry JR, Meyer AS. 2007. Evaluation of minimal *Trichoderma reesei* cellulase mixtures on differently pretreated barley straw substrates. Biotechnol Progr 23(6):1270-1276.

Rouvinen J, Bergfors T, Teeri T, Knowles J, Jones T. 1990. Three-dimensional structure of cellobiohydrolase II from *Trichoderma reesei*. Science 249(4967):380-386.

Ruiz-Duenas FJ, Martinez AT. 2009. Microbial degradation of lignin: how a bulky recalcitrant polymer is efficiently recycled in nature and how we can take advantage of this. Microb Biotechnol 2(2):164-177.

Runquist D, Hahn-Hagerdal B, Radstrom P. 2011. Comparison of heterologous xylose transporters in recombinant *Saccharomyces cerevisiae*. Biotechnol Biofuels 3:5.

Rychtera M, Wase DAJ. 1981. The growth of *Aspergillus terreus* and the production of itaconic acid in batch and continuous cultures. The influence of pH. J Chem Technol Biotechnol 31(1):509-521.

Saloheimo M, Nakari-SetäLä T, Tenkanen M, Penttilä M. 1997. cDNA cloning of a *Trichoderma reesei* cellulase and demonstration of endoglucanase activity by expression in yeast. Eur J Biochem 249(2):584-591.

Saloheimo M, Paloheimo M, Hakola S, Pere J, Swanson B, Nyyssonen E, Bhatia A, Ward M, Penttila M. 2002. Swollenin, a *Trichoderma reesei* protein with sequence similarity to the plant expansins, exhibits disruption activity on cellulosic materials. Eur J Biochem 269(17):4202-11.

Samorski M, Müller-Newen G, Büchs J. 2005. Quasi-continuous combined scattered light and fluorescence measurements: a novel measurement technique for shaken microtiter plates. Biotechnol Bioeng 92(1):61-8.

Sathitsuksanoh N, Zhu Z, Wi S, Percival Zhang YH. 2011. Cellulose solvent-based biomass pretreatment breaks highly ordered hydrogen bonds in cellulose fibers of switchgrass. Biotechnol Bioeng 108(3):521-529.

Schröter K, Flaschel E, Puhler A, Becker A. 2001. *Xanthomonas campestris* pv. *campestris* secretes the endoglucanases ENGXCA and ENGXCB: construction of an endoglucanase-deficient mutant for industrial xanthan production. Appl Microbiol Biotechnol 55(6):727-733.

Schuchardt S, Sickmann A. 2007. Protein identification using mass spectrometry: a method overview. EXS 97:141-170.

Schülein M. 1988. Cellulases of *Trichoderma reesei*. Methods Enzymol 160:234-242.

Selig MJ, Viamajala S, Decker SR, Tucker MP, Himmel ME, Vinzant TB. 2007. Deposition of lignin droplets produced during dilute acid pretreatment of maize stems retards enzymatic hydrolysis of cellulose. Biotechnol Progr 23(6):1333-1339.

Selig MJ, Vinzant TB, Himmel ME, Decker SR. 2009. The effect of lignin removal by alkaline peroxide pretreatment on the susceptibility of corn stover to purified cellulolytic and xylanolytic enzymes. Appl Biochem Biotechnol 155(1-3):397-406.

Selig MJ, Tucker MP, Sykes RW, Reichel KL, Brunecky R, Himmel ME, Davis MF, Decker SR. 2010. Lignocellulose recalcitrance screening by integrated high-throughput hydrothermal pretreatment and enzymatic saccharification. Ind Biotechnol 6(2):104-111.

Shallom D, Shoham Y. 2003. Microbial hemicellulases. Curr Opin Microbiol 6(3):219-228.

Shin D, Yoo A, Kim SW, Yang DR. 2006. Cybernetic modeling of simultaneous saccharification and fermentation for ethanol production from steam-exploded wood with *Brettanomyces custersii*. J Microbiol Biotechnol 16(9):1355-1361.

Shoemaker S, Watt K, Tsitovsky G, Cox R. 1983. Characterization and properties of cellulases purified from *Trichoderma reesei* strain-L27. Nat Biotechnol 1(8):687-690.

Singh A, Kumar PKR, Schügerl K. 1991. Adsorption and reuse of cellulases during saccharification of cellulosic materials. J Biotechnol 18:205–212.

Sjöström E, Alén R. 1999. Analytical methods in wood chemistry, pulping, and papermaking. Berlin, Heidelberg, New York: Springer Verlag.

Smith PK, Krohn RI, Hermanson GT, Mallia AK, Gartner FH, Provenzano MD, Fujimoto EK, Goeke NM, Olson BJ, Klenk DC. 1985. Measurement of protein using bicinchoninic acid. Anal Biochem 150(1):76-85.

Somerville C, Bauer S, Brininstool G, Facette M, Hamann T, Milne J, Osborne E, Paredez A, Persson S, Raab T and others. 2004. Toward a systems approach to understanding plant cell walls. Science 306(5705):2206-2211.

Somerville C, Youngs H, Taylor C, Davis SC, Long SP. 2010. Feedstocks for lignocellulosic biofuels. Science 329(5993):790-792.

Srisodsuk M, Reinikainen T, Penttila M, Teeri TT. 1993. Role of the interdomain linker peptide of *Trichoderma reesei* cellobiohydrolase I in its interaction with crystalline cellulose. J Biol Chem 268(28):20756-20761.

Stahlberg J, Johansson G, Pettersson G. 1991. A new model for enzymatic hydrolysis of cellulose based on the two-domain structure of cellobiohydrolase I. Nat Biotechnol 9(3):286-290.

Stals I, Sandra K, Geysens S, Contreras R, Van Beeumen J, Claeyssens M. 2004. Factors influencing glycosylation of *Trichoderma reesei* cellulases. I: postsecretorial changes of the O- and N-glycosylation pattern of Cel7A. Glycobiology 14(8):713-724.

Stephanopoulos G. 2007. Challenges in engineering microbes for biofuels production. Science 315(5813):801-4.

Takagi M. 1984. Inhibition of cellulase by fermentation products. Biotechnol Bioeng 26(12):1506-1507.

Tan HY, Ng TW, Liew OW. 2007. Effects of light spectrum in flatbed scanner densitometry of stained polyacrylamide gels. Biotechniques 42(4):474-478.

Tanaka M, Nakamura H, Taniguchi M, Morita T, Matsuno R, Kamikubo T. 1986. Elucidation of adsorption processes of cellulases during hydrolysis of crystalline cellulose. Appl Microbiol Biotechnol 23(3-4):263-268.

Teeri TT. 1997. Crystalline cellulose degradation: new insight into the function of cellobiohydrolases. Trends Biotechnol 15(5):160-167.

Tengborg C, Galbe M, Zacchi G. 2001. Influence of enzyme loading and physical parameters on the enzymatic hydrolysis of steam-pretreated softwood. Biotechnol Progr 17(1):110-117.

Tian S, Luo XL, Yang XS, Zhu JY. 2010. Robust cellulosic ethanol production from SPORL-pretreated lodgepole pine using an adapted strain *Saccharomyces cerevisiae* without detoxification. Bioresour Technol 101(22):8678-8685.

Tolan JS, Foody B. 1999. Cellulase from submerged fermentation. Adv Biochem Engin Biotechnol 65:41-67.

Tomme P, Vantilbeurgh H, Pettersson G, Vandamme J, Vandekerckhove J, Knowles J, Teeri T, Claeyssens M. 1988. Studies of the cellulolytic system of *Trichoderma reesei* QM 9414 - analysis of domain function in 2 cellobiohydrolases by limited proteolysis. Eur J Biochem 170(3):575-581.

Tuohy MG, Walsh DJ, Murray PG, Claeyssens M, Cuffe MM, Savage AV, Coughlan MP. 2002. Kinetic parameters and mode of action of the cellobiohydrolases produced by Talaromyces emersonii. Biochim Biophys Acta 1596(2):366-380.

Tur MK, Neef I, Jost E, Galm O, Jäger G, Stöcker M, Ribbert M, Osieka R, Klinge U, Barth S. 2009. Targeted restoration of down-regulated DAPK2 tumor suppressor activity induces apoptosis in Hodgkin lymphoma cells. J Immunother 32(5):431-441.

Ülker A, Sprey B. 1990. Characterization of an unglycosylated low molecular weight 1,4-β-glucan-glucanohydrolase of *Trichoderma reesei*. FEMS Microbiol Lett 69:215-219.

Väljamäe P, Sild V, Nutt A, Pettersson G, Johansson G. 1999. Acid hydrolysis of bacterial cellulose reveals different modes of synergistic action between cellobiohydrolase I and endoglucanase I. Eur J Biochem 266(2):327-334.

van Zyl WH, Lynd LR, den Haan R, McBride JE. 2007. Consolidated bioprocessing for bioethanol production using *Saccharomyces cerevisiae*. Adv Biochem Engin Biotechnol 108:205-235.

vom Stein T, Grande P, Sibilla F, Commandeur U, Fischer R, Leitner W, Dominguez de Maria P. 2010. Salt-assisted organic-acid-catalyzed depolymerization of cellulose. Green Chem 12:1844-1849.

vom Stein T, Grande PM, Kayser H, Sibilla F, Leitner W, Dominguez de Maria P. 2011. From biomass to feedstock: one-step fractionation of lignocellulose components by the selective organic acid-catalyzed depolymerization of hemicellulose in a biphasic system. Green Chem 13(7):1772-1777.

Voutilainen SP, Puranen T, Siika-Aho M, Lappalainen A, Alapuranen M, Kallio J, Hooman S, Viikri L, Vehmaanpera J, Koivula A. 2008. Cloning, expression, and characterization of novel thermostable family 7 cellobiohydrolases. Biotechnol Bioeng 101(3):515-528.

Wang LS, Zhang YZ, Gao PJ, Shi DX, Liu HW, Gao HJ. 2006. Changes in the structural properties and rate of hydrolysis of cotton fibers during extended enzymatic hydrolysis. Biotechnol Bioeng 93(3):443-456.

Wang M, Cai J, Huang L, Lv Z, Zhang Y, Xu Z. 2010. High-level expression and efficient purification of bioactive swollenin in *Aspergillus oryzae*. Appl Biochem Biotechnol 162(7):2027-2036.

Wang P, Broda P. 1992. Stable defined substrate for turbidimetric assay of endoxylanases. Appl Environ Microbiol 58(10):3433-3436.

Wasewar KL, Shende D, Keshav A. 2011. Reactive extraction of itaconic acid using tri-n-butyl phosphate and aliquat 336 in sunflower oil as a non-toxic diluent. J Chem Tech Biotech 86(2):319-323.

Wee YJ, Kim JN, Ryu HW. 2006. Biotechnological production of lactic acid and its recent applications. Food Technol Biotechnol 44(2):163-172.

Wei W, Yang C, Luo J, Lu C, Wu Y, Yuan S. 2010. Synergism between cucumber [alpha]-expansin, fungal endoglucanase and pectin lyase. J Plant Physiol 167(14):1204-1210.

Weiler E, Nover L. 2008. Allgemeine und molekulare Botanik. Stuttgart: Thieme.

Werpy T, Petersen G. 2004. Top value added chemicals from biomass. Volume I: results of screening for potential candidates from sugars and synthesis gas. Oak Ridge: U.S. Department of Energy, National Renewable Energy Laboratory (NREL).

Whitney SEC, Gidley MJ, McQueen-Mason SJ. 2000. Probing expansin action using cellulose/hemicellulose composites. Plant J 22(4):327-334.

Willke T, Vorlop KD. 2001. Biotechnological production of itaconic acid. Appl Microbiol Biotechnol 56(3-4):289-295.

Wilson CM. 1983. Staining of proteins on gels: comparisons of dyes and procedures. Methods Enzymol 91:236-247.

Winters MS, Day RA. 2003. Detecting protein-protein interactions in the intact cell of *Bacillus subtilis* (ATCC 6633). J Bacteriol 185(14):4268-4275.

Wood TM, Bhat KM. 1988. Methods for measuring cellulase activities. Method Enzymol 160:87-112.

Woodward J, Hayes MK, Lee NE. 1988. Hydrolysis of cellulose by saturating and non-saturating concentrations of cellulase - implications for synergism. Nat Biotechnol 6(3):301-304.

Woodward J. 1991. Synergism in cellulase systems. Bioresour Technol 36(1):67-75.

Wormald P, Wickholm K, Larsson PT, Iversen T. 1996. Conversions between ordered and disordered cellulose. Effects of mechanical treatment followed by cyclic wetting and drying. Cellulose 3(3):141-152.

Wright JD, Wyman CE, Grohmann K. 1988. Simultaneous saccharification and fermentation of lignocellulose: process evaluation. Appl Biochem Biotechnol 18:75-90.

Wyman CE. 1994. Ethanol from lignocellulosic biomass: technology, economics, and opportunities. Bioresour Technol 50(1):3-15.

Wyman CE. 2004. Ethanol fuel. In: Cleveland CJ, editor. Encyclopedia of energy. New York: Elsevier. p 541-555.

Wyman CE. 2007. What is (and is not) vital to advancing cellulosic ethanol. Trends Biotechnol 25(4):153-157.

Xu Q, Singh A, Himmel ME. 2009. Perspectives and new directions for the production of bioethanol using consolidated bioprocessing of lignocellulose. Curr Opin Biotechnol 20(3):364-371.

Yahiro K, Takahama T, Park YS, Okabe M. 1995. Breeding of *Aspergillus terreus* mutant TN-484 for itaconic acid production with high-yield. J Ferment Bioeng 79(5):506-508.

Yanase S, Yamada R, Kaneko S, Noda H, Hasunuma T, Tanaka T, Ogino C, Fukuda H, Kondo A. 2010. Ethanol production from cellulosic materials using cellulase-expressing yeast. Biotechnol J 5(5):449-455.

Yáñez R, Belén Moldes A, Alonso JL, Parajó JC. 2003. Production of D(-)-lactic acid from cellulose by simultaneous saccharification and fermentation using *Lactobacillus coryniformis* subsp. *torquens*. Biotechnol Lett 25(14):1161-1164.

Yang B, Willies DM, Wyman CE. 2006. Changes in the enzymatic hydrolysis rate of Avicel cellulose with conversion. Biotechnol Bioeng 94(6):1122-1128.

Yeh AI, Huang YC, Chen SH. 2010. Effect of particle size on the rate of enzymatic hydrolysis of cellulose. Carbohydr Polym 79(1):192-199.

Yuldashev B, Rakhimov M, Rabinovich ML. 1993. The comparative study of cellulase behaviour on the surface of cellulose and lignocellulose during enzymatic hydrolysis. Appl Biochem Microbiol 29:58-68.

Zavrel M, Schmidt T, Michalik C, Ansorge-Schumacher M, Marquardt W, Büchs J, Spiess AC. 2008. Mechanistic kinetic model for symmetric carboligations using benzaldehyde lyase. Biotechnol Bioeng 101:27-38.

Zhang M, Eddy C, Deanda K, Finkelstein M, Picataggio S. 1995. Metabolic engineering of a pentose metabolism pathway in ethanologenic *Zymomonas mobilis*. Science 267(5195):240-243.

Zhang S, Wolfgang DE, Wilson DB. 1999. Substrate heterogeneity causes the nonlinear kinetics of insoluble cellulose hydrolysis. Biotechnol Bioeng 66(1):35-41.

Zhang XZ, Zhang ZM, Zhu ZG, Sathitsuksanoh N, Yang YF, Zhang YHP. 2010. The noncellulosomal family 48 cellobiohydrolase from *Clostridium phytofermentans* ISDg: heterologous expression, characterization, and processivity. Appl Microbiol Biotechnol 86(2):525-533.

Zhang YH, Lynd LR. 2004. Toward an aggregated understanding of enzymatic hydrolysis of cellulose: noncomplexed cellulase systems. Biotechnol Bioeng 88(7):797-824.

Zhang YHP, Lynd LR. 2005. Determination of the number-average degree of polymerization of cellodextrins and cellulose with application to enzymatic hydrolysis. Biomacromolecules 6(3):1510-1515.

Zhang YHP, Himmel ME, Mielenz JR. 2006. Outlook for cellulase improvement: screening and selection strategies. Biotechnol Adv 24(5):452-481.

Zhang YHP, Ding SY, Mielenz JR, Cui JB, Elander RT, Laser M, Himmel ME, McMillan JR, Lynd LR. 2007. Fractionating recalcitrant lignocellulose at modest reaction conditions. Biotechnol Bioeng 97(2):214-223.

Zhao H, Kwak JH, Conrad Zhang Z, Brown HM, Arey BW, Holladay JE. 2007. Studying cellulose fiber structure by SEM, XRD, NMR and acid hydrolysis. Carbohydr Polym 68(2):235-241.

Zhu ZG, Sathitsuksanoh N, Zhang YHP. 2009. Direct quantitative determination of adsorbed cellulase on lignocellulosic biomass with its application to study cellulase desorption for potential recycling. Analyst 134(11):2267-2272.

Zwietering TN. 1958. Suspending of solid particles in liquid by agitators. Chem Eng Sci 8(3-4):244-253.

Appendix

Appendix A: Single Chromatographic Purification Steps

As described in Chapter 3.1.3.1, several chromatographic steps for purifying CBH I, CBH II, EG I, and EG II were performed. Figure 3-2 shows a flow diagram for these chromatographic steps. After every purification step, the fractions were comprehensively analyzed by SDS-polyacrylamide gel electrophoresis and cellulase activity assays using Avicel and CMC to differentiate CBHs and EGs, respectively. The chromatograms and fraction analysis (including SDS-polyacrylamide gel electrophoresis and cellulase activity assay) of each purification step are listed within this section. Moreover, the cellulases (CBH I, CBH II, EG I, and EG II) are marked within the SDS-polyacrylamide gels. These cellulases could be identified based on: molecular mass and isoelectric points (Table 1-2), determined cellulase activities (shown within the chromatograms), and mass spectrometry (data not shown).
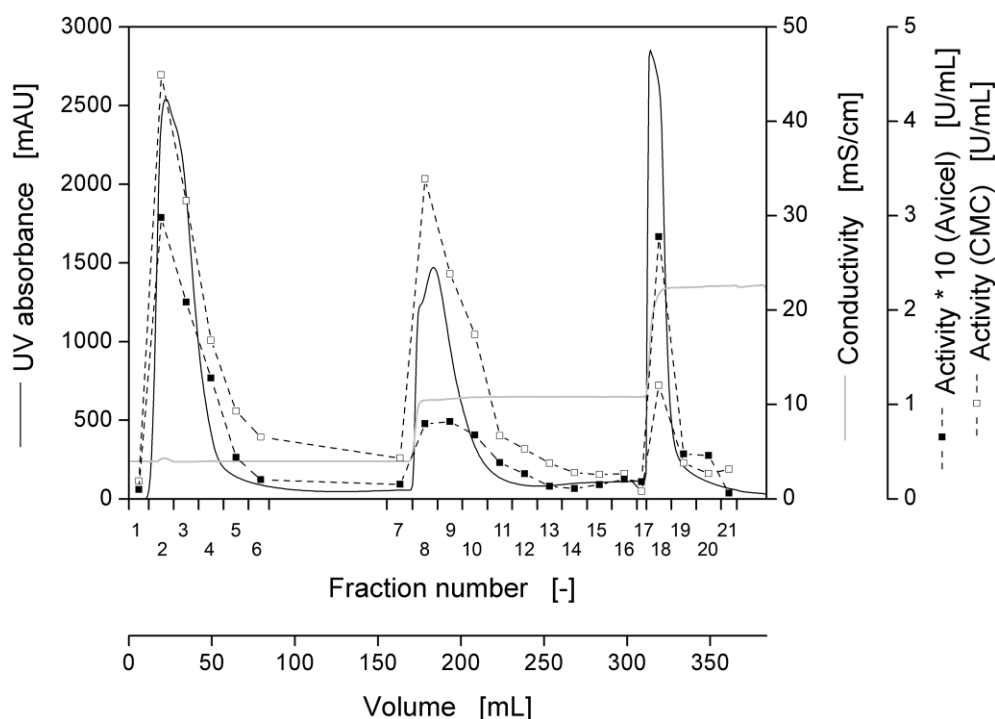
Figure A-1: Chromatographic purification step I according to Figure 3-2: chromatogram and cellulase activities of the collected fractions; purification: anion exchange chromatography, sample: 7.5 mL desalted Celluclast®, the purification procedure is described in Chapter 3.1.2.2; cellulase activity assay: 10 g/L Avicel or CMC in 0.1 M sodium acetate buffer (pH 4.8), 200 μL of the respective fraction, $T = 45°C$, $V_L = 1$ mL, $n = 1000$ rpm, $d_0 = 3$ mm, reaction time: 120 min (Avicel), 10 min (CMC). Avicel and CMC are model substrates to differentiate CBHs and EGs, respectively (Ghose, 1987; Zhang et al., 2006).
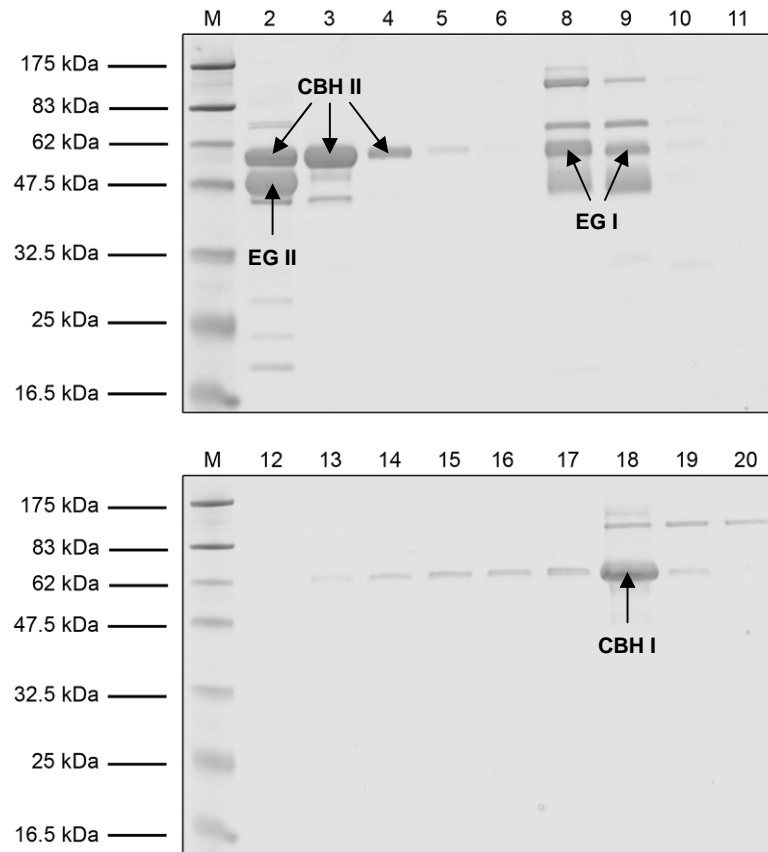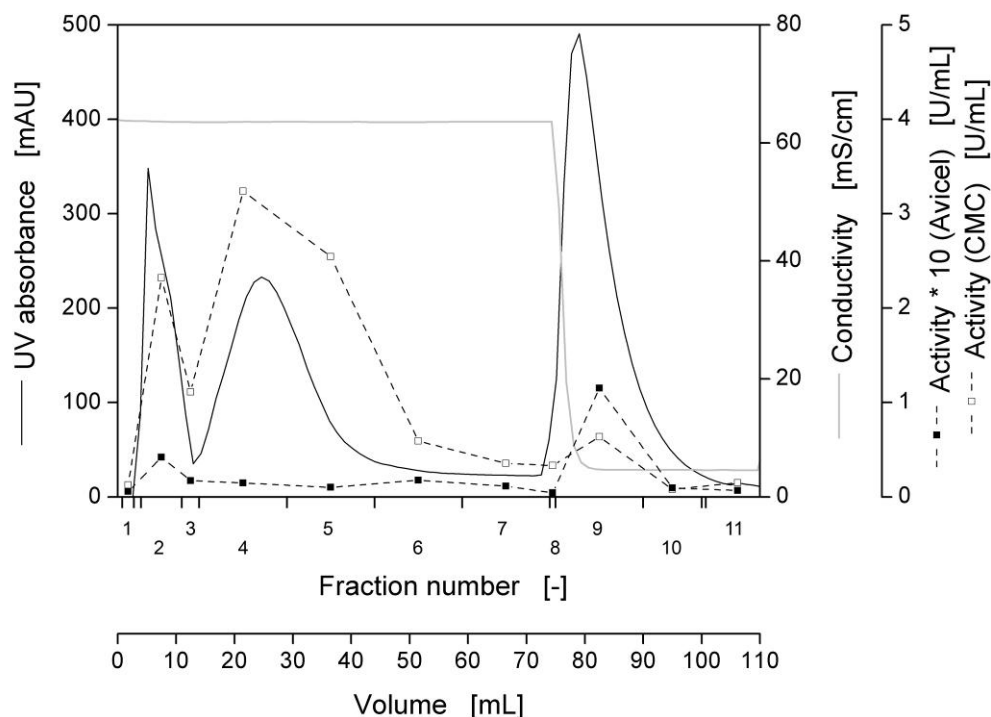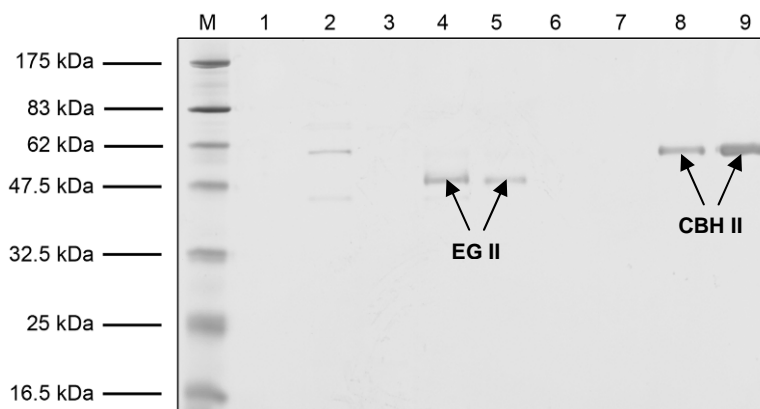
Figure A-2:   Chromatographic purification step I according to Figure 3-2: SDS-polyacrylamide gel electrophoresis of the collected fractions. (M) Molecular mass marker, fraction numbers refer to those shown in Figure A-1. The cellobiohydrolases (CBH) and endoglucanases (EG) could be identified based on: molecular mass and isoelectric points (Table 1-2), determined cellulase activities (Figure A-1), and mass spectrometry (data not shown); 12% polyacrylamide gel, the same volume of the collected fractions (15 µL) was loaded onto the particular slots.

Figure A-3:   Chromatographic purification step II according to Figure 3-2: chromatogram and cellulase activities of the collected fractions; purification: hydrophobic interaction chromatography, sample: 0.375 mL concentrated fractions of chromatographic purification step I (fractions: 2, 3, 4; two runs), the purification procedure is described in Chapter 3.1.2.2; cellulase activity assay: 10 g/L Avicel or CMC in 0.1 M sodium acetate buffer (pH 4.8), 200 μL of the respective fraction, $T = 45°C$, $V_L = 1$ mL, $n = 1000$ rpm, $d_0 = 3$ mm, reaction time: 120 min (Avicel), 10 min (CMC). Avicel and CMC are model substrates to differentiate CBHs and EGs, respectively (Ghose, 1987; Zhang et al., 2006).

Figure A-4:   Chromatographic purification step II according to Figure 3-2: SDS-polyacrylamide gel electrophoresis of the collected fractions. (M) Molecular mass marker, fraction numbers refer to those shown in Figure A-3. The cellobiohydrolases (CBH) and endoglucanases (EG) could be identified based on: molecular mass and isoelectric points (Table 1-2), determined cellulase activities (Figure A-3), and mass spectrometry (data not shown); 12% polyacrylamide gel, the same volume of the collected fractions (15 μL) was loaded onto the particular slots.
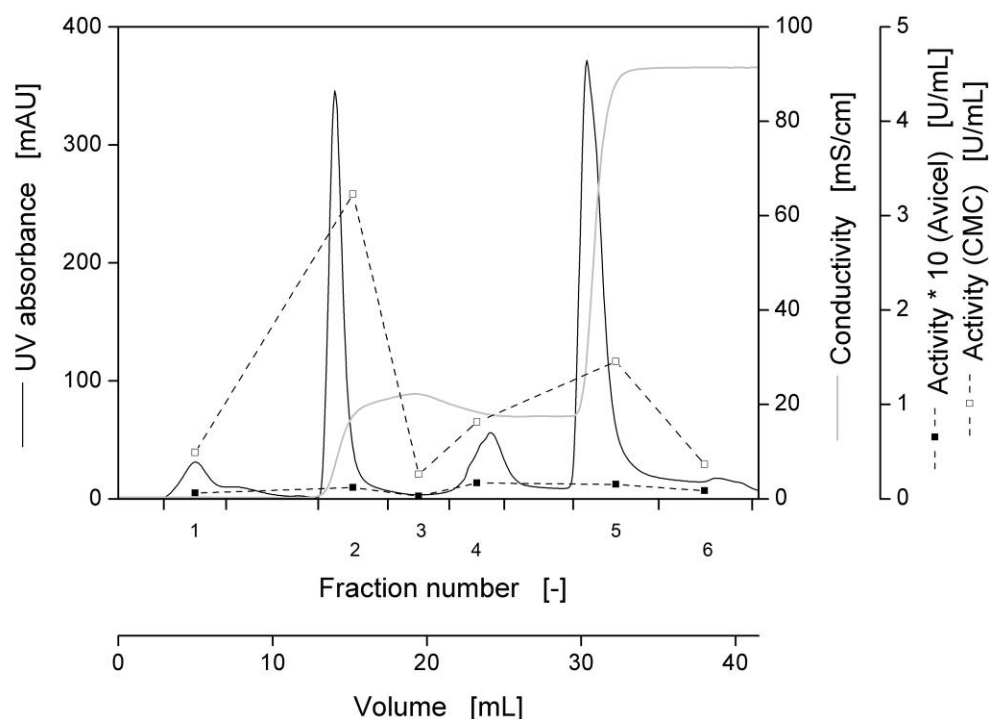
Figure A-5:   Chromatographic purification step III according to Figure 3-2: chromatogram and cellulase activities of the collected fractions; purification: cation exchange chromatography, sample: 0.375 mL concentrated fractions of chromatographic purification step I (fractions: 8, 9, 10; two runs), the purification procedure is described in Chapter 3.1.2.2; cellulase activity assay: 10 g/L Avicel or CMC in 0.1 M sodium acetate buffer (pH 4.8), 200 μL of the respective fraction, $T = 45°C$, $V_L = 1$ mL, $n = 1000$ rpm, $d_0 = 3$ mm, reaction time: 120 min (Avicel), 10 min (CMC). Avicel and CMC are model substrates to differentiate CBHs and EGs, respectively (Ghose, 1987; Zhang et al., 2006).
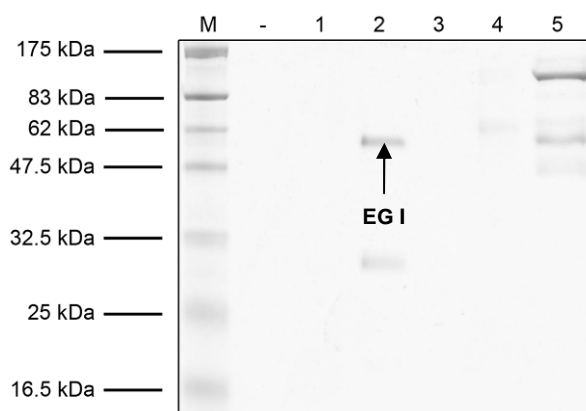

Figure A-6:   Chromatographic purification step III according to Figure 3-2: SDS-polyacrylamide gel electrophoresis of the collected fractions. (M) Molecular mass marker, fraction numbers refer to those shown in Figure A-5. The endoglucanase (EG) could be identified based on: molecular mass and isoelectric points (Table 1-2), determined cellulase activities (Figure A-5), and mass spectrometry (data not shown); 12% polyacrylamide gel, the same volume of the collected fractions (15 μL) was loaded onto the particular slots.
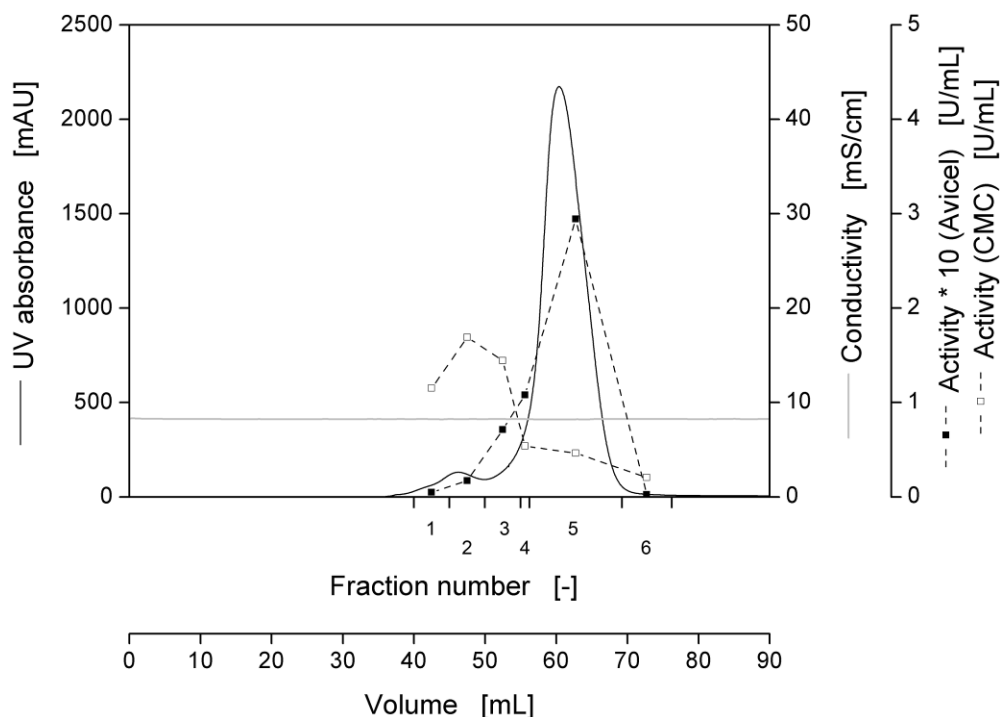
Figure A-7: Chromatographic purification step IV according to Figure 3-2: chromatogram and cellulase activities of the collected fractions; purification: size exclusion chromatography, sample: 0.6 mL concentrated fractions of chromatographic purification step I (fractions: 18, 19; two runs), the purification procedure is described in Chapter 3.1.2.2; cellulase activity assay: 10 g/L Avicel or CMC in 0.1 M sodium acetate buffer (pH 4.8), 200 µL of the respective fraction, $T = 45°C$, $V_L = 1$ mL, $n = 1000$ rpm, $d_0 = 3$ mm, reaction time: 120 min (Avicel), 10 min (CMC). Avicel and CMC are model substrates to differentiate CBHs and EGs, respectively (Ghose, 1987; Zhang et al., 2006).
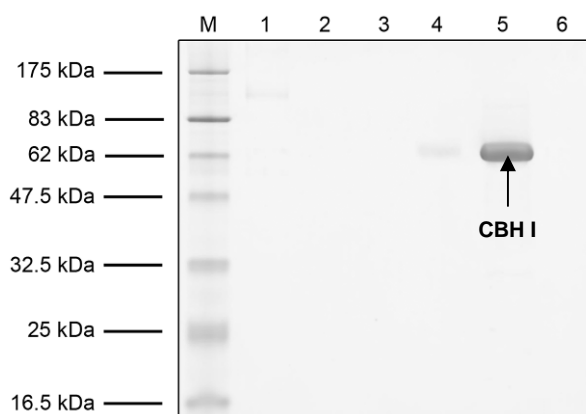

Figure A-8: Chromatographic purification step IV according to Figure 3-2: SDS-polyacrylamide gel electrophoresis of the collected fractions. (M) Molecular mass marker, fraction numbers refer to those shown in Figure A-7. The cellobiohydrolase (CBH) could be identified based on: molecular mass and isoelectric points (Table 1-2), determined cellulase activities (Figure A-7), and mass spectrometry (data not shown); 12% polyacrylamide gel, the same volume of the collected fractions (15 µL) was loaded onto the particular slots.
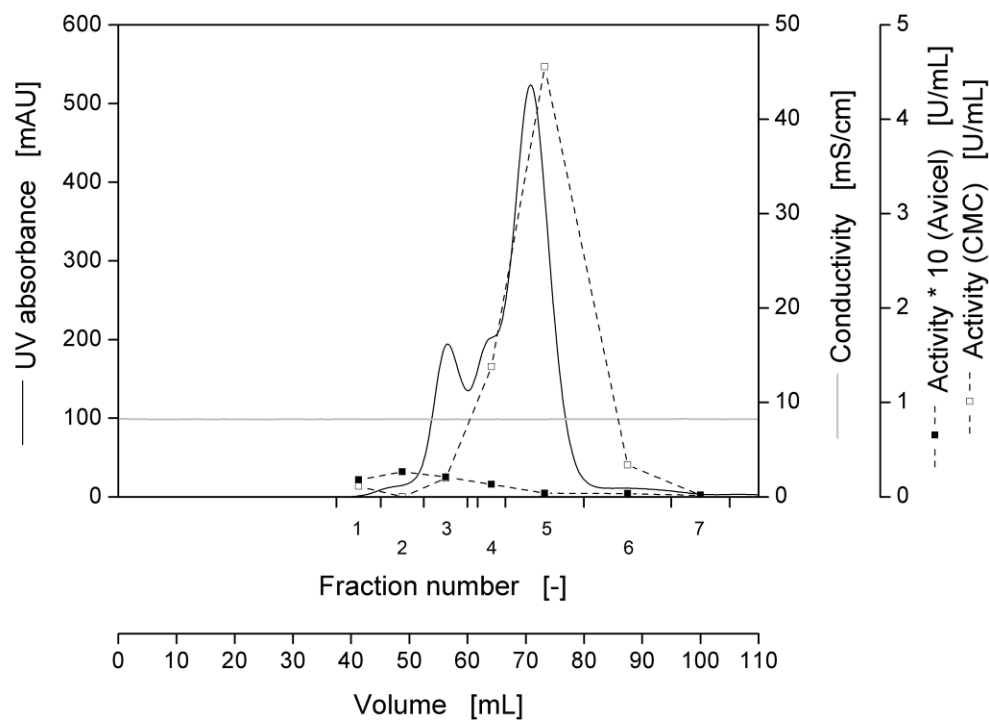
Figure A-9:   Chromatographic purification step V according to Figure 3-2: chromatogram and cellulase activities of the collected fractions; purification: size exclusion chromatography, sample: 0.5 mL concentrated fractions of chromatographic purification step II (fractions: 4, 5; eight runs), the purification procedure is described in Chapter 3.1.2.2; cellulase activity assay: 10 g/L Avicel or CMC in 0.1 M sodium acetate buffer (pH 4.8), 200 μL of the respective fraction, $T = 45°C$, $V_L = 1$ mL, $n = 1000$ rpm, $d_0 = 3$ mm, reaction time: 120 min (Avicel), 10 min (CMC). Avicel and CMC are model substrates to differentiate CBHs and EGs, respectively (Ghose, 1987; Zhang et al., 2006).
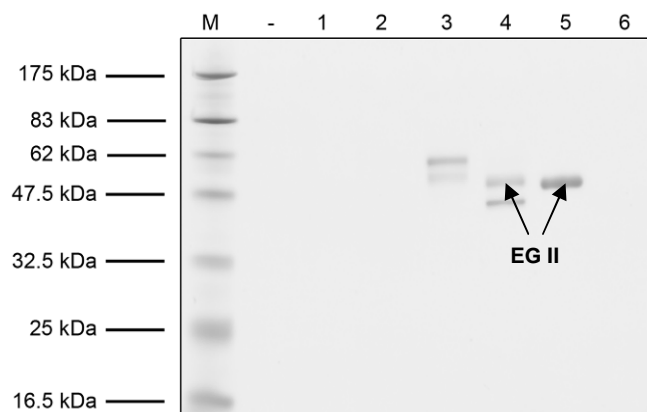

Figure A-10:   Chromatographic purification step V according to Figure 3-2: SDS-polyacrylamide gel electrophoresis of the collected fractions. (M) Molecular mass marker, fraction numbers refer to those shown in Figure A-9. The endoglucanase (EG) could be identified based on: molecular mass and isoelectric points (Table 1-2), determined cellulase activities (Figure A-9), and mass spectrometry (data not shown); 12% polyacrylamide gel, the same volume of the collected fractions (15 μL) was loaded onto the particular slots.
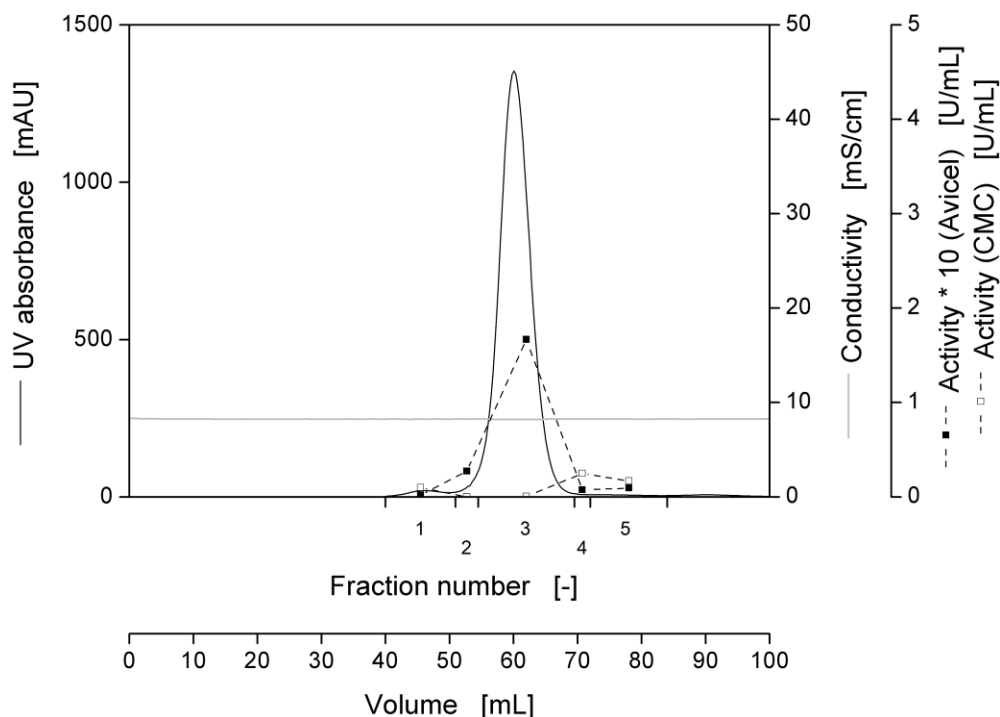
Figure A-11: Chromatographic purification step VI according to Figure 3-2: chromatogram and cellulase activities of the collected fractions; purification: size exclusion chromatography, sample: 0.5 mL concentrated fractions of chromatographic purification step II (fractions: 8, 9, 10; eight runs), the purification procedure is described in Chapter 3.1.2.2; cellulase activity assay: 10 g/L Avicel or CMC in 0.1 M sodium acetate buffer (pH 4.8), 200 μL of the respective fraction, $T = 45°C$, $V_L = 1$ mL, $n = 1000$ rpm, $d_0 = 3$ mm, reaction time: 120 min (Avicel), 10 min (CMC). Avicel and CMC are model substrates to differentiate CBHs and EGs, respectively (Ghose, 1987; Zhang et al., 2006).
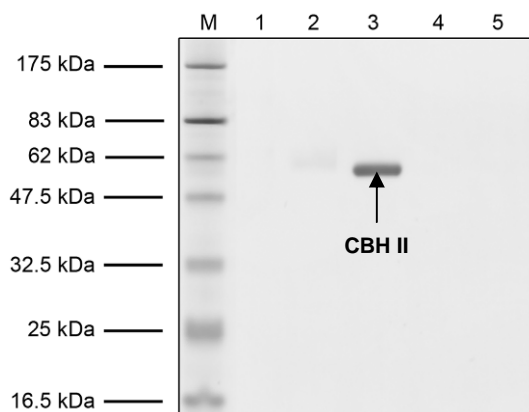

Figure A-12: Chromatographic purification step VI according to Figure 3-2: SDS-polyacrylamide gel electrophoresis of the collected fractions. (M) Molecular mass marker, fraction numbers refer to those shown in Figure A-11. The cellobiohydrolase (CBH) could be identified based on: molecular mass and isoelectric points (Table 1-2), determined cellulase activities (Figure A-11), and mass spectrometry (data not shown); 12% polyacrylamide gel, the same volume of the collected fractions (15 μL) was loaded onto the particular slots.
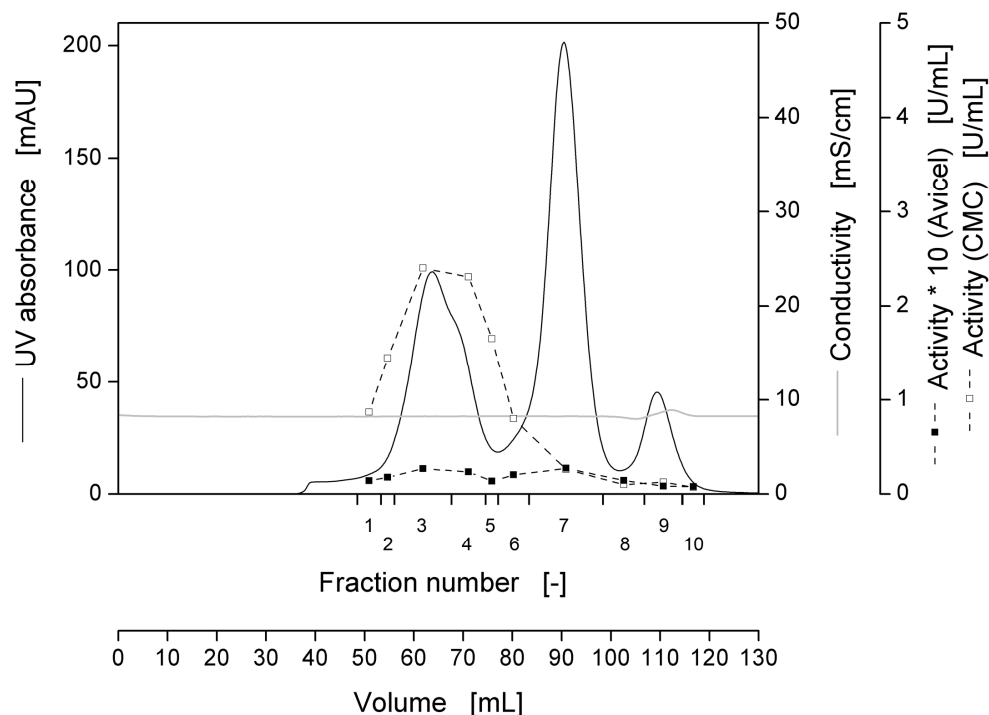
Figure A-13:   Chromatographic purification step VII according to Figure 3-2: chromatogram and cellulase activities of the collected fractions; purification: size exclusion chromatography, sample: 0.6 mL concentrated fractions of chromatographic purification step III (fractions: 2; 15 runs), the purification procedure is described in Chapter 3.1.2.2; cellulase activity assay: 10 g/L Avicel or CMC in 0.1 M sodium acetate buffer (pH 4.8), 200 μL of the respective fraction, $T = 45°C$, $V_L = 1$ mL, $n = 1000$ rpm, $d_0 = 3$ mm, reaction time: 120 min (Avicel), 10 min (CMC). Avicel and CMC are model substrates to differentiate CBHs and EGs, respectively (Ghose, 1987; Zhang et al., 2006).
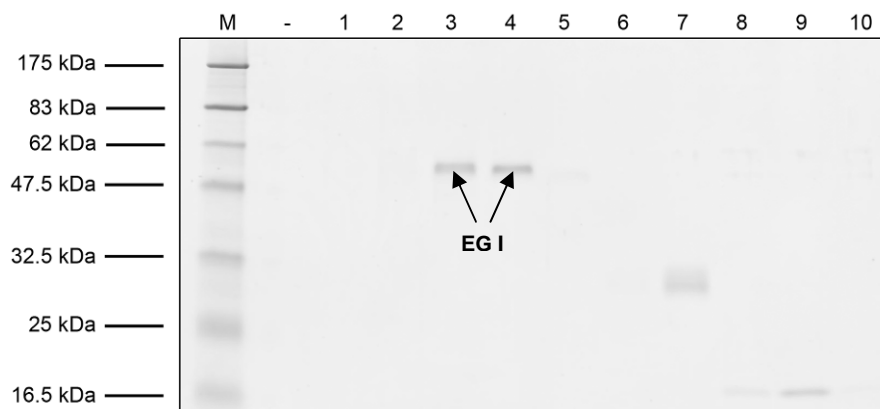

Figure A-14:   Chromatographic purification step VII according to Figure 3-2: SDS-polyacrylamide gel electrophoresis of the collected fractions. (M) Molecular mass marker, fraction numbers refer to those shown in Figure A-13. The endoglucanase (EG) could be identified based on: molecular mass and isoelectric points (Table 1-2), determined cellulase activities (Figure A-13), and mass spectrometry (data not shown); 12% polyacrylamide gel, the same volume of the collected fractions (15 μL) was loaded onto the particular slots.

Appendix B: Protein Markers

Table B-1: Description, source, and apparent molecular mass of the prestained proteins within the Prestained Protein Marker (New England Biolabs, Ipswich, USA).

Description[a]	Source[a]	Apparent molecular mass [kDa][a]
MBP-β-galactosidase	*E. coli*	175
MBP-paramyosin	*E. coli*	83
MBP-chitin binding domain	*E. coli*	62
Aldolase	Rabbit muscle	47.5
Triosephosphate isomerase	*E. coli*	32.5
β-Lactoglobulin A	Bovine milk	25
Lysozyme	Chicken egg white	16.5
Aprotinin	Bovine lung	6.5

MBP, maltose-binding protein.

[a] According to manufacture's data.

Table B-2: Description, source, and apparent molecular mass of the prestained proteins within the Plus Prestained Protein Ladder (Fermentas, Burlington, CA).

Description[a]	Source[a]	Apparent molecular mass [kDa][a]
Recombinant protein[b]	Prokaryote[b]	250
Recombinant protein[b]	Prokaryote[b]	130
Recombinant protein[b]	Prokaryote[b]	100
Recombinant protein[b]	Prokaryote[b]	70
Recombinant protein[b]	Prokaryote[b]	55
Recombinant protein[b]	Prokaryote[b]	35
Recombinant protein[b]	Prokaryote[b]	25
Recombinant protein[b]	Prokaryote[b]	15
Recombinant protein[b]	Prokaryote[b]	10

[a] According to manufacture's data.

[b] No additional information available; nondisclosure of the manufacture.

Lebenslauf

Name, Vorname	Jäger, Gernot
Geburtsdatum:	11.04.1983
Geburtsort:	Hilden
Staatsangehörigkeit:	Deutsch

Ausbildung

1989 - 2002   Evangelische Grundschule, Erkelenz

1993 - 2002   Abitur: Cusanus Gymnasium, Erkelenz

2002 - 2005   Studium: Biotechnologie (Bachelor of Science), RWTH Aachen
                  Abschlussarbeit: „Untersuchung des Suspendierzustandes von
                  Hydrogelkugeln für die Enzymimmobilisierung im gerührten
                  Reaktor", RWTH Aachen

2005 - 2007   Studium: Biotechnologie (Master of Science), RWTH Aachen
                  Abschlussarbeit: „Konstruktion, Expression, Reinigung und
                  Charakterisierung von CD30-Rezeptor bindenden Immunkinasen
                  (DAPK-basierend)", Fraunhofer IME

Berufstätigkeit

2008 - 2011   Doktorand / Wissenschaftlicher Mitarbeiter
                  Aachener Verfahrenstechnik - Bioverfahrenstechnik
                  (Prof. Dr.-Ing. Jochen Büchs), RWTH Aachen

seit 2011   Post-Doc / Wissenschaftlicher Mitarbeiter
                  Aachener Verfahrenstechnik - Bioverfahrenstechnik
                  (Prof. Dr.-Ing. Jochen Büchs), RWTH Aachen